DeepDive: A Data Management System for Automatic Knowledge Base Construction

by

Ce Zhang

A dissertation submitted in partial fulfillment of
the requirements for the degree of

Doctor of Philosophy

(Computer Sciences)

at the

UNIVERSITY OF WISCONSIN–MADISON

2015

Date of final oral examination: 08/13/2015

The dissertation is approved by the following members of the Final Oral Committee:

Jude Shavlik, Professor, Computer Sciences (UW-Madison)
Christopher Ré, Assistant Professor, Computer Science (Stanford University)
Jeffrey Naughton, Professor, Computer Sciences (UW-Madison)
David Page, Professor, Biostatistics and Medical Informatics (UW-Madison)
Shanan Peters, Associate Professor, Geosciences (UW-Madison)

ACKNOWLEDGMENTS

I owe Christopher Ré my career as a researcher, the greatest dream of my life. Since the day I first met Chris and told him about my dream, he has done everything he could, as a scientist, an educator, and a friend, to help me. I am forever indebted to him for his completely honest criticisms and feedback, the most valuable gifts an advisor can give. His training equipped me with confidence and pride that I will carry for the rest of my career. He is the role model that I will follow. If my whole future career achieves an approximation of what he has done so far in his, I will be proud and happy.

I am also indebted to Jude Shavlik and Miron Livny, who, after Chris left for Stanford, kindly helped me through all the paperwork and payments at Wisconsin. If it were not for their help, I would not have been able to continue my PhD studies. I am also profoundly grateful to Jude for being the chair of my committee. I am also likewise grateful to Jeffrey Naughton, David Page, and Shanan Peters for serving on my committee; and Thomas Reps for his feedback during defense.

DeepDive would have not been possible without all its users. Shanan Peters was the first user, working with it before it even got its name. He spent three years going through a painful process with us before we understood the current abstraction of DeepDive. I am grateful to him for sticking with us for this long process. I would also like to thank all the scientists and students who have interacted with me, without whose generous sharing of knowledge we could not have refined DeepDive to its current state. A very incomplete list includes Gabor Angeli, Gill Bejerano, Noel Heim, Arun Kumar, Pradap Konda, Emily Mallory, Christopher Manning, Jonathan Payne, Eldon Ulrich, Robin Valenza, and Yuke Zhu. DeepDive is now a team effort, and I am grateful to the whole DeepDive team, especially Jaeho Shin and Michael Cafarella, who help in managing the DeepDive team.

I am also extremely lucky to be surrounded by my friends. Heng Guo, Yinan Li, Linhai Song, Jia Xu, Junming Xu, Wentao Wu, and I have lunch frequently whenever we are in town, and this often amounts to the happiest hour in the entire day. Heng, a theoretician, has also borne the burden of listening to me pitch my system ideas for years, simply because he is, unfortunately for him, my roommate. Feng Niu mentored me through my early years at Wisconsin; even today, whenever I struggle to decide what the right thing to do is, I still imagine what he would have done in a similar situation. Victor Bittorf sparked my interest in modern hardware through his beautiful code and lucid tutorial. Over the years, I learned a lot from Yinan and Wentao about modern database systems, from Linhai about program analysis, and from Heng about counting.

Finally, I would also like to thank my parents for all their love over the last twenty-seven years and, I hope, in the future. Anything that I could write about them in any languages, even in my native Chinese, would pale beside everything they have done to support me in my life.

My graduate study has been supported by the Defense Advanced Research Projects Agency (DARPA) Machine Reading Program under Air Force Research Laboratory prime contract No. FA8750-09-C-0181, the DARPA DEFT Program under No. FA8750-13-2-0039, the National Science Foundation (NSF) EAGER Award under No. EAR-1242902, and the NSF EarthCube Award under No. ACI-1343760. Any opinions, findings, and conclusions or recommendations expressed in this material are those of the authors and do not necessarily reflect the views of DARPA, NSF, or the U.S. government.

The results mentioned in this dissertation come from previously published work [16, 84, 90, 148, 157, 171, 204–207]. Some descriptions are directly *from these papers. These papers are joint efforts with different authors, including: F. Abuzaid, G. Angeli, V. Bittorf, V. Govindaraju, S. Gupta, S. Hadjis, M. Premkumar, A. Kumar, M. Livny, C. Manning, F. Niu, C. Ré, S. Peters, C. Sa, A. Sadeghian, Z. Shan, J. Shavlik, J. Shin, J. Tibshirani, F. Wang, J. Wu, and S. Wu. Although this dissertation bears my name, this collection of research would not have been possible without the contributions of all these collaborators.*

ABSTRACT

Many pressing questions in science are macroscopic: they require scientists to consult information expressed in a wide range of resources, many of which are not organized in a structured relational form. Knowledge base construction (KBC) is the process of populating a knowledge base, i.e., a relational database storing factual information, from unstructured inputs. KBC holds the promise of facilitating a range of macroscopic sciences by making information accessible to scientists.

One key challenge in building a high-quality KBC system is that developers must often deal with data that are both diverse in type and large in size. Further complicating the scenario is that these data need to be manipulated by both relational operations and state-of-the-art machine-learning techniques. This dissertation focuses on supporting this complex process of building KBC systems. DeepDive is a data management system that we built to study this problem; its ultimate goal is to allow scientists to build a KBC system by declaratively specifying domain knowledge without worrying about any algorithmic, performance, or scalability issues.

DeepDive was built by generalizing from our experience in building more than ten high-quality KBC systems, many of which exceed human quality or are top-performing systems in KBC competitions, and many of which were built completely by scientists or industry users using DeepDive. From these examples, we designed a declarative language to specify a KBC system and a concrete protocol that iteratively improves the quality of KBC systems. This flexible framework introduces challenges of scalability and performance–Many KBC systems built with DeepDive contain statistical inference and learning tasks over terabytes of data, and the iterative protocol also requires executing similar inference problems multiple times. Motivated by these challenges, we designed techniques that make both the batch execution and incremental execution of a KBC program up to two orders of magnitude more efficient and/or scalable. This dissertation describes the DeepDive framework, its applications, and these techniques, to demonstrate the thesis that it is feasible to build an efficient and scalable data management system for the end-to-end workflow of building KBC systems.

SOFTWARE, DATA, AND VIDEOS

- DeepDive is available at `http://deepdive.stanford.edu`. It is a team effort to further develop and maintain this system.
- The DeepDive program of PaleoDeepDive (Chapter 4) is available at `http://deepdive.stanford.edu/doc/paleo.html` and can be executed with DeepDive v0.6.0α.
- The code for the prototype systems we developed to study the tradeoff of performance and scalability is also available separately.
  1. Elementary (Chapter 5.1): `http://i.stanford.edu/hazy/hazy/elementary`
  2. DimmWitted (Chapter 5.2): `http://github.com/HazyResearch/dimmwitted`. This was developed together with Victor Bittorf.
  3. Columbus (Chapter 6.1): `http://github.com/HazyResearch/dimmwitted/tree/master/columbus`. This was developed together with Arun Kumar.
  4. Incremental Feature Engineering (Chapter 6.2): DeepDive v0.6.0α. This was developed together with the DeepDive team, especially Jaeho Shin, Feiran Wang, and Sen Wu.
- Most data that we can legally release are available as DeepDive Open Datasets at `deepdive.stanford.edu/doc/opendata`. The computational resources to produce these data are made possible by millions of machine hours provided by the Center of High Throughput Computing (CHTC), led by Miron Livny at UW-Madison.
- These introductory videos in our YouTube channel are related to this dissertation:
  1. PaleoDeepDive: `http://www.youtube.com/watch?v=Cj2-dQ2nwoY`
  2. GeoDeepDive: `http://www.youtube.com/watch?v=X8uhs28O3eA`
  3. Wisci: `http://www.youtube.com/watch?v=Q1IpE9_pBu4`
  4. Columbus: `http://www.youtube.com/watch?v=wdTds3yg_G4`
  5. Elementary: `http://www.youtube.com/watch?v=Zf7sgMnR89c` and `http://www.youtube.com/watch?v=B5LxXGIkYe4`

DEPENDENCIES OF READING

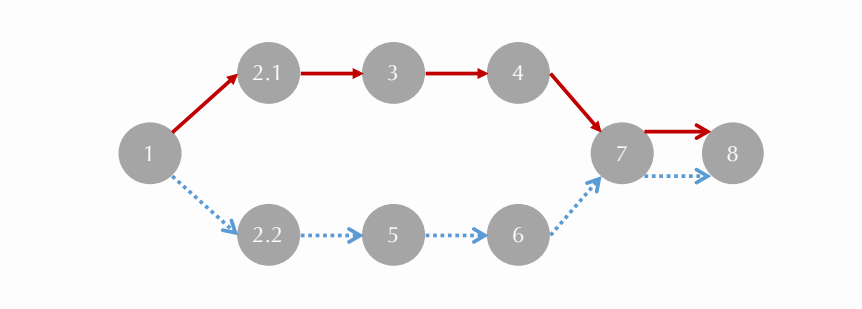

- **If** you are *only* interested in how DeepDive can be used to construct knowledge bases to help your applications and example systems built with DeepDive, you can read following the red solid line.
- **If** you are *only* interested in our work on efficient and scalable statistical analytics, you can read following the blue dotted line.
- **Otherwise**, you can read in linear order.

LIST OF FIGURES

LIST OF TABLES

1. Introduction

Science is built up of facts, as a house is with stones.

— Jules Henri Poincaré*, La Science et l'Hypothèse, 1901*

Knowledge Base Construction (KBC) is the process of populating a knowledge base (KB), i.e., a relational database storing factual information, from unstructured and/or structured input, e.g., text, tables, or even maps and figures. Because of its potential to answer key scientific questions, for decades, KBC has been conducted by scientists in various domains, such as the global compendia of marine animals compiled by Sepkoski in 1981 [167], the PaleoBioDB[1] project for biodiversity, and the PharmGKB [94] project for pharmacogenomics. The knowledge bases constructed by these projects contain up to one million facts and have contributed to hundreds of scientific discoveries.[2]

Despite their usefulness, it is typical for these knowledge bases to require a large amount of human resources to construct. For example, the PaleoBioDB project was constructed by an international group of more than 380 scientists with approximately nine continuous person years [148]. Partially motivated by the cost of building KBs manually, Automatic Knowledge Base Construction[3] has recently received tremendous interest from both academia [23, 32, 48, 71, 105, 134, 149, 170, 179, 200] and industry [73, 112, 133, 192, 209]. It is becoming clear that one key requirement for building a high-quality KBC system is to support processing data that are both diverse in type (e.g., text and tables) and large in size (e.g., larger than terabytes) with both relational operations and state-of-the-art machine learning techniques. One challenge introduced by this requirement is how to help domain scientists manage the complexity caused by these sophisticated operations and diverse data sources.

This dissertation demonstrates the thesis that *it is feasible to build a data management system to support the end-to-end workflow of building KBC systems; moreover, by providing such an integrated framework, we gain benefits that are otherwise harder to achieve.* We build DeepDive to demonstrate this thesis. In this chapter, we first present examples of the KBC workload; then, we present the goal of our study, and the technical contributions.

[1] `paleobiodb.org/#/`

[2] `paleobiodb.org/#/publications`; `www.pharmgkb.org/view/publications-pgkb.do`

[3] In the remaining part of this document, we use the term KBC to refer to an automatic KBC system.

1.1 Sample Target Workload

We present examples of KBC systems to illustrate the target workload that we focus on in this dissertation. The goal for this section is not to provide a complete description of the workload but instead to provide enough information to guide the reader through the rest of the chapter. A detailed description and examples of KBC workload are the topics of Chapter 2 and Chapter 4.

As illustrated in Figure 1.1, the input to a KBC system are resources such as journal articles, and the output is a relational database filled in with facts that can be supported by the input resources. For example, if a KBC system is given as an input a text snippet from a journal article that stating, "*The Namurian Tsingyuan Formation from Ningxia, China is divided into three members*," it could produce the following extractions. First, it could extract the phrase "Tsingyuan Formation" refers to a rock formation, "Ningxia, China" refers to a location, and "Namurian" refers to a temporal interval of age 326 to 313 million years. It will also extract relations between rock formation and their location and age as illustrated in Figure 1.1(a). Similar extractions can be extracted from other sources of input, such as tables, images, or even document layouts, as illustrated in Figure 1.1(b-d).

DeepDive has been used to build more than ten KBC systems similar to the one illustrated above, and these systems form the basis on which we justify our design decisions in DeepDive. In this dissertation, we focus on five KBC systems that the author of this dissertation involved in building for paleontology [148], geology [206], Freebase-like relations [16], genomics, and pharmacogenomics. These KBC systems have achieved high quality in these domains: the paleontology system has been featured in *Nature* [46] and achieves quality equal to (and sometimes better than) human experts [148], and the Freebase-like KBC system was the top-performing system for TAC-KBP 2014 slot-filling task. As DeepDive has become more mature recently, the development of KBC systems has been done more and more by domain scientists instead of the builder of DeepDive in its early stage.

1.2 The Goal of DeepDive

To achieve high quality in the process as illustrated above, an automatic KBC system is often designed to take advantage of multiple (noisy) input data sources, existing knowledge bases and taxonomies, domain knowledge from scientists, state-of-the-art natural language processing tools, and, as a growing trend, machine learning and statistical inference and learning. As a result, these KBC systems often need to deal with diverse types of data, and a diverse set of operations to manipulate

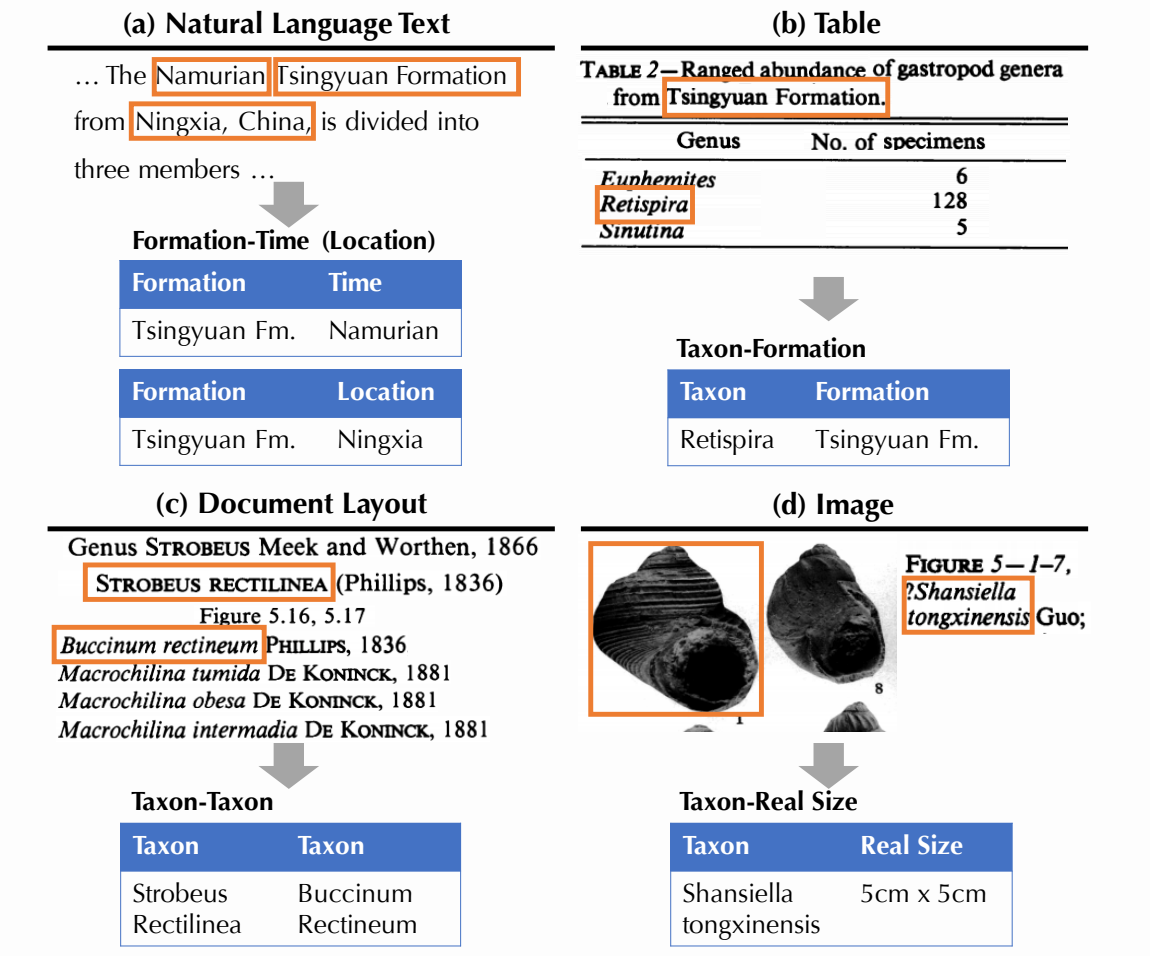

Figure 1.1: An illustration of the input and output of a KBC system built for paleontology.

the data. Apart from the diversity of data sources and operations, it is also typical for KBC systems to deal with Web-scale data sets and statistical operations that are not relational.

The goal of this thesis is to help domain experts, who want to build a KBC system, to deal with the sheer volume and diversity of data and operations required in KBC. Therefore, DeepDive is designed to be a data management system, which, if successful, will allow domain experts to build a KBC system by declaratively specifying domain knowledge without worrying about any algorithmic, performance, or scalability issues.

1.3 Technical Contributions

We divide the techniques of this dissertation into three categories.

(1) An Abstraction of General Workflow of KBC Systems. As the first step in building DeepDive, we focus on providing an abstraction to model the KBC workload. Ideally, this abstraction should support most common operations that users use while building KBC systems. To come up with this abstraction, we conducted case studies to build KBC systems in a diverse set of domains [16, 84, 148, 206]. Based on our observations from these case studies, we designed the execution model of DeepDive to consist of three phases: (1) feature extraction, (2) probabilistic knowledge engineering, and (3) statistical inference and learning. Given this execution model, to build a KBC system with DeepDive, domain experts first specify each of these phases with a declarative language, and iteratively improve each phase to achieve high quality. The first contribution is a Datalog-like language that allows domain experts to specify these three phases, and an iterative protocol to guide domain experts on debugging and improving each phase [157, 171]. This language and protocol has been applied to more than ten KBC systems, and the simplicity and flexibility of this language allows it to be used by users who are not computer scientists. This is the topic of Chapter 3 and Chapter 4.

(2) Performant and Scalable Statistical Inference and Learning. Given the three-phase framework of DeepDive, the next focus is to make each phase performant and scalable. One design decision we made is to rely on relational databases whenever possible, which allows us to take advantage of decades of study by the database community to speed up and scale up the feature extraction and probabilistic engineering phase. Therefore, this dissertation mainly focuses on speeding up and scaling up the statistical inference and learning phase that contains non-relational operations seen in statistical analytics, e.g., generalized linear models and Gibbs sampling. The second contribution is the study of (1) speeding up a subset of statistical analytics models on modern multi-socket, multi-core, non-uniform memory access (NUMA) machines with SIMD instructions when these models fit in the main memory [207]; and (2) scaling up a subset of statistical analytics models when the model does not fit in the main memory [206]. These techniques enable improvement of up to two orders of magnitude on the performance and scalability of these operations, which, together with classic relational techniques, helps to free the domain experts from worrying about the performance and scalability issues in building KBC systems with DeepDive. This is the topic of Chapter 5.

(3) Performant Iterative Debugging and Development. A common development pattern in KBC, as we observed in case studies, is that building a KBC system is an iterative exploratory process. That is, a domain expert often executes a set of different, but similar, KBC systems to find suitable features, input sources, and domain knowledge to use. Therefore, the last focus of this dissertation is to further optimize this iterative development pattern by supporting incremental execution of a KBC system. The technical challenge is that some operations in KBC are not relational, and, therefore, classic techniques developed for incrementally maintaining relational database systems cannot be used directly. The third contribution is to develop techniques to speed up exploratory feature selection and engineering with generalized linear models [204] and statistical inference and learning [171]. These techniques provide a speedup of another two orders of magnitude on the real workload we observed in KBC systems built by DeepDive users. This is the topic of Chapter 6.

Summary The central goal of this dissertation is to introduce a system, DeepDive, that can support the end-to-end workflow of building KBC systems to deal with inputs that are both diverse and large in size. DeepDive aims at supporting the thesis of this work, that is *it is feasible to build a data management system to support the end-to-end workflow of building KBC systems; moreover, by providing such an integrated framework, we gain benefits that are otherwise harder to achieve.* The main technical challenges are (1) what abstraction this system should provide to non-CS domain scientists, and (2) the performance in executing a KBC system built with this abstraction. For the first challenge, we design the framework by generalizing from more than ten KBC systems that we built in the past; and for the second challenge, we study techniques of both batch execution and incremental execution.

2. Preliminaries

In this chapter, we describe two pieces of critical background material for this thesis:

1. **A walkthough on what a KBC system is**, specifically, (1) concrete examples of KBC systems; (2) a KBC model that is an abstraction of objects used in KBC systems; and (3) a list of common operations that the user conducts while building KBC systems. The goal of this part is not to describe the technique or abstraction of DeepDive but, rather to get to the same page regarding the type of systems and workload we want to support with DeepDive.
2. **A description of the factor graph**, a type of probabilistic graphical model that is the abstraction we used for statistical inference and learning. The goal is to set up the notation and definition that the rest of this document will consistently exploit.

2.1 Knowledge Base Construction (KBC)

The *input* to a KBC system is a heterogeneous collection of unstructured, semi-structured, and structured data, ranging from text documents to existing but incomplete KBs. The *output* of the system is a relational database containing facts extracted from the input and put into the appropriate schema. Creating the knowledge base may involve extraction, cleaning, and integration.

Example 2.1. *Figure 1.1(a) shows a knowledge base with pairs of rock formations and locations that the rock formation is found. The input to the system is a collection of journal articles published in paleontology journals; the output is a KB containing pairs of rock formations and their location. In this example, a KBC system populates the KB with linguistic patterns, e.g., '... from ...' between a pairs of mentions (e.g., "Tsingyuan Fm" and "Ningxia"). As we will see later, these linguistic patterns are called* features *in DeepDive, and roughly, these features are then put in a classifier deciding whether this pair of mentions indicates that a formation appears in a location (in the* Formation-Location*) relation. KBC systems can also populate knowledge bases from resources other than natural language text. Figure 1.1(b-d) illustrate examples of KBC systems built to extract information from tables, document*

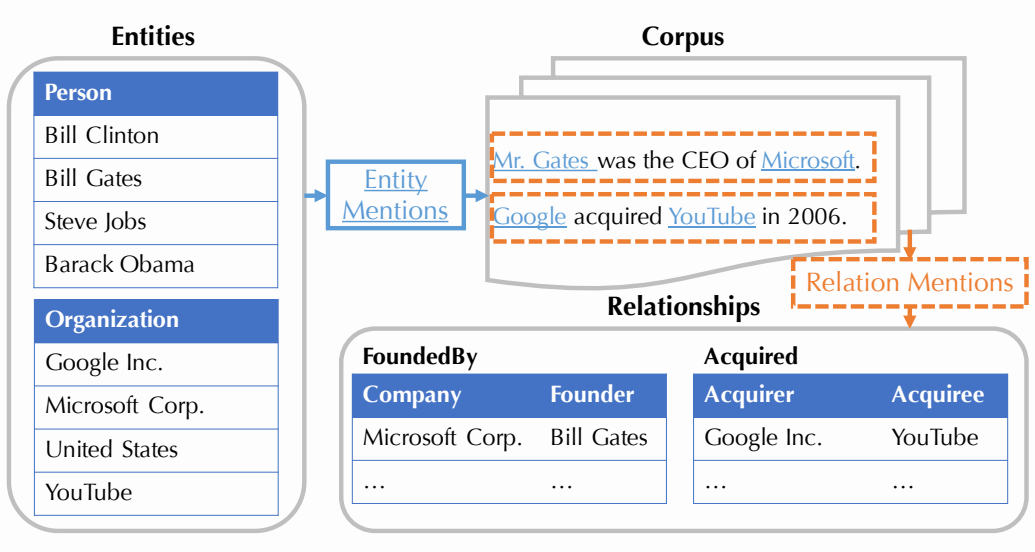

Figure 2.1: An illustration of the KBC model.

layout, and image. In practice, it is not uncommon for scientists to require a KBC system to deal with all these resources to answer their scientific questions [148].

Example 2.1 shows a KBC system for paleontology. Similar examples can also be found in other domains. For example, considering a knowledge base with pairs of individuals that are married to each other. In this case, The input to the system is a collection of news articles and an incomplete set of married persons; the output is a KB containing pairs of person that are married. A KBC system extracts linguistic patterns, e.g., "... and his wife ..." between a pair of mentions of individuals (e.g.,"Barack Obama" and "M. Obama") to decide whether this pair of mentions indicates that they are married (in the HasSpouse) relation. As another example, in pharmacogenomics, scientists might want to populate a knowledge base with pairs of gene and drug that interacts with each other by extracting features from journal articles. These similar examples of KBC systems in different domains can be characterized by (1) a KBC model, and (2) a list of common operations executed over the KBC model. We now describe these two parts in details.

2.1.1 The KBC Model

As we can see from Example 2.1, a KBC system needs to interact with different data sources. A KBC model is the abstraction of these data sources. We adopt standard KBC model that has been

developed by the KBC community for decades and used in standard KBC competitions, e.g., ACE.[1]

There are four types of objects that a KBC system seeks to extract from input documents, namely *entities*, *relations*, *mentions*, and *relation mentions*.

1. **Entity:** An entity is a real-world person, place, or thing. For example, the entity "Michelle_Obama_1" represents the actual entity for a person whose name is "Michelle Obama".

2. **Relation:** A relation associates two (or more) entities, and represents the fact that there exists a relationship between these entities. For example, the entity "Barack_Obama_1" and "Michelle_Obama_1" participate in the HasSpouse relation, which indicates that they are married.

3. **Mention:** a mention is a span of text in an input document that refers to an entity or relationship: "Michelle" may be a mention of the entity "Michelle_Obama_1." An entity might have mentions of different from; for example, apart from "Michelle", mentions of the form "M. Obama" or "Michelle Obama" can also refer to the same entity "Michelle_Obama_1." The process of mapping mentions to entities is called *entity linking*.

4. **Relation Mention:** A *relation mention* is a phrase that connects two mentions that participate in a relation, e.g., the phrase "and his wife" that connects the mentions "Barack Obama" and "M. Obama".

Figure 2.1 illustrates the examples and the relationship between these four types of objects. As we will see later in Chapter 3, DeepDive provides an abstraction to represent each type of objects as database relations and random variables, and provides a language for the user to specify indicators and the correlations between these objects.

2.1.2 Common Operations of KBC

Section 2.1.1 shows a data model of different types of objects inside a KBC system, and we now describe a set of operations a KBC system needs to support over this data model. This list of operations come from our our observations from the users of DeepDive while building different KBC systems.

[1] http://www.itl.nist.gov/iad/mig/tests/ace/2000/

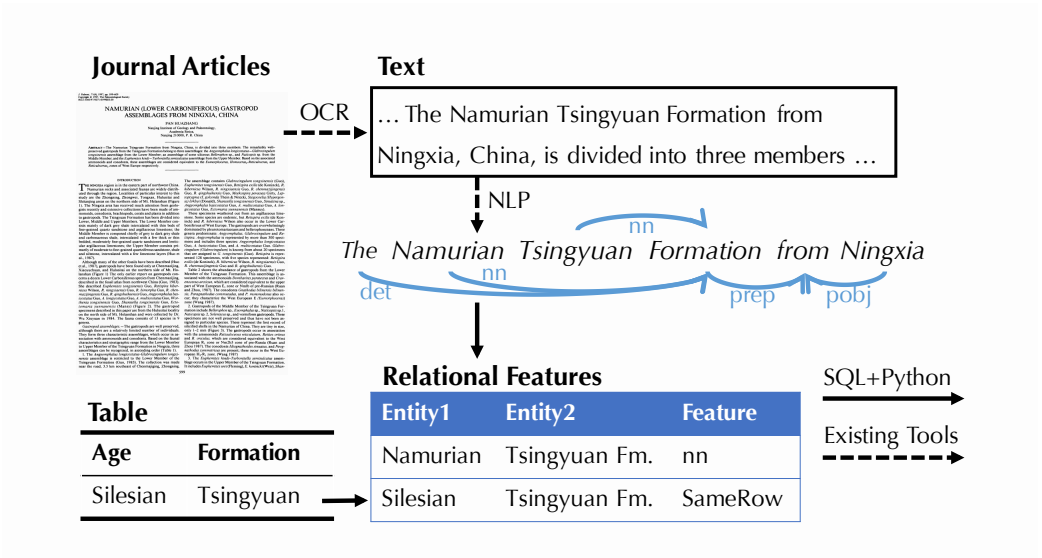

Figure 2.2: An illustration of features extracted for a KBC system.

Feature Extraction. The concept of a feature is one of the most important concepts for building KBC systems. We already see some example of features in Example 2.1; we now describe feature extraction in more details.

To extract features, the user specifies a mapping that takes as input both structured and unstructured information, and output features associated with entities, mentions, relations, or relation mentions. Intuitively, each feature will then be used as "evidience" to make prediction about the associated object. For example, Figure 2.2 illustrates features extracted for predicting relation mentions between temporal intervals and rock formations.

Given the diversity of input sources and target domains, the features extracted by the user is also higely diverse. For example:

- The user might need to run existing tools, such as Optical Character Recognition (OCR) and Natural Language Processing (NLP) tools to acquire information from text, HTML, or images. The output might contain JSON objects to represent parse trees or DOM structures.

- The user might also write user defined functions (UDF) in their favorite languages, e.g., Python, Perl, or SQL, to further process the information produced by existing tools. Examples include the word sequence features between two mentions as we see in Example 2.1, or the features derived from parse trees or table structures as illustrated in Figure 2.2.

One should notice that different features might be different regarding how "strong" they are as indicators of the target task. For example, the feature "... wife of ..." between two mentions could be a strong indicator of the HasSpouse relation, while the feature "... met ..." is much weaker. As we will see later in Chapter 3, DeepDive provides a way for the user to write these feature extractors, and automatically learn the weight, i.e., strengths, of features from training example provided by the user.

Domain Knowledge Integration. Another way to improve the quality of KBC systems is to integrate knowledge specific to the application domain. Such knowledge are assertions that are (statistically) true in the domain. Examples include

- To help extract the HasSpouse relation between persons, one can integrate the knowledge that "One person is *likely* to be the spouse of only one person."
- To help extract the HasAge relation between rock formations and temporal intervals, one can integrate the knowledge that "The same rock formation is not *likely* to have ages spanning 100 million years long."
- To help extract the BodySize relation between species and size measurements, one can integrate the knowledge that "Adult T. Rex are larger than humans."
- To help extract the HasFormula relation between chemical names and chemical formulae, one can integrate the knowledge that "C as in benzene can only make four chemical bonds."

To see how domain knowledge helps KBC systems, consider the effect of integrating the rule "one person is likely to be the spouse of only one person." With this rule, given a single entity "Barack_Obama," this rule gives positive preference to the case where only one of (Barack_Obama, Michelle_Obama) and (Barack_Obama, Michelle_Williams) is true. Therefore, even if the KBC system makes a wrong prediction about (Barack_Obama, Michelle_Williams) according to a wrong feature or a misleading document, integrating domain knowledge provides the opportunities to correct this.

One should also notice from this example that domain knowledge does not need to be always correct to be useful. As we will see later in Chapter 3, DeepDive provides a way for the user to specify her "confidence" of domain knowledge by either manually specifying or letting DeepDive automatically learn a real-valued *weight*.

Supervision. As we have described in previous paragraphs, both the features extracted and domain knowledge integrated need a *weight* to indicate how strong an indicator they are to the target task. One way to do that is for the user to manually specify the weight, which we support in DeepDive; however, another more easy, consistent, and effective way is for DeepDive to automatically learn the weight with machine learning techniques.

One challenge with building a machine learning system for KBC is collecting on training examples. As the number of predicates in the system grows, specifying training examples for each relation is tedious and expensive. Although DeepDive supports the standard supervised machine learning paradigm in which the user provides manually labelled training example, another common technique to cope with this is distant supervision. Distant supervision starts with an (incomplete) entity-level knowledge base and a corpus of text. The user then defines a (heuristic) mapping between entities in the database and text. This map is used to generate (noisy) training data for mention-level relations [61, 96, 131]. We illustrate this procedure by an example.

Example 2.2 (Distant Supervision)**.** *Consider the mention-level relation HasSpouse. To find training data, we find sentences that contain mentions of pairs of entities that are married, and we consider the resulting sentences positive examples. Negative examples could be generated from pairs of persons who are, say, parent-child pairs. Ideally, the patterns that occur between pairs of mentions corresponding to mentions will contain indicators of marriage more often than those that are parent-child pairs (or other pairs). Selecting those indicative phrases or features allows us to find features for these relations and generate training data. Of course, engineering this mapping is a difficult task in practice and requires many iterations.*

One should notice that the training examples generated by distant supervision are not necessarily always real training examples of the relation. For example, the fact that we see "Barack Obama" and "Michelle Obama" in the same sentence does not necesarily mean that this sentence contains linguistic indicator of the HasSpouse relation. The hope of distant supervision is that, statistically speaking, most distantly generated training examples are correct. As we will see later in Chapter 3, DeepDive provides a way for the user to write distant supervision rules as relational mappings.

Iterative Refinement As the reader might already notice, all of the above three operations do not necessarily produce completely correct data. In the meantime, we observe that KBC systems built

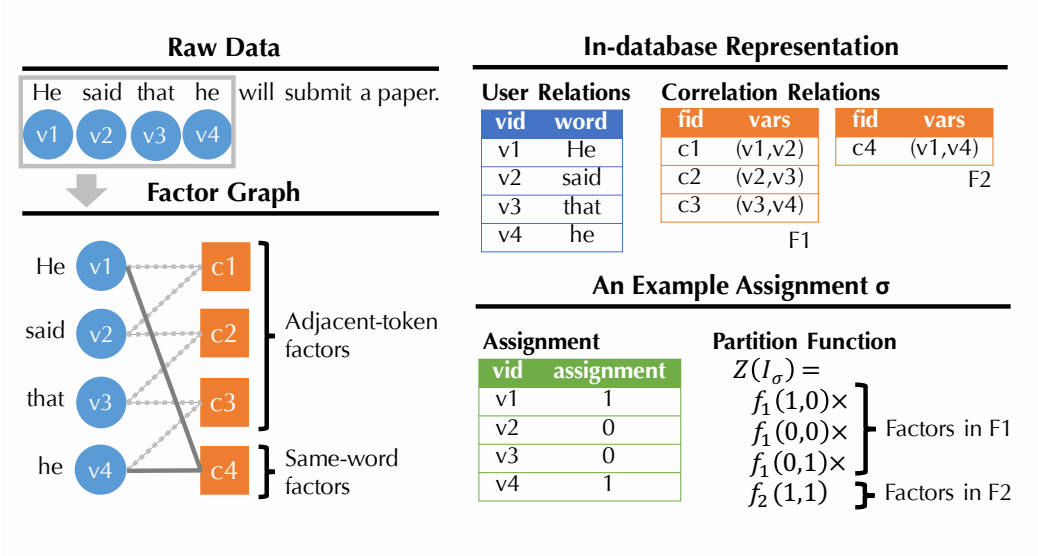

Figure 2.3: An example factor graph that represents a simplified skip-chain CRF; more sophisticated versions of this model are used in named-entity recognition and parsing. There is one user relation containing all tokens, and there are two correlation relations for adjacent-token correlation (F1) and same-word correlation (F2) respectively. The factor function associated to F1 (resp. F2), called f_1 (resp. f_2), is stored in a manner similar to a user-defined function.

with DeepDive achieves higher than 95% accuracy, sometimes even higher than human experts on the same task, with these imperfect data. These two facts together might look counter-intuitive – *How can a system make accurate predictions with less accurate data?*

Part of this is achieved by iteratively improving the above three phases by the user of DeepDive to eliminate noise that matters. For example, the user might look at the errors made by a KBC system, and refine her feature extractors, domain knowledge, or ways of generating distantly supervised training examples. As we will see later in Chapter 3, DeepDive provides a concrete protocol for the user to follow in this iterative refinement process. It also provides different ways for the user to diagnose different reasons of errors made in a KBC system.

2.2 Factor Graphs

As we will see later in Chapter 3, DeepDive heavily relies on factor graphs, one type of probabilistic graphical models, for its statistical inference and learning phase. We present preliminaries on factor graphs, and the inference and learning operations over factor graphs.

Factor graphs have been used to model complex correlations among random variables for decades [188], and have recently been adopted as one underlying representation for probabilistic databases [165, 189, 194]. In this work, we describe factor graph following the line of work of probabilistic databases; and the reader can find other types of formalization in classic textbooks [111, 188]. We first describe the definition of a factor graph, and then how to do inference and learning over factor graphs with Gibbs sampling.

2.2.1 Factor Graphs

A key principle of factor graphs is that random variables should be separated from the correlation structure. Following this principle, we define a probabilistic database to be $\mathcal{D} = (\mathcal{R}, \mathcal{F})$, where $\mathcal{R}$ is called the *user schema* and $\mathcal{F}$ is called the *correlation schema*. Relations in the user schema (resp. correlation schema) are called *user relations* (resp. *correlation relations*). A user's application interacts with the user schema, while the correlation schema captures correlations among tuples in the user schema. Figure 2.3 gives a schematic view of the concepts in this section.

User Schema Each tuple in a user relation $R_i \in \mathcal{R}$ has a unique tuple ID, which takes values from a *variable ID domain* $\mathbb{D}$, and is associated with a random variable[2] taking values from a *variable value domain* $\mathbb{V}$. We assume that $\mathbb{V}$ is Boolean. For some random variables, their value may be fixed as input, and we call these variables *evidence variables*. We denote the set of positive evidence variables as $\mathbb{P} \subseteq \mathbb{D}$, and the set of negative evidence variables as $\mathbb{N} \subseteq \mathbb{D}$. Each distinct *variable assignment* $\sigma : \mathbb{D} \mapsto \mathbb{V}$ defines a *possible world* I_σ that is equivalent to a standard database instantiation of the user schema. We say a variable assignment is *consistent* with $\mathbb{P}$ and $\mathbb{N}$ if it assigns True for all variables in $\mathbb{P}$ and False for all variables in $\mathbb{N}$. Let $\mathcal{I}$ be the set of all possible worlds, and $\mathcal{I}_e$ be the set of all possible worlds that are consistent with evidence $\mathbb{P}$ and $\mathbb{N}$.

Correlation Schema The correlation schema defines a probability distribution over the possible worlds as follows. Intuitively, each correlation relation $F_j \in \mathcal{F}$ represents one type of correlation over the random variables in $\mathbb{D}$ by specifying *which* variables are correlated and *how* they are correlated. To specify *which*, the schema of F_j has the form $F_j(\underline{fid}, \bar{v})$ where fid is a unique factor ID taking values from a *factor ID domain* $\mathbb{F}$, and $\bar{v} \in \mathbb{D}^{a_j}$ where a_j is the number of random variables that

[2]Either modeling the existence of a tuple (for Boolean variables) or in the form of a special attribute of R_i.

are correlated by each factor.[3] In Figure 2.3, variables v_1 and v_4 are correlated. To specify *how*, F_j is associated with a function $f_j : \mathbb{V}^{a_j} \mapsto \mathbb{R}$ and a real-number weight w_j. Given a possible world I_σ, for any $t = (fid, v_1, \ldots, v_{a_j}) \in F_j$, define $g_j(t, I_\sigma) = w_j f_j(\sigma(v_1), \ldots, \sigma(v_{a_j}))$. Define vars$(fid) = \{v_1, \ldots, v_{a_j}\}$. To explain independence in the graph, we need the notion of the *Markov blanket* [146, 188] of a variable v, denoted $\mathbf{mb}(v)$, and defined to be

$$\mathbf{mb}(v_i) = \{v \mid v \neq v_i,\ \exists fid \in \mathbb{F} \text{ s.t. } \{v, v_i\} \subseteq \text{vars}(fid)\}.$$

In Figure 2.3, $\mathbf{mb}(v_1) = \{v_2, v_4\}$. In general, a variable v is conditionally independent of a variable $v' \notin \mathbf{mb}(v)$ given $\mathbf{mb}(v)$. Here, v_1 is independent of v_3 given $\{v_2, v_4\}$.

Probability Distribution Given $\mathcal{I}$, the set of all possible worlds, we define the *partition function* $Z : \mathcal{I} \mapsto \mathbb{R}_+$ over any possible world $I \in \mathcal{I}$ as

$$Z(I) = \exp\left\{\sum_{F_j \in \mathcal{F}} \sum_{t \in F_j} g_j(t, I)\right\} \tag{2.1}$$

The probability of a possible world $I \in \mathcal{I}$ is

$$\Pr[I] = Z(I)\left(\sum_{J \in \mathcal{I}} Z(J)\right)^{-1}. \tag{2.2}$$

It is well known that this representation can encode all discrete distributions over possible worlds [24].

2.2.2 Inference and Query Answering

In a factor graph, which defines a probability distribution, (marginal) *inference* refers to the process of computing the probability that a random variable will take a particular value. Marginal inference on factor graphs is a powerful framework. For each variable v_i, let $\mathcal{I}_e^+$ be all possible worlds consistent with evidences in which v_i is assigned to True and $\mathcal{I}_e^-$ be all possible worlds consistent with evidences in which v_i is assigned to False, the marginal probability of v_i is defined as

$$\Pr[v_i] = \frac{\sum_{I \in \mathcal{I}_e^+} Z(I)}{\sum_{I \in \mathcal{I}_e^+} Z(I) + \sum_{I \in \mathcal{I}_e^-} Z(I)}$$

[3] Our representation supports factors with varying arity as well, but we focus on fixed-arity factors for simplicity.

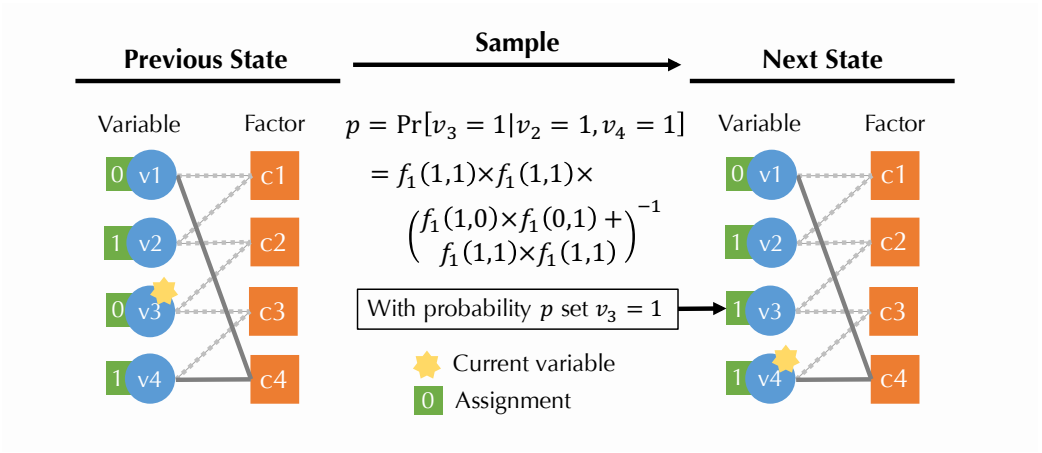

Figure 2.4: A step of Gibbs sampling. To sample a variable v_3, we read the current values of variables in $\mathbf{mb}(v_3) = \{v_2, v_4\}$ and calculate the conditional probability $\Pr[v_3|v_2, v_4]$. Here, the sample result is $v_3 = 1$. We update the value of v_3 and then proceed to sample v_4.

Gibbs Sampling As exact inference for factor graphs is well-known to be intractable [146, 188], a commonly used inference approach is to sample, and then use the samples to compute the marginal probabilities of random variables (e.g., by averaging the outcomes). The main idea of Gibbs sampling is as follows. We start with a random possible world I_0. For each variable $v \in \mathbb{D}$, we sample a new value of v according to the conditional probability $\Pr[v|\mathbf{mb}(v)]$. A routine calculation shows that computing this probability requires that we retrieve the assignment to the variables in $\mathbf{mb}(v)$ and the factor functions associated with the factor nodes that neighbor v. Then we update v in I_0 to the new value. After scanning all variables, we obtain a first sample I_1. We repeat this to get I_{k+1} from I_k.

Example 2.3. *We continue our example (see Figure 2.3) of skip-chain conditional random field [182], a type of factor graphs used in named-entity recognition [74]. Figure 2.4 illustrates one step in Gibbs sampling to update a single variable, v_3: we compute the probability distribution over v_3 by retrieving factors c_2 and c_3, which determines $\mathbf{mb}(v_3)$. Then, we find the values of v_2 and v_4. Using Equation 2.2, one can check that the probability that $v_3 = 1$ is given by the equation in Figure 2.4 (conditioned on $\mathbf{mb}(v_3)$, the remaining factors cancel out).*

There are several popular optimization techniques for Gibbs sampling. One class of techniques improves the sample quality, e.g., *burn-in*, in which we discard the first few samples, and *thinning*, in which we retain every k^{th} sample for some integer k [15]. A second class of techniques improves throughput using parallelism. The key observation is that variables that do not share factors may be

sampled independently and so in parallel [197]. These techniques are essentially orthogonal to our contributions, and we do not discuss them further in this dissertation.

2.2.3 Weight Learning

Another operation over factor graph is to learn the weight associated with each factor. Given the set of possible worlds that are consistent with evidences $\mathcal{I}_e$, weight learning tries to find the weight that maximizes the probability of these possible worlds

$$\arg\max_{w_j} \frac{\sum_{I \in \mathcal{I}_e} Z(I)}{\sum_{I \in \mathcal{I}} Z(I)}$$

There are different ways of solving this optimization problem, and they are out of the scope of this dissertation. In DeepDive, we follow the standard procedure of stochastic gradient descent and estimate the gradient with samples draw with Gibbs sampling [111, 188].

2.2.4 Discussion

In DeepDive, the default algorithm implemented for inference and learning is Gibbs sampling and stochastic gradient descent. However, there are many other well-studied approaches that can be used to solve the problem of inference and learning over factor graphs, e.g., junction trees [111], log-determinant relaxation [187], or belief propagation [188], etc. In principle, these approaches could be implemented and plug in directly into DeepDive just as different solvers. We do not discuss them in this dissertation because they are orthogonal to the contributions of DeepDive.

3. The DeepDive Framework

> *The world that I was programming in back then has passed, and the goal now is for things to be easy, self-managing, self-organizing, self-healing, and mindless. Performance is not an issue. Simplicity is a big issue.*
>
> — Jim Gray, *An Interview by Marianne Winslett, 2002*

In this chapter, we present DeepDive, a data management system built to support the KBC workload as described in Chapter 2.1. The goal of DeepDive is to provide a simple, but flexible, framework for domain experts to deal with diverse types of data and integrate domain knowledge. This chapter is organized as follows:

1. **DeepDive Program.** We describe *DeepDive program*, the program that the user writes to build a KBC system. A DeepDive program allows the user to specify features, domain knowledge, and distant supervision, all in an unified framework.

2. **Semantic and Execution of DeepDive Programs.** Given a DeepDive program, we define its semantics and how it is executed in DeepDive.

3. **Debugging a DeepDive Program.** Building a KBC system is an iterative process, and we describe a concrete protocol that the user can follow to improve a KBC system via repeated error analysis.

In this chapter, our focus is to define at a high level how DeepDive supports the KBC workload, and how a real KBC system is built with DeepDive. We do not discuss the specific techniques that make the execution and debugging of DeepDive programs performant and scalable, which will be the topics of Chapter 5 and Chapter 6.

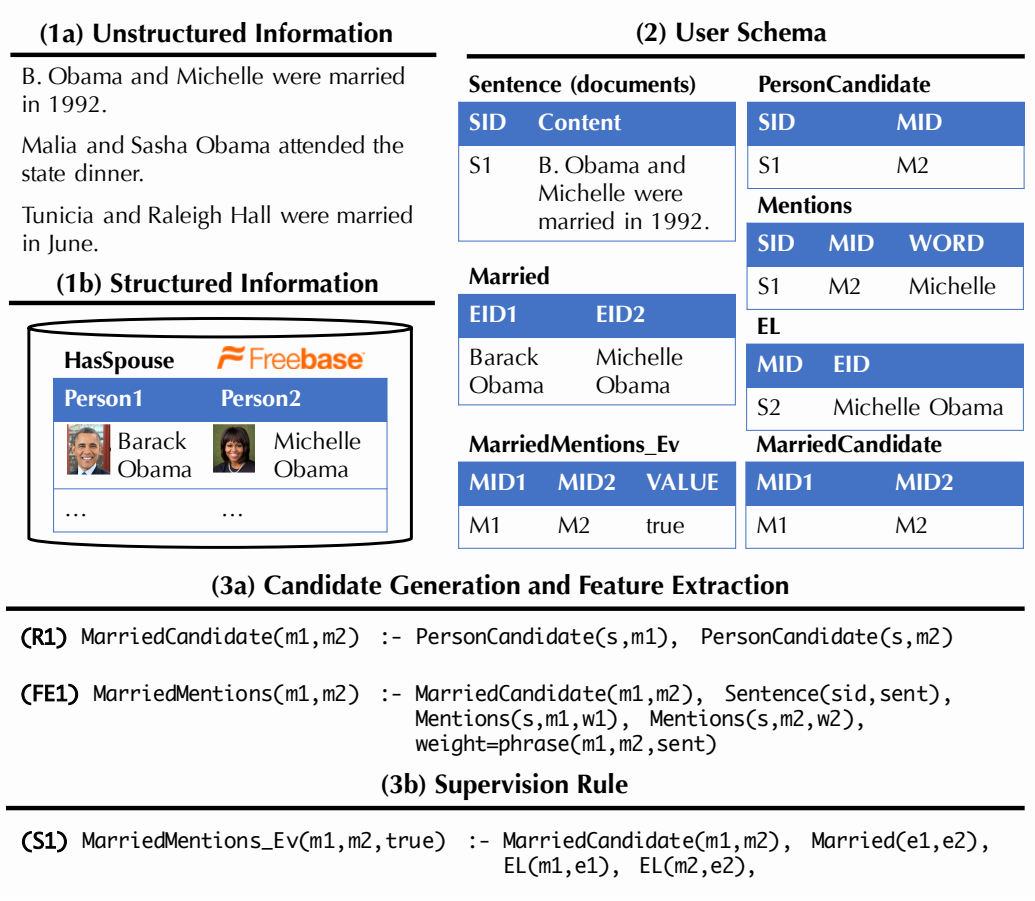

Figure 3.1: An example DeepDive program for a KBC system.

3.1 A DeepDive Program

DeepDive is an end-to-end framework for building KBC systems, as shown in Figure 3.2.[1] We walk through each phase. DeepDive supports both SQL and Datalog, but we use Datalog syntax for exposition. The rules we describe in this section are manually created by the user of DeepDive and the process of creating these rules is application-specific.

Candidate Generation and Feature Extraction All data in DeepDive is stored in a relational database. The first phase populates the database using a set of SQL queries and user-defined functions (UDFs) that we call *feature extractors*. By default, DeepDive stores all documents in the database in one sentence per row with markup produced by standard NLP pre-processing tools, including HTML

[1]For more information, including examples, please see `http://deepdive.stanford.edu`. Note that our engine is built on Postgres and Greenplum for all SQL processing and UDFs. There is also a port to MySQL.

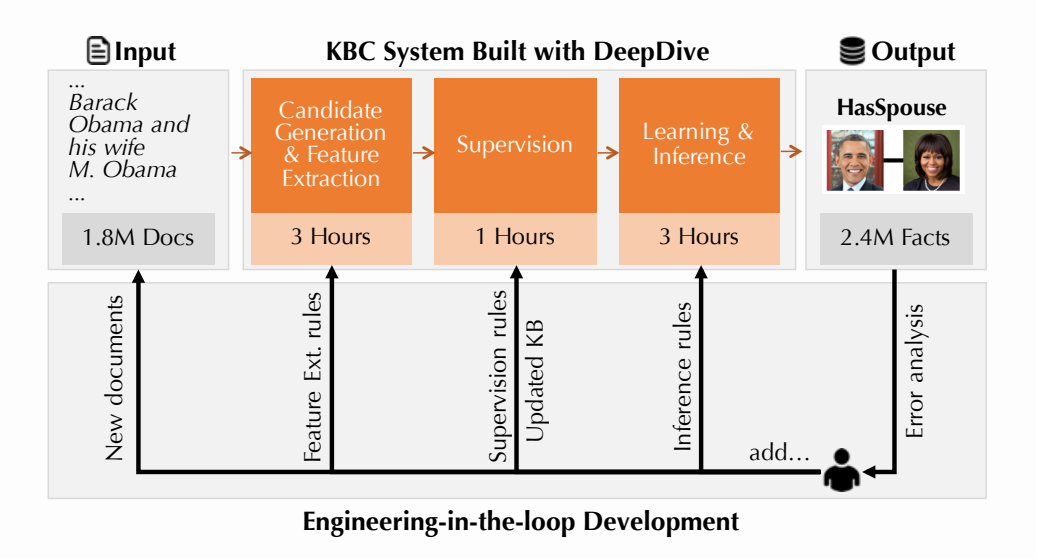

Figure 3.2: A KBC system takes as input unstructured documents and outputs a structured knowledge base. The runtimes are for the TAC-KBP competition system (News). To improve quality, the developer adds new rules and new data.

stripping, part-of-speech tagging, and linguistic parsing. After this loading step, DeepDive executes two types of queries: (1) *candidate mappings*, which are SQL queries that produce possible mentions, entities, and relations, and (2) *feature extractors* that associate features to candidates, e.g., "... and his wife ..." in Example 2.1.

Example 3.1. *Candidate mappings are usually simple. Here, we create a relation mention for every pair of candidate persons in the same sentence (s):*

$$\texttt{(R1)}\ \texttt{MarriedCandidate}(m1, m2)\texttt{:-}$$
$$\texttt{PersonCandidate}(s, m1), \texttt{PersonCandidate}(s, m2).$$

Candidate mappings are simply SQL queries with UDFs.[2] Such rules must be high recall: if the union of candidate mappings misses a fact, DeepDive has no chance to extract it.

We also need to extract features, and we extend classical Markov Logic in two ways: (1) user-defined functions and (2) weight tying, which we illustrate by example.

Example 3.2. *Suppose that* $\mathsf{phrase}(m1, m2, sent)$ *returns the phrase between two mentions in the*

[2]These SQL queries are similar to low-precision but high-recall ETL scripts.

sentence, e.g., "and his wife" in the above example. The phrase between two mentions may indicate whether two people are married. We would write this as:

$$\begin{aligned}(FE1)\ \ & \texttt{MarriedMentions}(m1, m2) :\text{-} \\ & \texttt{MarriedCandidate}(m1, m2), \texttt{Mention}(sid, m1), \\ & \texttt{Mention}(sid, m2), \texttt{Sentence}(sid, sent) \\ & weight = \mathsf{phrase}(m1, m2, sent).\end{aligned}$$

One can think about this like a classifier: This rule says that whether the text indicates that the mentions $m1$ *and* $m2$ *are married is* influenced *by the phrase between those mention pairs. The system will infer based on training data its confidence (by estimating the weight) that two mentions are indeed indicated to be married.*

Technically, phrase returns an identifier that determines which weights should be used for a given relation mention in a sentence. If phrase returns the same result for two relation mentions, they receive the *same* weight. We explain weight tying in more detail later. In general, phrase could be an arbitrary UDF that operates in a per-tuple fashion. This allows DeepDive to support common examples of features such as "bag-of-words" to context-aware NLP features to highly domain-specific dictionaries and ontologies. In addition to specifying sets of classifiers, DeepDive inherits Markov Logic's ability to specify rich correlations between entities via weighted rules. Such rules are particularly helpful for data cleaning and data integration.

Supervision DeepDive can use training data or evidence about any relation; in particular, each user relation is associated with an evidence relation with the same schema and an additional field that indicates whether the entry is true or false. Continuing our example, the evidence relation $MarriedMentions\_Ev$ could contain mention pairs with positive and negative labels. Operationally, two standard techniques generate training data: (1) hand-labeling, and (2) *distant supervision*, which we illustrate below.

Example 3.3. Distant supervision *[61, 96, 131] is a popular technique to create evidence in KBC systems. The idea is to use an incomplete KB of married entity pairs to* heuristically *label (as* `True` *evidence) all*

relation mentions that link to a pair of married entities:

$$\textit{(S1)}\ \texttt{MarriedMentions\_Ev}(m1, m2, true)\text{ :-}$$
$$\texttt{MarriedCandidates}(m1, m2), \texttt{EL}(m1, e1),$$
$$\texttt{EL}(m2, e2), \texttt{Married}(e1, e2).$$

Here, `Married` is an (incomplete) list of married real-world persons that we wish to extend. The relation EL is for "entity linking" that maps mentions to their candidate entities. At first blush, this rule seems incorrect. However, it generates noisy, imperfect examples of sentences that indicate two people are married. Machine learning techniques are able to exploit redundancy to cope with the noise and learn the relevant phrases (e.g., "and his wife"). Negative examples are generated by relations that are largely disjoint (e.g., siblings). Similar to DIPRE [41] and Hearst patterns [92], distant supervision exploits the "duality" [41] between patterns and relation instances; furthermore, it allows us to integrate this idea into DeepDive's unified probabilistic framework.

Learning and Inference In the learning and inference phase, DeepDive generates a factor graph. The inference and learning are done using standard techniques (Gibbs Sampling).

Error Analysis DeepDive runs the above three phases in sequence, and at the end of the learning and inference, it obtains a marginal probability p for each candidate fact. To produce the final KB, the user often selects facts in which we are highly confident, e.g., $p > 0.95$. Typically, the user needs to inspect errors and repeat, a process that we call *error analysis*. Error analysis is the process of understanding the most common mistakes (incorrect extractions, too-specific features, candidate mistakes, etc.) and deciding how to correct them [157]. To facilitate error analysis, users write standard SQL queries. The concrete procedure of doing error analysis is the focus of Section 3.3.

3.2 Semantics of a DeepDive Program

A DeepDive program is a set of rules with weights. During inference, the values of all weights w are assumed to be known, while, in learning, one finds the set of weights that maximizes the probability of the evidence. As shown in Figure 3.3, a DeepDive program defines a factor graph. First, we directly

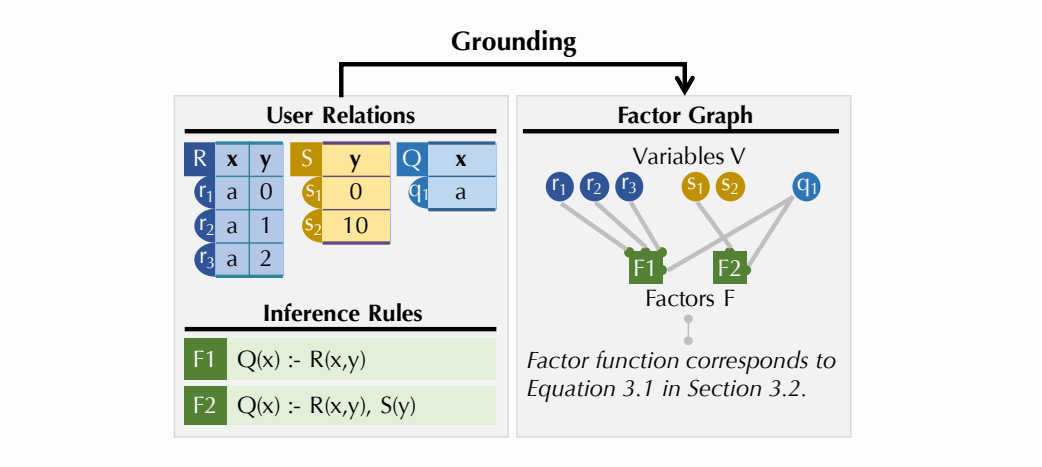

Figure 3.3: Schematic illustration of grounding. Each tuple corresponds to a Boolean random variable and node in the factor graph. We create one factor for every set of groundings.

define the probability distribution for rules that involve weights, as it may help clarify our motivation. Then, we describe the corresponding factor graph on which inference takes place.

Each possible tuple in the user schema–both IDB and EDB predicates–defines a Boolean random variable (r.v.). Let $\mathbb{V}$ be the set of these r.v.'s. Some of the r.v.'s are fixed to a specific value, e.g., as specified in a supervision rule or by training data. Thus, $\mathbb{V}$ has two parts: a set $\mathcal{E}$ of *evidence* variables (those fixed to a specific values) and a set $\mathcal{Q}$ of *query* variables whose value the system will infer. The class of evidence variables is further split into *positive evidence* and *negative evidence*. We denote the set of positive evidence variables as $\mathcal{P}$, and the set of negative evidence variables as $\mathcal{N}$. An assignment to each of the query variables yields a *possible world* I that must contain all positive evidence variables, i.e., $I \supseteq \mathcal{P}$, and must not contain any negatives, i.e., $I \cap \mathcal{N} = \emptyset$.

Boolean Rules We first present the semantics of *Boolean* inference rules. For ease of exposition only, we assume that there is a single domain $\mathbb{D}$. A rule γ is a pair (q, w) such that q is a Boolean query and w is a real number. An example is as follows:

$$q() :\text{-}\ R(x, y), S(y) \quad weight = w.$$

We denote the body predicates of q as $body(\bar{z})$ where $\bar{z}$ are all variables in the body of $q()$, e.g., $\bar{z} = (x, y)$ in the example above. Given a rule $\gamma = (q, w)$ and a possible world I, we define the *sign of*

Semantics	$g(n)$
Linear	n
Ratio	$\log(1+n)$
Logical	$\mathbb{I}_{\{n>0\}}$

Table 3.1: Semantics for g in Equation 3.1.

γ *on* I as $\mathsf{sign}(\gamma, I) = 1$ if $q() \in I$ and -1 otherwise.

Given $\bar{c} \in \mathbb{D}^{|\bar{z}|}$, a *grounding* of q w.r.t. $\bar{c}$ is a substitution $body(\bar{z}/\bar{c})$, where the variables in $\bar{z}$ are replaced with the values in $\bar{c}$. For example, for q above with $\bar{c} = (a, b)$ then $body(\bar{z}/(a, b))$ yields the grounding $R(a, b), S(b)$, which is a conjunction of facts. The *support* $\mathsf{n}(\gamma, I)$ of a rule γ in a possible world I is the number of groundings $\bar{c}$ for which $body(\bar{z}/\bar{c})$ is satisfied in I:

$$\mathsf{n}(\gamma, I) = |\{\bar{c} \in \mathbb{D}^{|\bar{z}|} \ : \ I \models body(\bar{z}/\bar{c}) \ \}|$$

The *weight of* γ *in* I is the product of three terms:

$$\mathsf{w}(\gamma, I) = w \ \mathsf{sign}(\gamma, I) \ g(\mathsf{n}(\gamma, I)), \tag{3.1}$$

where g is a real-valued function defined on the natural numbers. For intuition, if $w(\gamma, I) > 0$, it adds a weight that indicates that the world is more likely. If $w(\gamma, I) < 0$, it indicates that the world is less likely. As motivated above, we introduce g to support multiple semantics. Table 3.1 shows choices for g that are supported by DeepDive, which we compare in an example below.

Let Γ be a set of Boolean rules, the weight of Γ on a possible world I is defined as

$$\mathsf{W}(\Gamma, I) = \sum_{\gamma \in \Gamma} \mathsf{w}(\gamma, I).$$

This function allow us to define a probability distribution over the set J of possible worlds:

$$\Pr[I] = \mathsf{Z}^{-1} \exp(\mathsf{W}(\Gamma, I)) \text{ where } \mathsf{Z} = \sum_{I \in J} \exp(\mathsf{W}(\Gamma, I)), \tag{3.2}$$

and Z is called the *partition function*. This framework is able to compactly specify much more sophisticated distributions than traditional probabilistic databases [180].

Example 3.4. *We illustrate the semantics by example. From the Web, we could extract a set of relation mentions that supports* "Barack Obama was born in Hawaii" *and another set of relation mentions that support* "Barack Obama was born in Kenya." *These relation mentions provide conflicting information, and one common approach is to "vote." We abstract this as up or down votes about a fact* $q()$.

$$q() \text{ :- } Up(x) \qquad weight = 1.$$

$$q() \text{ :- } Down(x) \qquad weight = -1.$$

We can think of this as a having a single random variable $q()$ *in which the size of* Up *(resp.* $Down$*) is an evidence relation that indicates the number of "Up" (resp. "Down") votes. There are only two possible worlds: one in which* $q() \in I$ *(is true) and not. Let* $|Up|$ *and* $|Down|$ *be the sizes of* Up *and* $Down$*. Following Equation 3.1 and 3.2, we have*

$$\Pr[q()] = \frac{e^W}{e^{-W} + e^W}$$

where

$$W = g(|Up|) - g(|Down|).$$

Consider the case when $|Up| = 10^6$ *and* $|Down| = 10^6 - 100$*. In some scenarios, this small number of differing votes could be due to random noise in the data collection processes. One would expect a probability for* $q()$ *close to* 0.5*. In the linear semantics* $g(n) = n$*, the probability of* q *is* $(1 + e^{-200})^{-1} \approx 1 - e^{-200}$*, which is extremely close to* 1*. In contrast, if we set* $g(n) = \log(1 + n)$*, then* $\Pr[q()] \approx 0.5$*. Intuitively, the probability depends on their* ratio *of these votes. The* logical *semantics* $g(n) = \mathbb{1}_{n>0}$ *gives exactly* $\Pr[q()] = 0.5$*. However, it would do the same if* $|Down| = 1$*. Thus, logical semantics may ignore the strength of the voting information. At a high level, ratio semantics can learn weights from examples with different raw counts but similar ratios. In contrast, linear is appropriate when the raw counts themselves are meaningful.*

No semantic subsumes the other, and each is appropriate in some application. We have found that in many cases the ratio semantics is more suitable for the application that the user wants to model. Intuitively, sampling converges faster in the logical or ratio semantics because the distribution is less sharply peaked, which means that the sampler is less likely to get stuck in local minima.

Extension to General Rules. Consider a general inference rule $\gamma = (q, w)$, written as:

$$q(\bar{y}) \text{ :- } body(\bar{z}) \quad \text{weight} = w(\bar{x}).$$

where $\bar{x} \subseteq \bar{z}$ and $\bar{y} \subseteq \bar{z}$. This extension allows *weight tying*. Given $\bar{b} \in \mathbb{D}^{|\bar{x} \cup \bar{y}|}$ where $\bar{b}_x$ (resp. $\bar{b}_y$) are the values of $\bar{b}$ in $\bar{x}$ (resp. $\bar{y}$), we expand γ to a set Γ of Boolean rules by substituting $\bar{x} \cup \bar{y}$ with values from $\mathbb{D}$ in all possible ways.

$$\Gamma = \{(q_{\bar{b}_y}, w_{\bar{b}_x}) \mid q_{\bar{b}_y}() \text{ :- } body(\bar{z}/\bar{b}) \text{ and } w_{\bar{b}_x} = w(\bar{x}/\bar{b}_x)\}$$

where each $q_{\bar{b}_y}()$ is a *fresh* symbol for distinct values of $\bar{b}_t$, and $w_{\bar{b}_x}$ is a real number. Rules created this way may have free variables in their bodies, e.g., $q(x)$:- $R(x, y, z)$ with $w(y)$ create $|\mathbb{D}|^2$ different rules of the form $q_a()$:- $R(a, b, z)$, one for each $(a, b) \in \mathbb{D}^2$, and rules created with the same value of b share the same weight. Tying weights allows one to create models succinctly.

Example 3.5. *We use the following as an example:*

$$Class(x) \text{ :- } R(x, f) \quad weight = w(f).$$

This declares a binary classifier as follows. Each binding for x is an object to classify as in $Class$ or not. The relation R associates each object to its features. E.g., $R(a, f)$ indicates that object a has a feature f. $weight = w(f)$ indicates that weights are functions of feature f; thus, the same weights are tied across values for a. This rule declares a logistic regression classifier.

It is straightforward formal extension to let weights be functions of the return values of UDFs as we do in DeepDive.

3.2.1 Inference on Factor Graphs

As in Figure 3.3, DeepDive explicitly constructs a factor graph for inference and learning using a set of SQL queries. Recall that a factor graph is a triple $(V, F, \hat{w})$ in which V is a set of nodes that correspond to Boolean random variables, F is a set of hyperedges (for $f \in F$, $f \subseteq V$), and $\hat{w} : F \times \{0, 1\}^V \to \mathbb{R}$ is a weight function. We can identify possible worlds with assignments since each node corresponds

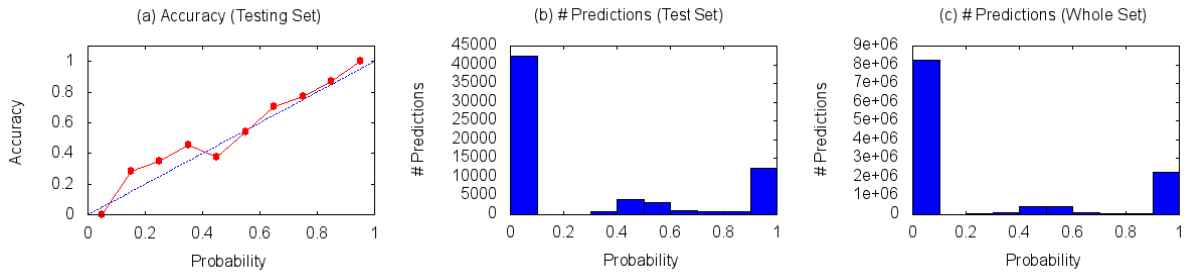

Figure 3.4: Illustration of calibration plots automatically generated by DeepDive.

to a tuple; moreover, in DeepDive, each hyperedge f corresponds to the set of groundings for a rule γ. In DeepDive, V and F are explicitly created using a set of SQL queries. These data structures are then passed to the sampler, which runs outside the database, to estimate the marginal probability of each node or tuple in the database. Each tuple is then reloaded into the database with its marginal probability.

Example 3.6. *Take the database instances and rules in Figure 3.3 as an example, each tuple in relation R, S, and Q is a random variable, and V contains all random variables. The inference rules $F1$ and $F2$ ground factors with the same name in the factor graph as illustrated in Figure 3.3. Both $F1$ and $F2$ are implemented as SQL in DeepDive.*

To define the semantics, we use Equation 3.1 to define $\hat{w}(f, I) = w(\gamma, I)$, in which γ is the rule corresponding to f. As before, we define $\hat{W}(F, I) = \sum_{f \in F} \hat{w}(f, I)$, and then the probability of a possible world is the following function:

$$\Pr[I] = Z^{-1} \exp\left\{\hat{W}(F, I)\right\} \text{ where } Z = \sum_{I \in J} \exp\{\hat{W}(F, I)\}$$

The main task that DeepDive conducts on factor graphs is statistical inference, i.e., for a given node, what is the marginal probability that this node takes the value 1? Since a node takes value 1 when a tuple is in the output, this process computes the marginal probability values returned to users. In general, computing these marginal probabilities is ♯P-hard [188]. Like many other systems, DeepDive uses Gibbs sampling to estimate the marginal probability of every tuple in the database.

3.3 Debugging and Improving a KBC System

A DeepDive system is only as good as its features, rules, and the quality of data sources. We found in our experience that understanding which features to add is the most critical—but often the most overlooked—step in the process. Without a systematic analysis of the errors of the system, developers often add rules that do not significantly improve their KBC system, and they settle for suboptimal quality. In this section, we describe our process of error analysis, which we decompose into two stages: a macro-error analysis that is used to guard against statistical errors and gives an at-a-glance description of the system and a fine-grained error analysis that actually results in new features and code being added to the system.

3.3.1 Macro Error Analysis: Calibration Plots

In DeepDive, *calibration plots* are used to summarize the overall quality of the KBC results. Because DeepDive uses a joint probability model, each random variable is assigned a marginal probability. Ideally, if one takes all the facts to which DeepDive assigns a probability score of 0.95, then 95% of these facts are correct. We believe that probabilities remove a key element: the developer reasons about features, not the algorithms underneath. This is a type of *algorithm independence* that we believe is critical.

DeepDive programs define one or more test sets for each relation, which are essentially a set of labeled data for that particular relation. This set is used to produce a calibration plot. Figure 3.4 shows an example calibration plot for the Formation-Time relation for the paleontology application, which provides an aggregated view of how the KBC system behaves. By reading each of the subplots, we can get a rough assessment of the next step to improve our KBC system. We explain each component below.

As shown in Figure 3.4, a calibration plot contains three components: (a) accuracy, (b) # predictions (test set), which measures the number of extractions in the test set with a certain probability; and (c) # predictions (whole set), which measures the number of extractions in the whole set with a certain probability. The test set is assumed to have labels so that we can measure accuracy, while the whole set does not.

(a) Accuracy. To create the accuracy histogram, we bin each fact extracted by DeepDive on the test set by the probability score assigned to each fact; e.g., we round to the nearest value in the set $k/10$ for $k = 1, \ldots, 10$. For each bin, we compute the fraction of those predictions that is correct. Ideally, this line would be on the (0,0)-(1,1) line, which means that the DeepDive-produced probability value is calibrated, i.e., it matches the *test-set accuracy*. For example, Figure 3.4(a) shows a curve for calibration. Differences in these two lines can be caused by noise in the training data, quantization error due to binning, sparsity in the training data, or overfitting in the learning algorithms.

(b) # Predictions (Testing Set). We also create a histogram of the number of predictions in each bin. In a well-tuned system, the # Predictions histogram should have a "U" shape. That is, most of the extractions are concentrated at high probability and low probability. We do want a number of low-probability events, as this indicates DeepDive is considering plausible but ultimately incorrect alternatives. Figure 3.4(b) shows a U-shaped curve with some masses around 0.5-0.6. Intuitively, this suggests that there is some hidden type of example for which the system has insufficient features. More generally, facts that fall into bins that are not in (0,0.1) or (0.9,1.0) are candidates for improvements, and one goal of improving a KBC system is to "push" these probabilities into either (0,0.1) or (0.9,1.0). To do this, we may want to sample from these examples and add more features to resolve this uncertainty.

(c) # Predictions (Whole Set). The final histogram is similar to Figure 3.4(b), but illustrates the behavior of the system, for which we do not necessarily have any training examples (generated by human labelling and/or distant supervision). We can visually inspect that Figure 3.4(c) has a similar shape to (b); If not, this would suggest possible overfitting or some bias in the selection of the hold-out set.

3.3.2 Micro Error Analysis: Per-Example Analysis

Calibration plots provide a high-level summary of the quality of a KBC system, from which developers can get an abstract sense of how to improve it. For developers to produce rules that can improve the system, they need to actually look at data. We describe this fine-grained error analysis.

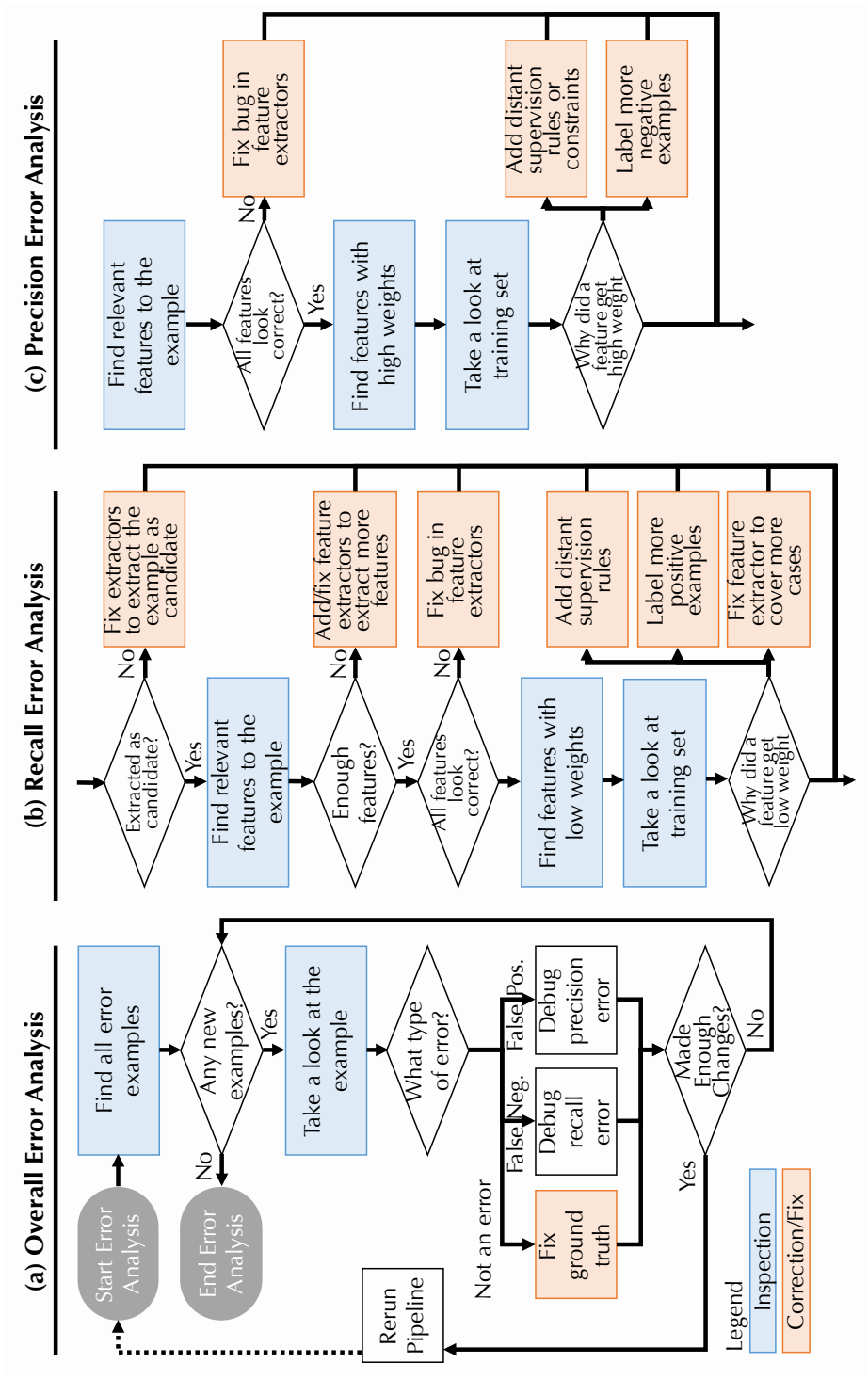

Figure 3.5: Error analysis workflow of DeepDive.

Figure 3.5(a) illustrates the overall workflow of error analysis. The process usually starts with the developer finding a set of errors, which is a set of random variables having predictions that are inconsistent with the training data. Then, for each random variable, the developer looks at the corresponding tuples in the user relation (recall that each tuple in the user relation corresponds to a random variable) and tries to identify the types of errors. We describe two broad classes of errors that we think of as improving the recall and the precision, which we describe below.

Recall Error Analysis. A recall error, i.e., a false negative error, occurs when DeepDive is expected to extract a fact but fails to do so. In DeepDive's data model, this usually means that a random variable has a low probability or that the corresponding fact is not extracted as a candidate. Figure 3.5(b) illustrates the process of debugging a recall error.

First, it is possible that the corresponding fact that is expected to be extracted does not appear as a candidate. In this case, there is no random variable associated with this fact, so it is impossible for DeepDive to extract it. For example, this case might happen when the corresponding fact appears in tables, but we only have a text-based extractor. In this case, the developer needs to write extractors to extract these facts as candidates.

Another common scenario is when the corresponding fact appears as a candidate but is not assigned a high enough probability by DeepDive. In this case, the developer needs to take a series of steps, as shown in Figure 3.5(b), to correct the error. First, it is possible that this candidate is not associated with any features or that the corresponding features have an obvious bug. In this case, one needs to fix the extractors of the features. Second, it is possible that the corresponding features have a relatively low weight learned by DeepDive. In that case, one needs to look at the training data to understand the reason. For example, one might want to add more distant supervision rules to increase the number of positive examples that share the same feature or even manually label more positive examples. One might also want to change the feature extractors to collapse the current features with other features to reduce the sparsity.

Precision Error Analysis. A precision error, i.e., a false positive error, occurs when DeepDive outputs a high probability for a fact, but it is an incorrect one or not supported by the corresponding document. Figure 3.5(c) illustrates the process of debugging a precision error. Similar to debugging recall errors, for precision errors, the developer needs to look at the features associated with the

random variable. The central question to investigate is why some of these features happen to have high weights. In our experience, this usually means that we do not have enough negative examples for training. If this is the case, the developer adds more distant supervision rules or (less commonly) manually labels more negative examples.

Avoiding Overfitting. One possible pitfall for the error analysis at the per-example level is overfitting, in which the rules written by the developer overfit to the corpus or the errors on which the error analysis is conducted. To avoid this problem, we have insisted that all our applications to generate careful held-out sets to produce at least (1) a training set; (2) a testing set; and (3) an error analysis set. In the error analysis process, the developer is only allowed to look at examples in the error analysis set, and validate the score on the testing set.

3.4 Conclusion

In this chapter, we present the abstraction that DeepDive provides to the developer of KBC systems. To build a KBC system with DeepDive, a developer writes a DeepDive program in a high-level declarative language. We described the semantic of a DeepDive program, and a concrete iterative protocol of debugging a DeepDive program to produce KBC systems with higher quality. The ultimate goal of this abstraction is to be flexible and simple such that domain experts can deal with diverse types of data and integrate domain knowledge easily.

4. Applications using DeepDive

It's a little scary, the machines are getting that good.

— Mark Uhen (George Mason University) on PaleoDeepDive*, Nature, 2015*

I think it's one of the best innovations that palaeontology has had in a very long time.

— Jonathan Tennant (Imperial College London) on PaleoDeepDive*, Nature, 2015*

In this chapter, we describe applications that have been built with DeepDive using the framework we discussed in the previous chapter. This chapter is organized in two parts.

1. **PaleoDeepDive.** We describe a KBC system that we built called PaleoDeepDive. The goal is to illustrate in details how DeepDive's framework can be used to build a KBC system and describe an intensive study on the quality of a KBC system built with DeepDive.

2. **TAC-KBP.** We describe a KBC system that we built for the TAC-KBP competition. In contrast to PaleoDeepDive, which is targeted for a specific scientific domain, TAC-KBP is a popular competition that attracts dozens of international teams to compete every year. The goal here is to illustrate that, for this type of public benchmark, KBC systems built with DeepDive also achieve high quality.

Many more KBC systems have been built with DeepDive by the users instead of the developers of DeepDive. For these applications, the domain experts write the DeepDive programs on their own, while the DeepDive team only provides technical support. In this dissertation, we do not describe these works, but interested readers can find an up-to-date subset at the Showcase section on the DeepDive Web site.[1]

[1] `http://deepdive.stanford.edu/doc/showcase/apps.html`

4.1 PaleoDeepdive

We describe PaleoDeepDive as an example of how a KBC system can be built with the DeepDive. In this section, we first describe the use-case of PaleoDeepDive and the scientific questions enabled by PaleoDeepDive; we then describe the relationship between PaleoDeepDive and the DeepDive framework we introduced in previous sections. At the end, we report on intensive study of the quality of PaleoDeepDive.

4.1.1 Motivation and Application

Palaeontology is based on the description and biological classification of fossils, an enterprise that has played out in an untold number of scientific publications over the past four centuries. The construction of synthetic databases that aggregate fossil data in a way that enables large-scale questions to be addressed has expanded the intellectual reach of palaeontology [21, 29, 155, 166] and led to many fundamental new insights into macroevolutionary processes [8, 10, 98, 107] and the timing and nature of biotic responses to global environmental change [35, 76]. Nevertheless, palaeontologists remain data limited, both in terms of the pace of description of new fossils and in terms of their ability to synthesize existing knowledge. Many other sciences, particularly those for which physical samples and specimens are the source of data, face similar challenges.

One of the largest and most successful efforts to compile data on the fossil record to date is the Paleobiology Database (PBDB). Founded nearly two decades ago by a small team of palaeontologists and geoscientists who generated the first sampling-standardized global Phanerozoic biodiversity curves [11,12], the PBDB has since grown to include an international team of more than 300 scientists with diverse research agendas. Collectively, this group has spent nearly 10 continuous person years entering more than 290,000 taxonomic names, 500,000 opinions on the status and classification of those names, and 1.17 million fossil occurrences (i.e., temporally and geographically resolved instances of taxonomically classified fossils). Some data derive from the fieldwork and taxonomic studies of the contributors, but the majority of the data were acquired from some 40,000 publications.

Although the PBDB has enjoyed tremendous scientific success by yielding novel results for more than 200 official publications, the database leverages only a small fraction of all published palaeontological knowledge. One of the principal reasons for sparse representation of many parts of the literature is that there is a vast and ever-growing body of published work, and manually finding

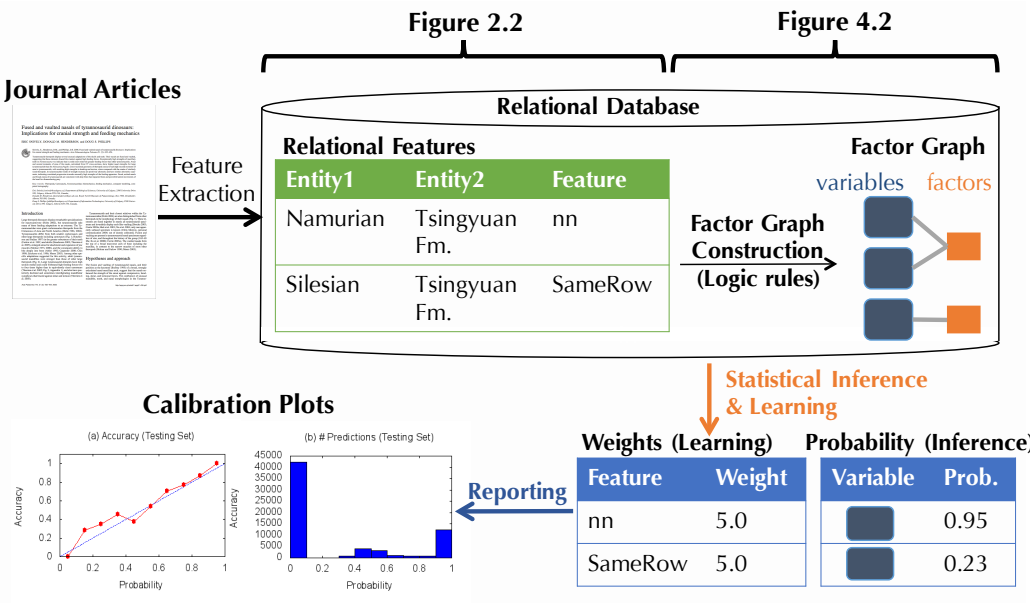

Figure 4.1: Illustration of the PaleoDeepDive workflow. PaleoDeepDive contains two phases: (1) Feature Extraction, and (2) Statistical Inference and Learning. For details of these two phases, see Figure 2.2 and Figure 4.2.

and entering data into the database is labor intensive. Heterogeneous coverage of the literature and incomplete extraction of data can also be attributed to the priorities of individual researchers and to decisions made during database design, which predetermine the types of data that are accommodated. Moreover, because the end product is a list of facts that are divorced from most, if not all, original contexts, assessing the quality of the database and the reproducibility of its results is difficult and has never before been done on a large scale.

This motivated PaleoDeepDive, a statistical machine reading and learning system developed with DeepDive. The goal of PaleoDeepDive is to automatically extract fossil occurrence data from the published literature. PaleoDeepDive's goal is threefold. First, we aim to quantitatively test the reproducibility of the PBDB and key macroevolutionary results that are used to frame much of our understanding of the large-scale history of life. Second, we aim to improve upon previous generation machine reading systems by overcoming challenges posed by ambiguity at a large scale and scope. Third, we aim to develop a system that has the capacity to change the practice of science in many disciplines by removing substantial time and cost barriers to large-scale data synthesis and integration. In so doing, we hope to shift the balance of effort away from data compilation efforts and towards creative hypothesis testing and the more efficient and focused generation of new primary data.

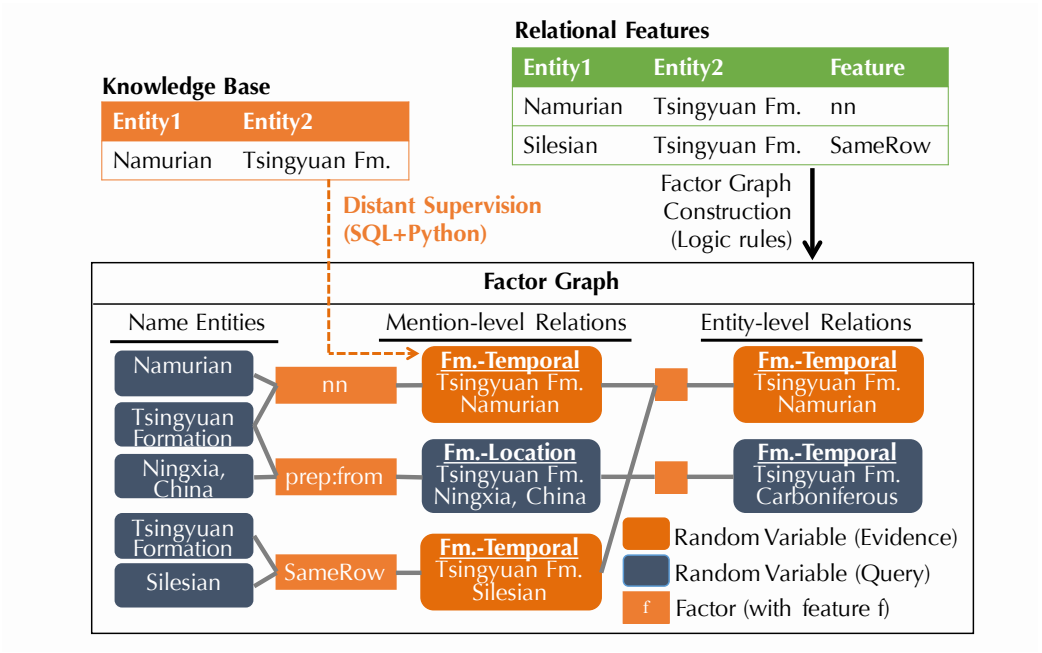

Figure 4.2: Illustration of the PaleoDeepDive workflow: Statistical Inference and Learning.

4.1.2 System Walkthrough

We walk through the PaleoDeepDive system as illustrated in Figure 4.1. The input to PaleoDeepDive is a set of journal articles, e.g., PDF and HTML documents, and an (incomplete) knowledge base that we would like to complete. One prominent feature of PaleoDeepDive is that the PaleoDeepDive approach uses the text, tables, figures, and layout to extract information: We have found that some information that PaleoDeepDive extracts have high quality non-textual feature, e.g., the taxonomy relation heavily relies on layout-based information, e.g., section headers or their layout in tabular data. The output of PaleoDeepDive is a set of tuples with a score. In PaleoDeepDive, the confidence score is the marginal probability that PaleoDeepDive assigns based on its probability model (conditioned on all available evidence). In PaleoDeepDive, we output all facts with the confidence higher than a threshold (say 0.95) to the user. In addition to estimated probabilities, PaleoDeepDive also outputs a real number weight for each feature (defined later), which intuitively specifies how strongly a feature contributes to predictions. These weights help the developer understand what factors the systems estimates are useful in extracting tuples (we define them formally below). PaleoDeepDive also outputs a set of statistics and plots for a developer to debug and improve the current version of PaleoDeepDive as described in Section 3.3.

Layer	Features
Name Entities	Dictionary (English dictionary, GeoNames, PaleoDB, Species2000, etc.) Part-of-speech tag from StanfordCoreNLP Name-entity tag from StanfordCoreNLP Name entity mentions in the same sentences/paragraphs/documents)
Mention-level Relations	Word sequence between name entities Dependency path between name entities Name-entity tag from StanfordCoreNLP Table caption-content association Table cell-header association Section headers (for Taxonomy)
Entity-level Relations	Temporal interval containment (e.g., Namurian $\subseteq$ Carboniferous) Location containment (e.g., Ningxia, China $\subseteq$ China) One formation does not likely span > 200 million years

Table 4.1: List of features and rules used in PaleoDeepDive.

To produce these outputs from the given input, PaleoDeepDive goes through three phases. These three phases are consistent with the DeepDive framework that we described, and we focus on giving concrete examples of these phases.

Feature Extraction In the feature extraction phase, PaleoDeepDive takes PDF documents and an incomplete knowledge base, and produce a *factor graph*. In PaleoDeepDive, all features are encoded as tables in a relational database as shown in Figure 2.2. For example, given the raw input PDF, one extractor that invokes the OCR software will translate the PDF into a set of text snippets, and PaleoDeepDive will store them one per row in a table in the database. Then, one extractor that invokes natural language processing tools, e.g., Stanford CoreNLP, will take as input one text snippet, and outputs a linguistic parse tree. Again, PaleoDeepDive will store each tree per row in another table. These two examples, although simple, are representative of all feature extractors in PaleoDeepDive. A feature extractor in PaleoDeepDive contains two components: (1) one SQL query; and (2) a executable program that takes as input one row in a SQL query, and output a set of rows. By writing a set of feature extractors in this unified representation, PaleoDeepDive is able to produce a set of in-database relations. One can see more examples in Figure 2.2, and Table 4.1 shows the list of features that are used in PaleoDeepDive. The simplicity of these features belies the difficulty in finding the right simple features, which is an iterative process.

Distant Supervision One key challenge of PaleoDeepDive is how to generate training data for learning. As we discussed before, training data is a set of random variables whose values are

Relation	Tuple in Knowledge Base	Positive Examples	Negative Examples
Taxonomy	(Taxon, Taxon) (t_1, t_2)	$\{(t_1, t_2)\}$	$\{(t_1, t_2') : t_2' \neq t_2\}$
Formation	(Taxon, Fm.) (t, f)	$\{(t, f)\}$	Pos. examples of other relations
Fm.-Age (Mention)	(Fm.,Age) (t, i)	$\{(t, i') : intersect(i, i')\}$	$\{(t, i') : \neg intersect(i, i')\}$
Fm.-Age (Entity)	(Fm.,Age) (t, i)	$\{(t, i') : intersect(i, i') \wedge \neg contain(i', i)\}$	$\{(t, i') : \neg intersect(i, i')\}$
Fm.-Loc. (Mention)	(Fm.,Location) (t, l)	$\{(t, l') : intersect(l, l')\}$	$\{(t, l') : \neg intersect(l, l')\}$
Fm.-Loc. (Entity)	(Fm.,Location) (t, l)	$\{(t, l') : intersect(l, l') \wedge \neg contain(l', l)\}$	$\{(t, l') : \neg intersect(l, l')\}$

Table 4.2: List of distant supervision rules used in PaleoDeepDive. Function $contain(x, y)$ and $intersect(x, y)$ return True if the interval (or locations) x contains or intersects with y.

known. Traditional way of generating training data includes human expert annotation (e.g., the vast amount of labeled data in LDC[2]) and crowd-sourcing [47]. We use these approaches, but they can be expensive. In PaleoDeepDive, we make extensive use of a substantial generalization of Hearst patterns called *distant supervision* [96, 131, 205] that we describe by example.

An Example To use distant supervision, PaleoDeepDive requires an (incomplete) knowledge base. In PaleoDeepDive, this knowledge can be PaleoDB that is built by human volunteers. The goal is to complete the knowledgebase (as much as possible). Let us assume that we know that Tsingyuan Formation dates from Namurian. The first step of distant supervision is to provide a set of rules to generate heuristic examples, e.g., Hearst patterns that involve a formation name and an age. For example, if we know the fact that Tsingyuan Formation has the age Namurian, the developer might provide a rule that all variables that assign Tsingyuan Formation to an age that overlaps with Namurian, e.g., Silesian, should be considered as a *positive examples*; Otherwise, *negative example*, whose value is always False. This rule will not be at the propositional level, but will be at the first-order level: meaning all formations whose age overlaps with their recorded age will be considered as positive examples. This rule is not perfect, and the statistical system will appropriately assign weights to these samples. The developer writes more sophisticated inference rules to help refine the quality of these heuristic examples. This addition of rules is a novel component of PaleoDeepDive.

As we can see, using this technique does not require expensive human annotation. In our recent study, we showed that training data generated by distant supervision may have higher quality training than paid human annotations from Amazon Mechanical Turk [205]. Table 4.2 shows a set of distant supervision rules that we used in PaleoDeepDive.

Statistical Learning and Inference Given the rules specified in the previous phases, PaleoDeepDive now produces a factor graph via grounding, and runs statistical inference and learning.

Factor Graph Construction After the user provides a set of feature extractors that produce feature relations inside database, the next step is to generate a factor graph, on which PaleoDeepDive will run statistical inference and learning to produce the output that we described before. For example, in Figure 4.2, the tuple FormationTemporal(Tsingyuan Fm, Namurian) corresponds to a random varaible, which takes the value 1 or true if Tsingyuan formation has the age Namurian.

[2]https://www.ldc.upenn.edu/

To specify a correlation, say that if FormationTemporal(Tsingyuan Fm, Namurian) is true, then it is likely that FormationTemporal(Tsingyuan Fm, Silesian) is also true, then we could encode a factor that connects these two random variables. This is only a statistical implication, and PaleoDeepDive will estimate the strength of this implication on data.

Factor Graphs in PaleoDeepDive The final factor graph in PaleoDeepDive has an intuitive structure. Our graph contains random variables that can be viewed as being in three layers as shown in Figure 4.2. The first layer corresponds to the set of name entities detected from the text, which contains a set of Boolean random variables, each of which corresponds to one name entity mention. If one random variable has a value equal to true, it means that the corresponding name entity mention is correct. The second layer corresponds to a set of relation candidates between mentions extracted from text, and the third layer corresponds to a set of relation candidates between entities. One can think of the second layer as a per document layer and the third layer as the "aggregation" of the second layer cross all documents in the corpus. These layers are simply for software engineering reasons: the statistical inference uses information from all layers at the inference and learning time.

Variables in PaleoDeepDive's factor graph are connected by factors. Variables in the first and second layers are connected by factors that indicate whether a mention-level relation candidate is true, and variables in the second and third layers are connected by factors that "aggregate" mention-level extractions to entity-level extractions. Variables in the third layer are also connected inside the same layer, e.g., if one formation is extracted to be in Cambrian, then our confidence of that a formation from the same document is also in Cambrian may increase.

High-performance Statistical Inference and Learning Given the factor graph, PaleoDeepDive will then (1) learn the weight for each factor; and (2) run inference to decide the probability of each random variable. In PaleoDeepDive, this factor graph contains more than 200 million random variables and 300 million factors with 12 million distinct weights. Running inference and learning at this scale is computationally challenging. To meet this challenge, we develop a set of techniques that are the topic of Chapter 5 and Chapter 6.

4.1.3 Extension: Image Processing as Feature Extractors

We describe an extension of PaleoDeepDive to extract information from images. This extension is more preliminary compared with the main functionality of PaleoDeepDive; however, it shows off the ability of DeepDive to support a diverse set of KBC workload. As we will see in this section, the image-processing tools are all act like feature extractors, and DeepDive's framework is general enough to accommodate these feature extractors.

We describe the approach that we used for extracting body size of taxons from images. An example of such extraction is shown in Figure 1.1(d). To be concrete, the target relation that we want to extract is

$$(Taxon, FigureName, FigureLabel, Magnification, ImageArea)$$

where $ImageArea$ is one region on the PDF document with known DPI such that we can know its actual size on a printed paper. The following table is an example of the extracted relation.

Vediproductus wedberensis	Fig. 381	2a	X1	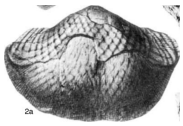
Compressoproductus compressus	Fig. 382	1a	X0.8	
Devonoproductus walcotti	Fig. 383	1b	X2.0	

The PaleoDeepDive approach to body size extraction contains two components, namely (1) Image processing, and (2) text extraction. In PaleoDeepDive, these two components are done jointly in the same factor graph. We describe these two components.

Image Processing The goal of the image processing component is to associate each image area with a figure label. To achieve this goal, PaleoDeepDive needs to (1) detect image areas and figure

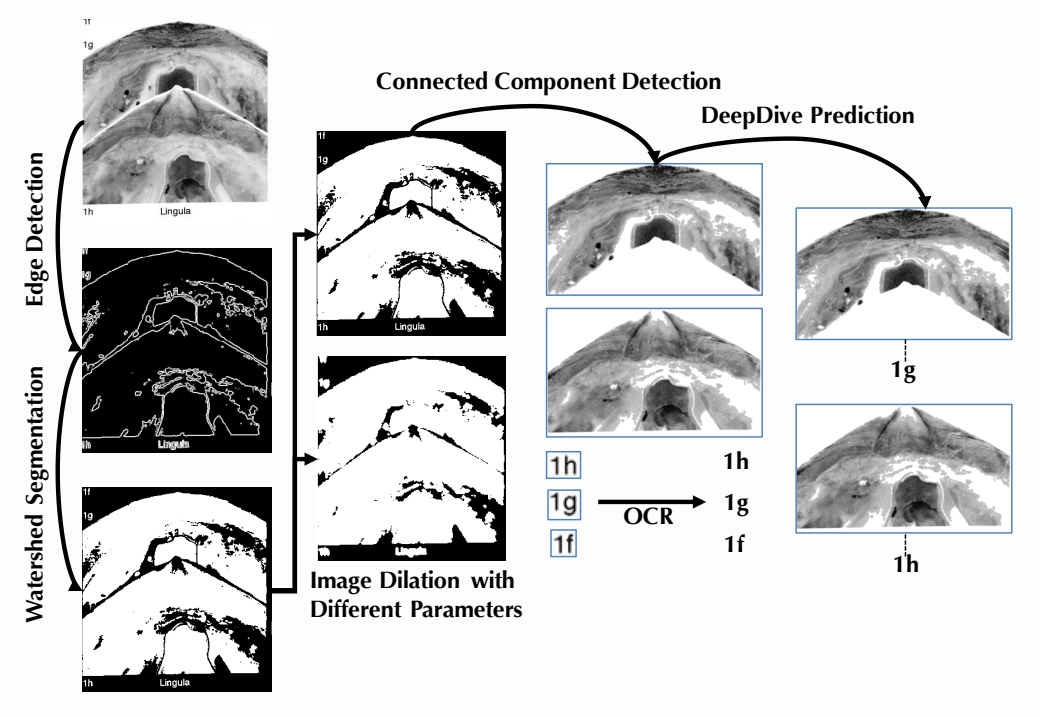

Figure 4.3: Image Processing Component for Body Size Extraction. Note that this examples contains the illustration of a *partial* body.

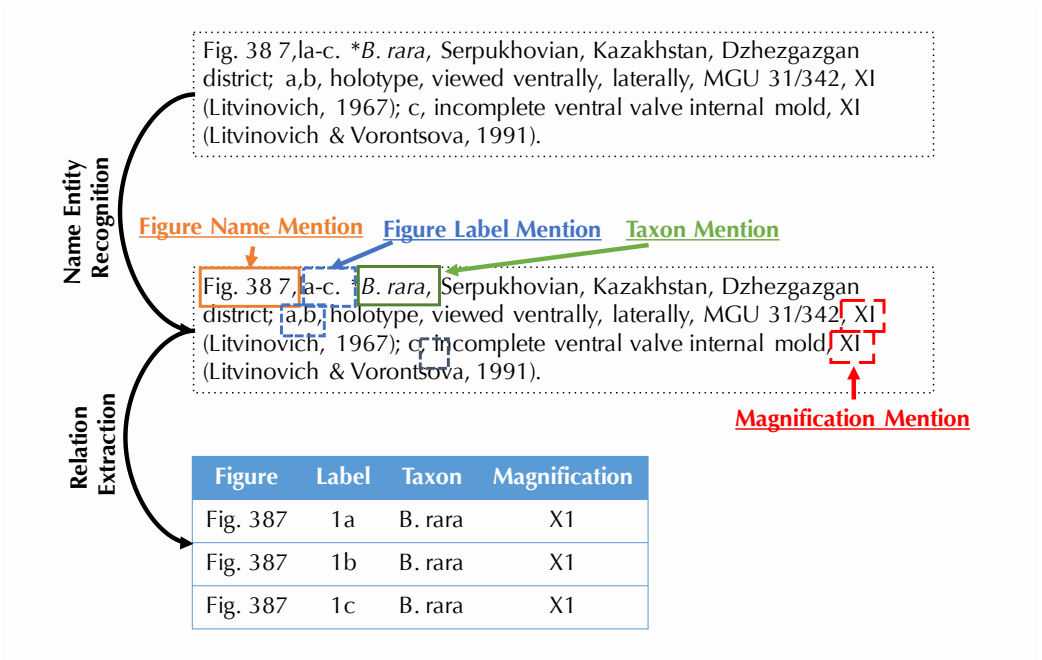

Figure 4.4: Relation Extraction Component for Body Size Extraction.

labels from PDF documents, and (2) associate image areas with figure labels. Figure 4.3 illustrates these two steps.

Detection of Image Areas and Figure Labels PaleoDeepDive extracts image areas and figure labels from PDF documents using state-of-the-art image segmentation algorithms available in open-source toolkits, e.g., OpenCV[3], or scikit-image.[4] As shown in Figure 4.3, these steps include (1) Edge detection; (2) Watershed Segmentation; (3) Image Dilation; and (4) Connected-component Detection. We did all these steps following standard online-tutorials of scikit-image, with one variant for Image Dilation that we describe as follows. In the image dilation step, one needs to specify a parameter for dilation. Instead of specifying one value for the parameter, we try a range of parameters and generate different versions of segmentations. PaleoDeepDive then trains a logistic regression classifiers to choose between these segments trained on a human-labeled corpus with a set of features including segments containment and OCR results.

Associate Image Areas with Figure Labels After recognizing a set of image regions and their corresponding OCR results, PaleoDeepDive tries to predict the association of figure labels and image areas as shown in Figure 4.3. Similar for relation extraction, PaleoDeepDive introduces one Boolean random variable for each pair of label and image area, and builds a logistic regression models. Features used in this step include the distance between label and image areas, and whether a label is nearest to an image area and vice versa.

Text Extraction PaleoDeepDive also extracts information from text as shown in Figure 4.4. The extraction phase is similar to what we introduced before for extracting diversity-related relations. In the name entity recognition component, PaleoDeepDive extracts different types of mentions, including Figure name (e.g., "Fig. 387"), Figure labels (e.g., "1a-c"), Taxon (e.g., "*B. rara*"), and magnitude (e.g., "X1"). Figure 4.4 shows an example of these mentions (raw text with OCR errors). PaleoDeepDive then extracts relations between these mentions using the same set of features as other diversity-related relations, and populate the target relation as shown in Figure 4.4.

[3] `http://opencv.org/`.
[4] `http://scikit-image.org/`.

Joint Inference Both image processing component and text extraction component creates a factor graph that populates two relations with schema

$$(FigureLabel, ImageArea)$$

and

$$(Taxon, FigureName, FigureLabel, Magnitude).$$

PaleoDeepDive joins these two intermediate relations to form a large factor graph to populate the target relation, and run jointly inference on the whole factor graph.

4.1.4 Descriptive Statistics of PaleoDeepDive

In this section, we present descriptive statistics of PaleoDeepDive, e.g., the corpus on which PaleoDeepDive runs, and the number of extractions produced by PaleoDeepDive.

Corpus PaleoDeepDive is executed on two corpora, namely the (1) overlapping corpus and (2) the whole corpus. The overlapping corpus contains journal articles that also appear in the human-built PaleoDB, and we use it for comparison between PaleoDeepDive and PaleoDB. The whole corpus is our best-effort corpus in collecting as many document as possible given our access to different publishers and library, and we use it to illustrate the scaling behavior of PaleoDeepDive. We run exactly the same operations, including feature extraction, and statistical learning and inference, on these two corpora. In total, the overlapping corpus has 11,782 distinct references in total, and covers 25% of all references in PaleoDB. The whole corpus contains In total, we have 277,309 PDF documents in the whole corpus.

Factor Graph Table 4.3 shows the statistics of the factor graph generated using both overlapping corpus and the whole corpus, and the ratio between the whole corpus and the overlapping corpus. We see that the whole corpus contains more than 292 million random variables, 308 million factors, and 12 million distinct weights.

We describe the scaling behavior by comparing the factor graph generated from the overlapping corpus and the whole corpus. As shown in Table 4.3, the whole corpus contains 23$\times$ more PDF documents, and we observe that the number of variables and factors scales in a similar factor (22$\times$

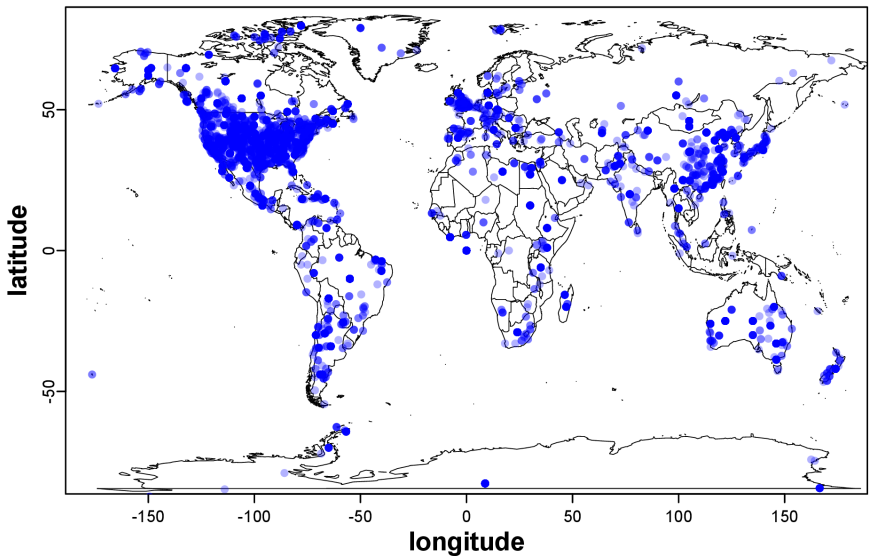

Figure 4.5: Spatial distribution of PaleoDeepDive's extraction (Overlapping Corpus).

and 20×). The whole corpus contains 13× more distinct features than the overlapping set, and it is expected that this number has a sub-linear growth with the corpus size because adding a new document may not necessarily introduces new features.

One interesting observation is that the whole corpus contains only 2× more evidence variables than the overlapping corpus. This is expected because all these variables are generated using distant supervision–the more overlap between the knowledge base and the corpus, the more evidence variables that we can generate. For the overlapping corpus, the overlap between knowledge base and the corpus is much better because the knowledge base is built using the same set of documents.

Extraction Result Table 4.4 shows the number of extractions after statistical inference and learning for both overlapping corpus and the whole corpus. Figure 4.5 shows a spatial representation of these extractions from the overlapping corpus and the whole corpus.

For the extraction results, we observe that the number of authorities scales 10× and the number of taxon candidates scales 22× for a 23× larger data set (Table 4.4). This is expected because all taxon mentions of the same authority will only contribute once for the authority extraction. The number of occurrences scale sub-linearly (6×). The reason for the sub-linear-growth of occurrences is not all documents in the whole corpus are related to occurrences.

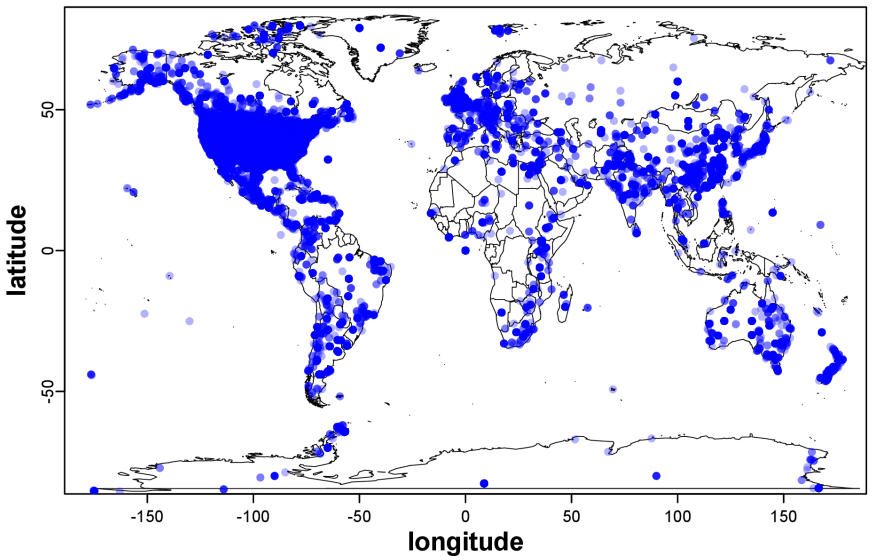

Figure 4.6: Spatial distribution of PaleoDeepDive's extraction (Whole Corpus).

	Overlapping Corpus	Whole Corpus	Ratio (W./O.)
# Variables	13,138,987	292,314,985	22×
# Evidence Variables	980,023	2,066,272	2×
# Factors	15,694,556	308,943,168	20×
# Distinct Features (Weight)	945,117	12,393,865	13×
Documents	11,782	280,280	23×

Table 4.3: Statistics of the factor graphs on different corpora. Ratio = Whole/Overlapping.

4.1.5 Quality of PaleoDeepDive

We validate that PaleoDeepDive achieves high precision and recall for extracting relations between taxa, rock formations, temporal intervals, and locations.

End-to-end Quality The quality of PaleoDeepDive's data extractions was assessed in three ways. The first uses DeepDive's pipeline, which produces internal measures of precision for every entity and relationship. All of the extractions used here have a precision of $\geq$95% according to this criterion. We also conducted blind assessment experiments of two types. In the first double blind experiment, we randomly sampled 100 relations from the PaleoDB and PaleoDeepDive and then randomized the combined 200 extractions into a single list. This list was then manually assessed for accuracy relative to the source document. In this assessment, PaleoDeepDive achieves $\geq$92% accuracy in all cases, which is as greater or greater than the accuracy estimated for the PaleoDB. In the second blind experiment, eight scientists with different levels of investment in the PaleoDB were presented with

		Overlapping Corpus	Whole Corpus	Ratio (W/O)
Mention-level	Taxon	6,049,257	133,236,518	22×
	Formation	523,143	23,250,673	44×
	Interval	1,009,208	16,222,767	16×
	Location	1,096,079	76,688,898	76×
	Opinions	1,868,195	27,741,202	15×
	Taxon-Formation	545,628	4,332,132	8×
	Formation-Temporal	208,821	3,049,749	14×
	Formation-Location	239,014	5,577,546	23×
Entity-level	Authorities	163,595	1,710,652	10×
	Opinions	192,365	6,605,921	34×
	Collections	23,368	125,118	5×
	Occurrences	93,445	539,382	6×
	Documents	11,782	280,280	23×

Table 4.4: Extraction statistics. Ratio = Whole/Overlapping.

the same five documents and the same 481 randomly selected taxonomic facts, which were extracted by both humans and PaleoDeepDive. No indication was given regarding which system generated the facts. Humans measured a mean error frequency in the PaleoDeepDive-constructed database of 10%, with a standard deviation of ±6%. This is comparable to the error rate of 14 ±5% they estimated for those same documents in the human-constructed PaleoDB. Variability in the error rate estimates between annotators reflects a combination of assessment error and divergent interpretations. Although these blind experiments suggest that the error rate is comparable between the PaleoDB and PaleoDeepDive, the comparisons are not strictly equivalent. For example, PaleoDeepDive currently understands only parent-child relationships and synonymy, which comprise a large fraction (90% and 5%, respectively) but not all of the opinions in the PaleoDB. Human data enterers also selectively enter data that are deemed important or non-redundant with data in other documents because the data entry process is time consuming.

The third approach we took to assessing the quality of PaleoDeepDive was conducted at the aggregate level of Phanerozoic macroevolutionary patterns [77], which represent some of the key synthetic results that motivated the manual construction of the PaleoDB [12]. After processing the PaleoDB and PaleoDeepDive databases with the same algorithms in order to generate a working taxonomy and a list of occurrences that meet the same threshold for temporal resolution, we find good overall agreement in macroevolutionary quantities (Figure 4.7; data are binned into the same 52 time intervals, mean duration 10.4 Myr). Both long-term trends and interval-to-interval changes in genus-level diversity and turnover rates are strongly positively correlated, indicating that both

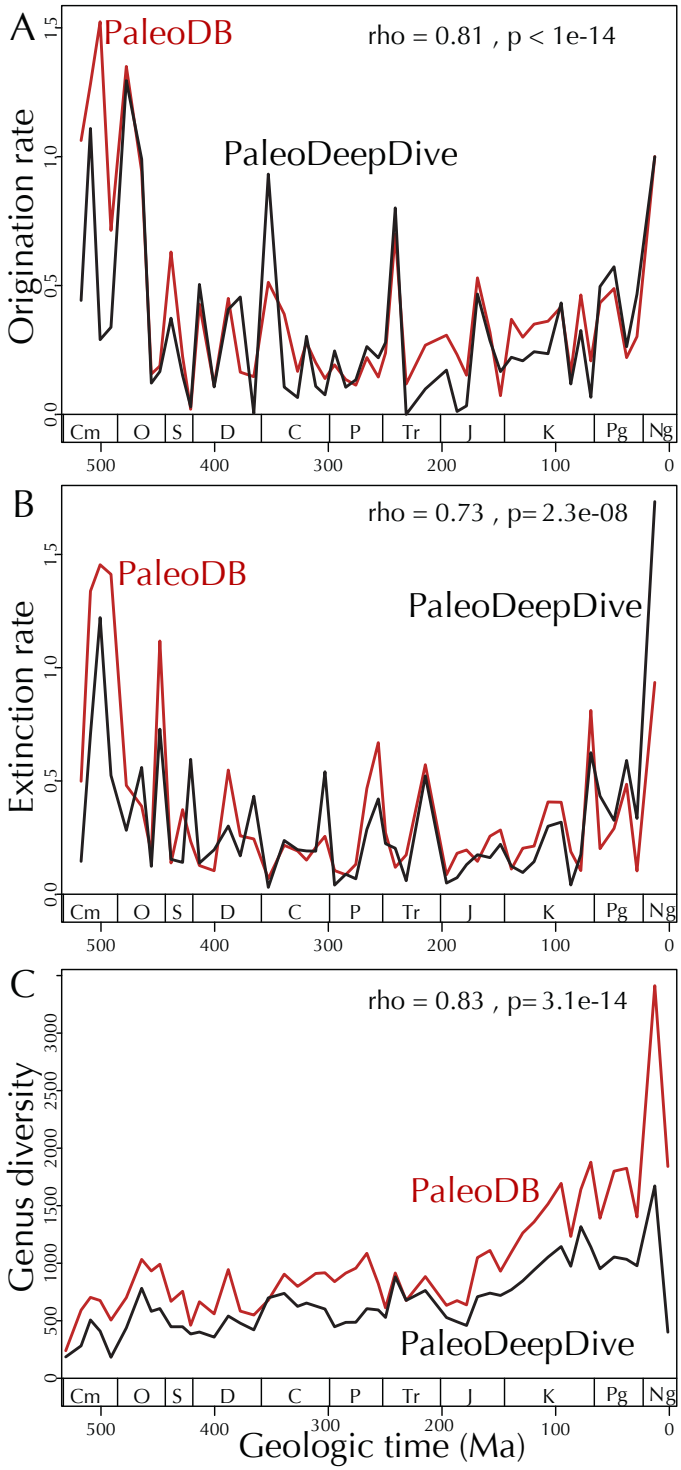

Figure 4.7: Machine- and human-generated macroevolutionary results for the overlapping document set. Human-generated in red, machine-generated in black. Spearman rank order correlations for first differences shown. (a) Per capita, per interval origination rates (27). (b) Per capita, per interval extinction rates. (c) Total range-through diversity.

closely capture the same signal. The number of genus-level occurrences in each time interval, which is important to sampling standardization approaches [9, 129], are also positively correlated (for first differences, Spearman rho = 0.65; p = $5.7x10^{-7}$). The times of first and last occurrence of 6,708 taxonomically and temporally resolved genera common to both database are also congruent (Figure 4.8).

Differences between synethic results (Fig. 4.7) can be attributed to a combination of errors and inconsistencies in the human-constructed database, as well as to data recovery and inference errors committed by PaleoDeepDive. For example, the human database contains typographical errors introduced during data entry. But, there are more insidious inconsistencies in the PaleoDB that cause most of the differences observed in Figure 4.7. For example, there are groups of occurrences in the PaleoDB that derive from multiple documents, even though only one document is cited as the source of data. Groups of occurrences in the PaleoDB are also sometimes attributed to a reference that contains no data but that instead cites the PaleoDB or some other archive that we did not access. A much more common source of discrepancy between the PaleoDeepDive and PaleoDB involves the injection of facts and interpretations by humans during data entry. Most notably, approximately 50% of the ages assigned to PaleoDB fossil occurrences are not mentioned in the cited reference. Although problematic in some senses, this is well justified scientifically. The stated age for an fossil occurrence is often not the best age that is available, and the PaleoDB has no capacity to dynamically assign ages to fossil occurrences based on all evidence. Humans attempt to account for these limitations by entering what they determine, on the basis of other sources, to be the best age for a fossil occurrence in a given document. PaleoDeepDive replicated aspects of this behavior by inferring across all documents the most precise and recently published age for a given geological unit and location, but this is not sufficient to cover the full range of sources that were consulted by humans. Thus, a disproportionate number of the occurrences extracted by PaleoDeepDive have a temporal resolution (e.g., period-level) that results in exclusion from the macroevolutionary quantities shown in Figure 4.7. Including occurrences with low-resolution causes the human- and machine-generated diversity curves (Fig. 4.7c) to more closely converge.

Errors and limitations in the current PaleoDeepDive system also account for some divergence in results (Fig. 4.7). For example, OCR-related document processing failures, often involving tables, are among the leading causes of data omissions by PaleoDeepDive. The current version of PaleoDeepDive

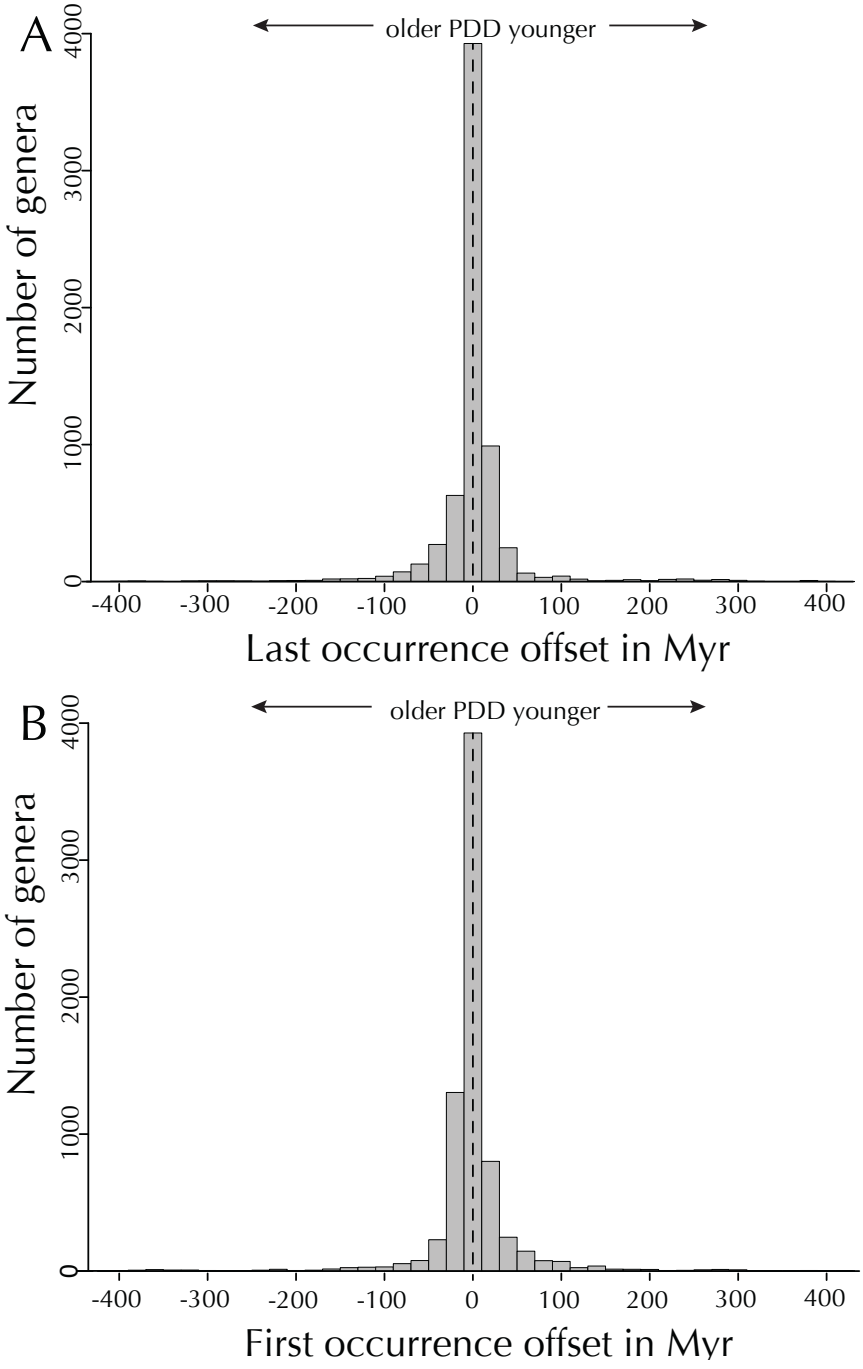

Figure 4.8: Difference in genus range end points for 6,708 genera common to the PaleoDB and PaleoDeepDive. (a) Last occurrence differences. Median is 0 Myr, mean is +1.7 Myr. (b) First occurrence offset. Median is 0 Myr, mean is -0.3 Myr.

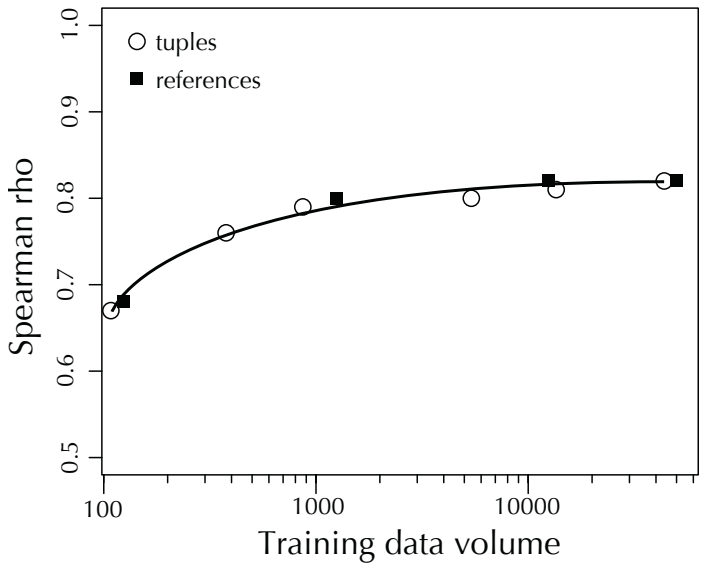

Figure 4.9: Effect of changing PBDB training database size on PDD quality. Spearman rho is correlation between human- and machine- generated time series of diversity, as in Figure 4.7c.

also has elements of design that cause some facts to be omitted, even though they are included in the PaleoDB. For example, PaleoDeepDive now places great importance on formal geologic units, which means that no occurrences are recognized in references that do not have well defined geologic units. Because this situation is more prevalent in recent time intervals, the lower total diversity recovered by PaleoDeepDive towards the recent (Fig. 4.7) is largely attributable to this design decision. Differences between the PaleoDeepDive and PaleoDB databases also occur when a fact is correctly extracted by PaleoDeepDive, but with a probability that is <0.95, the threshold used to generate the results shown in Figure 4.7. This type of confidence-related error can be overcome by defining new features or rules that remove sources of ambiguity.

Despite identification of errors in both the human- and machine-generated databases, the results from the overlapping corpus demonstrate that PaleoDeepDive performs comparably to humans in many complex data extraction tasks. This is an important result that demonstrates the reproducibility of key results in the PaleoDB and that addresses several long-standing challenges in computer science. However, it is also the case that macroevolutionary quantities, which are based on large numbers of taxa, are robust to random errors introduced at the level of individual facts [3, 19, 168]. Thus, PaleoDeepDive's macroevolutionary results (Fig. 4.7) could be interpreted as evidence for the presence of a strong signal in the palaeontological literature that is readily recovered, regardless of

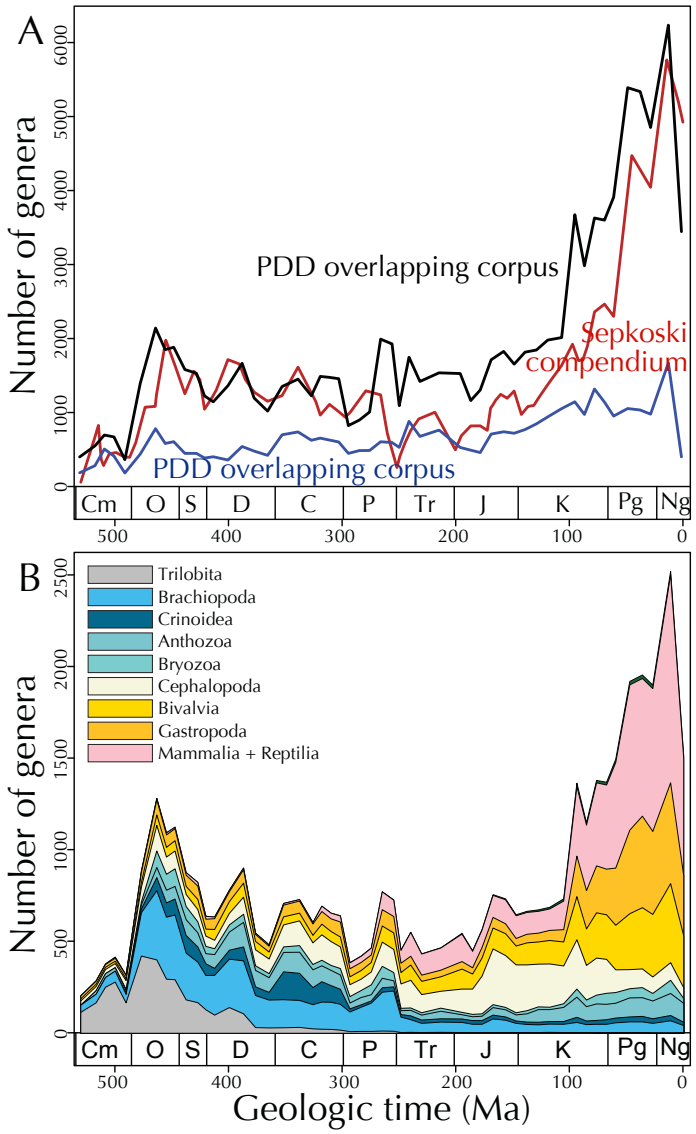

Figure 4.10: Genus-level diversity generated by PaleoDeepDive for the whole document set. (a) Total genus diversity calculated as in Figure 4.7. For comparison, Sepkoski's genus-level diversity curve (3) is plotted using his stage-level timescale. (b), Diversity partitioned by genera resolved to select classes by PDD.

the precision of the approach. The narrow distribution of range offsets on a per-genus basis (Fig. 4.8), however, suggests that PDD's precision is high even at the scale of individual facts.

Robustness to the Size of the Knowledge Base One important component in PaleoDeepDive is distant supervision, which uses an existing knowledge base to produce labeled training data for weight learning (Section 4.1.2). In this section, we validate that PaleoDeepDive's quality is robust to

Percentage of KB	# Evidence Variables	Subject Entities
0.1%	552	61
1%	9,056	556
10%	97,286	5,489
50%	515,593	27,825
100%	980,023	55,454

Table 4.5: Statistics of lesion study on the size of knowledge base.

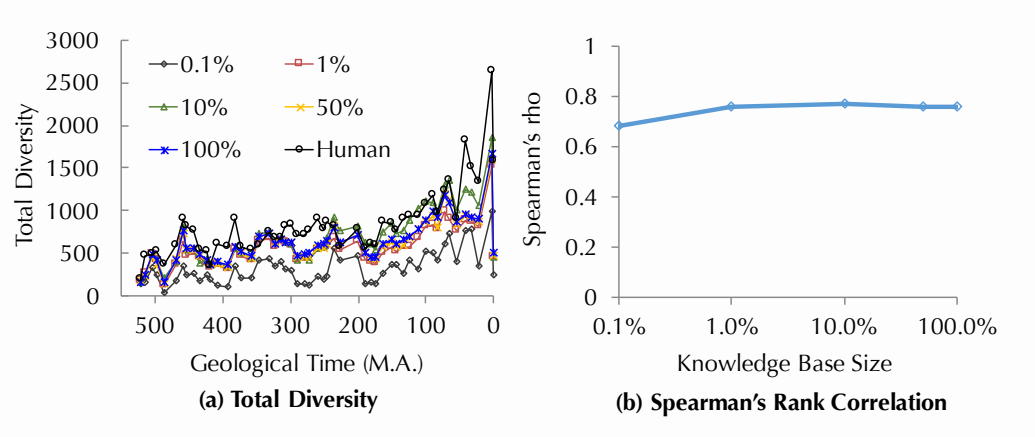

Figure 4.11: Lesion study of the size of knowledge base (random sample).

the size of the knowledge base used for distant supervision.

Random Sub-sampling of Knowledge Base The core question is: how large a Knolwedge Base does one need to obtain high quality? To understand this question, we conduct the following experiment.

We take the whole PaleoDB dump and produce a series of knowledge bases by uniformly random sub-sampling each table, i.e., $KB^{(0.1\%)}$, $KB^{(1\%)}$, $KB^{(10\%)}$, $KB^{(50\%)}$. Let $KB^{(100\%)}$ be the whole PaleoDB knowledge base. For each sub-sampled knowledge base, we run PaleoDeepDive by only using it for distant supervision, while all other components keep the same. We run all runs on the overlapping corpus, and produce the biodiversity curve for each run that uses different knowledge base, and report the total diversity curve and the Spearman's rho tested with the human version. We run this process three times for each knowledge base size, and report only one of them here (All runs have similar result). Table 4.5 shows statistics of the training data produced by each knowledge base. The smallest knowledge base $KB^{(0.1\%)}$ produces 552 evidence random variables, which correspond to relations related to 61 distinct entities. The largest knowledge base $KB^{(100\%)}$ contains more than

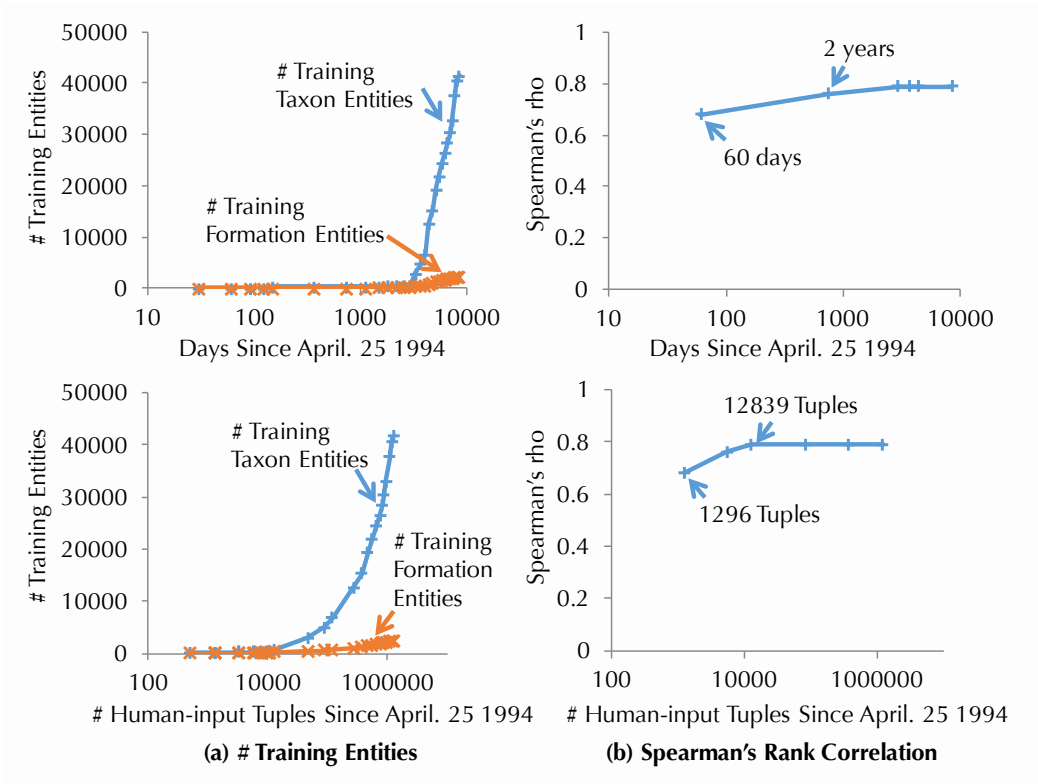

Figure 4.12: Lesion study of the size of knowledge base (chronological).

980K evidence variables, which correspond to relations related to 55K distinct entities.

Figure 4.11 shows the result. We see from Figure 4.11(a) that using an extremely small knowledge base ($KB^{(0.1\%)}$) produces a biodiversity curve with significantly less total diversity than the full knowledge base ($KB^{(100\%)}$). This difference is also supported by the Spearman's rho in Figure 4.11(b), where $KB^{(0.1\%)}$ is 0.68 and $KB^{(100\%)}$ is 0.79. This is because when the number of training variables is too small, it is hard for DeepDive to learn high-confident weight from the training data. We also observe that $KB^{(1\%)}$, which contains only 1% tuples of the full PaleoDB, achieves a similar total diversity than $KB^{(100\%)}$, and the Spearman's rho for $KB^{(1\%)}$ is 0.76. This implies the robustness of PaleoDeepDive's quality to the size of the underlying knowledge base.

In principle, as long as PaleoDB contains the relevant information of these 556 entities, PaleoDeepDive is able to produces a biodiversity curve on the overlapping corpus with Spearman's rho 0.76.

Chronological Replay of PaleoDB History The previous experiment uniformly samples the knowledge base, and now we study one question that *How long would it have taken for PaleoDB volunteers to build a PaleoDB snapshot that is large enough to effectively construct PaleoDeepDive?*. To understand this question, we conduct the following experiment that "chronologically replay" snapshots of PaleoDB.[5]

Each tuple in PaleoDB has a field called creation time, and we order all tuples by this field, and create one snapshot every 30 days. This gives us a series of knowledge bases. For each knowledge base, we use it to supervise PaleoDeepDive and report the results in Figure 4.12.

Figure 4.12(a) shows the statistics of the training data produced by this series of knowledge bases. One see that as the number of days (since April 25 1994, the date of the first tuple) or the number of human-input tuples grows, the number of entities appears in the training set grows. Figure 4.12(b) shows the Spearman's rho for each knowledge base. We find that the first non-empty PaleoDeepDive training set happens after 60 days, when there are 1296 human-input tuples. This achieves a Spearman's rho of 0.65, which is much worse than the one we can get on the full PaleoDB dump (0.79). However, with the dump on April 1996 (2 years), we can produce a diversity curve with Spearman's rho 0.76. This dumps only contains 12K human input tuple. The 2 year figure is somewhat biased: the PaleoDB project did not have a large number of volunteers initially; in contrast, by 2004 it would take only 1 month for volunteers to input a sufficient number of tuples.

4.2 TAC-KBP

We briefly describe another KBC application built with DeepDive. Different from PaleoDeepDive, this application is built for a KBC competition called TAC-KBP, which is a public benchmark data set on non-scientific applications.[6] This allows us to compare the KBC system built with DeepDive not only to human volunteers as we did in PaleoDeepDive, but also other state-of-the-art KBC systems. We first describe the task of TAC-KBP, then describe the submission system we built that is the top-performing system in TAC-KBP 2014 slot filling task among 18 teams and 65 submissions.

[5] One confounding effect that should be noted is that we use the same rules that we have constructed for the final system; and the extra information may have been helpful in debugging or creating these rules.

[6] `http://www.nist.gov/tac/2014/KBP/`

Entities	Relations		
Person	**Person-related Relations**		**Organization-related Relations**
Location	age	parents	alternate_names
	alternate_names	religion	city_of_headquarters
Organization	cause_of_death	schools_attended	country_of_headquarters
	charges	siblings	date_dissolved
Date	children	Spouse	date_founded
	countries_of_residence	title	founded_by
Cause of Death	country_of_birth	cities_of_residence	member_of
	country_of_death	city_of_birth	members
Title	date_of_birth	city_of_death	number_of_employees_members
	date_of_death	origin	parents
URL	employee_or_member_of		political_religious_affiliation
	other_family		shareholders
	stateorprovince_of_birth		stateorprovince_of_headquarters
	stateorprovince_of_death		subsidiaries
	statesorprovinces_of_residence		top_members_employees
			website

Figure 4.13: The set of entities and relations in TAC-KBP competition.

4.2.1 Description of the Submission System

The slot filling task of TAC-KBP 2014 aims at extracting information from 1.8M news articles. The target relation is similar to those appear in Freebase or Wikipedia's information box. Figure 4.13 illustrates the set of entities and relations that a submission system needs to extract from news articles. In totaly, there are totally 41 target relations for person entity or organization entity. We describe system details of the two runs we submitted with DeepDive, with a focus on the lessons we learned during the development of these systems.

Input Data Preparation The input to DeepDive is a text corpus with NLP-markups that are stored as a database relation. The baseline system we built contains all NLP-markups produced by Stanford CoreNLP. During our development, we find that in one system snapshot with recall=0.45, parsing-related errors contribute to 31% of recall errors. A further analysis shows that some of these sentences do have a correct parsing result in other parsers. Motivated by this observation, our final submission contains the union of parsing result from three parsers, namely, Stanford CoreNLP [126], Malt parser [143], and BBN's SERIF [36]. Among these three parsers, we run Stanford CoreNLP and Malt parser by ourselves, and the result of SERIF is shipped with the TAC 2014 KBP English Source Corpus (LDC2014E13). We conduct post-processing on the result of Malt parser and SERIF to make sure they share the same format as the output of Stanford CoreNLP. For Malt parser, we collapse

the dependency tree as in Stanford CoreNLP; for SERIF, we use Stanford CoreNLP to translate the constitute parsing result into collapsed dependencies. These post-processing steps make sure we can use exactly the same DeepDive program to process the output of all these three parsers, and therefore, do not need to change the DeepDive program.

Feature Extraction The features we used in our submission largely follow state-of-the-art work. Baseline features that we use include the dependency paths and word sequences between a mention pair. For each baseline feature, we apply one or a conjunction of the following operations to generate a new feature, including (1) replace a verb (resp. noun) with its POS or NER tag; (2) replace a verb (resp. noun) with its WordNet synset; (3) replace a verb (resp. noun) with its WordNet hypernyms. These are basic features that we used for a mention pair in the sentence. Another class of features that we used involves a mention pair and a keyword (e.g., president, chair, marry, etc.) in the sentence. Given two mentions m_1, m_2, and a keyword w, we create a feature that is a conjunction between (1) (m_1, w)'s feature; (2) (m_2, w)'s feature; and (3) w's lemma form. For (m_i, w)'s feature, we use the same feature extractor as we defined for a single mention pairs. The dictionary of keywords is generated in a way described below.

Distant Supervision We follow the standard practice of distant supervision to produce positive and negative examples. To improve upon this component, our goal is to harvest more (distantly) labeled training examples. Therefore, our submission involves a labeling phase that is motivated by the success of Hearst's patterns [92] in harvesting high-quality taxonomic relations.

Our labeling effort starts from the result of standard distant supervision, which is a set of tuples of mention pairs that are labeled as positive examples for relation R, denoted as $R(m_1, m_2)$, and for each mention pair, we have the set of features associated with it, denoted as a relation $F(m_1, m_2, f)$. Then, we pick all features f that (1) are associated with at least one mention pair in R, and (2) appeared in the whole corpus at least twice for distinct sentences. For each feature, we manually label it as an indicator of the relation or not. For features labeled as indicators, we only use them in the following way–We include all mention pairs associated with this feature as newly generated positive examples (and negative examples for other relations). One simple optimization we conducted is that if a more general feature (e.g., the feature after substituting a noun to its POS tag) is labeled as correct, then all features that are more specific than this feature should also be correct and do not

need a human label. We manually labeled 100K features in this way. Although 100K features sounds like a large amount of features to label, we find that it only takes the author 2 days, and after getting familiar with this task, the labeling speed could be as fast as one feature per second.

Error Analysis We conducted error analysis after the score and ground truth was released to classify errors that our submission made into multiple categories. This error analysis is conducted on our submission with F1=0.36 (Precision=0.54 and Recall=0.27) and focuses mainly on precision.

Out of all 509 proposed relations, 276 of them are labeled as correct, 154 wrong, 53 inexact, and 26 redundant. We mainly focus on the 154+54 wrong and inexact relations, which constitute 40 points of precision loss. Because this submission system uses a probability threshold 0.8 to propose relations, 20 points of these errors are expected due to errors in relation extraction. In the remaining 20 points of precision loss, we find that entity linking errors contribute to 7 points of precision loss. One common pattern is that DeepDive confuses entities which are different from the query entity but share the same name. For example, if the query asks about “Barack Obama” and there are mentions of “Barack Obama” and “Michelle Obama” in the same document, our system sometimes mistakenly links a mention “Obama” referring to “Michelle Obama” to the query. Another 7 points of precision loss are caused by normalizing answers that are of the type date, age, and title. For example, our system did not normalize the date to the format “yyyy-mm-dd”, and these answers are labelled as “incorrect” by the annotators. These two classes of errors require deeper understanding of entities that appear in the corpus.

5. Batch Execution

But the speed was power,
and the speed was joy,
and the speed was pure beauty.

— Richard Bach, *Jonathan Livingston Seagull, 1970*

The thesis of this dissertation is that it is feasible to build DeepDive as a data management system in which the user specifies *what* he wants to do in each phase instead of *how* these operations are physically conducted. We have illustrated how DeepDive allows this declarative way of specifying a KBC system. One question remains: *Can we make the execution of DeepDive efficient and scalable?*

The answer to this question is well-studied for some phases. For example, both the feature extraction and probabilistic knowledge engineering phases rely on SQL with user-defined functions. Because the data model of DeepDive is relational, the efficiency and scalability of these two phases can be achieved by relying on modern (distributed) relational databases.

However, the statistical inference and learning phase requires more study. Because the operations in this phase are not relational, making them scalable and efficient it is an active research problem that has attracted intensive interests in recent years, as we will discuss in Chapter 7. This chapter described two techniques that we developed for this topic. The first technique aims to scale up one algorithm for statistical inference and learning, namely Gibbs sampling, over factor graphs whose size exceeds tera-bytes and thus does not fit in main memory. The technical contribution is to revisit the design of a buffer manager for statistical inference and learning algorithms. The second technique aims to speed up statistical analytics algorithms when the problem fits in main memory. The technical contribution is to study the system tradeoff of building an in-memory analytics system on modern hardware. As we will see in this chapter, both techniques can lead to more than two orders of magnitude speed up in some workloads. These techniques together allow DeepDive to support a large range of statistical inference and learning tasks with different-sized problems and different computational resources. Given these techniques, the user can focus more on constructing a DeepDive program instead of worrying about how a statistical inference task could be done on billions of random variables.

5.1 Scalable Gibbs Sampling

Factor graphs are the abstraction DeepDive uses for statistical inference and learning. Other than its application in DeepDive, factor graphs also capture and unify a range of data-driven statistical tasks in predictive analytics, and pricing and actuarial models that are used across many industries. For example, Moody's rating service uses Gibbs sampling and generalized linear models (GLMs) [174], as do leading insurance actuaries [17,72]. Increasingly, more sophisticated factor graph models are used. For example, Yahoo and Google use latent Dirichlet allocation (LDA) for topic modeling [34,122,173], and Microsoft's EntityCube uses Markov logic [69, 140, 163, 209]. Most inference or parameter estimation problems for factor graphs are intractable to solve exactly [188]. To perform these tasks, one often resorts to sampling. Arguably the most popular of these approaches, and the one on which we focus, is Gibbs sampling [159].

Not surprisingly, frameworks that combine factor graphs and Gibbs sampling are popular and widely used. For example, the OpenBUGS framework has been used widely since the 1980s [125]. More recent examples include PGibbs [82] and Factorie [128]. For any factor graph, given a fixed time budget, an implementation of Gibbs sampling that produces samples at a higher throughput, achieves higher-quality results [174]. Thus, a key technical challenge is to create an implementation of *high-throughput* Gibbs samplers.

Achieving high throughput for Gibbs sampling is well studied for factor graphs that fit in main memory, but there is a race to apply these approaches to larger amounts of data, e.g., in defense and intelligence [136], enterprise [93], and web applications [173]. In DeepDive, the factor graph produced for KBC can easily exceed terabytes, which does not always fit in main memory.

A key pain point of existing approaches on scalable Gibbs sampling is that for each specific model, a scalable implementation is hand tuned, e.g., Greenplum's MADlib [93] and Yahoo [173] implement hand-tuned versions of LDA. High-performance implementations of Gibbs sampling often require a tedious process of trial-and-error optimization. Further complicating an engineer's job is that the variety of storage backends has exploded in the last few years: traditional files, relational databases, and HDFS-based key-value stores, like HBase or Accumulo. The lack of scalable Gibbs samplers forces developers to revisit I/O tradeoffs for each new statistical model and each new data storage combination. We first show that a baseline approach that picks classically optimal points in this tradeoff space may lose almost two orders of magnitude of throughput.

We select three classical techniques that are used to improve query performance in database storage managers: materialization, page-oriented layout, and buffer-replacement policy. These techniques are simple to implement (so they may be implemented in practice), and they have stood the test of four decades of use.[1] Our study examines these techniques for a handful of popular storage backends: main-memory based, traditional unix files, and key-value stores.

Applying these classical techniques is not as straightforward as one may think. The tradeoff space for each technique has changed due to at least one of two new characteristics of sampling algorithms (versus join data processing): (1) data are mutable during processing (in contrast to a typical join algorithm), and (2) data are repeatedly accessed in an order that changes randomly across executions, which means that we cannot precompute an ideal order. However, within any given sampling session, the data is accessed in a fixed order. We consider the tradeoff space analytically, and use our analysis of the tradeoff space to design a simple proof-of-concept storage manager. We use this storage manager to validate our claimed tradeoff space in scaling Gibbs sampling.

As we show through experiments, our prototype system is competitive with even state-of-the-art, hand-tuned approaches for factor graphs that are larger than main memory. Thus, it is possible to achieve competitive performance using this handful of classical techniques.

5.1.0.1 Overview of Technical Contributions

The input to Gibbs sampling is a factor graph as we described in Chapter 2, which can be modeled as a labeled bipartite graph $G = (X, Y, E)$ where X and Y are sets of nodes and $E \subseteq X \times Y$ is a set of edges. To obtain a sample for a single variable x, we perform three steps: (1) retrieve all neighboring factors[2] and the assignments for all variables in those factors, (2) evaluate these neighboring factors with the retrieved assignments, and (3) aggregate the evaluation results to compute a conditional distribution from which we select a new value for x. This operation, which we call the *core operation*, is repeated for every variable in the factor graph (in a randomly selected order). We loop over the variables many times to obtain a high-quality sample.

Since the bulk (often over 99%) of the execution time is spent in the core operation, we focus on optimizing this operation. To this end, we identify three tradeoffs for the core operation of Gibbs sampling: (1) materialization, (2) page-oriented layout, and (3) buffer-replacement policy. Note that

[1] Although sampling approaches have been integrated with data processing systems, notably the MCDB project [100], the above techniques have not been applied to the area of high-throughput samplers.

[2] The set of neighboring factors are factors that connect a given variable and its Markov blanket.

all these three tradeoffs are among the most popular tradeoffs studied by the database community, and our effort in adapting these general tradeoffs to more ad hoc workload is in a very similar spirit to prior arts in database [185].

1. **Materialization tradeoffs.** During Gibbs sampling, we access the bipartite graph structure many times. An obvious optimization is to materialize a portion of the graph to avoid repeated accesses. A twist is that the value of a random variable is updated during the core operation. Thus, materialization schemes that introduce redundancy may require many (random) writes. This introduces a new cost in materialization schemes, and so we re-explore lazy and eager materialization schemes, along with two co-clustering schemes [153, ch. 16]. The two co-clustering schemes together analytically and empirically dominate both eager and lazy schemes – but neither dominates the other. Thus, we design a simple optimizer based on statistics from the data to choose between these two approaches.

2. **Page-oriented layout.** Once we have decided how to materialize or co-cluster, we are still free to assign variables and factors to pages to minimize the number of page fetches from the storage manager during the core operation. In cases in which the sampling is I/O bound, minimizing the number of page fetches helps reduce this bottleneck. Since Gibbs sampling proceeds through the variables in a random order, we want a layout that has good average-case performance. Toward this goal, we describe a simple heuristic that outperforms a naïve random layout by up to an order of magnitude. We then show that extending this heuristic is difficult: assuming P $\neq$ NP, no polynomial time algorithm has a constant-factor approximation for the layout that minimizes page fetches during execution.

3. **Buffer-Replacement Policy.** A key issue, when dealing with data that is larger than available main memory, is deciding which data to retain and which to discard from main memory, i.e., the buffer-replacement policy. Although the data is visited in random order, one will typically perform many passes over the data in the same random order. Thus, after the first pass over the data, we have a great deal of information about which pages will be selected during execution. It turns out that this enables us to use a classical result from Bélády in 1966 [26] to define a theoretically optimal eviction strategy: *evict the item that will be used latest in the future*. We implement this approach and show that it performs optimally, but that its improvement over more traditional strategies based on MRU/LRU is only 5–10%. It also requires some non-trivial

implementation, and so it may be too complex for the performance gain. A technical serendipity is that we use Bélády's result to characterize an optimal buffer-replacement strategy, which is needed to establish our hardness result described in page-oriented layout.

We present our technical contributions in Section 5.1.1, and an empirical validation in Section 5.1.2. We discuss related work together with other techniques in Chapter 7. We conclude in Section 5.1.3.

5.1.1 Storage-Manager tradeoffs to Scale Gibbs Sampling

We show that Gibbs sampling essentially performs joins and updates on a view over several base relations that represent the factor graph. Thus, we can apply classical data management techniques (such as view materialization, page-oriented layout, and buffer-replacement policy) to achieve scalability and high I/O efficiency.

5.1.1.1 Gibbs Sampling as a View

Given a database with a user schema and correlation schema as defined in Chapter 2, we define two simple relations that represent the edge relation of the factor graph and the sampled possible world:

$$E(v, f) = \{(v, f) | f \in \mathbb{F},\ v \in \text{vars}(f)\} \text{ and } A(\underline{v}, a) \subseteq \mathbb{D} \times \mathbb{V}$$

In Figure 2.3, E encodes the bipartite graph and each tuple in A corresponds to a possible assignment of a label of a variable. Note that each variable is assigned a single value (so v is a key of A) and A will be modified during Gibbs sampling.

The following view describes the input factor graph for Gibbs sampling:

$$Q(v, f, v', a') \leftarrow E(v, f), E(v', f), A(v', a'), v \neq v'.$$

When running Gibbs sampling, we group Q by the first field v. Notice that the corresponding group of tuples in Q contains all variables in the Markov blanket $\mathbf{mb}(v)$ along with all the factor IDs incident to v. This is all the information we need to generate a sample. For each group, corresponding to a variable v, we sample a new value (denoted by a) for v according to the conditional probability

	Reads		Writes	Storage
	from A	from E	A	
Lazy	$\lvert\mathbf{mb}(v)\rvert$	d_v	1	$O(\lvert E\rvert + \lvert A\rvert)$
V-CoC	$\lvert\mathbf{mb}(v)\rvert$	0	1	$O(\sum_v \lvert\mathbf{mb}(v)\rvert + \lvert A\rvert)$
F-CoC	0	d_v	d_v	$O(\lvert E\rvert)$
Eager	0	0	$\lvert\mathbf{mb}(v)\rvert$	$O(\sum_v \lvert\mathbf{mb}(v)\rvert)$

Table 5.1: I/O costs for sampling one variable under different materialization strategies. For a variable v, d_v is the number of factors in which v participates. Reads (resp. writes) are random reads (resp. random writes). The cost for each strategy is the total number of reads and writes.

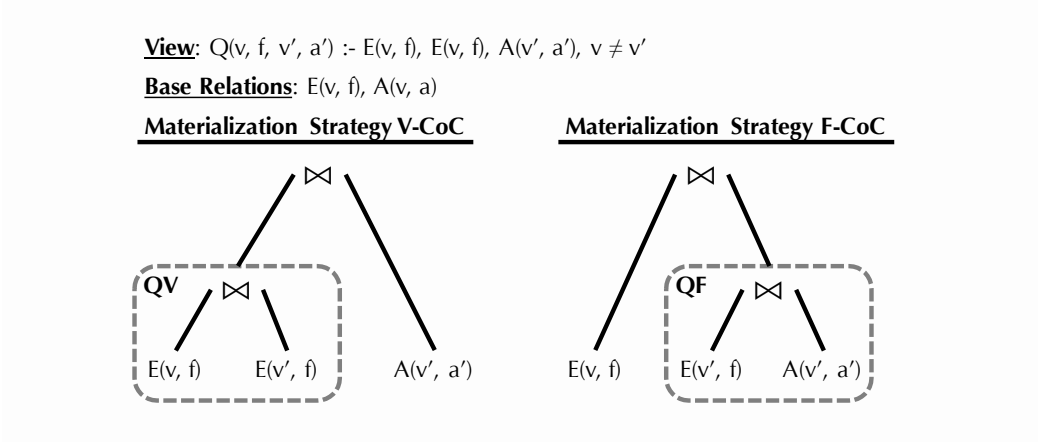

Figure 5.1: Strategies V-CoC and F-CoC.

$\Pr[v|\mathbf{mb}(v)]$. The twist is that after we obtain a, we must update A before we proceed to the next variable to be sampled. In our implementation, we proceed through the groups in a random order.[3]

After one pass through Q, we obtain a new possible world (represented by A). We repeat this process to obtain multiple samples. By counting the number of occurrences of an event, e.g., a variable taking a particular value, we can use these samples to perform marginal inference.

We describe how we optimize the data access to Q using classical data management techniques such as view materialization and page-oriented layout. To study these tradeoffs, we implement a simple storage system. We store E and A using slotted pages [153] and a single-pool buffer manager.[4]

5.1.1.2 Materializing the Factor Graph

The view Q involves a three-way join. All join operators perform an index nested-loop join (see Figure 5.1) with a small twist: the join keys are also *record IDs*, hence we do not need to perform an actual index look-up to find the appropriate page. We examine materialization strategies to improve the performance of these joins.[5]

Materialization can reduce the number of random reads. However, a key twist is that the base relation A is updated after we examine each group. Thus, if we replicate A we could incur many random writes. We study this tradeoff by comparing four different materialization strategies in terms of random read/write costs and space requirements of different strategies described as follows.

- **Lazy:** we only materialize base tables. This strategy incurs the most random reads for on-the-fly joins, but the fewest random writes.
- **V-CoC:** we co-cluster on the variable side

$$QV(v, f, v') \leftarrow E(v, f), E(v', f), v \neq v'$$

  Compared to the lazy strategy, this strategy eliminates random reads on E and retains a single copy of A.

- **F-CoC:** we co-cluster on the factor side

$$QF(f, v', a) \leftarrow E(v', f), A(v', a)$$

  Compared to the lazy strategy, this strategy eliminates random reads on A at the cost of more random writes to update A within QF.

- **Eager:** we eagerly materialize Q. This strategy eliminates all random reads at the cost of high random writes during the core operation.

[3] Our strategy is independent of the order. The order, however, empirically does change the convergence rate, and it is future work to understand the tradeoff of order and convergence.

[4] We use variable and factor IDs as record IDs, and so can look up the column v or f in both E and A using one random access (similar to RID lists [153, ch. 16]).

[5] Since we run many iterations of Gibbs sampling, the construction cost of materialized views is often smaller than the cost of running Gibbs sampling in all strategies. (In all of our experiments, the construction cost is less than 25% of the total run time.)

Figure 5.1 illustrates the two co-clustering strategies.

From Table 5.1, we see that V-CoC dominates Lazy and F-CoC dominates Eager in terms of random accesses (Assuming each factor contains at least two variables, $|\mathbf{mb}(v)| \geq 2d_v$). Our experiments confirm these analytic models (see Section 5.1.2.3). Therefore, our system selects between V-CoC and F-CoC. To determine which approach to use, our system selects the materialization strategy with the smallest random I/O cost according to our cost model.

5.1.1.3 Page-oriented Layout

With either V-CoC or F-CoC, Q is an index nested-loop join between one relation clustered on variables and another relation clustered on factors. How the data are organized into pages impacts I/O efficiency in any environment.

We formalize the problem of page-oriented layout for Gibbs sampling as follows, GLAYOUT. The input to the problem is a tuple (V, F, E, μ, S, P) where (V, F, E) define a factor graph; that is, $V = \{v_1, \ldots, v_N\}$ is a set of variables, $F = \{f_1, \ldots, f_M\}$ is the set of factors, and $E = \{(v, f) \mid v \in \text{vars}(f)\}$ defines the edge relation. The order μ is a total order on the variables, V, which captures the fact that at each iteration of Gibbs sampling, one scans the variables in V in a random order, and S the page size (i.e., the maximum number of variables a page can store), and P the set of pages.

Any solution for GLAYOUT is a tuple (α, β, π) where $\alpha : V \mapsto P$ (resp. $\beta : F \mapsto P$) map variables (resp. factors) to pages. The order $\pi = (e_1, \ldots, e_L)$ defines the order of edges that the algorithm visits. That is, given a fixed variable visit order $\mu = (v_1, \ldots, v_N)$, we only consider tuple orders π that respect μ; we denote this set of orders as $\Pi(\mu)$.[6]

As we will see, it is possible in Gibbs sampling to construct an *optimal* page eviction strategy. For the moment, to simplify our presentation, we assume that there are only two buffer pages: one for variables and one for factors. We return to this point later. Then any ordering $\pi = (e_1, \ldots, e_L)$ would incur an I/O cost (for fetching factors from disk):

$$\text{cost}(\pi, \beta) = 1 + \sum_{i=2}^{L} \mathbb{I}\left[\beta(e_i.f) \neq \beta(e_{i-1}.f)\right]$$

The goal is to find an ordering $\pi \in \Pi(\mu)$ and mapping β that minimizes the above I/O cost.

[6] $\Pi(\mu) = \{\pi = (e_1, \ldots, e_L) \mid \forall i, j.1 \leq i \leq j \leq L, e_i.v \preceq_\mu e_j.v\}$, where $x \preceq_\mu y$ indicates that x precedes y in μ.

Algorithm We use the following simple heuristic to construct (α, β, π) ordering F: we sort the factors in F in dictionary order by μ, that is, by the position of the earliest variable that occurs in a given factor. We then greedily pack F-tuples onto disk pages in this order. We show empirically that this layout has one order of magnitude improvement over randomly ordering and paging tuples.

We find that extending this heuristic for better performance is theoretically challenging:

Proposition 5.1. *Assuming* P≠NP*, an algorithm does not exist that runs in polynomial time to find the optimal solution to* GLAYOUT. *More strongly, assuming* P≠NP*, no polynomial time algorithm can even guarantee a constant approximation factor for* cost.

We prove this proposition in the Appendix A.1 by encoding the multi-cut partition problem [14]. Under slightly more strict complexity assumptions (about randomized complexity classes), it also follows that getting a good layout *on average* is computationally difficult.

Multi-page Buffer We return to the issue of more than two buffer pages. Since variables are accessed sequentially, MRU is optimal for the variable pages. One could worry that the additional number of buffer pages could be used intelligently to lower the cost. We show that we are able to reduce the multiple-page buffer case to the two-page case (and so an approximation result similar to Proposition 5.1); intuitively, given the instance generated for the two-buffer case, we include extra factors whose role in the reduction is to ensure that any optimal buffering strategy essentially incurs I/O only on the sequence of buffer pages that it would in the two-buffer case. Our proof examines the set of pages in Bélády's [26] optimal strategy, which we describe in the next section.

5.1.1.4 Buffer-Replacement Policy

When a data set does not fit in main memory, we must choose which page to evict from main memory. A key twist here is that we will be going over the same data set many times. After the first pass, we know the full reference sequence for the remainder of the execution. This enables us to use a classical result from Bélády in the 1960s [26] to define a theoretically optimal eviction strategy: *evict the item that will be used latest in the future*.

Recall that we scan variables in sequential order, so MRU is optimal for those pages. However, the factor pages require a bit more care. On the first pass of the data, we store the entire reference sequence of factors in a file, i.e., sequence $f_{i_1}, f_{i_2}, \ldots,$ lists each factor. For each reference, we then

Systems	LR	CRF	LDA	Storage	Parallelism
Elementary	✓	✓	✓	Multiple	Multi-thread
Factorie	✓	✓	✓	RAM	Single-thread
PGibbs	✓	✓	✓	RAM	Multi-thread
OpenBUGS	✓		✓	RAM	Single-thread
MADlib			✓	Database	Multi-thread

Table 5.2: Key features of each system that implements Gibbs sampling. OpenBUGS and MADlib do not support skip-chain CRFs. MADlib supports **LR** but not a full Bayesian (sampling) treatment; its support for LDA is via specialized UDFs.

do a pass over this log to compute when each factor is used next in the sequence. At the end of the first scan, we have a log that consists of pairs of factor IDs and when each factor appears next. The resulting file may be several GB in size. However, during the subsequent passes, we only need the head of this log in main memory. We use this information to maintain, for each frame in the buffer manager, when that frame will be used next.

In our experiments, we evaluate under what situations this optimal strategy is worth the extra overhead. We find that the optimal strategy is close to the standard LRU in terms of run time–even if we allow the potentially unfair advantage of holding the entire reference sequence in main memory. In both cases, the number of page faults is roughly 5%–10% smaller using the optimal approach. However, we found that simple schemes based on MRU/LRU are essentially optimal in two tasks (**LR** and **CRF** in the next section), and in the third task (**LDA** in the next section) the variables share factors that are far apart, and so even the optimal strategy cannot mitigate all random I/O.

5.1.2 Experiments

We validate that (1) our system is able to scale to factor graphs that are larger than main memory, and (2) for inference on factor graphs that are larger than main memory, we achieve throughput that is competitive with specialized approaches. We then validate the details of our technical claims about materialization, page-oriented layout, and buffer-replacement policy that we described.

5.1.2.1 Experimental Setup

We run experiments on three popular statistical models: 1) logistic regression (**LR**), 2) skip-chain conditional random field [182] (**CRF**), and 3) latent Dirichlet allocation (**LDA**). We use **LR** and **CRF** for text chunking, and **LDA** for topic modeling. We select **LR** because it can be solved exactly and so

Models	Bench (1x)			Perf (1,000x)			Scale (100,000x)		
	$\|V\|$	$\|F\|$	Size	$\|V\|$	$\|F\|$	Size	$\|V\|$	$\|F\|$	Size
LR	47K	47K	2MB	47M	47M	2GB	5B	5B	0.19TB
CRF	47K	94K	3MB	47M	94M	3GB	5B	9B	0.3TB
LDA	0.4M	12K	10M	0.4B	10M	9GB	39B	0.2B	0.9TB

Table 5.3: Data sets sizes. We omit the 10x, 100x, and 10,000x cases from this table.

can be used as a simple benchmark. We select **CRF** as it is widely used in text-related applications and inference is often performed with Gibbs sampling, and **LDA** as it is intuitively the most challenging model that is supported by all systems in our experiments.

Data Sets To compare the quality and efficiency with other systems, we use public data sets that we call *Bench*. We run **LR** and **CRF** on CoNLL[7] and **LDA** on AP.[8] For scalability experiments and tradeoff efficiency experiments, we scale up *Bench* from 1x to 100,000x by adding more documents which are randomly selected from a one-day web crawl (5M documents, 400GB). We call the 1,000x data set *Perf* and the 100,000x data set *Scale*. Table 5.3 shows the number of variables, factors, and size.

Metrics We use two metrics to measure the quality: (1) the F1 score of the final result for data sets with ground truth (when ground truth is available) and (2) the *squared loss* [194] between the marginal probabilities that are the output of each sampling system and a gold standard on each data set (when there is no ground truth). For **LR**, we compute the gold standard using exact inference. For **CRF** and **LDA**, it is intractable to compute the exact distribution; and the standard approach is to use the results from Gibbs sampling after running many iterations beyond convergence [194]. In particular, we get an approximate gold standard for both **CRF** and **LDA** on *Bench* by running Gibbs sampling for 10M iterations. For efficiency, we measure the *throughput* as the number of samples produced by a system per second.

Competitor Systems We compare our system with four state-of-the-art Gibbs sampling systems: (1) PGibbs on GraphLab [82], (2) Factorie [128], and (3) OpenBUGS [125], which are main memory systems, and MADlib [93], a scalable in-database implementation of LDA. PGibbs and MADlib[9] are implemented using C++, OpenBUGS is implemented using Pascal and C, and Factorie is implemented

[7] `http://www.cnts.ua.ac.be/conll2000/chunking/`
[8] `http://www.cs.princeton.edu/~blei/lda-c/`
[9] `http://doc.madlib.net/v0.3/group__grp__plda.html`

Setting Name	Page Size	Buffer Size
Sp/Sb	4KB	40KB
Lp/Sb	4MB	40MB
Sp/Lb	4KB	4GB
Lp/Lb	4MB	4GB
Lp/MAXb	4MB	40GB

Table 5.4: Different configuration settings of Elementary. Sp (resp. Lp) means *small (resp. large) page size*; Sb (resp. Lb) means *small (resp. large) buffer-size*.

using Java. We use Greenplum 4.2.1.0 for MADlib. The key features of each system are shown in Table 5.2. For each model (i.e., **LR**, **CRF**, and **LDA**), all systems take the same factor graph as their input. We modify each system to output squared loss after each iteration, and we do not count this time as part of the execution time.

Details of our Prototype We call our prototype system Elementary, and compare three variants of our system by plugging in different storage backends: **EleMM**, **EleFILE**, and **EleHBASE**. We use main memory, traditional unix files, and HBase,[10] respectively, for these three variants. **EleMM** is used to compare with other main memory systems. **EleFILE** and **EleHBASE** use different secondary storage and are used to validate scalability and I/O tradeoffs.

Our system is implemented using C++ and bypasses the OS disk-page cache to support its own buffer manager. We compile all C++ code using GCC 4.7.2 and all Java code using Java 1.7u4. All experiments are run on a RHEL6.1 workstation with two 2.67GHz Intel Xeon CPUs (12 cores, 24 hyper-threaded), 128GB of RAM, and 12×2TB RAID0 drives. All data and temporary files are stored on a RAID, and all software is installed on a separate disk. We use the latest HBase-0.94.1 on a single machine[11] and follow best practices to tune HBase.[12]

We use various page-size/buffer-size combinations, as shown in Table 5.4. These configuration settings correspond to small/large page sizes and small/large buffer sizes. We explored more settings but the high-level conclusions are similar to these four settings so we omit those results. The **Lp/MAXb** setting is used for end-to-end experiments.

[10] `http://hbase.apache.org`

[11] Our system can use HBase on multiple machines to get even higher scalability. We only discuss the one-machine case to be fair to other systems.

[12] http://hbase.apache.org/book/performance.html

	# thread = 1			# threads = 20		
	LR	**CRF**	**LDA**	**LR**	**CRF**	**LDA**
EleMM	24	18	12	12x	9x	6x
EleFILE	34	24	33	9x	6x	4x
EleHBASE	101	70	92	9x	7x	4x
PGibbs	38	42	CRASH	9x	5x	CRASH
MADLib	N/A	N/A	17	N/A	N/A	8x
Factorie	95	120	6	N/A	N/A	N/A
OpenBUGS	150	N/A	CRASH	N/A	N/A	N/A

Table 5.5: The time in seconds (speedup for 20-threads case) needed to achieve squared loss below 0.01 for *Bench* data set. N/A means that the task is not supported.

5.1.2.2 End-to-end Efficiency and Scalability

We validate that our system achieves state-of-the-art quality by demonstrating that it converges to the gold-standard probability distribution on each task. We then compare our system's efficiency and scalability with that of our competitors.

Quality We validate that our system converges to the gold-standard probability distribution on several tasks. We run all systems on *Bench* using the configuration **Lp/MAXb**. We take a snapshot after each system produces a sample; we output the squared loss and F1 score of that snapshot. Table 5.5 shows the time that each system needs to converge to a solution with a squared loss less than 0.01. We chose 0.01 since a smaller loss does not improve the F1 score, i.e., when the loss is less than 0.01, **LR** converges to F1=0.79 and **CRF** to F1=0.81, which are the gold-standard values for these tasks. This validates that all systems achieve the same quality, and thus a more interesting question is to understand the rate at which they achieve the quality.

Efficiency To understand the rate at which a system achieves the gold-standard quality, we run PGibbs, MADlib, Factorie, and OpenBUGS and measure when they are within 0.01 of the optimal loss. If a system can take advantage of multi-threading, we also run it with 20 threads and report the speedup factor compared with one thread. We chose our materialization strategy to be consistent with what is hard coded in state-of-the-art competitors, i.e., V-CoC for **LR** and **CRF**, and F-CoC for **LDA**. Table 5.5 shows the results.

When there is one thread and all the data fit in main memory, we observe that all systems converge to gold-standard probability distribution within roughly comparable times. This is likely due to the fact that main memory Gibbs sampling uses a set of well-known techniques, which are widely

implemented. There are, however, some minor differences in runtime. On **LR** and **CRF**, EleMM has comparable efficiency to PGibbs, but is slightly faster. After reviewing PGibbs' code, we believe the efficiency difference ($<$2x) is caused by the performance overhead of PGibbs explicitly representing factor functions as a table. For **LR** and **CRF**, EleMM is 4–10x faster than Factorie, and we believe that this is because Factorie is written in Java (not C++). OpenBUGS is more than one order of magnitude slower than EleMM. This difference in OpenBUGS is due to the inefficiency in how it records the samples of each variable. PGibbs requires explicit enumeration of all outcomes for each factor, and so the input size to PGibbs is exponential in the size of the largest factor. As **LDA** involves factors with hundreds or more variables, we could not run **LDA** on PGibbs. OpenBUGS crashed on **LDA** while compiling the model and data with the error message "illegal memory read." Elementary with secondary storage backends has similar performance trends, but is overall 2–5x slower than EleMM, due to the overhead of I/O.

For 20-thread cases, we observe speedups for all multi-threading systems. EleFILE and EleHBASE gets smaller speedups compared with EleMM because of the overhead of I/O requests. PGibbs also gets slightly smaller speedups than EleMM, and we believe that this marginal difference is caused by the overhead of MPI, which is used by PGibbs.

Scalability We validate that our system can scale to larger data sets by using secondary storage backends. We run all systems on data sets scaling from 1x (*Bench*) to 100,000x (*Scale*) using one thread and **Lp/MAXb**. We let each system run for 24 hours and stop it afterwards. Figure 5.2 shows the results for **LR** and **LDA**. We also run a baseline system, **Baseline**, that uses the file system as storage and disables all of our optimizations (lazy materialization, and no buffer management).

Not surprisingly, only systems that use secondary storage backends, i.e., EleFILE, EleHBASE, and MADlib (only for LDA), scale to the largest data sets; in contrast, main memory systems crash or thrash at scaling factors of 10x or more. As the core operation is scan based, it also not surprising that each system scales up almost linearly (if it is able to run).

However, the performance of the various approaches can be quite different. The Baseline system is three orders of magnitude slower than EleMM (it does not finish the first iteration within 24 hours on the 100x scale factor). This shows that buffer management is crucial to implementing an I/O-efficient Gibbs sampler. Due to higher I/O overheads, EleHBASE is 3x slower than EleFILE.

MADlib uses PostgreSQL as the storage backend, and is 2x faster than EleFILE. However, MADlib

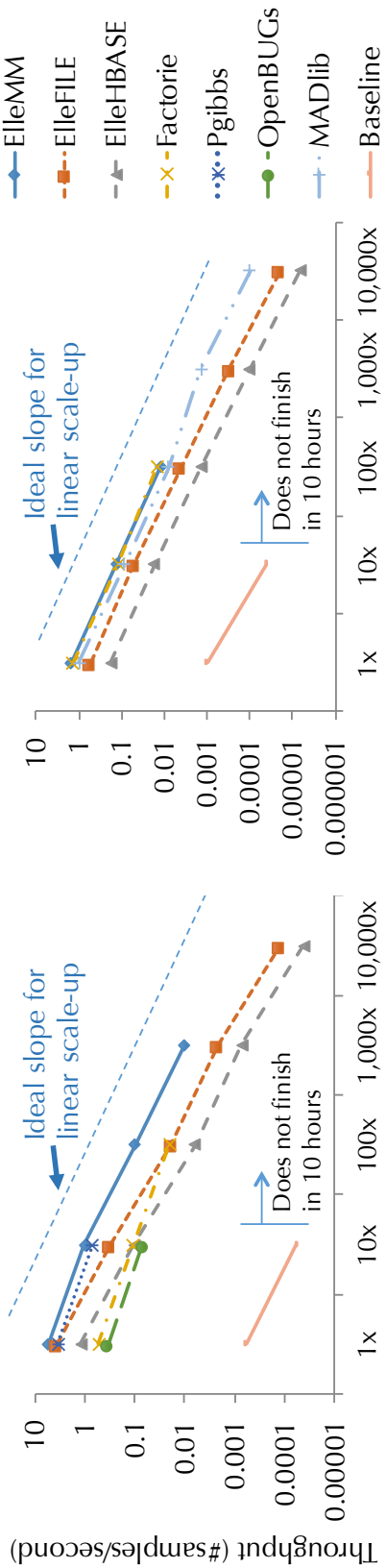

Figure 5.2: Scalability of Different Systems.

Model	A	E	QV	QF	Q
LR	0.18	1.4	1.4	1.4	1.4
CRF	0.18	2.0	3.2	2.0	3.2
LDA	1.66	9.0	100T+	9.0	100T+

Table 5.6: Size of intermediate state in *Perf* dataset (see Sec. 5.1.1). All sizes in GB, except where noted.

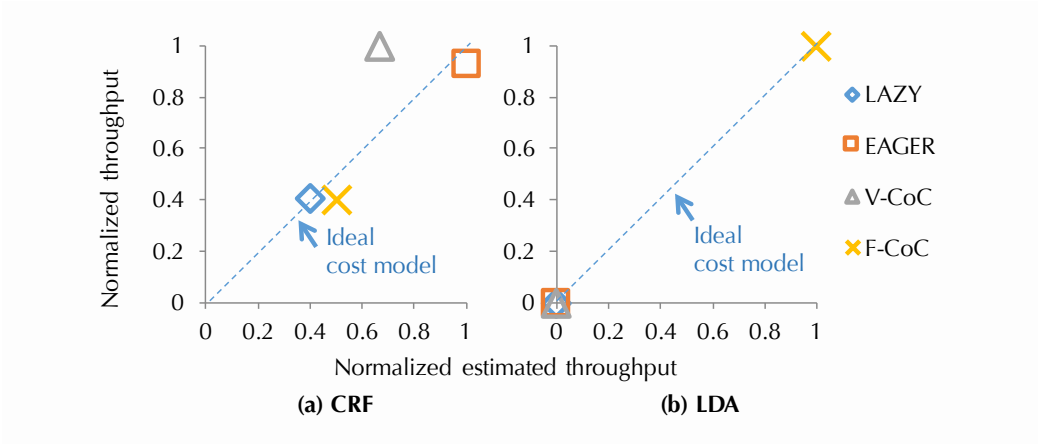

Figure 5.3: Accuracy of cost model of different materialization strategies for Gibbs sampling.

uses an approximate sampler for LDA, while our system implements an exact sampler. If we allow EleFILE to run this approximate sampler, EleFILE is between 10-20% faster.

5.1.2.3 I/O tradeoffs

We validate that both the materialization tradeoff and the page-oriented layout tradeoff in Section 5.1.1 affect the throughput of Gibbs sampling on factor graphs that are larger than main memory, while the buffer-replacement tradeoff only has a marginal impact. We also validate that we can automatically select near-optimal strategies based on our I/O cost model.

View Materialization We validate that (1) the co-clustering strategies that we explored in Section 5.1.1 outperform both Lazy and Eager strategies, and (2) neither of the co-clustering strategies dominates the other. We compare the four materialization strategies; our GLAYOUT heuristic page-oriented layout is used. We report results for both EleFILE and EleHBASE on **CRF** and **LDA**.

As shown in Figure 5.4(a), for **CRF**, V-CoC dominates other strategies for all settings. We looked into the buffer manager; we found that (1) V-CoC outperforms Lazy (resp. F-CoC) by incurring 75% fewer read misses on **Sp/Sb** (resp. **Sp/Lb**); and (2) V-CoC incurs 20% fewer dirty page writes

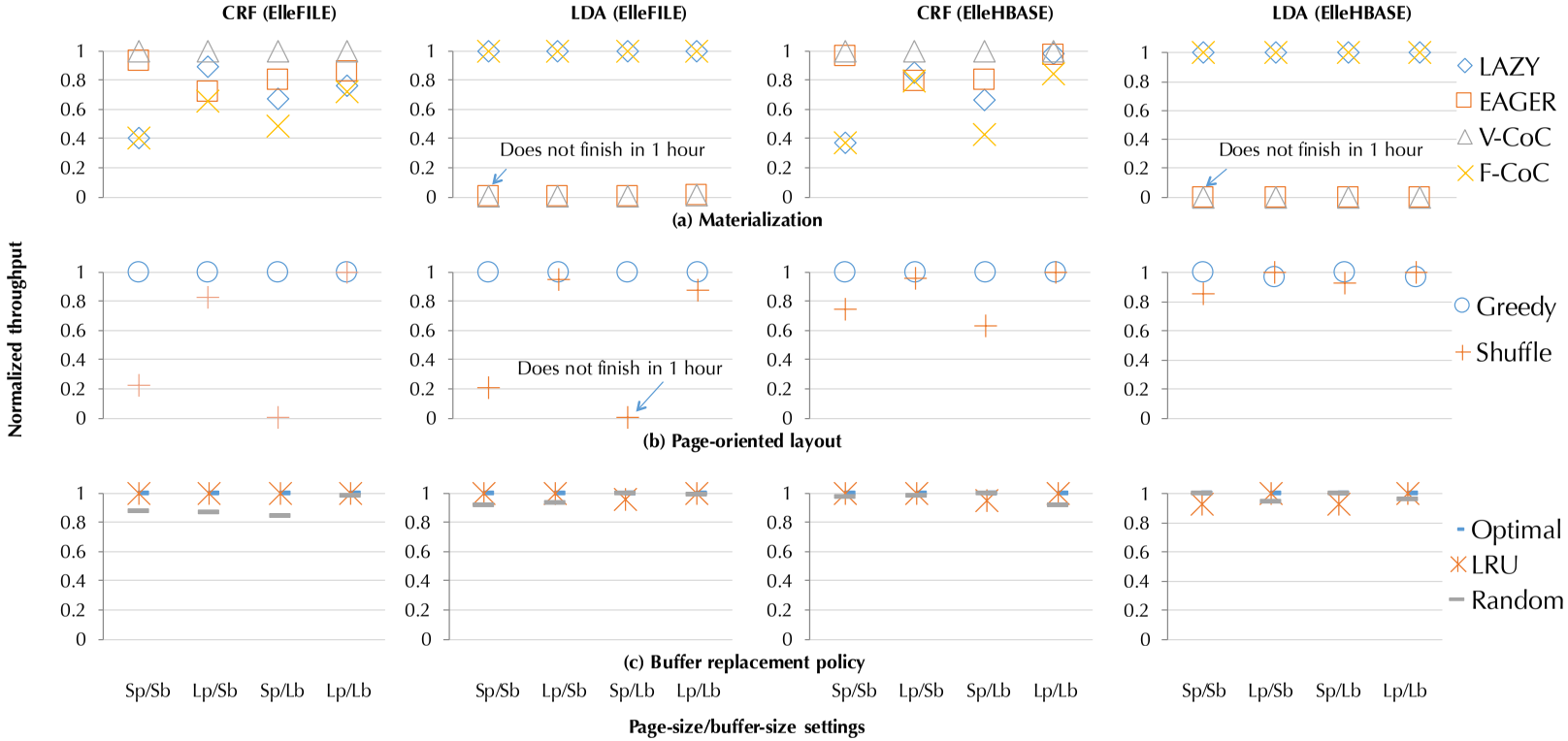

Figure 5.4: I/O tradeoffs on *Perf* dataset. Recall that Sp (resp. Lp) means *small (resp. large) page size*; Sb (resp. Lb) means *small (resp. large) buffer size*. See Table 5.4 for the exact definitions of page and buffer size settings

than Eager. The situation, however, is reversed in **LDA**. Here, F-CoC dominates, as both V-CoC and Eager fail to run **LDA** as they would require 100TB+ of disk space for materialization. Thus, neither co-clustering strategy dominates the other, but one always dominates both Eager and Lazy. The same observation holds for both EleFILE and EleHBASE.

A key difference between these tasks is that the number of variables in most factors in **LDA** is much larger (can be larger than 1,000) than **LR** and **CRF** (fewer than 3). Thus, some pre-materialization strategies are expensive in **LDA**. On the other hand, for **LR** and **CRF**, the time needed to look up factors is the bottleneck (which is optimized by V-CoC).

We then validate that one can automatically select between different materialization strategies by using the cost model shown in Table 5.1. For each model and materialization strategy, we estimated the throughput as the inverse of the estimated total amount of I/O. For each materialization strategy, we plot its estimated and actual throughput. Figure 5.3 shows the results for EleFILE (**Sp/Lb**). We can see that the throughput decreases when the estimated throughput decreases. Based on this cost model, we can select the near-optimal materialization strategy.

Page-oriented Layout We validate that our heuristic ordering strategy can improve sampling throughput over a random ordering. We focus on the F-CoC materialization strategy here because the V-CoC setting has similar results. We compare two page-oriented layout strategies: (1) **Shuffle**, in which we randomly shuffle the factor table, and (2) **Greedy**, which use our greedy heuristic to layout the factor table. As shown in Figure 5.4(b), **Greedy** dominates **Shuffle** on all data sets in both settings. For **CRF**, the heuristic can achieve two orders of magnitude of speedup. We found that for **Sp/Lb**, heuristic ordering incurs two orders of magnitude fewer page faults than random ordering. These results show that the tradeoff in page-oriented layout impacts the throughput of Gibbs sampling on factor graphs that do not fit in memory.

Buffer-Replacement Policy We validate that the optimal buffer-replacement strategy can only achieve a marginal improvement of sampling throughput over LRU. We compare three settings: (1) **Optimal**, which uses the optimal caching strategy on tables with random access, (2) **LRU**, which uses LRU on tables with random access; and (3) **Random**, which uses a random replacement policy. We use MRU on tables with sequential scan. We use V-CoC for **LR** and **CRF**, F-CoC for **LDA**, and **Greedy** for all page-oriented layouts because they are the optimal strategies for these tasks. As

shown in Figure 5.4(c), **Optimal** achieves 10% higher throughput than **Random** for **CRF**, and 5% higher throughput than **LRU** for **LDA**. For **CRF**, the access pattern of factors is much like a sequence scan, and therefore **LRU** is near-optimal. As **Optimal** requires non-trivial implementation and is not implemented in existing data processing systems, an engineer may opt against implementing it in a production system.

Discussion On this small set of popular tasks, experiments demonstrate that our prototype can achieve competitive (and sometimes better) throughput and scalability than state-of-the-art systems for Gibbs sampling from factor graphs that are larger than main memory. What is interesting to us about this result is that we used a set of generic optimizations inspired by classical database techniques. Of course, in any given problem, there may be problem-specific optimizations that can dramatically improve throughput. For example, in higher-level languages like MCDB or Factorie, there may be additional optimization opportunities. Our goal, however, is not to exhaustively enumerate such optimizations; instead, we view the value of our work as articulating a handful of tradeoffs that may be used to improve the throughput of either specialized or generic systems for Gibbs sampling from factor graphs. These tradeoffs have not been systematically studied in previous work. Also, our techniques are orthogonal to optimizations that choose between various sampling methods to improve runtime performance, e.g., Wang et al. [189]. A second orthogonal direction is distributing the data to many machines; such an approach would allow us to achieve higher scalability and performance. We believe that the optimizations that we describe are still useful in the distributed setting. However, there are new tradeoffs that may need to be considered, e.g., communication and replication tradeoffs are obvious areas to explore.

5.1.3 Conclusion to Scalable Gibbs Sampling

We studied how to run Gibbs sampling over factor graphs, the abstraction DeepDive used for statistical inference and learning phase. Our goal is to make a highly scalable Gibbs sampler. All other things being equal, a Gibbs sampler that produces samples with higher throughput allows us to obtain high quality more quickly. Thus, the central technical challenge is how to create a high-throughput sampler. In contrast to previous approaches that optimize sampling by proposing new algorithms, we examined whether or not traditional database optimization techniques could be used to improve the core operation of Gibbs sampling. In particular, we study the impact of a handful of classical

data management tradeoffs on the throughput of Gibbs sampling on factor graphs that are larger than main memory. Our work articulates a handful of tradeoffs that may be used to improve the throughput of such systems, including materialization, page-oriented layout, and buffer-management tradeoffs. After analytically examining the tradeoff space for each technique, we described novel materialization strategies and a greedy page-oriented layout strategy.

Our experimental study found that our techniques allowed us to achieve up to two orders of magnitude improvement in throughput over classical techniques. Using a classical result due to Bélády, we implemented the optimal page-replacement strategy, but found empirically that it offered only modest improvement over traditional techniques. Overall, we saw that by optimizing for only these classical tradeoffs, we were able to construct a prototype system that achieves competitive (and sometimes much better) throughput than prior Gibbs sampling systems for factor graphs.

5.2 Efficient In-memory Statistical Analytics

We now focus on the task of running statistical inference and learning when the data fit in main memory. In this section, we extend our scope boarder to not only consider factor graph, but also a more general class of problem called statistical analytics, that contains more (sometimes simpler) models such as linear regression, support vector machines, or logistic regression. As we will show in Section 5.2.4, this study allows us to apply what we learned from statistical analytics to factor graph.

Statistical analytics is one of the hottest topics in data-management research and practice. Today, even small organizations have access to machines with large main memories (via Amazon's EC2) or for purchase at $5/GB. As a result, there has been a flurry of activity to support main-memory analytics in both industry (Google Brain [116], Impala, and Pivotal) and research (GraphLab [123], and MLlib [176]). Each of these systems picks one design point in a larger tradeoff space. The goal of this section is to define and explore this space. We find that today's research and industrial systems under-utilize modern hardware for analytics—sometimes by two orders of magnitude. We hope that our study identifies some useful design points for the next generation of such main-memory analytics systems.

Throughout, we use the term *statistical analytics* to refer to those tasks that can be solved by *first-order methods*–a class of iterative algorithms that use gradient information; these methods are the core algorithm in systems such as MLlib, GraphLab, and Google Brain. Our study examines

analytics on commodity multi-socket, multi-core, non-uniform memory access (NUMA) machines, which are the de facto standard machine configuration and thus a natural target for an in-depth study. Moreover, our experience with several enterprise companies suggests that, after appropriate preprocessing, a large class of enterprise analytics problems fit into the main memory of a single, modern machine. While this architecture has been recently studied for traditional SQL-analytics systems [51], it has not been studied for *statistical* analytics systems.

Statistical analytics systems are different from traditional SQL-analytics systems. In comparison to traditional SQL-analytics, the underlying methods are intrinsically robust to error. On the other hand, traditional statistical theory does not consider which operations can be efficiently executed. This leads to a fundamental tradeoff between *statistical efficiency* (how many steps are needed until convergence) and *hardware efficiency* (how efficiently those steps can be carried out).

To describe such tradeoffs more precisely, we describe the setup of the analytics tasks that we consider in this section. The input data is a matrix in $\mathbb{R}^{N \times d}$ and the goal is to find a vector $x \in \mathbb{R}^d$ that minimizes some (convex) loss function, say the logistic loss or the hinge loss (SVM). Typically, one makes several complete passes over the data while updating the model; following conventions, we call each such pass an *epoch*. There may be some communication at the end of the epoch, e.g., in bulk-synchronous parallel systems such as Spark [201]. We identify three tradeoffs that have not been explored in the literature: (1) *access methods for the data*, (2) *model replication*, and (3) *data replication*. Current systems have picked one point in this space; we explain each space and discover points that have not been previously considered. Using these new points, we can perform 100$\times$ faster than previously explored points in the tradeoff space for several popular tasks.

Access Methods Analytics systems access (and store) data in either row-major or column-major order. For example, systems that use *stochastic gradient descent methods* (SGD) access the data row-wise; examples include MADlib [93] in Impala and Pivotal, Google Brain [116], and MLlib in Spark [176]; and *stochastic coordinate descent methods* (SCD) access the data column-wise; examples include GraphLab [123], Shogun [175], and Thetis [177]. These methods have essentially identical statistical efficiency, but their wall-clock performance can be radically different due to hardware efficiency. However, this tradeoff has not been systematically studied. We introduce a storage abstraction that captures the access patterns of popular statistical analytics tasks and a prototype called DimmWitted. In particular, we identify three access methods that are used in popular analytics

tasks, including standard supervised machine learning models such as SVMs, logistic regression, and least squares; and more advanced methods such as neural networks and Gibbs sampling on factor graphs. For different access methods for the same problem, we find that the time to converge to a given loss can differ by up to 100×.

We also find that no access method dominates all others, so an engine designer may want to include both access methods. To show that it may be possible to support both methods in a single engine, we develop a simple cost model to choose among these access methods. We describe a simple cost model that selects a nearly optimal point in our data sets, models, and different machines.

Data and Model Replication We study two sets of tradeoffs: the level of granularity, and the mechanism by which mutable state and immutable data are shared in analytics tasks. We describe the tradeoffs we explore in both (1) mutable state sharing, which we informally call *model replication*, and (2) *data replication*.

(1) Model Replication During execution, there is some state that the task mutates (typically an update to the model). We call this state, which may be shared among one or more processors, a *model replica*. We consider three different granularities at which to share model replicas:

- The PerCPU approach treats a NUMA machine as a distributed system in which every core is treated as an individual machine, e.g., in bulk-synchronous models such as MLlib on Spark or event-driven systems such as GraphLab. These approaches are the classical shared-nothing and event-driven architectures, respectively. In PerCPU, the part of the model that is updated by each core is only visible to that core until the end of an epoch. This method is efficient and scalable from a hardware perspective, but it is less statistically efficient, as there is only coarse-grained communication between cores.

- The PerMachine approach acts as if each processor has uniform access to memory. This approach is taken in Hogwild! [141] and Google Downpour [66]. In this method, the hardware takes care of the coherence of the shared state. The PerMachine method is statistically efficient due to high communication rates, but it may cause contention in the hardware, which may lead to suboptimal running times.

- A natural hybrid is PerNode, in which a node is a NUMA node that contains multiple CPU cores; this method uses the fact that PerCPU communication through the last-level cache (LLC) is dramatically faster than communication through remote main memory. This method is novel; for some models, PerNode can be an order of magnitude faster.

Because model replicas are mutable, a key question is *how often should we synchronize model replicas?* We find that it is beneficial to synchronize the models as much as possible—so long as we do not impede throughput to data in main memory. A natural idea, then, is to use PerMachine sharing, in which the hardware is responsible for synchronizing the replicas. However, this decision can be suboptimal, as the cache-coherence protocol may stall a processor to preserve coherence, but this information may not be worth the cost of a stall from a statistical efficiency perspective. We find that the PerNode method, coupled with a simple technique to batch writes across sockets, can dramatically reduce communication and processor stalls. The PerNode method can result in an over $10\times$ runtime improvement. This technique depends on the fact that we do not need to maintain the model consistently: we are effectively delaying some updates to reduce the total number of updates across sockets (which lead to processor stalls).

(2) Data Replication The data for analytics is immutable, so there are no synchronization issues for data replication. The classical approach is to partition the data to take advantage of higher aggregate memory bandwidth. However, each partition may contain skewed data, which may slow convergence. Thus, an alternate approach is to replicate the data fully (say, per NUMA node). In this approach, each node accesses that node's data in a different order, which means that the replicas provide non-redundant statistical information; in turn, this reduces the variance of the estimates based on the data in each replicate. We find that for some tasks, fully replicating the data four ways can converge to the same loss almost $4\times$ faster than the sharding strategy.

Summary of Contributions Westudy the three tradeoffs listed above for main-memory statistical analytics systems. These tradeoffs are not intended to be an exhaustive set of optimizations, but they demonstrate our main conceptual point: *treating NUMA machines as distributed systems or SMP is suboptimal for statistical analytics*. We design a storage manager, DimmWitted, that shows it is possible to exploit these ideas on real data sets. Finally, we evaluate our techniques on multiple real datasets, models, and architectures.

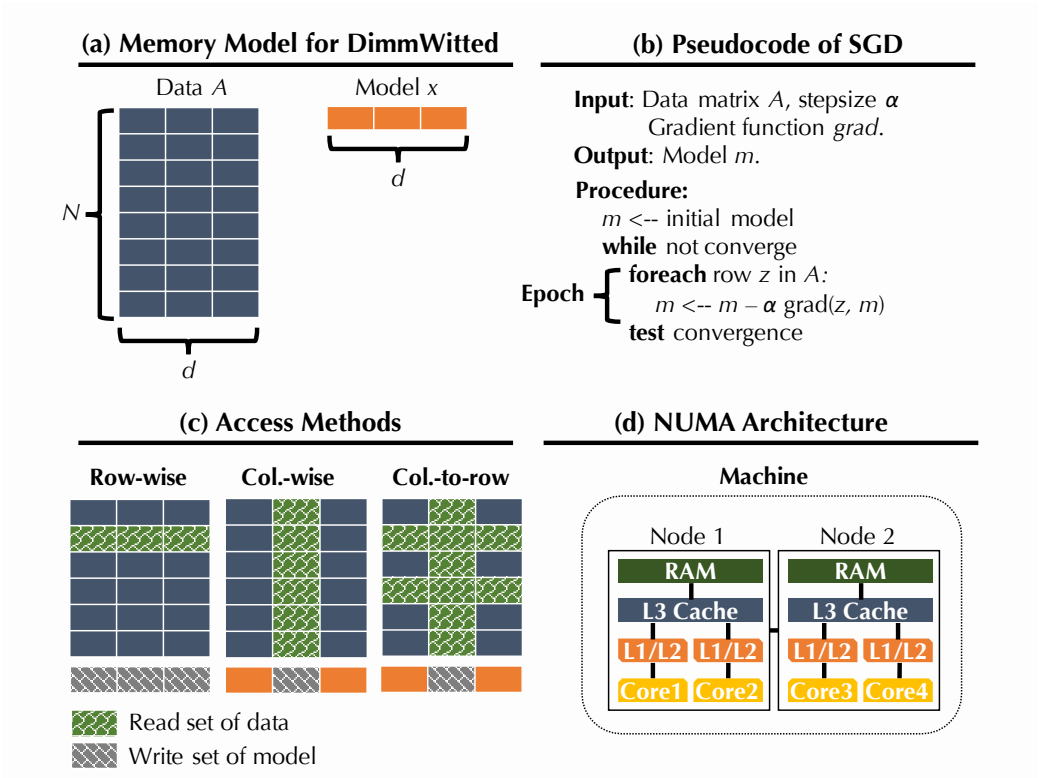

Figure 5.5: Illustration of (a) DimmWitted's Memory Model, (b) Pseudocode for SGD, (c) Different Statistical Methods in DimmWitted and Their Access Patterns, and (d) NUMA Architecture.

5.2.1 Background

In this section, we describe the memory model for DimmWitted, which provides a unified memory model to implement popular analytics methods. Then, we recall some basic properties of modern NUMA architectures.

Data for Analytics The data for an analytics task is a pair (A, x), which we call the data and the model, respectively. For concreteness, we consider a matrix $A \in \mathbb{R}^{N \times d}$. In machine learning parlance, each row is called an *example*. Thus, N is often the number of examples and d is often called the dimension of the model. There is also a model, typically a vector $x \in \mathbb{R}^d$. The distinction is that the data A is read-only, while the model vector, x, will be updated during execution. From the perspective of this section, the important distinction we make is that data is an immutable matrix, while the model (or portions of it) are mutable data.

First-Order Methods for Analytic Algorithms DimmWitted considers a class of popular algorithms called *first-order methods*. Such algorithms make several passes over the data; we refer to each such pass as an *epoch*. A popular example algorithm is stochastic gradient descent (SGD), which is widely used by web-companies, e.g., Google Brain and VowPal Wabbit [4], and in enterprise systems such as Pivotal, Oracle, and Impala. Pseudocode for this method is shown in Figure 5.5(b). During each epoch, SGD reads a single example z; it uses the current value of the model and z to estimate the derivative; and it then updates the model vector with this estimate. It reads each example in this loop. After each epoch, these methods test convergence (usually by computing or estimating the norm of the gradient); this computation requires a scan over the complete dataset.

5.2.1.1 Memory Models for Analytics

We design DimmWitted's memory model to capture the trend in recent high-performance sampling and statistical methods. There are two aspects to this memory model: the *coherence level* and the *storage layout*.

Coherence Level Classically, memory systems are coherent: reads and writes are executed atomically. For analytics systems, we say that a memory model is *coherent* if reads and writes of the entire model vector are atomic. That is, access to the model is enforced by a critical section. However, many modern analytics algorithms are designed for an *incoherent* memory model. The Hogwild! method showed that one can run such a method in parallel without locking but still provably converge. The Hogwild! memory model relies on the fact that writes of individual components are atomic, but it does not require that the entire vector be updated atomically. However, atomicity at the level of the cacheline is provided by essentially all modern processors. Empirically, these results allow one to forgo costly locking (and coherence) protocols. Similar algorithms have been proposed for other popular methods, including Gibbs sampling [103, 173], stochastic coordinate descent (SCD) [158, 175], and linear systems solvers [177]. This technique was applied by Dean et al. [66] to solve convex optimization problems with billions of elements in a model. This memory model is distinct from the classical, *fully coherent* database execution [153].

The DimmWitted prototype allows us to specify that a region of memory is coherent or not. This region of memory may be shared by one or more processors. If the memory is only shared per thread,

Algorithm	Access Method	Implementation
Stochastic Gradient Descent	Row-wise	MADlib, Spark, Hogwild!
Stochastic Coordinate Descent	Column-wise Column-to-row	GraphLab, Shogun, Thetis

Table 5.7: Algorithms and Their Access Methods.

then we can simulate a shared-nothing execution. If the memory is shared per machine, we can simulate Hogwild!.

Access Methods We identify three distinct access paths used by modern analytics systems, which we call row-wise, column-wise, and column-to-row. They are graphically illustrated in Figure 5.5(c). Our prototype supports all three access methods. All of our methods perform several epochs, that is, passes over the data. However, the algorithm may iterate over the data row-wise or column-wise.

- In *row-wise access*, the system scans each row of the table and applies a function that takes that row, applies a function to it, and then updates the model. This method may write to all components of the model. Popular methods that use this access method include stochastic gradient descent, gradient descent, and higher-order methods (such as l-BFGS).
- In *column-wise access*, the system scans each column j of the table. This method reads just the j component of the model. The write set of the method is typically a single component of the model. This method is used by stochastic coordinate descent.
- In *column-to-row access*, the system iterates conceptually over the columns. This method is typically applied to sparse matrices. When iterating on column j, it will read all rows in which column j is non-zero. This method also updates a single component of the model. This method is used by non-linear support vector machines in GraphLab and is the de facto approach for Gibbs sampling.

DimmWitted is free to iterate over rows or columns in essentially any order (although typically some randomness in the ordering is desired). Table 5.7 classifies popular implementations by their access method.

Name (abbrv.)	#Node	#Cores/Node	RAM/Node (GB)	CPU Clock (GHz)	LLC (MB)
local2 (l2)	2	6	32	2.6	12
local4 (l4)	4	10	64	2.0	24
local8 (l8)	8	8	128	2.6	24
ec2.1 (e1)	2	8	122	2.6	20
ec2.2 (e2)	2	8	30	2.6	20

Table 5.8: Summary of Machines. Tested with STREAM [30], local2 has intra-node bandwidth 6GB/s and inter-node QPI 12 GB/s.

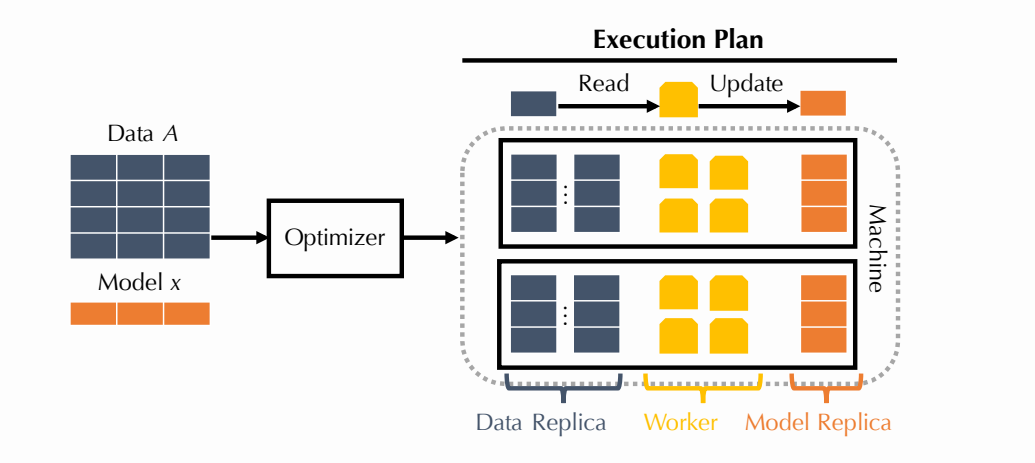

Figure 5.6: Illustration of DimmWitted's engine.

5.2.1.2 Architecture of NUMA Machines

We briefly describe the architecture of a modern NUMA machine. As illustrated in Figure 5.5(d), a NUMA machine contains multiple NUMA nodes. Each node has multiple cores and processor caches, including the L3 cache. Each node is directly connected to a region of DRAM. NUMA nodes are connected to each other by buses on the main board; in our case, this connection is the Intel Quick Path Interconnects (QPIs), which has a bandwidth as high as 25.6GB/s. To access DRAM regions of other NUMA nodes, data is transferred across NUMA nodes using the QPI. These NUMA architectures are cache coherent, and the coherency actions use the QPI. Table 5.8 describes the configuration of each machine that we use in this section. Machines controlled by us have names with the prefix "local"; the other machines are Amazon EC2 configurations.

Tradeoff	Strategies	Existing Systems
Access Methods	Row-wise	SP, HW
	Column-wise	GL
	Column-to-row	GL
Model Replication	Per Core	GL, SP
	Per Node	
	Per Machine	HW
Data Replication	Sharding	GL, SP, HW
	Full Replication	

Table 5.9: A Summary of DimmWitted's Tradeoffs and Existing Systems (GraphLab (GL), Hogwild! (HW), Spark (SP)).

5.2.2 The DimmWitted Engine

We describe the tradeoff space that DimmWitted's optimizer considers, namely (1) access method selection, (2) model replication, and (3) data replication. To help understand the statistical-versus-hardware tradeoff space, we present some experimental results in a *Tradeoffs* paragraph within each subsection. We describe implementation details for DimmWitted in Appendix A.2.

5.2.2.1 System Overview

We describe analytics tasks in DimmWitted and the execution model of DimmWitted.

System Input For each analytics task that we study, we assume that the user provides data $A \in \mathbb{R}^{N \times d}$ and an initial model that is a vector of length d. In addition, for each access method listed above, there is a function of an appropriate type that solves the same underlying model. For example, we provide both a row- and column-wise way of solving a support vector machine. Each method takes two arguments; the first is a pointer to a model.

- f_{row} captures the the row-wise access method, and its second argument is the index of a single row.
- f_{col} captures the column-wise access method, and its second argument is the index of a single column.
- f_{ctr} captures the column-to-row access method, and its second argument is a pair of one column index and a set of row indexes. These rows correspond to the non-zero entries in a data matrix for a single column.[13]

[13]Define $S(j) = \{i : a_{ij} \neq 0\}$. For a column j, the input to f_{ctr} is a pair $(j, S(j))$.

Algorithm	Read	Write (Dense)	Write (Sparse)
Row-wise	$\sum_i n_i$	dN	$\sum_i n_i$
Column-wise	$\sum_i n_i$	d	d
Column-to-row	$\sum_i n_i^2$	d	d

Table 5.10: Per Epoch Execution Cost of Row- and Column-wise Access. The Write column is for a single model replica. Given a dataset $A \in \mathbb{R}^{N \times d}$, let n_i be the number of non-zero elements a_i.

Each of the functions modifies the model to which they receive a pointer in place. However, in our study, f_{row} can modify the whole model, while f_{col} and f_{ctr} only modify a single variable of the model. We call the above tuple of functions a *model specification*. Note that a model specification contains either f_{col} or f_{ctr} but typically not both.

Execution Given a model specification, our goal is to generate an execution plan. An execution plan, schematically illustrated in Figure 5.6, specifies three things for each CPU core in the machine: (1) a subset of the data matrix to operate on, (2) a replica of the model to update, and (3) the access method used to update the model. We call the set of replicas of data and models *locality groups*, as the replicas are described physically; i.e., they correspond to regions of memory that are local to particular NUMA nodes, and one or more workers may be mapped to each locality group. The data assigned to distinct locality groups may overlap. We use DimmWitted's engine to explore three tradeoffs:

(1) Access methods, in which we can select between either the row or column method to access the data.

(2) Model replication, in which we choose how to create and assign replicas of the model to each worker. When a worker needs to read or write the model, it will read or write the model replica that it is assigned.

(3) Data replication, in which we choose a subset of data tuples for each worker. The replicas may be overlapping, disjoint, or some combination.

Table 5.9 summarizes the tradeoff space. In each section, we illustrate the tradeoff along two axes, namely (1) the *statistical efficiency*, i.e., the number of epochs it takes to converge, and (2) *hardware efficiency*, the time that each method takes to finish a single epoch.

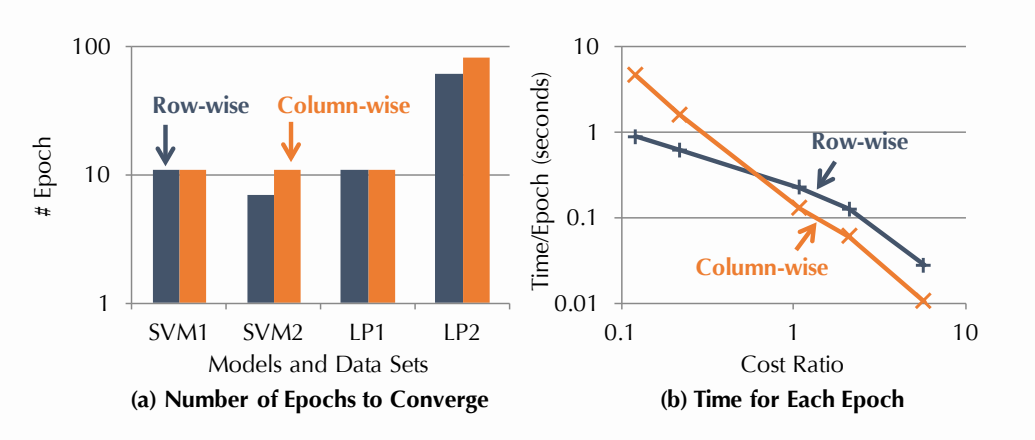

Figure 5.7: Illustration of the Method Selection Tradeoff. (a) These four datasets are RCV1, Reuters, Amazon, and Google, respectively. (b) The "cost ratio" is defined as the ratio of costs estimated for row-wise and column-wise methods: $(1+\alpha)\sum_i n_i/(\sum_i n_i^2+\alpha d)$, where n_i is the number of non-zero elements of i^{th} row of A and α is the cost ratio between writing and reads. We set $\alpha = 10$ to plot this graph.

5.2.2.2 Access Method Selection

In this section, we examine each access method: row-wise, column-wise, and column-to-row. We find that the execution time of an access method depends more on hardware efficiency than on statistical efficiency.

Tradeoffs We consider the two tradeoffs that we use for a simple cost model (Table 5.10). Let n_i be the number of non-zeros in row i; when we store the data as sparse vectors/matrices in CSR format, the number of reads in a row-wise access method is $\sum_{i=1}^{N} n_i$. Since each example is likely to be written back in a dense write, we perform dN writes per epoch. Our cost model combines these two costs linearly with a factor α that accounts for writes being more expensive, on average, because of contention. The factor α is estimated at installation time by measuring on a small set of datasets. The parameter α is in 4 to 12 and grows with the number of sockets; e.g., for local2, $\alpha \approx 4$, and for local8, $\alpha \approx 12$. Thus, α may increase in the future.

Statistical Efficiency. We observe that each access method has comparable *statistical efficiency*. To illustrate this, we run all methods on all of our datasets and report the number of epochs that one method converges to a given error to the optimal loss, and Figure 5.7(a) shows the result on four datasets with 10% error. We see that the gap in the number of epochs across different methods is small (always within 50% of each other).

Hardware Efficiency. Different access methods can change the time per epoch by up to a factor of $10\times$, and there is a cross-over point. To see this, we run both methods on a series of synthetic datasets where we control the number of non-zero elements per row by subsampling each row on the Music dataset (see Section 5.2.3 for more details). For each subsampled dataset, we plot the cost ratio on the x-axis, and we plot their actual running time per epoch in Figure 5.7(b). We see a cross-over point on the time used per epoch: when the cost ratio is small, row-wise outperforms column-wise by $6\times$, as the column-wise method reads more data; on the other hand, when the ratio is large, the column-wise method outperforms the row-wise method by $3\times$, as the column-wise method has lower write contention. We observe similar cross-over points on our other datasets.

Cost-based Optimizer DimmWitted estimates the execution time of different access methods using the number of bytes that each method reads and writes in one epoch, as shown in Table 5.10. For writes, it is slightly more complex: for models such as SVM, each gradient step in row-wise access only updates the coordinates where the input vector contains non-zero elements. We call this scenario a *sparse* update; otherwise, it is a *dense* update.

DimmWitted needs to estimate the ratio of the cost of reads to writes. To do this, it runs a simple benchmark dataset. We find that, for all the eight datasets, five statistical models, and five machines that we use in the experiments, the cost model is robust to this parameter: as long as writes are $4\times$ to $100\times$ more expensive than reading, the cost model makes the correct decision between row-wise and column-wise access.

5.2.2.3 Model Replication

In DimmWitted, we consider three model replication strategies. The first two strategies, namely PerCPU and PerMachine, are similar to traditional shared-nothing and shared-memory architecture, respectively. We also consider a hybrid strategy, PerNode, designed for NUMA machines.

Granularity of Model Replication The difference between the three model replication strategies is the granularity of replicating a model. We first describe PerCPU and PerMachine and their relationship with other existing systems (Table 5.9). We then describe PerNode, a simple, novel hybrid strategy that we designed to leverage the structure of NUMA machines.

1. PerCPU. In the PerCPU strategy, each core maintains a mutable state, and these states are combined to form a new version of the model (typically at the end of each epoch). This is essentially a shared-nothing architecture; it is implemented in Impala, Pivotal, and Hadoop-based frameworks. PerCPU is popularly implemented by state-of-the-art statistical analytics frameworks such as Bismarck, Spark, and GraphLab. There are subtle variations to this approach: in Bismarck's implementation, each worker processes a partition of the data, and its model is averaged at the end of each epoch; Spark implements a minibatch-based approach in which parallel workers calculate the gradient based on examples, and then gradients are aggregated by a single thread to update the final model; GraphLab implements an event-based approach where each different task is dynamically scheduled to satisfy the given consistency requirement. In DimmWitted, we implement PerCPU in a way that is similar to Bismarck, where each worker has its own model replica, and each worker is responsible for updating its replica.[14] As we will show in the experiment section, DimmWitted's implementation is 3-100$\times$ faster than either GraphLab and Spark. Both systems have additional sources of overhead that DimmWitted does not, e.g., for fault tolerance in Spark and a distributed environment in both. We are not making an argument about the relative merits of these features in applications, only that they would obscure the tradeoffs that we study in this section.

2. PerMachine. In the PerMachine strategy, there is a single model replica that all workers update during execution. PerMachine is implemented in Hogwild! and Google's Downpour. Hogwild! implements a lock-free protocol, which forces the hardware to deal with coherence. Although different writers may overwrite each other and readers may have dirty reads, Niu et al. [141] prove that Hogwild! converges.

3. PerNode. The PerNode strategy is a hybrid of PerCPU and PerMachine. In PerNode, each NUMA node has a single model replica that is shared among all cores on that node.

Model Synchronization Deciding how often the replicas synchronize is key to the design. In Hadoop-based and Bismarck-based models, they synchronize at the end of each epoch. This is a shared-nothing approach that works well in user-defined aggregations. However, we consider finer

[14] We implemented MLlib's minibatch in DimmWitted. We find that the Hogwild!-like implementation always dominates the minibatch implementation. DimmWitted's column-wise implementation for PerMachine is similar to GraphLab, with the only difference that DimmWitted does not schedule the task in an event-driven way.

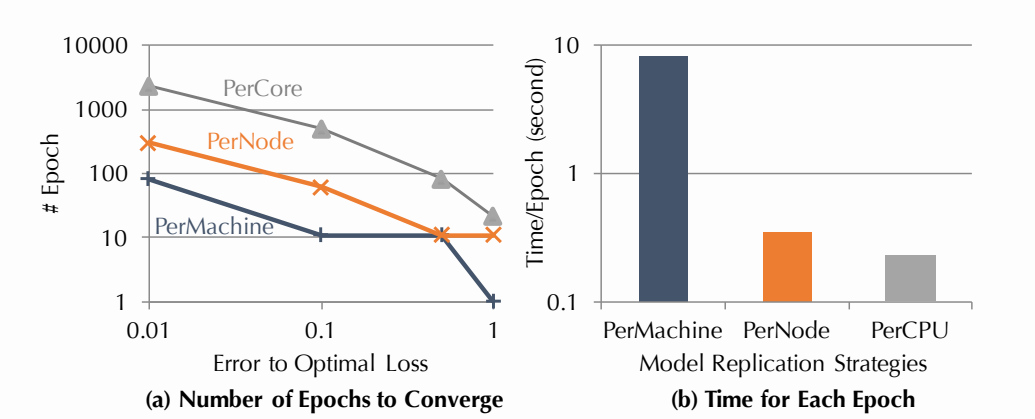

Figure 5.8: Illustration of Model Replication Tradeoff in DimmWitted.

granularities of sharing. In DimmWitted, we chose to have one thread that periodically reads models on all other cores, averages their results, and updates each replica.

One key question for model synchronization is *how frequently should the model be synchronized?* Intuitively, we might expect that more frequent synchronization will lower the throughput; on the other hand, the more frequently we synchronize, the fewer number of iterations we might need to converge. However, in DimmWitted, we find that the optimal choice is to communicate as frequently as possible. The intuition is that the QPI has staggering bandwidth (25GB/s) compared to the small amount of data we are shipping (megabytes). As a result, in DimmWitted, we implement an asynchronous version of the model averaging protocol: a separate thread averages models, with the effect of batching many writes together across the cores into one write, reducing the number of stalls.

Tradeoffs We observe that PerNode is more hardware efficient, as it takes less time to execute an epoch than PerMachine; PerMachine might use fewer number of epochs to converge than PerNode.

Statistical Efficiency. We observe that PerMachine usually takes fewer epochs to converge to the same loss compared to PerNode, and PerNode uses fewer number of epochs than PerCPU. To illustrate this observation, Figure 5.8(a) shows the number of epochs that each strategy requires to converge to a given loss for SVM (RCV1). We see that PerMachine always uses the least number of epochs to converge to a given loss: intuitively, the single model replica has more information at each step, which means that there is less redundant work. We observe similar phenomena when comparing PerCPU and PerNode.

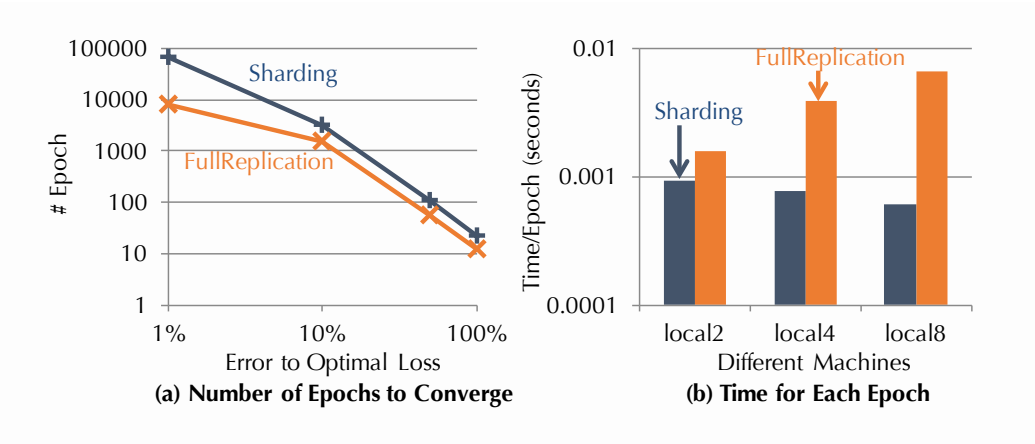

Figure 5.9: Illustration of Data Replication Tradeoff in DimmWitted.

Hardware Efficiency. We observe that PerNode uses much less time to execute an epoch than PerMachine. To illustrate the difference in the time that each model replication strategy uses to finish one epoch, we show in Figure 5.8(b) the execution time of three strategies on SVM (RCV1). We see that PerNode is 23× faster than PerMachine and that PerCPU is 1.5× faster than PerNode. PerNode takes advantage of the locality provided by the NUMA architecture. Using PMUs, we find that PerMachine incurs 11× more cross-node DRAM requests than PerNode.

Rule of Thumb For SGD-based models, PerNode usually gives optimal results, while for SCD-based models, PerMachine does. Intuitively, this is caused by the fact that SGD has a denser update pattern than SCD, so, PerMachine suffers from hardware efficiency.

5.2.2.4 Data Replication

In DimmWitted, each worker processes a subset of data and then updates its model replica. To assign a subset of data to each worker, we consider two strategies.

1. Sharding**.** Sharding is a popular strategy implemented in systems such as Hogwild!, Spark, and Bismarck, in which the dataset is partitioned, and each worker only works on its partition of data. When there is a single model replica, Sharding avoids wasted computation, as each tuple is processed once per epoch. However, when there are multiple model replicas, Sharding might increase the variance of the estimate we form on each node, lowering the statistical efficiency. In DimmWitted, we implement Sharding by randomly partitioning the rows (resp. columns) of

a data matrix for the row-wise (resp. column-wise) access method. In column-to-row access, we also replicate other rows that are needed.

2. FullReplication. A simple alternative to Sharding is FullReplication, in which we replicate the whole dataset many times (PerCPU or PerNode). In PerNode, each NUMA node will have a full copy of the data. Each node accesses its data in a different order, which means that the replicas provide non-redundant statistical information. Statistically, there are two benefits of FullReplication: (1) averaging different estimates from each node has a lower variance, and (2) the estimate at each node has lower variance than in the Sharding case, as each node's estimate is based on the whole data. From a hardware efficiency perspective, reads are more frequent from local NUMA memory in PerNode than in PerMachine. The PerNode approach dominates the PerCPU approach, as reads from the same node go to the same NUMA memory. Thus, we do not consider PerCPU replication from this point on.

Tradeoffs Not surprisingly, we observe that FullReplication takes more time for each epoch than Sharding. However, we also observe that FullReplication uses fewer epochs than Sharding, especially to achieve low error. We illustrate these two observations by showing the result of running SVM on Reuters using PerNode in Figure 5.9.

Statistical Efficiency. FullReplication uses fewer epochs, especially to low-error tolerance. Figure 5.9(a) shows the number of epochs that each strategy takes to converge to a given loss. We see that, for within 1% of the loss, FullReplication uses $10\times$ fewer epochs on a two-node machine. This is because each model replica sees more data than Sharding, and therefore has a better estimate. Because of this difference in the number of epochs, FullReplication is $5\times$ faster in wall-clock time than Sharding to converge to 1% loss. However, we also observe that, at high-error regions, FullReplication uses more epochs than Sharding and causes a comparable execution time to a given loss.

Hardware Efficiency. Figure 5.9(b) shows the time for each epoch across different machines with different numbers of nodes. Because we are using the PerNode strategy, which is the optimal choice for this dataset, the more nodes a machine has, the slower FullReplication is for each epoch. The slow-down is roughly consistent with the number of nodes on each machine. This is not surprising because each epoch of FullReplication processes more data than Sharding.

Model	Dataset	#Row	#Col.	NNZ	Size (Sparse)	Size (Dense)	Sparse
SVM, LR, LS	RCV1	781K	47K	60M	914MB	275GB	✓
	Reuters	8K	18K	93K	1.4MB	1.2GB	✓
	Music	515K	91	46M	701MB	0.4GB	
	Forest	581K	54	30M	490MB	0.2GB	
LP	Amazon	926K	335K	2M	28MB	>1TB	✓
	Google	2M	2M	3M	25MB	>1TB	✓
QP	Amazon	1M	1M	7M	104MB	>1TB	✓
	Google	2M	2M	10M	152MB	>1TB	✓
Gibbs	Paleo	69M	30M	108M	2GB	>1TB	✓
NN	MNIST	120M	800K	120M	2GB	>1TB	✓

Table 5.11: Dataset Statistics. NNZ refers to the Number of Non-zero elements. The # columns is equal to the number of variables in the model.

5.2.3 Experiments

We validate that exploiting the tradeoff space that we described enables DimmWitted's orders of magnitude speedup over state-of-the-art competitor systems. We also validate that each tradeoff discussed in this section affects the performance of DimmWitted.

5.2.3.1 Experiment Setup

Datasets and Statistical Models We validate the performance and quality of DimmWitted on a diverse set of statistical models and datasets. For statistical models, we choose five models that are among the most popular models used in statistical analytics: (1) Support Vector Machine (SVM), (2) Logistic Regression (LR), (3) Least Squares Regression (LS), (4) Linear Programming (LP), and (5) Quadratic Programming (QP). For each model, we choose datasets with different characteristics, including size, sparsity, and under- or over-determination. For SVM, LR, and LS, we choose four datasets: Reuters[15], RCV1[16], Music[17], and Forest.[18] Reuters and RCV1 are datasets for text classification that are sparse and underdetermined. Music and Forest are standard benchmark datasets that are dense and overdetermined. For QP and LR, we consider a social-network application, i.e., network analysis, and use two datasets from Amazon's customer data and Google's Google+ social networks.[19] Table 5.11 shows the dataset statistics.

[15] archive.ics.uci.edu/ml/datasets/Reuters-21578+Text+Categorization+Collection
[16] about.reuters.com/researchandstandards/corpus/
[17] archive.ics.uci.edu/ml/datasets/YearPredictionMSD
[18] archive.ics.uci.edu/ml/datasets/Covertype
[19] snap.stanford.edu/data/

Dataset		Within 1% of the Optimal Loss					Within 50% of the Optimal Loss				
		GraphLab	GraphChi	MLlib	Hogwild!	DW	GraphLab	GraphChi	MLlib	Hogwild!	DW
SVM	Reuters	58.9	56.7	15.5	**0.1**	**0.1**	13.6	11.2	0.6	**0.01**	**0.01**
	RCV1	> 300.0	> 300.0	> 300	61.4	**26.8**	> 300.0	> 300.0	58.0	0.71	**0.17**
	Music	> 300.0	> 300.0	156	33.32	**23.7**	31.2	27.1	7.7	0.17	**0.14**
	Forest	16.2	15.8	2.70	0.23	**0.01**	1.9	1.4	0.15	0.03	**0.01**
LR	Reuters	36.3	34.2	19.2	**0.1**	**0.1**	13.2	12.5	1.2	**0.03**	**0.03**
	RCV1	> 300.0	> 300.0	> 300.0	38.7	**19.8**	> 300.0	> 300.0	68.0	0.82	**0.20**
	Music	> 300.0	> 300.0	> 300.0	35.7	**28.6**	30.2	28.9	8.9	0.56	**0.34**
	Forest	29.2	28.7	3.74	0.29	**0.03**	2.3	2.5	0.17	0.02	**0.01**
LS	Reuters	132.9	121.2	92.5	4.1	**3.2**	16.3	16.7	1.9	0.17	**0.09**
	RCV1	> 300.0	> 300.0	> 300	27.5	**10.5**	> 300.0	> 300.0	32.0	1.30	**0.40**
	Music	> 300.0	> 300.0	221	40.1	**25.8**	> 300.0	> 300.0	11.2	0.78	**0.52**
	Forest	25.5	26.5	1.01	0.33	**0.02**	2.7	2.9	0.15	0.04	**0.01**
LP	Amazon	2.7	2.4	> 120.0	> 120.0	**0.94**	2.7	2.1	120.0	1.86	**0.94**
	Google	13.4	11.9	> 120.0	> 120.0	**12.56**	2.3	2.0	120.0	3.04	**2.02**
QP	Amazon	6.8	5.7	> 120.0	> 120.0	**1.8**	6.8	5.7	> 120.0	> 120.00	**1.50**
	Google	12.4	10.1	> 120.0	> 120.0	**4.3**	9.9	8.3	> 120.0	> 120.00	**3.70**

Table 5.12: End-to-End Comparison (time in seconds). The column DW refers to DimmWitted. We take 5 runs on local2 and report the average (standard deviation for all numbers $< 5\%$ of the mean). Entries with $>$ indicate a timeout.

Metrics We measure the quality and performance of DimmWitted and other competitors. To measure the quality, we follow prior art and use the loss function for all functions. For end-to-end performance, we measure the wall-clock time it takes for each system to converge to a loss that is within 100%, 50%, 10%, and 1% of the optimal loss.[20] When measuring the wall-clock time, we do not count the time used for data loading and result outputting for all systems. We also use other measurements to understand the details of the tradeoff space, including (1) local LLC request, (2) remote LLC request, and (3) local DRAM request. We use Intel Performance Monitoring Units (PMUs) and follow the manual[21] to conduct these experiments.

Experiment Setting We compare DimmWitted with four competitor systems: GraphLab [123], GraphChi [113], MLlib [176] over Spark [201], and Hogwild! [141]. GraphLab is a distributed graph processing system that supports a large range of statistical models. GraphChi is similar to GraphLab but with a focus on multi-core machines with secondary storage. MLlib is a package of machine learning algorithms implemented over Spark, an in-memory implementation of the MapReduce framework. Hogwild! is an in-memory lock-free framework for statistical analytics. We find that all four systems pick some points in the tradeoff space that we considered in DimmWitted. In GraphLab and GraphChi, all models are implemented using stochastic coordinate descent (column-wise access); in MLlib and Hogwild!, SVM and LR are implemented using stochastic gradient descent (row-wise access). We use implementations that are provided by the original developers whenever possible. For models without code provided by the developers, we only change the corresponding gradient function.[22] For GraphChi, if the corresponding model is implemented in GraphLab but not GraphChi, we follow GraphLab's implementation.

We run experiments on a variety of architectures. These machines differ in a range of configurations, including the number of NUMA nodes, the size of last-level cache (LLC), and memory bandwidth. See Table 5.8 for a summary of these machines. DimmWitted, Hogwild!, GraphLab, and GraphChi are implemented using C++, and MLlib/Spark is implemented using Scala. We tune both GraphLab and MLlib according to their best practice guidelines.[23] For both GraphLab, GraphChi,

[20] We obtain the optimal loss by running all systems for one hour and choosing the lowest.

[21] `software.intel.com/en-us/articles/performance-monitoring-unit-guidelines`

[22] For sparse models, we change the dense vector data structure in MLlib to a sparse vector, which only improves its performance.

[23] MLlib:`spark.incubator.apache.org/docs/0.6.0/tuning.html`;
GraphLab: `graphlab.org/tutorials-2/fine-tuning-graphlab-performance/`;
For GraphChi, we tune the memory buffer size to ensure all data fit in memory and that there are no disk I/Os.

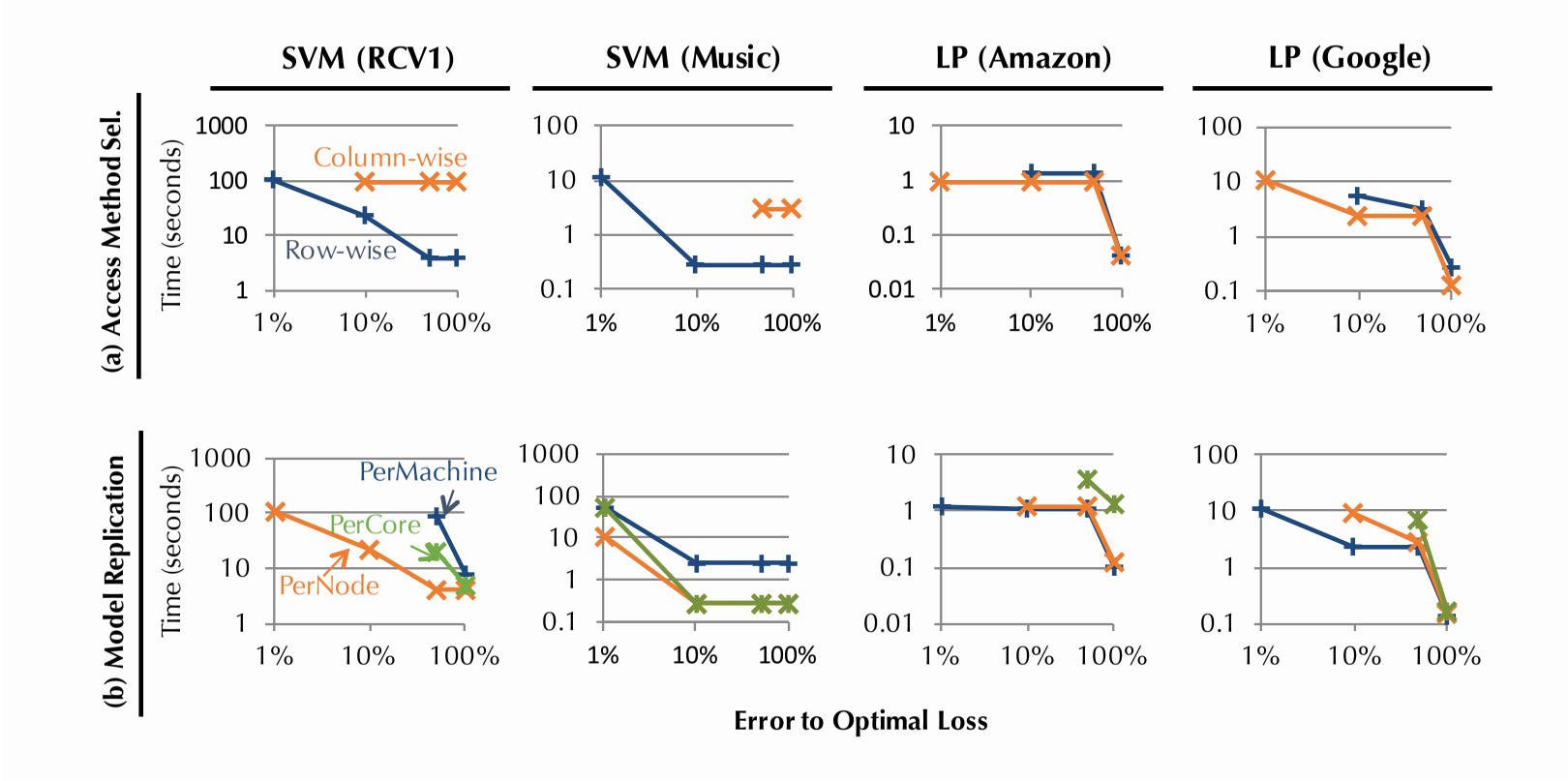

Figure 5.10: Tradeoffs in DimmWitted. Missing points timeout in 120 seconds.

and MLlib, we try different ways of increasing locality on NUMA machines, including trying to use numactl and implementing our own RDD for MLlib. Systems are compiled with g++ 4.7.2 (-O3), Java 1.7, or Scala 2.9.

5.2.3.2 End-to-End Comparison

We validate that DimmWitted outperforms competitor systems in terms of end-to-end performance and quality. Note that both MLlib and GraphLab have extra overhead for fault tolerance, distributing work, and task scheduling. Our comparison between DimmWitted and these competitors is intended only to demonstrate that existing work for statistical analytics has not obviated the tradeoffs that we study here.

Protocol For each system, we grid search their statistical parameters, including step size ({100.0, 10.0, ..., 0.0001}) and mini-batch size for MLlib ({1%, 10%, 50%, 100%}); we always report the best configuration, which is essentially the same for each system. We measure the time it takes for each system to find a solution that is within 1%, 10%, and 50% of the optimal loss. Table 5.12 shows the results for 1% and 50%; the results for 10% are similar. We report end-to-end numbers from local2, which has two nodes and 24 logical cores, as GraphLab does not run on machines with more than 64 logical cores. Table 5.14 shows the DimmWitted's choice of point in the tradeoff space on local2.

As shown in Table 5.12, DimmWitted always converges to the given loss in less time than the other competitors. On SVM and LR, DimmWitted could be up to 10× faster than Hogwild!, and more than two orders of magnitude faster than GraphLab and Spark. The difference between DimmWitted and Hogwild! is greater for LP and QP, where DimmWitted outperforms Hogwild! by more than two orders of magnitude. On LP and QP, DimmWitted is also up to 3× faster than GraphLab and GraphChi, and two orders of magnitude faster than MLlib.

Tradeoff Choices We dive more deeply into these numbers to substantiate our claim that there are some points in the tradeoff space that are not used by GraphLab, GraphChi, Hogwild!, and MLlib. Each tradeoff selected by our system is shown in Table 5.14. For example, GraphLab and GraphChi uses column-wise access for all models, while MLlib and Hogwild! use row-wise access for all models and allow only PerMachine model replication. These special points work well for some but not all models. For example, for LP and QP, GraphLab and GraphChi are only 3× slower than

DimmWitted, which chooses column-wise and PerMachine. This factor of 3 is to be expected, as GraphLab also allows distributed access and so has additional overhead. However there are other points: for SVM and LR, DimmWitted outperforms GraphLab and GraphChi, because the column-wise algorithm implemented by GraphLab and GraphChi is not as efficient as row-wise on the same dataset. DimmWitted outperforms Hogwild! because DimmWitted takes advantage of model replication, while Hogwild! incurs 11× more cross-node DRAM requests than DimmWitted; in contrast, DimmWitted incurs 11× more local DRAM requests than Hogwild! does.

For SVM, LR, and LS, we find that DimmWitted outperforms MLlib, primarily due to being located at a different point in the tradeoff space. In particular, MLlib uses batch-gradient-descent with a PerCPU implementation, while DimmWitted uses stochastic gradient and PerNode. We find that, for the Forest dataset, DimmWitted takes 60× fewer number of epochs to converge to 1% loss than MLlib. For each epoch, DimmWitted is 4× faster. These two factors contribute to the 240× speed-up of DimmWitted over MLlib on the Forest dataset (1% loss). MLlib has overhead for scheduling, so we break down the time that MLlibuses for scheduling and computation. We find that, for Forest, out of the total 2.7 seconds of execution, MLlib uses 1.8 seconds for computation and 0.9 seconds for scheduling. We also implemented a batch-gradient-descent and PerCPU implementation inside DimmWitted to remove these and C++ versus Scala differences. The 60× difference in the number of epochs until convergence still holds, and our implementation is only 3× faster than MLlib. This implies that the main difference between DimmWitted and MLlib is the point in the tradeoff space—not low-level implementation differences.

For LP and QP, DimmWitted outperforms MLlib and Hogwild! because the row-wise access method implemented by these systems is not as efficient as column-wise access on the same data set. GraphLab does have column-wise access, so DimmWitted outperforms GraphLab and GraphChi because DimmWitted finishes each epoch up to 3× faster, primarily due to low-level issues. This supports our claims that the tradeoff space is interesting for analytic engines and that no one system has implemented all of them.

Throughput We compare the throughput of different systems for an extremely simple task: parallel sums. Our implementation of parallel sum follows our implementation of other statistical models (with a trivial update function), and uses all cores on a single machine. Table 5.13 shows the throughput on all systems on different models on one dataset. We see from Table 5.13 that DimmWitted

	SVM (RCV1)	LR (RCV1)	LS (RCV1)	LP (Google)	QP (Google)	Parallel Sum
GraphLab	0.2	0.2	0.2	0.2	0.1	0.9
GraphChi	0.3	0.3	0.2	0.2	0.2	1
MLlib	0.2	0.2	0.2	0.1	0.02	0.3
Hogwild!	1.3	1.4	1.3	0.3	0.2	13
DimmWitted	5.1	5.2	5.2	0.7	1.3	21

Table 5.13: Comparison of Throughput (GB/seconds) of Different Systems on local2.

Model and Dataset		Access Method	Model Replication	Data Replication
SVM, LR, LS	Reuters RCV1 Music	Row-wise	PerNode	FullReplication
LP, QP	Amazon Google	Column-wise	PerMachine	FullReplication

Table 5.14: Plans that DimmWitted Chooses for Each Dataset on Machine local2.

achieves the highest throughput of all the systems. For parallel sum, DimmWitted is 1.6$\times$ faster than Hogwild!, and we find that DimmWitted incurs $8\times$ fewer LLC cache misses than Hogwild!. Compared with Hogwild!, in which all threads write to a single copy of the sum result, DimmWitted maintains one single copy of the sum result per NUMA node, so the workers on one NUMA node do not invalidate the cache on another NUMA node. When running on only a single thread, DimmWitted has the same implementation as Hogwild!. Compared with GraphLab and GraphChi, DimmWitted is $20\times$ faster, likely due to the overhead of GraphLab and GraphChi dynamically scheduling tasks and/or maintaining the graph structure. To compare DimmWitted with MLlib, which is written in Scala, we implemented a Scala version, which is $3\times$ slower than C++; this suggests that the overhead is not just due to the language. If we do not count the time that MLlibuses for scheduling and only count the time of computation, we find that DimmWitted is 15$\times$ faster than MLlib.

5.2.3.3 Tradeoffs of DimmWitted

We validate that all the tradeoffs described in this section have an impact on the efficiency of DimmWitted. We report on a more modern architecture, local4 with four NUMA sockets, in this section. We describe how the results change with different architectures.

Access Method Selection We validate that different access methods have different performance, and that no single access method dominates the others. We run DimmWitted on all statistical models

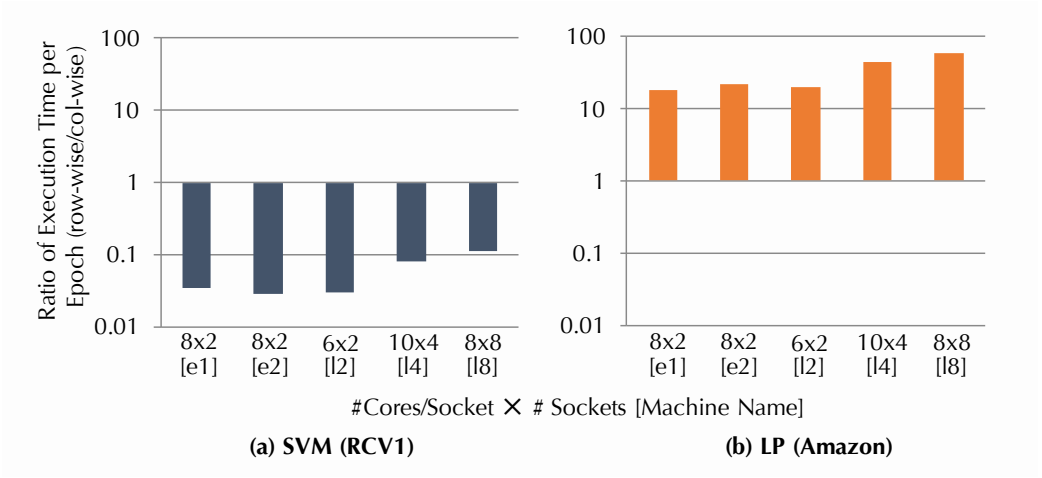

Figure 5.11: Ratio of Execution Time per Epoch (row-wise/column-wise) on Different Architectures. A number larger than 1 means that row-wise is slower. l2 means local2, e1 means ec2.1, etc.

and compare two strategies, row-wise and column-wise. In each experiment, we force DimmWitted to use the corresponding access method, but report the best point for the other tradeoffs. Figure 5.10(a) shows the results as we measure the time it takes to achieve each loss. The more stringent loss requirements (1%) are on the left-hand side. The horizontal line segments in the graph indicate that a model may reach, say, 50% as quickly (in epochs) as it reaches 100%.

We see from Figure 5.10(a) that the difference between row-wise and column-to-row access could be more than $100\times$ for different models. For SVM on RCV1, row-wise access converges at least $4\times$ faster to 10% loss and at least $10\times$ faster to 100% loss. We observe similar phenomena for Music; compared with RCV1, column-to-row access converges to 50% loss and 100% loss at a $10\times$ slower rate. With such datasets, the column-to-row access simply requires more reads and writes. This supports the folk wisdom that gradient methods are preferable to coordinate descent methods. On the other hand, for LP, column-wise access dominates: row-wise access does not converge to 1% loss within the timeout period for either Amazon or Google. Column-wise access converges at least 10-100$\times$ faster than row-wise access to 1% loss. We observe that LR is similar to SVM and QP is similar to LP. Thus, no access method dominates all the others.

The cost of writing and reading are different and is captured by a parameter that we called α in Section 5.2.2.2. We describe the impact of this factor on the relative performance of row- and column-wise strategies. Figure 5.11 shows the ratio of the time that each strategy uses (row-wise/column-wise) for SVM (RCV1) and LP (Amazon). We see that, as the number of sockets on a

machine increases, the ratio of execution time increases, which means that row-wise becomes slower relative to column-wise, i.e., with increasing α. As the write cost captures the cost of a hardware-resolved conflict, we see that this constant is likely to grow. Thus, if next-generation architectures increase in the number of sockets, the cost parameter α and consequently the importance of this tradeoff are likely to grow.

Cost-based Optimizer We observed that, for all datasets, our cost-based optimizer selects row-wise access for SVM, LR, and LS, and column-wise access for LP and QP. These choices are consistent with what we observed in Figure 5.10.

Model Replication We validate that there is no single strategy for model replication that dominates the others. We force DimmWitted to run strategies in PerMachine, PerNode, and PerCPU and choose other tradeoffs by choosing the plan that achieves the best result. Figure 5.10(b) shows the results.

We see from Figure 5.10(b) that the gap between PerMachine and PerNode could be up to 100×. We first observe that PerNode dominates PerCPU on all datasets. For SVM on RCV1, PerNode converges 10× faster than PerCPU to 50% loss, and for other models and datasets, we observe a similar phenomenon. This is due to the low statistical efficiency of PerCPU, as we discussed in Section 5.2.2.3. Although PerCPU eliminates write contention inside one NUMA node, this write contention is less critical. For large models and machines with small caches, we also observe that PerCPU could spill the cache.

These graphs show that neither PerMachine nor PerNode dominates the other across all datasets and statistical models. For SVM on RCV1, PerNode converges 12× faster than PerMachine to 50% loss. However, for LP on Amazon, PerMachine is at least 14× faster than PerNode to converge to 1% loss. For SVM, PerNode converges faster because it has 5× higher throughput than PerMachine, and for LP, PerNode is slower because PerMachine takes at least 10× fewer epochs to converge to a small loss. One interesting observation is that, for LP on Amazon, PerMachine and PerNode do have comparable performance to converge to 10% loss. Compared with the 1% loss case, this implies that PerNode's statistical efficiency decreases as the algorithm tries to achieve a smaller loss. This is not surprising, as one must reconcile the PerNode estimates.

We observe that the relative performance of PerMachine and PerNode depends on (1) the number of sockets used on each machine and (2) the sparsity of the update.

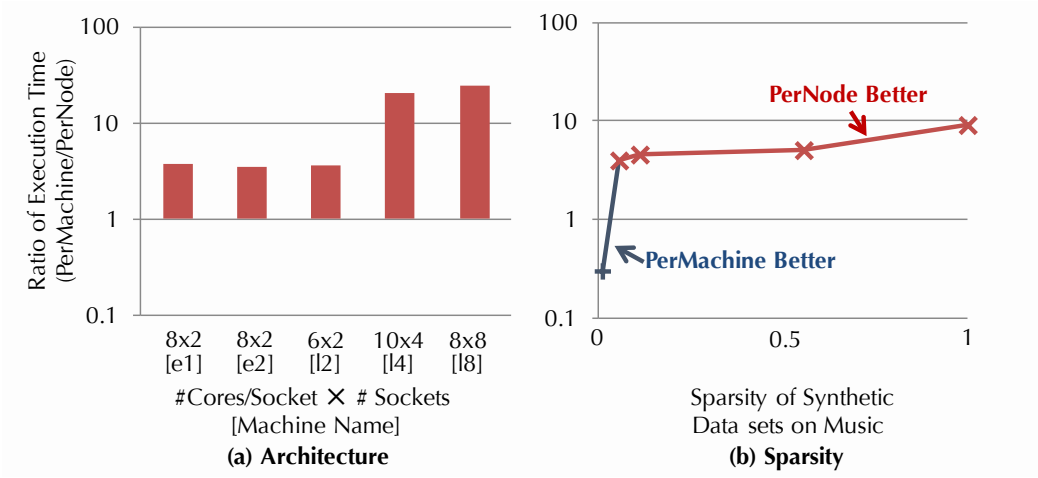

Figure 5.12: The Impact of Different Architectures and Sparsity on Model Replication. A ratio larger than 1 means that PerNode converges faster than PerMachine to 50% loss.

To validate (1), we measure the time that PerNode and PerMachine take on SVM (RCV1) to converge to 50% loss on various architectures, and we report the ratio (PerMachine/PerNode) in Figure 5.12. We see that PerNode's relative performance improves with the number of sockets. We attribute this to the increased cost of write contention in PerMachine.

To validate (2), we generate a series of synthetic datasets, each of which subsamples the elements in each row of the Music dataset; Figure 5.12(b) shows the results. When the sparsity is 1%, PerMachine outperforms PerNode, as each update touches only one element of the model; thus, the write contention in PerMachine is not a bottleneck. As the sparsity increases (i.e., the update becomes denser), we observe that PerNode outperforms PerMachine.

Data Replication We validate the impact of different data replication strategies. We run DimmWitted by fixing data replication strategies to FullReplication or Sharding and choosing the best plan for each other tradeoff. We measure the execution time for each strategy to converge to a given loss for SVM on the same dataset, RCV1. We report the ratio of these two strategies as FullReplication/Sharding in Figure 5.13(a). We see that, for the low-error region (e.g., 0.1%), FullReplication is 1.8-2.5× faster than Sharding. This is because FullReplication decreases the skew of data assignment to each worker, so hence each individual model replica can form a more accurate estimate. For the high-error region (e.g., 100%), we observe that FullReplication appears to be 2-5× slower than Sharding. We find that, for 100% loss, both FullReplication and Sharding converge in a single epoch, and Sharding

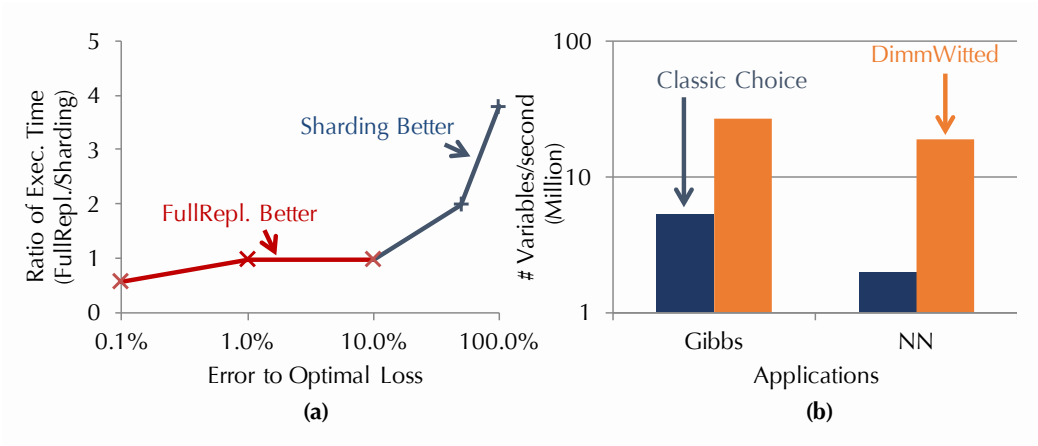

Figure 5.13: (a) Tradeoffs of Data Replication. A ratio smaller than 1 means that FullReplication is faster. (b) Performance of Gibbs Sampling and Neural Networks Implemented in DimmWitted.

may therefore be preferred, as it examines less data to complete that single epoch. In all of our experiments, FullReplication is never substantially worse and can be dramatically better. Thus, if there is available memory, the FullReplication data replication seems to be preferable.

5.2.4 Gibbs Sampling

We briefly describe how to run Gibbs sampling (which uses a column-to-row access method). Using the same tradeoffs, we achieve a significant increase in speed over the classical implementation choices of these algorithms.

Gibbs sampling is one of the most popular algorithms to solve statistical inference and learning over probabilistic graphical models [159]. We briefly observe that its main step is a column-to-row access. A factor graph can be thought of as a bipartite graph of a set of variables and a set of factors. To run Gibbs sampling, the main operation is to select a single variable, and calculate the conditional probability of this variable, which requires the fetching of all factors that contain this variable and all assignments of variables connected to these factors. This operation corresponds to the column-to-row access method. Similar to first-order methods, recently, a Hogwild! algorithm for Gibbs was established [103]. As shown in Figure 5.13(b), applying the technique in DimmWitted to Gibbs sampling achieves 4$\times$ the throughput of samples as the PerMachine strategy.

5.2.5 Conclusion to In-memory Statsitical Analytics

For statistical analytics on main-memory, NUMA-aware machines, we studied tradeoffs in access methods, model replication, and data replication. We found that using novel points in this tradeoff space can have a substantial benefit: our DimmWitted prototype engine can run at least one popular task at least 100$\times$ faster than other competitor systems. This comparison demonstrates that this tradeoff space may be interesting for current and next-generation statistical analytics systems.

5.3 Conclusion

In this chapter, we focus on speeding up the execution of statistical inference over a range of models, e.g., logistic regression, support vector machines, and factor graphs. Our study considers two cases: (1) the data fit in main memory and (2) the data does not fit in main memory. For both cases, we study the system tradeoff of conducting statistical inference and learning, and our experiments show that our study of the tradeoff contributes to up to two orders of magnitude speed up compared with existing tools. The techniques we designed in this chapter helps the user of DeepDive to focus more on integrating high-level knowledge, instead of low-level efficiency and scalability details.

6. Incremental Execution

> *We need to face up to the need for iterative procedures in data analysis. It is nice to plan to make but a single analysis... it is also nice to be able to carry out an individual analysis in a single straightforward step to avoid iteration and repeated computation. But it is not realistic to believe that good data analysis is consistent with either of these niceties.*
>
> — John W. Tukey, *The Future of Data Analysis, 1962*

In previous chapters, we described how to write a DeepDive program to specify a KBC system and how to execute it in an efficient and scalable way given a batch of documents. However, as we described in Chapter 3, developing this KBC program is not an one-shot process; instead, it requires the user to follow an iterative protocol to deciding on the right features, external sources, domain knowledge, and supervision rules to use in a KBC program. This iterative protocol requires the user to execute a series of KBC systems that differ only slightly from the others. In this chapter, we focus on a different question that the previous chapter; instead of focusing on how to efficiently execute a KBC system over a batch of documents and a given KBC program, we focus on the following question: *Can we make the execution of a series of KBC systems with slightly different KBC programs efficient?*

We study this question in two ways. First, we focus on a problem called *feature selection*, in which the user already knows a set of candidate features but wants to select a subset from these features. By allowing the user to select a subset of features, we help her to better explain the KBC systems she built and also help avoid overfitting. One observation is that the process of feature selection is often a human-in-the-loop iterative process using automatic feature selection algorithms. The first technique that we developed is a DSL language that enables iterative feature selection for a range of popular statistical models, and we study how to make this process efficient. Our second focus is on how to *develop* a set of new features, supervision rules, or domain knowledge rules instead of just selecting a subset, which we call feature engineering. The second technique that we developed is a technique to incrementally maintain the inference and learning results over factor graphs and validate it over five KBC systems we built. As we will see, both techniques achieve up to two orders of magnitude speed up on their target workloads. We describe these two techniques in this chapter.

6.1 Incremental Feature Selection

One of the most critical stages in the data analytics process is *feature selection*; in feature selection, an analyst selects the inputs or features of a model to help improve modeling accuracy or to help an analyst understand and explore their data. These features could come from a KBC system, e.g., to select the subset of dependency paths between mention pairs that are actual indicators of relations; or could come from other analytics tasks, e.g., bioinformatics, genomics, or business intelligence. With the increased interest in data analytics, a pressing challenge is to improve the efficiency of the feature selection process. In this work, we propose Columbus, the first data-processing system designed to support the feature-selection process.

To understand the practice of feature selection, we interviewed analysts in enterprise settings. This included an insurance company, a consulting firm, a major database vendor's analytics customer, and a major e-commerce firm. Uniformly, analysts agreed that they spend the bulk of their time on the feature selection process. Confirming the literature on feature selection [89, 104], we found that features are selected (or not) for many reasons: their statistical performance, their real-world explanatory power, legal reasons,[1] or for some combination. Thus, feature selection is practiced as an interactive process with an analyst in the loop. Analysts use feature selection algorithms, data statistics, and data manipulations as a dialogue that is often specific to their application domain. Nevertheless, the feature selection process has structure: analysts often use domain-specific cookbooks that outline best practices for feature selection [89].

Although feature selection cookbooks are widely used, the analyst must still write low-level code, increasingly in R, to perform the subtasks in the cookbook that comprise a feature selection task. In particular, we have observed that such users are forced to write their own custom R libraries to implement simple routine operations in the feature selection literature (e.g., stepwise addition or deletion [89]). Over the last few years, database vendors have taken notice of this trend, and now, virtually every major database engine ships a product with some R extension: Oracle's OR, IBM's SystemML [80], SAP HANA, and Revolution Analytics on Hadoop and Teradata. These R-extension layers (RELs) transparently scale operations, such as matrix-vector multiplication or the determinant, to larger sets of data across a variety of backends, including multicore main memory, database engines, and Hadoop. We call these REL operations *ROPs*.

[1] Using credit score as a feature is considered a discriminatory practice by the insurance commissions in both California and Massachusetts.

However, we observed that one major source of inefficiency in analysts' code is not addressed by ROP optimization: *missed opportunities for reuse and materialization across ROPs*. Our first contribution is to demonstrate a handful of materialization optimizations that can improve performance by orders of magnitude. Selecting the optimal materialization strategy is difficult for an analyst, as the optimal strategy depends on the reuse opportunities of the feature selection task, the error the analyst is willing to tolerate, and properties of the data and compute node, such as parallelism and data size. Thus, an optimal materialization strategy for an R script for one dataset may not be the optimal strategy for the same task on another data set. As a result, it is difficult for analysts to pick the correct combination of materialization optimizations.

To study these tradeoffs, we introduce Columbus, an R language extension and execution framework designed for feature selection. To use Columbus, a user writes a standard R program. Columbus provides a library of several common feature selection operations, such as *stepwise addition*, i.e., *"add each feature to the current feature set and solve."* This library mirrors the most common operations in the feature selection literature [89] and what we observed in analysts' programs. Columbus's optimizer uses these higher-level, declarative constructs to recognize opportunities for data and computation reuse. To describe the optimization techniques that Columbus employs, we introduce the notion of a *basic block*.

A basic block is Columbus's main unit of optimization. A basic block captures a feature selection task for *generalized linear models*, which captures models like linear and logistic regression, support vector machines, lasso, and many more; see Def. 6.1. Roughly, a basic block B consists of a data matrix $A \in \mathbb{R}^{N \times d}$, where N is the number of examples and d is the number of features, a target $b \in \mathbb{R}^N$, several feature sets (subsets of the columns of A), and a (convex) loss function. A basic block defines a set of regression problems on the same data set (with one regression problem for each feature set). Columbus compiles programs into a sequence of basic blocks, which are optimized and then transformed into ROPs. Our focus is not on improving the performance of ROPs, but on how to use widely available ROPs to improve the performance of feature selection workloads.

We describe the opportunities for reuse and materialization that Columbus considers in a basic block. As a baseline, we implement classical batching and materialization optimizations. In addition, we identify three novel classes of optimizations, study the tradeoffs each presents, and then describe a cost model that allows Columbus to choose between them. These optimizations are novel in that

Materialization Strategy	Error Tolerance	Sophistication of Tasks	Reuse
Lazy Eager	Low (Exact Solution)	Medium	Low
Naïve Sampling	High (Without Guarantee)		High
Coreset	Medium-High (With Guarantee)	Small	
QR	Low (Exact Solution)	Large	

Table 6.1: A summary of tradeoffs in Columbus.

they have not been considered in traditional SQL-style analytics (but all the optimizations have been implemented in other areas).

Subsampling Analysts employ subsampling to reduce the amount of data the system needs to process to improve runtime or reduce overfitting. These techniques are a natural choice for analytics, as both the underlying data collection process and solution procedures are only reliable up to some tolerance. Popular sampling techniques include naïve random sampling and importance sampling (coresets). Coresets [38, 114] is a relatively recent importance-sampling technique; when $d \ll N$, coresets allow one to create a sample whose size depends on d (the number of features)–as opposed to N (the number of examples)–and that can achieve strong approximation results: essentially, the loss is preserved on the sample for *any* model. In enterprise workloads (as opposed to web workloads), we found that the overdetermined problems ($d \ll N$), well-studied in classical statistics, are common. Thus, we can use a coreset to optimize the result with provably small error. However, computing a coreset requires computing importance scores that are more expensive than a naïve random sample. We study the cost-benefit tradeoff for sampling-based materialization strategies. Of course, sampling strategies have the ability to improve performance by an order of magnitude. On a real data set, called Census,[2] we found that d was 1000x smaller than N, as well as that using a coreset outperforms a baseline approach by 89x, while still getting a solution that is within 1% of the loss of the solution on the entire dataset.

Transformation Materialization Linear algebra has a variety of decompositions that are analogous to sophisticated materialized views. One such decomposition, called a (thin) QR decomposition [81], is widely used to optimize regression problems. Essentially, after some preprocessing, a QR decomposition allows one to solve a class of regression problems in a single scan over the matrix. In feature selection, one has to solve *many* closely related regression problems, e.g., for various subsets of

[2] `https://archive.ics.uci.edu/ml/datasets/Census+Income`

features (columns of A). We show how to adapt QR to this scenario as well. When applicable, QR can outperform a baseline by more than $10\times$; QR can also be applied together with coresets, which can result in $5\times$ more speed up. Of course, there is a cost-benefit tradeoff that one must make when materializing QR, and Columbus develops a simple cost model for this choice.

Model Caching Feature selection workloads require that analysts solve many similar problems. Intuitively, it should be possible to reuse these partial results to "warmstart" a model and improve its convergence behavior. We propose to cache several models, and we develop a technique that chooses which model to use for a warmstart. The challenge is to be able to find "nearby" models, and we introduce a simple heuristic for model caching. Compared with the default approach in R (initializing with a random start point or all 0's), our heuristic provides a 13x speedup; compared with a simple strategy that selects a random model in the cache, our heuristic achieves a 6x speedup. Thus, the cache and the heuristic contribute to our improved runtime.

We tease apart the optimization space along three related axes: *error tolerance*, the *sophistication* of the task, and the amount of *reuse* (see Section 6.1.2). Table 6.1 summarizes the relationship between these axes and the tradeoffs. Of course, the correct choice also depends on computational constraints, notably parallelism. We describe a series of experiments to validate this tradeoff space and find that no one strategy dominates another. Thus, we develop a cost-based optimizer that attempts to select an optimal combination of the above materialization strategies. We validate that our heuristic optimizer has performance within 10% of the optimal optimization strategy (found offline by brute force) on all our workloads. Many of the subproblems of the optimizer are classically NP-hard, justifying heuristic optimizers.

Contributions This section makes three contributions: (1) We propose Columbus, which is the first data processing system designed to support the feature selection dialogue; (2) we are the first to identify and study both existing and novel optimizations for feature selection workloads as data management problems; and (3) we use the insights from (2) to develop a novel cost-based optimizer. We validate our results on several real-world programs and datasets patterned after our conversations with analysts. Additionally, we validate Columbus across two backends from main memory and REL for an RDBMS. We argue that these results suggest that feature selection is a promising area for

```
1  e  = SetErrorTolerance(0.01)        # Set Error Tolerance
2  d1 = Dataset("USCensus")            # Register the dataset
3  s1 = FeatureSet("NumHouses", ...)   # Population-related features
4  l1 = CorrelationX(s1, d1)           # Get mutual correlations
5  s1 = Remove(s1, "NumHouses")        # Drop the feature "NumHouses"
6  l2 = CV(lsquares_loss, s1, d1, k=5) # Cross validation (least squares)
7  d2 = Select(d1,"Income >= 10000")   # Focus on high-income areas
8  s2 = FeatureSet("Income", ...)      # Economic features
9  l3 = CV(logit_loss, s2, d2, k=5)    # Cross validation with (logit loss)
10 s3 = Union(s1, s2)                  # Use both sets of features
11 s4 = StepAdd(logit_loss, s3, d1)    # Add in one other feature
12 Final(s4)                           # Session ends with chosen features
```

Figure 6.1: Example snippet of a Columbus program.

future data management research. Additionally, we are optimistic that the technical optimizations we pursue apply beyond feature selection to areas like scientific databases and tuning machine learning.

Outline The rest of this section is organized as follows. In Section 6.1.1, we provide an overview of the Columbus system. In Section 6.1.2, we describe the tradeoff space for executing a feature selection program and our cost-based optimizer. We describe experimental results in Section 6.1.3. We discuss related work in Chapter 7.

The key task of Columbus is to compile and optimize an extension of the R language for feature selection. We compile this language into a set of *REL operations*, which are R-language constructs implemented by today's language extenders, including ORE, Revolution Analytics, etc. One key design decision in Columbus is *not* to optimize the execution of these REL operators; these have already been studied intensively and are the subjects of major ongoing engineering efforts. Instead, we focus on how to compile our language into the most common of these REL operations (ROPs). Figure 6.3 shows all ROPs that are used in Columbus.

6.1.1 System Overview

6.1.1.1 Columbus Programs

In Columbus, a user expresses their feature selection program against a set of high-level constructs that form a domain specific language for feature selection. We describe these constructs next, and we selected these constructs by talking to a diverse set of analysts and following the state-of-the-art

	Logical Operators
Data Transform	Select, Join, Union, ...
Evaluate	Mean, Variance, Covariance, Pearson Correlation Cross Validation, AIC
Regression	Least Squares, Lasso, Logistic Regression
Explore	Feature Set Operation Stepwise Addition, Stepwise Deletion Forward Selection, Backward Selection

Table 6.2: A summary of operators in Columbus.

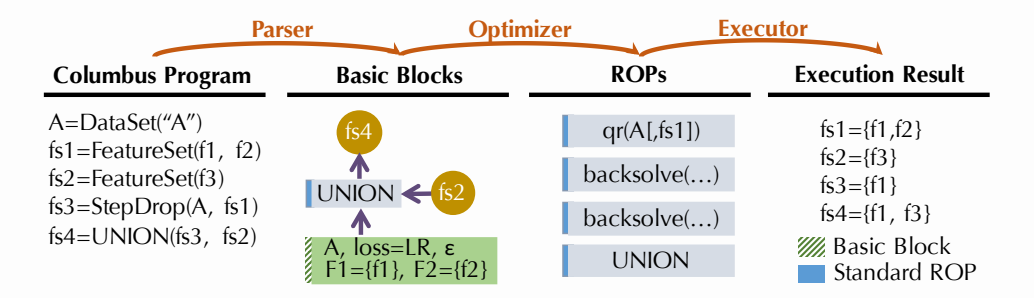

Figure 6.2: Architecture of Columbus.

literature in feature selection. Columbus's language is a strict superset of R, so the user still has access to the full power of R.[3] We found that this flexibility was a requirement for most of the analysts surveyed. Figure 6.1 shows an example snippet of a Columbus program. For example, the 9^{th} line of the program executes logistic regression and reports its score using cross validation.

Columbus has three major datatypes: A *data set*, which is a relational table $R(A_1, \ldots, A_d)$.[4] A *feature set* F for a dataset $R(A_1, \ldots, A_d)$ is a subset of the attributes $F \subseteq \{A_1, \ldots, A_d\}$. A *model* for a feature set is a vector that assigns each feature a real-valued weight. As shown in Table 6.2, Columbus supports several operations. We classify these operators based on what types of output an operator produces and order the classes in roughly increasing order of the sophistication of optimization that Columbus is able to perform for such operations (see Table 6.2 for examples): (1) *Data Transformation Operations*, which produce new data sets; (2) *Evaluate Operations*, which evaluate data sets and models; (3) *Regression Operations*, which produce a model given a feature set; and (4) *Explore Operations*, which produce new feature sets:

(1) Data Transform. These operations are standard data manipulations to slice and dice the

[3] We also have expressed the same language over Python, but for simplicity, we stick to the R model in this section.

[4] Note that the table itself can be a view; this is allowed in Columbus, and the tradeoffs for materialization are standard, so we omit the discussion of them in the section.

dataset. In Columbus, we are aware only of the schema and cardinality of these operations; these operations are executed and optimized directly using a standard RDBMS or main-memory engine. In R, the frames can be interpreted either as a table or an array in the obvious way. We map between these two representations freely.

(2) Evaluate. These operations obtain various numeric scores given a feature set including descriptive scores for the input feature set, e.g., mean, variance, or Pearson correlations and scores computed after regression, e.g., cross-validation error (e.g., of logistic regression), and Akaike Information Criterion (AIC) [89]. Columbus can optimize these calculations by batching several together.

(3) Regression. These operations obtain a model given a feature set and data, e.g., models trained by using logistic regression or linear regression. The result of a regression operation is often used by downstream *explore operations*, which produces a new feature set based on how the previous feature set performs. These operations also take a termination criterion (as they do in R): either the number of iterations or until an error criterion is met. Columbus supports either of these conditions and can perform optimizations based on the type of model (as we discuss).

(4) Explore. These operations enable an analyst to traverse the space of feature sets. Typically, these operations result in training many models. For example, a STEPDROP operator takes as input a data set and a feature set, and outputs a new feature set that removes one feature from the input by training a model on each candidate feature set. Our most sophisticated optimizations leverage the fact that these operations operate on features in *bulk*. The other major operation is STEPADD. Both are used in many workloads and are described in Guyon et al. [89].

Columbus is not intended to be comprehensive. However, it does capture the workloads of several analysts that we observed, so we argue that it serves as a reasonable starting point to study feature selection workloads.

6.1.1.2 Basic Blocks

In Columbus, we compile a user's program into a directed-acyclic-dataflow graph with nodes of two types: R functions and an intermediate representation called a *basic block*. The R functions are opaque to Columbus, and the central unit of optimization is the basic block (extensible optimizers [85]).

Definition 6.1. *A* task *is a tuple* $\mathtt{t} = (A, b, \ell, \epsilon, F, R)$ *where* $A \in \mathbb{R}^{N \times d}$ *is a data matrix,* $b \in \mathbb{R}^N$ *is a*

label (or target), $\ell : \mathbb{R}^2 \to \mathbb{R}^+$ *is a loss function,* $\epsilon > 0$ *is an error tolerance,* $F \subseteq [d]$ *is a feature set, and* $R \subseteq [N]$ *is a subset of rows. A task specifies a regression problem of the form:*

$$L_{\mathsf{t}}(x) = \sum_{i \in R} \ell(z_i, b_i) \text{ s.t. } z = A\Pi_F x$$

Here Π_F *is the axis-aligned projection that selects the columns or feature sets specified by* F.[5] *Denote an optimal solution of the task* $x_*(\mathsf{t})$ *defined as*

$$x_*(\mathsf{t}) = \operatorname*{argmin}_{x \in \mathbb{R}^d} L_{\mathsf{t}}(x)$$

Our goal is to find an $x(\mathsf{t})$ *that satisfies the error*[6]

$$\|L_{\mathsf{t}}(x(\mathsf{t})) - L_{\mathsf{t}}(x_*(\mathsf{t}))\|_2 \leq \epsilon$$

A basic block, B, *is a set of tasks with common data* (A, b) *but with possibly different feature sets* $\bar{F}$ *and subsets of rows* $\bar{R}$.

Columbus supports a family of popular non-linear models, including support vector machines, (sparse and dense) logistic regression, ℓ_p regression, lasso, and elastic net regularization. We give an example to help clarify the definition.

Example 6.2. *Consider the* 6^{th} *line in Figure 6.1, which specifies a five-fold cross validation operator with least squares over data set* d_1 *and feature set* s_1. *Columbus will generate a basic block* B *with five tasks, one for each fold. Let* $t_i = (A, b, l, \epsilon, F, R)$. *Then,* A *and* b *are defined by the data set* d_1 *and* $l(x, b) = (x - b)^2$. *The error tolerance* ϵ *is given by the user in the* 1^{st} *line. The projection of features* $F = s_1$ *is found by a simple static analysis. Finally,* R *corresponds to the set of examples that will be used by the* i^{th} *fold.*

The basic block is the unit of Columbus's optimization. Our design choice is to combine several operations on the same data at a high-enough level to facilitate bulk optimization, which is our focus in the next section.

[5] For $F \subseteq [d]$, $\Pi_F \in \mathbb{R}^{d \times d}$ where $(\Pi_F)_{ii} = 1$ if $i \in F$ and all other entries are 0.

[6] We allow termination criteria via a user-defined function or the number of iterations. The latter simplifies reuse calculations in Section 6.1.2, while arbitrary code is difficult to analyze (we must resort to heuristics to estimate reuse). We present the latter as the termination criterion to simplify the discussion and as it brings out interesting tradeoffs.

Columbus's compilation process creates a task for each regression or classification operator in the program; each of these specifies all of the required information. To enable arbitrary R code, we allow black box code in this work flow, which is simply executed. Selecting how to both optimize and construct basic blocks that will execute efficiently is the subject of Section 6.1.2.

REL Operations To execute a program, we compile it into a sequence of *REL Operations* (ROPs). These are operators that are provided by the R runtime, e.g., R and ORE. Figure 6.3 summarizes the host-level operators that Columbus uses, and we observe that these operators are present in both R and ORE. Our focus is how to optimize the compilation of language operators into ROPs.

6.1.1.3 Executing a Columbus Program

To execute a Columbus program, our prototype contains three standard components, as shown in Figure 6.2: (1) parser; (2) optimizer; and (3) executor. At a high-level, these three steps are similar to the existing architecture of any data processing system. The output of the parser can be viewed as a directed acyclic graph, in which the nodes are either basic blocks or standard ROPs, and the edges indicate data flow dependency. The optimizer is responsible for generating a "physical plan." This plan defines which algorithms and materialization stategies are used for each basic block; the relevant decisions are described in Sections 6.1.2.1 and 6.1.2.2. The optimizer may also merge basic blocks together, which is called *multiblock optimization*, which is described in Section 6.1.2.4. Finally, there is a standard executor that manages the interaction with the REL and issues concurrent requests.

6.1.2 The Columbus Optimizer

We begin with optimizations for a basic block that has a least-squares cost, which is the simplest setting in which Columbus's optimizations apply. We then describe how to extend these ideas to basic blocks that contain nonlinear loss functions and then describe a simple technique called model caching.

Optimization Axes To help understand the optimization space, we present experimental results on the CENSUS data set using Columbus programs modeled after our experience with insurance analysts.

(a) ROPs Used in Columbus and Their Running Times

ROPs	Semantic	Cost
A <- B[1:n,1:d]	matrix sub-selection	DN+dn
A %*% C	matrix multiplication	dnm
A * E	element-wise multiplication	dn
solve(W [,b])	calculate W^{-1} or $W^{-1}b$	d^3
qr(A)	QR decomposition of A	d^2n
sample(V, prob)	Sample element in V with prob	n
backsolve(W [,b])	solve() for triangular matrix W	d^2

(b) Materialization Strategies and ROPs Used by Each Strategy

Materialization Strategies	Materialization ROPs	Execution ROPs
Lazy	N/A	<-, %*%, solve
Eager	<-	%*%, solve
Naïve Sampling	<-, sample	%*%, solve
Coreset	<-, %*%, solve, sample, *	%*%, solve
QR	<-, qr	backsolve

Legend
A: n×d B: N×D C: d×m E: n×d V: n×1 W: d×d
The cost of an op. with **black** font face dominates the cost of any **green** op. for that ROP.

Figure 6.3: (a) ROPs used in Columbus and their costs; (b) Cost model of materializations in Columbus. When data are stored in main memory, the cost for matrix sub-selection ($a \leftarrow B[1:n, 1:d]$) is only dn. In (b), **Materialization ROPs** are the set of ROPs used in the materialization phase for an operator, while **Execution ROPs** are those ROPs used during execution (i.e., while solving the model). The materialization cost and execution cost for each strategy can be estimated by summing the cost of each ROPs they produce in (a).

Figure 6.4 illustrates the crossover points for each optimization opportunity along three axes that we will refer to throughout this section:[7]

(1) Error tolerance depends on the analyst and task. For intuition, we think of different types of error tolerances, with two extremes: *error tolerant* $\epsilon = 0.5$ and *high quality* $\epsilon = 10^{-3}$. In Figure 6.4, we show $\epsilon \in \{0.001, 0.01, 0.1, 0.5\}$.

(2) Sophistication of the feature selection task, namely the loss function (linear or not), the number of feature sets or rows selected, and their degree of overlap. In Figure 6.4, we set the number of features as $\{10, 100, 161\}$ and the number of tasks in each block as $\{1, 10, 20, 50\}$.

[7]For each combination of parameters below, we execute Columbus and record the total execution time in a main memory R backend. This gives us about 40K data points, and we only summarize the best results in this section. Any omitted data point is dominated by a shown data point.

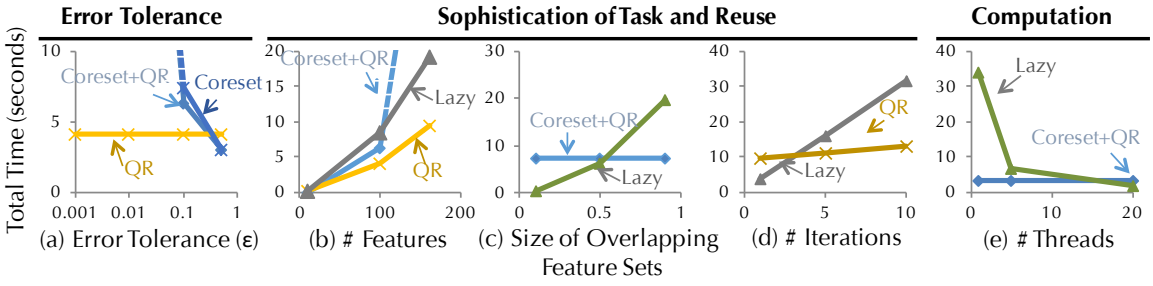

Figure 6.4: An Illustration of the Tradeoff Space of Columbus, which is defined in Section 6.1.2.

(3) Reuse is the degree to which we can reuse computation (and that it is helpful to do so). The key factors are the amount of overlap in the feature sets in the workloads[8] and the number of available threads that Columbus uses, which we set here to $\{1, 5, 10, 20\}$.[9]

We discuss these graphs in paragraphs marked *Tradeoff*.

6.1.2.1 A Single, Linear Basic Block

We consider three families of optimizations: (1) classical database optimizations, (2) sampling-based optimizations, and (3) transformation-based optimizations. The first optimization is essentially unaware of the feature-selection process; in contrast, the last two of these leverage the fact that we are solving several regression problems. Each of these optimizations can be viewed as a form of precomputation (materialization). Thus, we describe the mechanics of each optimization, the cost it incurs in materialization, and its cost at runtime. Figure 6.3 summarizes the cost of each ROP and the dominant ROP in each optimization. Because each ROP is executed once, one can estimate the cost of each materialization from this figure.[10]

To simplify our presentation, in this subsection, we let $\ell(x, b) = (x - b)^2$, i.e., the least-squares loss, and suppose that all tasks have a single error ε. We return to the more general case in the next subsection. Our basic block can be simplified to $\mathsf{B} = (A, b, \bar{F}, \bar{R}, \varepsilon)$, for which we compute:

$$x(R, F) = \operatorname*{argmin}_{x \in \mathbb{R}^d} \| \Pi_R \left(A \Pi_F x - b \right) \|_2^2 \text{ where } R \in \bar{R}, F \in \bar{F}$$

[8] Let $G = (\cup_{F \in \bar{F}} F, E)$ be a graph, in which each node corresponds to a feature. An edge $(f_1, f_2) \in E$ if there exists $F \in \bar{F}$ such that $f_1, f_2 \in F$. We use the size of the largest connected component in G as a proxy for overlap.

[9] Note that Columbus supports two execution models, namely batch mode and interactive mode.

[10] We ran experiments on three different types of machines to validate that the cost we estimated for each operator is close to the actual running time.

Our goal is to compile the basic block into a set of ROPs. We explain the optimizations that we identify below.

Classical Database Optimizations We consider classical eager and lazy view materialization schemes. Denote $F^{\cup} = \cup_{F \in \bar{F}} F$ and $R^{\cup} = \cup_{R \in \bar{R}}$ in the basic block. It may happen that A contains more columns than $F^{\cup}$ and more rows than $R^{\cup}$. In this case, one can project away these extra rows and columns—analogous to materialized views of queries that contain selections and projections. As a result, classical database materialized view optimizations apply. Specially, Columbus implements two strategies, namely *Lazy* and *Eager*. The *Lazy* strategy will compute these projections at execution time, and *Eager* will compute these projections at materialization time and use them directly at execution time. When data are stored on disk, e.g., as in ORE, *Eager* could save I/Os versus *Lazy*.

Tradeoff Not surprisingly, *Eager* has a higher materialization cost than *Lazy*, while *Lazy* has a slightly higher execution cost than *Eager*, as one must subselect the data. Note that if there is ample parallelism (at least as many threads as feature sets), then Lazy dominates. The standard tradeoffs apply, and Columbus selects between these two techniques in a cost-based way. If there are disjoint feature sets $F_1 \cap F_2 = \emptyset$, then it may be more efficient to materialize these two views separately. The general problem of selecting an optimal way to split a basic block to minimize cost is essentially a weighted set cover, which is NP-hard. As a result, we use a simple heuristic: split disjoint feature sets. With a feature selection workload, we may know the number of times a particular view will be reused, which Columbus can use to more intelligently chose between Lazy and Eager (rather than not having this information). These methods are insensitive to error and the underlying loss function, which will be major concerns for our remaining feature-selection-aware methods.

Sampling-Based Optimizations Subsampling is a popular method to cope with large data and long runtimes. This optimization saves time simply because one is operating on a smaller dataset. This optimization can be modeled by adding a subset selection ($R \in \bar{R}$) to a basic block. In this section, we describe two popular methods: *naïve random sampling* and a more sophisticated importance-sampling method called *coresets* [38, 114]; we describe the tradeoffs these methods provide.

Naïve Sampling Naïve random sampling is widely used, and in fact, analysts often ask for it by name. In naïve random sampling, one selects some fraction of the data set. Recall that A has N

rows and d columns; in naïve sampling, one selects some fraction of the N rows (say 10%). The cost model for both materialization and its savings of random sampling is straightforward, as one performs the same solve—only on a smaller matrix. We perform this sampling using the ROP SAMPLE.

Coresets A recent technique called *coresets* allows one to sample from an overdetermined system $A \in \mathbb{R}^{N \times d}$ with a sample size that is proportional to d and independent of N with much stronger guarantees than naïve sampling. In some enterprise settings, d (the number of features) is often small (say 40), but the number of data points is much higher, say millions, and coresets can be a large savings. We give one such result:

Proposition 6.3 (Boutsidis et al. [38]). *For $A \in \mathbb{R}^{N \times d}$ and $b \in \mathbb{R}^N$. Define $s(i) = a_i^T \left(A^T A\right)^{-1} a_i$. Let $\tilde{A}$ and $\tilde{b}$ be the result of sampling m rows, where row i is selected with probability proportional to $s(i)$. Then,* for all *$x \in \mathbb{R}^d$, we have*

$$\Pr\left[\left|\|Ax - b\|_2^2 - \frac{N}{m}\|\tilde{A}x - \tilde{b}\|_2^2\right| < \varepsilon\|Ax - b\|_2^2\right] > \frac{1}{2}$$

So long as $m > 2\varepsilon^{-2} d \log d$.

This guarantee is strong.[11] To understand how strong, observe that naïve sampling cannot meet this type of guarantee, without sampling proportional to N. To see this, consider the case in which a feature occurs in only a single example, e.g., $A_{1,1} = 1$ and $A_{i,1} = 0$ for $i = 2, \ldots, N$. It is not hard to see that the only way to achieve a similar guarantee is to make sure the first row is selected. Hence, naïve sampling will need roughly N samples to guarantee this is selected. Note that Prop 6.3 does not use the value b. Columbus uses this fact later to optimize basic blocks with changing b.

Tradeoff Looking at Figure 6.4, one can see a clear tradeoff space: coresets require two passes over the data to compute the sensitivity scores. However, the smaller sample size (proportional to d) can be a large savings when the error ϵ is moderately large. But as either d or ϵ^{-1} grows, coresets become less effective, and there is a cross-over point. In fact, coresets are useless when $N = d$. One benefit of coresets is that they have explicit error guarantees in terms of ϵ. Thus, our current implementation of Columbus will not automatically apply *Naïve Sampling* unless the user requests it. With optimal settings for sample size, naïve sampling can get better performance than coresets.

[11] Note that one can use $\log_2 \delta^{-1}$ independent trials to boost the probability of success to $1 - \delta$.

Transformation-Based Optimizations In linear algebra, there are decomposition methods to solve (repeated) least-squares efficiently; the most popular of these is called the QR decomposition [81]. At a high level, we use the QR decomposition to transform the data matrix A so that *many* least-squares problems can be solved efficiently. Typically, one uses a QR to solve for many different values of b (e.g., in Kalman filter updates). However, in feature selection, we use a different property of the QR: that it can be used across many *different feature sets*. We define the QR factorization (technically the thin QR), describe how Columbus uses it, and then describe its cost model.

Definition 6.4 (Thin QR Factorization)**.** *The QR decomposition of a matrix $A \in R^{N \times d}$ is a pair of matrices (Q, R) where $Q \in \mathbb{R}^{N \times d}$, $R \in \mathbb{R}^{d \times d}$, and A=QR. Q is an orthogonal matrix, i.e., $Q^T Q = I$ and R is upper triangular.*

We observe that since $Q^{-1} = Q^T$ and R is upper triangular, one can solve $Ax = b$ by setting $QRx = b$ and multiplying through by the transpose of Q so that $Rx = Q^T b$. Since R is upper triangular, one can solve can this equation with back substitution; back substitution does not require computing the inverse of R, and its running time is linear in the number of entries of R, i.e., $O(d^2)$.

Columbus leverages a simple property of the QR factorization: upper triangular matrices are closed under multiplication, i.e., if U is upper triangular, then so is RU. Since Π_F is upper triangular, we can compute *many* QR factorizations by simply reading off the inverse of $R\Pi_F$.[12] This simple observation is critical for feature selection. Thus, if there are several different row selectors, Columbus creates a separate QR factorization for each.

Tradeoff As summarized in Figure 6.3, QR's materialization cost is similar to importance sampling. In terms of execution time, Figure 6.4 shows that QR can be much faster than coresets: solving the linear system is quadratic in the number of features for QR but cubic for coresets (without QR). When there are a large number of feature sets and they overlap, QR can be a substantial win (this is precisely the case when coresets are ineffective). These techniques can also be combined, which further modifies the optimal tradeoff point. An additional point is that QR does not introduce error (and is often used to improve numerical stability), which means that QR is applicable in error tolerance regimes when sampling methods cannot be used.

[12]Notice that $\Pi_R Q$ is not necessarily orthogonal, so $\Pi_R Q$ may be expensive to invert.

Discussion of Tradeoff Space Figure 6.4 shows the crossover points for the tradeoffs we described in this section for the CENSUS dataset. We describe why we assert that each of the following aspects affects the tradeoff space.

Error For error-tolerant computation, naïve random sampling provides dramatic performance improvements. However, when low error is required, then one must use classical database optimizations or the QR optimization. In between, there are many combinations of QR, coresets, and sampling that can be optimal. As we can see in Figure 6.4(a), when the error tolerance is small, coresets are significantly slower than QR. When the tolerance is 0.01, the coreset we need is even larger than the original data set, and if we force Columbus to run on this large coreset, it would be more than 12x slower than QR. For tolerance 0.1, coreset is 1.82x slower than QR. We look into the breakdown of materialization time and execution time, and we find that materialization time contributes to more than 1.8x of this difference. When error tolerance is 0.5, Coreset+QR is 1.37x faster than QR. We ignore the curve for Lazy and Eager because they are insensitive to noises and are more than 1.24x slower than QR.

Sophistication One measure of sophistication is the number of features the analyst is considering. When the number of features in a basic block is much smaller than the data set size, coresets create much smaller but essentially equivalent data sets. As the number of features, d, increases, or the error decreases, coresets become less effective. On the other hand, optimizations, like QR, become more effective in this regime: although materialization for QR is quadratic in d, it reduces the cost to compute an inverse from roughly d^3 to d^2.

As shown in Figure6.4(b), as the number of features grows, CoreSet+QR slows down. With 161 features, the coreset will be larger than the original data set. However, when the number of features is small, the gap between CoreSet+QR and QR will be smaller. When the number of features is 10, CoreSet+QR is 1.7x faster than QR. When the number of feature is small, the time it takes to run a QR decomposition over the coreset could be smaller than over the original data set, hence, the 1.7x speedup of CoreSet+QR over QR.

Reuse In linear models, the amount of overlap in the feature sets correlates with the amount of reuse. We randomly select features but vary the size of overlapping feature sets. Figure6.4(c) shows the result. When the size of the overlapping feature sets is small, Lazy is 15x faster than CoreSet+QR.

This is because CoreSet wastes time in materializing for a large feature set. Instead, Lazy will solve these problems independently. On the other hand, when the overlap is large, CoreSet+QR is 2.5x faster than Lazy. Here, CoreSet+QR is able to amortize the materialization cost by reusing it on different models.

Available Parallelism If there is a large amount of parallelism and one needs to scan the data only once, then a lazy materialization strategy is optimal. However, in feature selection workloads where one is considering hundreds of models or repeatedly iterating over data, parallelism may be limited, so mechanisms that reuse the computation may be optimal. As shown by Figure 6.4(e), when the number of threads is large, Lazy is 1.9x faster than CoreSet+QR. The reason is that although the reuse between models is high, all of these models could be run in parallel in Lazy. Thus, although CoreSet+QR does save computation, it does not improve the wall-clock time. On the other hand, when the number of threads is small, CoreSet+QR is 11x faster than Lazy.

6.1.2.2 A Single, Non-linear Basic Block

We extend our methods to non-linear loss functions. The same tradeoffs from the previous section apply, but there are two additional techniques we can use. We describe them below.

Recall that a task solves the problem

$$\min_{x \in R^d} \sum_{i=1}^{N} \ell(z_i, b_i) \text{ subject to } z = Ax$$

where $\ell : \mathbb{R}^2 \to \mathbb{R}^+$ is a convex function.

Iterative Methods We select two methods: stochastic gradient descent (SGD) [31, 37, 169], and iterative reweighted least squares (IRLS), which is implemented in R's generalized linear model package.[13] We describe an optimization, warmstarting, that applies to such models as well as to ADMM.

ADMM There is a classical, general purpose method that allows one to *decompose* such a problem into a least-squares problem and a second simple problem. The method we explore is one of the most popular, called *the Alternating Direction Method of Multipliers (ADMM)* [39], which has been widely

[13] `stat.ethz.ch/R-manual/R-patched/library/stats/html/glm.html`

used since the 1970s. We explain the details of this method to highlight a key property that allows us to reuse the optimizations from the previous section.

ADMM is iterative and defines a sequence of triples (x^k, z^k, u^k) for $k = 0, 1, 2, \ldots$. It starts by randomly initializing the three variables (x^0, z^0, u^0), which are then updated by the following equations:

$$\begin{aligned} x^{(k+1)} &= \underset{x}{\operatorname{argmin}} \frac{\rho}{2}||Ax - z^{(k)} + u^{(k)}||_2^2 \\ z^{(k+1)} &= \underset{z}{\operatorname{argmin}} \sum_{i=1}^{N} l(z_i, b_i) + \frac{\rho}{2}||Ax^{(k+1)} - z + u^{(k)}||_2^2 \\ u^{(k+1)} &= u^{(k)} + Ax^{(k+1)} - z^{(k+1)} \end{aligned}$$

The constant $\rho \in (0, 2)$ is a step size parameter that we set by a grid search over five values.

There are two key properties of the ADMM equations that are critical for feature selection applications:

(1) Repeated Least Squares The solve for $x^{(k+1)}$ is a linear basic block from the previous section since z and u are fixed and the A matrix is *unchanged* across iteration. In nonlinear basic blocks, we solve multiple feature sets concurrently, so we can reuse the transformation optimizations of the previous section for each such update. To take advantage of this, Columbus logically rewrites ADMM into a sequence of linear basic blocks with custom R functions.

(2) One-dimensional z We can rewrite the update for z into a series of independent, one-dimensional problems. That is,

$$z_i^{(k+1)} = \underset{z_i}{\operatorname{argmin}}\, l(z_i, b_i) + \frac{\rho}{2}(q_i - z_i)^2, \text{ where } q = Ax^{(k+1)} + u^{(k)}$$

This one-dimensional minimization can be solved by fast methods, such as bisection or Newton. To update $x^{(k+1)}$, the bottleneck is the ROP "solve," whose cost is in Figure 6.3. The cost of updating z and u is linear in the number of rows in A, and can be decomposed into N problems that may be solved independently.

Tradeoffs In Columbus, ADMM is our default solver for non-linear basic blocks. Empirically, on all of our applications in our experiments, if one first materializes the QR computation for the least-squares subproblem, then we find that ADMM converges faster than SGD to the same loss. Moreover, there is sharing *across* feature sets that can be leveraged by Columbus in ADMM (using our earlier optimization about QR). One more advanced case for reuse is when we must fit hyperparameters, like ρ above or regularization parameters; in this case, ADMM enables opportunities for high degrees of sharing.

6.1.2.3 Warmstarting by Model-Caching

In feature selection workloads, our goal is to solve a model after having solved many similar models. For iterative methods like gradient descent or ADMM, we should be able to partially reuse these similar models. We identify three situations in which such reuse occurs in feature-selection workloads: (1) We downsample the data, learn a model on the sample, and then train a model on the original data. (2) We perform stepwise removal of a feature in feature selection, and the "parent" model with all features is already trained. (3) We examine several nearby feature sets interactively. In each case, we should be able to reuse the previous models, but it would be difficult for an analyst to implement effectively in all but the simplest cases. In contrast, Columbus can use warmstart to achieve up to 13x performance improvement for iterative methods without user intervention.

Given a cache of models, we need to choose a model: we observe that computing the loss of each model on the cache on a sample of the data is inexpensive. Thus, we select the model with the lowest sampled loss. To choose models to evict, we simply use an LRU strategy. In our workloads, the cache does not become full, so we do not discuss it. However, if one imagines several analysts running workloads on similar data, the cache could become a source of challenges and optimizations.

6.1.2.4 Multiblock Optimization

There are two tasks we need to do across blocks: (1) We need to decide on how coarse or fine to make a basic block, and (2) we need to execute the sequence of basic blocks across the backend.

Multiblock Logical Optimization Given a sequence of basic blocks from the parser, Columbus must first decide how coarse or fine to create individual blocks. Cross validation is, for example, merged into a single basic block. In Columbus, we greedily improve the cost using the obvious

	Features	Tuples	Size	# Basic Blocks	# Tasks /Basic Blocks	# Lines of Code	Type of Basic Blocks
KDD	481	191 K	235 MB	6	10	28	6 LR Blocks
Census	161	109 K	100 MB	4	0.2 K	16	3 LS, 1 LR
Music	91	515 K	1 GB	4	0.1 K	16	3 LS, 1 LR
Fund	16	74 M	7 GB	1	2.5 K	4	1 LS
House	10	2 M	133 MB	1	1.0 K	4	1 LS

Table 6.3: Dataset and Program Statistics. LS refers to Least Sqaures. LR refers to Logistic Regression.

estimates from Figure 6.3. The problem of deciding the optimal partitioning of many feature sets is NP-hard by a reduction to WEIGHTEDSETCOVER. The intuition is clear, as one must cover all the different features with as few basic blocks as possible. However, the heuristic merging can have large wins, as operations like cross validation and grid searching parameters allow one to find opportunities for reuse.

Cost-based Execution Recall that the executor of Columbus executes ROPs by calling the required database or main-memory backend. The executor is responsible for executing and coordinating multiple ROPs that can be executed in parallel; Columbus executor simply creates one thread to manage each of these ROPs. The actual execution of each physical operator is performed by the backend statistical framework, e.g., R or ORE. Nevertheless, we need to decide how to schedule these ROPs for a given program. We experimented with the tradeoff of how coarsely or finely to batch the execution. Many of the straightforward formulations of the scheduling problems are, not surprisingly, NP-hard. Nevertheless, we found that a simple greedy strategy (to batch as many operators as possible, i.e., operators that do not share data flow dependencies) was within 10% of the optimal schedule obtained by a brute-force search. After digging into this detail, we found that many of the host-level substrates already provide sophisticated data processing optimizations (e.g. sharing scans).

6.1.3 Experiments

Using the materialization tradeoffs we have outlined, we validate that Columbus is able to speed up the execution of feature selection programs by orders of magnitude compared to straightforward implementations in state-of-the-art statistical analytics frameworks across two different backends: R (in-memory) and a commercial RDBMS. We validate the details of our technical claims about the tradeoff space of materialization and our (preliminary) multiblock optimizer.

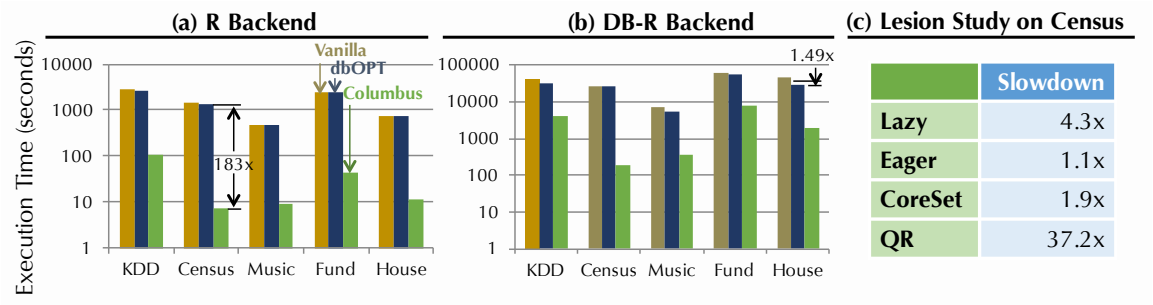

Figure 6.5: End-to-end Performance of Columbus. All approaches return a loss within 1% optimal loss.

6.1.3.1 Experiment Setting

Based on conversations with analysts, we selected a handful of datasets and created programs that use these datasets to mimic analysts' tasks in different domains. We describe these programs and other experimental details.

Datasets and Programs To compare the efficiency of Columbus with baseline systems, we select five publicly available data sets: (1) **Census**, (2) **House**, (3) **KDD**, (4) **Music**, and (5) **Fund**.[14] These data sets have different sizes, and we show the statistics in Table 6.3. We categorize them by the number of features in each data set.

Both **House**, a dataset for predicting household electronic usage, and **Fund**, a dataset for predicting the donation that a given agency will receive each year, have a small number of features (fewer than 20). In these data sets, it is feasible to simply try and score almost all combinations of features. We mimic this scenario by having a large basic block that regresses a least-squares model on feature sets of sizes larger than 5 on House and 13 on Fund and then scores the results using AIC. These models reflect a common scenario in current enterprise analytics systems.

At the other extreme, **KDD** has a large number of features (481), and it is infeasible to try many combinations. In this scenario, the analyst is guided by automatic algorithms, like Lasso [184] (that selects a few sparse features), manual intervention (moving around the feature space), and heavy use of cross-validation techniques.[15] **Census** is a dataset for the task of predicting mail responsiveness of people in different Census blocks, each of which contains a moderate number of features (161). In

[14]These data sets are publicly available on Kaggle (`www.kaggle.com/`) or the UCI Machine Learning Repository. (`archive.ics.uci.edu/ml/`)

[15] The **KDD** program contains six basic blocks, each of which is a 10-fold cross-validation. These six different basic blocks work on non-overlappings set of features specified by the user manually.

this example, analysts use a mix of automatic and manual specification tasks that are interleaved.[16] This is the reason that we select this task for our running example. **Music** is similar to **Census**, and both programs contain linear models (least squares) and non-linear models (logistic regression) to mimic the scenario in which an analyst jointly explores the feature set to select and the model to use.

R Backends We implemented Columbus on multiple backends and report on two: (1) *R*, which is the standard, main-memory R and (2) *DB-R*, commercial R implementation over RDBMS. We use R 2.15.2, and the most recent available versions of the commercial systems.

For all operators, we use the result of the corresponding main memory R function as the gold standard. All experiments are run on instances on Amazon EC2 (cr1.8xlarge), which has 32 vCPU, 244 GB RAM, and 2x120GB SSD and runs Ubuntu 12.04.[17]

6.1.3.2 End-to-End Efficiency

We validate that Columbus improves the end-to-end performance of feature selection programs. We construct two families of competitor systems (one for each backend): VANILLA, and DBOPT. VANILLA is a baseline system that is a straightforward implementation of the corresponding feature selection problem using the ROPs; thus it has the standard optimizations. DBOPT is Columbus, but we enable only the optimizations that have appeared in classical database literature, i.e., Lazy, Eager, and batching. DBOPT and Columbus perform scheduling in the same way to improve parallelism to isolate the contributions of the materialization. Figure 6.5 shows the result of running these systems over all five data sets with error tolerance ϵ set to 0.01.

On the R-based backend, Columbus executes the same program using less time than R on all datasets. On Census, Columbus is two orders of magnitude faster, and on Music and Fund, Columbus is one order of magnitude faster. On Fund and House, Columbus chooses to use CoreSet+QR as the materialization strategy for all basic blocks and chooses to use QR for other data sets. This is because for data sets that contain fewer rows and more columns, QR dominates CoreSet-based approaches, as described in the previous Section. One reason that Columbus improves more on Census than on Music and Fund is that Census has more features than Music and Fund; therefore, operations like StepDrop produce more opportunities for reuse than Census.

[16] The **Census** program contains four basic blocks, each of which is a STEPDROP operation on the feature set output by the previous basic block.

[17] We also run experiments on other dedicated machines. The tradeoff space is similar to what we report in this section.

To understand the classical points in the tradeoff space, compare the efficiency of DBOPT with the baseline system, VANILLA. When we use R as a backend, the difference between DBOPT and R is less than 5%. The reason is that R holds all data in memory, and accessing a specific portion of the data does not incur any IO cost. In contrast, we observe that when we use the DB backend, DBOPT is 1.5x faster than VANILLA on House. However, this is because the underlying database is a row store, so the time difference is due to IO and deserialization of database tuples.

We can also see that the new forms of reuse we outline are significant. If we compare the execution time of Census and Music, we see a difference between the approaches. While Census is smaller than Music, baseline systems, e.g., VANILLA, are slower on Census than on Music. In contrast, Columbus is faster on Census than on Music. This is because Census contains more features than Music; therefore, the time that VANILLA spent on executing complex operators like STEPDROP is larger in CENSUS. In contrast, by exploiting the new tradeoff space of materialization, Columbus is able to reuse computation more efficiently for feature selection workloads.

6.1.3.3 Linear Basic Blocks

We validate that all materialization tradeoffs that we identified affect the efficiency of Columbus. In Section 6.1.2, we designed experiments to understand the tradeoff between different materialization strategies with respect to three axes, i.e., error tolerance, sophistication of tasks and reuse, and computation. Here, we validate that each optimization contributes to the final results in a full program (on Census). We then validate our claim that the cross-over points for optimizations change based on the dataset but that the space essentially stays the same. We only show results on the main-memory backend.

Lesion Study We validate that each materialization strategy has an impact on the performance of Columbus. For each parameter setting used to create Figure 6.4, we remove a materialization strategy. Then, we measure the maximum slowdown of an execution with that optimization removed. We report the maximum slowdown across all parameters in Figure 6.5(c) in main memory on Census. We see that Lazy, QR, and CoreSet all have significant impacts on quality, ranging from 1.9x to 37x. This means that if we drop any of them from Columbus, one would expect a 1.9x to 37x slowdown on the whole Columbus system. Similar observations hold for other backends. The only major difference is that our DB-backend is a row store, and Eager has a larger impact (1.5x slowdown).

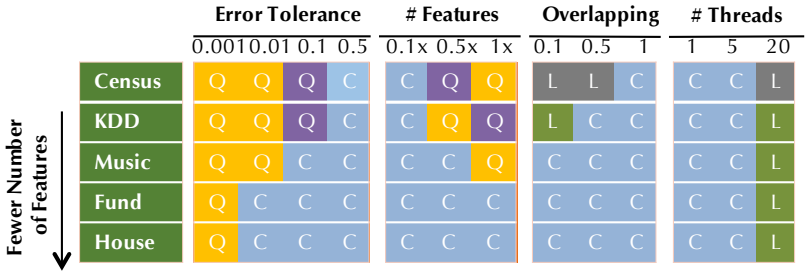

Figure 6.6: Robustness of Materialization Tradeoffs Across Datasets. For each parameter setting (one column in the table), we report the materialization strategy that has the fastest execution time given the parameter setting. Q refers to QR, C refers to CoreSet+QR, and L refers to Lazy. The protocol is the same as Figure 6.4 in Section 6.1.2.

We validate our claim that the high-level principles of the tradeoffs remain the same across datasets, but we contend that the tradeoff points change across data sets. Thus, our work provides a guideline about these tradeoffs, but it is still difficult for an analyst to choose the optimal point. In particular, for each parameter setting, we report the name of the materialization strategy that has the fastest execution time. Figure 6.6 shows that across different data sets, the same pattern holds, but with different crossover points. Consider the *error tolerance*. On all data sets, for high error tolerance, CoreSet+QR is always faster than QR. On Census and KDD, for the lowest three error tolerances, QR is faster than CoreSet+QR, while on Music, only for the lowest two error tolerance is QR faster than CoreSet+QR. While on Fund and House, for all error tolerances except the lowest one, CoreSet+QR is faster than QR. Thus, the cross-over point changes.

6.1.3.4 Non-Linear Basic Blocks with ADMM

Columbus uses ADMM as the default non-linear solver, which requires that one solves a least-squares problem that we studied in linear basic blocks. Compared with linear basic blocks, one key twist with ADMM is that it is iterative–thus, it has an additional parameter, the number of iterations to run. We validate that tradeoffs similar to the linear case still apply to non-linear basic blocks, and we describe how convergence impacts the tradeoff space. For each data set, we vary the number of iterations to run for ADMM and try different materialization strategies. For CoreSet-based approaches, we grid search the error tolerance, as we did for the linear case. As shown in Figure 6.4(d), when the number of iterations is small, QR is 2.24x slower than Lazy. Because there is only one iteration, the least-squares problem is only solved once. Thus, Lazy is the faster strategy compared with QR.

However, when the number of iterations grows to 10, QR is 3.8x faster than Lazy. This is not

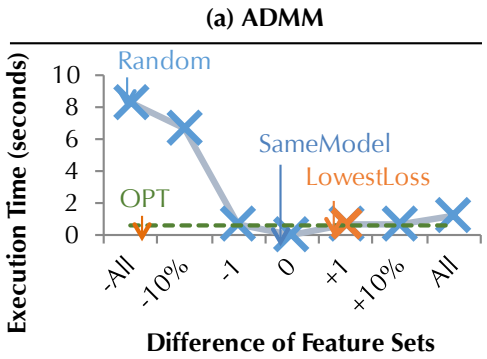

(b) SGD and IRLS

	% to Optimal Loss	
	10%	100%
SGD	4x	1x
IRLS	12x	3x

Figure 6.7: (a) The Impact of Model Caching for ADMM. The execution time is measured by the time needed to converge to 1% optimal loss. (b) The Speed-up of Model Caching. Different iterative approaches are compared to a given loss with a random initial model.

surprising based on our study for linear cases–by running more iterations, the opportunities for reuse increase. We expect an even larger speedup if we run more iterations.

Warmstart Using Model Caching We validate the model-caching tradeoff for different iterative models, including ADMM, SGD, and IRLS. We use logistic regression as an example throughout (as it is the most common non-linear loss).

Given a feature set F, we construct seven feature sets to mimic different scenarios of model caching, and we call them F^{-All}, $F^{-10\%}$, F^{-1}, F^{0} F^{+1}, $F^{+10\%}$, F^{+All}. Where F^{-All} mimics the cold start problem when the analyst has not trained any models for this data set, we initialize with a random data point (this is RANDOM); F^{+All} means that the analyst has a "super parent" model trained for all features and has selected some features for warmstart; $F^{-10\%}$ (resp. $F^{+10\%}$) is when we warmstart with a model different from F by removing (resp. adding) $10\%|F|$ of randomly picked features; F^{+1} and F^{-1} mimic models generated by StepDrop or StepAdd, which are different from F by removing or adding only a single feature. F^{0} is when we have the same F (we call it SAMEMODEL). For each data set, we run ADMM with the initial model set to the model obtained from training different Fs. Then, we measure the time needed to converge to 1%, 10%, and 2x of the optimal loss for F. Our heuristic, LOWESTLOSS, chooses a single model based on which has the lowest loss, and OPT chooses the lowest execution time among all Fs, except F^{0}. Because the process relies on randomly selecting features to add or remove, we randomly select 10 feature sets and train a model for each them and report the average.

We first consider this for ADMM, and Figure 6.7(a) shows the result. We see that LOWESTLOSS

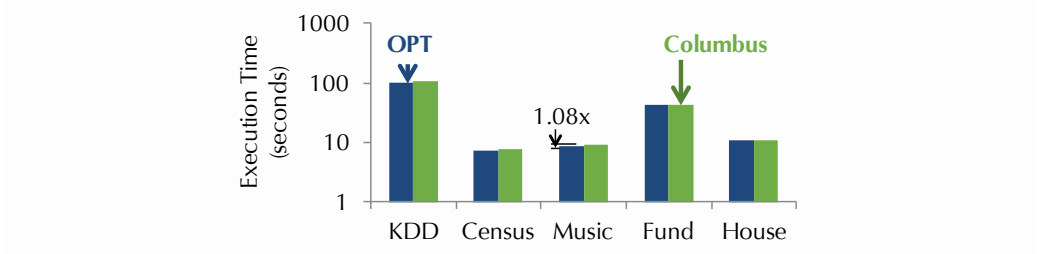

Figure 6.8: Greedy versus optimal optimizer

is 13x faster than RANDOM. Also, if we disable our heuristic and just pick a random feature set to use for warmstart, we could be 11x slower in the worst case. Compared with OPT, LOWESTLOSS is 1.03x slower. This validates the effectiveness of our warmstart heuristic. Another observation is that when we use a feature set that is a superset of F (F^{+1}, $F^{+10\%}$), we can usually expect better performance than using a subset (F^{-1}, $F^{-10\%}$). This is not surprising because the superset contains more information relevant to all features in F.

Other Iterative Approaches We validate that warmstart also works for other iterative approaches, namely SGD and IRLS (the default in R). We run all approaches and report the speedup using our proposed lowest-loss-heuristic compared with RANDOM. As shown in Figure 6.7(b), we see that both SGD and IRLS are able to take advantage of warmstarting to speed up their convergence by up to 12x.

6.1.3.5 Multiblock Optimization

We validate that our greedy optimizer for multi-block optimization has comparable performance to the optimal. We compare the plan that is picked by the Columbus optimizer, which uses a greedy algorithm to choose between different physical plans, and the optimal physical plan that we find by brute-force search.[18] We call the optimal physical plan OPT and show the result in Figure 6.8.

As shown in Figure 6.8, Columbus's greedy optimizer is slower than OPT on KDD, Census, and Music; however, it is slower within a range of less than 10%. For Fund and House, OPT has the same performance as Columbus's greedy optimizer, because there is only one basic block, and the optimal strategy is picked by Columbus's greedy optimizer. When OPT selects a better plan than our greedy optimizer, we found that the greedy optimizer does not accurately estimate the amount of reuse.

[18]For each physical plan, we terminate the plan if it runs longer than the plan picked by the greedy scheduler.

6.1.4 Conclusion to Interative Feature Selection

Columbus is the first system to treat the feature selection dialogue as a database systems problem. Our first contribution is a declarative language for feature selection, informed by conversations with analysts over the last two years. We observed that there are reuse opportunities in analysts' workloads that are not addressed by today's R backends. To demonstrate our point, we showed that simple materialization operations could yield orders of magnitude performance improvements on feature selection workloads. As analytics grows in importance, we believe that feature selection will become a pressing data management problem.

6.2 Incremental Feature Engineering

The ultimate goal of KBC is to obtain high-quality structured data from unstructured information. These databases are richly structured with tens of different entity types in complex relationships. Typically, quality is assessed using two complementary measures: precision (how often a claimed tuple is correct) and recall (of the possible tuples to extract, how many are actually extracted). These systems can ingest massive numbers of documents–far outstripping the document counts of even well-funded human curation efforts. Industrially, KBC systems are constructed by skilled engineers in a months-long process–not a one-shot algorithmic task. Arguably, the most important question in such systems is how to best use skilled engineers' time to rapidly improve data quality. In its full generality, this question spans a number of areas in computer science, including programming languages, systems, and HCI. We focus on a narrower question, with the axiom that *the more rapid the programmer moves through the KBC construction loop, the more quickly she obtains high-quality data.*

This section describes how DeepDive enables this fast KBC construction loop. Recall that DeepDive's execution model go through two main phases: (1) *grounding*, in which one evaluates a sequence of SQL queries to produce a data structure called a *factor graph* that describes a set of random variables and how they are correlated. Essentially, every tuple in the database or result of a query is a random variable (node) in this factor graph; (2) the *inference* phase takes the factor graph from grounding and performs statistical inference using standard techniques, e.g., Gibbs sampling [195,206]. The output of inference is the marginal probability of every tuple in the database. As with Google's Knowledge Vault [70] and others [142], DeepDive also produces marginal probabilities

that are *calibrated*: if one examined all facts with probability 0.9, we would expect that approximately 90% of these facts would be correct. To calibrate these probabilities, DeepDive estimates (i.e., learns) parameters of the statistical model from data. Inference is a subroutine of the learning procedure and is the critical loop. Inference and learning are computationally intense (hours on 1TB RAM/48-cores).

In our experience with DeepDive, we found that KBC is an iterative process. In the past few years, DeepDive has been used to build dozens of high-quality KBC systems by a handful of technology companies, a number law enforcement agencies via DARPA's MEMEX, and scientists in fields such as paleobiology, drug repurposing, and genomics. In all cases, we have seen the process of developing KBC systems is iterative: quality requirements change, new data sources arrive, and new concepts are needed in the application. This led us to develop techniques to make the entire pipeline incremental in the face of changes both to the data and to the DeepDive program. Our primary technical contributions are to make the grounding and inference phases more incremental.

Incremental Grounding Grounding and feature extraction are performed by a series of SQL queries. To make this phase incremental, we adapt the algorithm of Gupta, Mumick, and Subrahmanian [88]. In particular, DeepDive allows one to specify "delta rules" that describe how the output will change as a result of changes to the input. Although straightforward, this optimization has not been applied systematically in such systems and can yield up to $360\times$ speedup in KBC systems.

Incremental Inference Due to our choice of incremental grounding, the input to DeepDive's inference phase is a factor graph along with a set of changed data and rules. The goal is to compute the output probabilities computed by the system. Our approach is to frame the incremental maintenance problem as one of approximate inference. Previous work in the database community has looked at how machine learning data products change in response to both to new labels [110] and to new data [52,53]. In KBC, both the program and data change on each iteration. Our proposed approach can cope with both types of change simultaneously.

The technical question is which approximate inference algorithms to use in KBC applications. We choose to study two popular classes of approximate inference techniques: *sampling-based materialization* (inspired by sampling-based probabilistic databases such as MCDB [100]) and *variational-based materialization* (inspired by techniques for approximating graphical models [187]). Applying these techniques to incremental maintenance for KBC is novel, and it is not theoretically clear how the

techniques compare. Thus, we conducted an experimental evaluation of these two approaches on a diverse set of DeepDive programs.

We found these two approaches are sensitive to changes along three largely orthogonal axes: the size of the factor graph, the sparsity of correlations, and the anticipated number of future changes. The performance varies by up to two orders of magnitude in different points of the space. Our study of the tradeoff space highlights that neither materialization strategy dominates the other. To automatically choose the materialization strategy, we develop a simple rule-based optimizer.

Experimental Evaluation Highlights We used DeepDive programs developed by our group and DeepDive users to understand whether the improvements we describe can speed up the iterative development process of DeepDive programs. To understand the extent to which DeepDive's techniques improve development time, we took a sequence of six snapshots of a KBC system and ran them with our incremental techniques and completely from scratch. In these snapshots, our incremental techniques are 22$\times$ faster. The results for each snapshot differ at most by 1% for high-quality facts (90%+ accuracy); fewer than 4% of facts differ by more than 0.05 in probability between approaches. Thus, essentially the same facts were given to the developer throughout execution using the two techniques, but the incremental techniques delivered them more quickly.

Outline The rest of the section is organized as follows. We discuss the different techniques for incremental maintenance in Section 6.2.1. We also present the results of the exploration of the tradeoff space and the description of our optimizer. Our experimental evaluation is presented in Section 6.2.2.

6.2.1 Incremental KBC

To help the KBC system developer be more efficient, we developed techniques to incrementally perform the grounding and inference step of KBC execution.

Problem Setting Our approach to incrementally maintaining a KBC system runs in two phases. **(1) Incremental Grounding.** The goal of the incremental grounding phase is to evaluate an update of the DeepDive program to produce the "delta" of the modified factor graph, i.e., the modified variables ΔV and factors ΔF. This phase consists of relational operations, and we apply classic incremental

view maintenance techniques. **(2) Incremental Inference.** The goal of incremental inference is given $(\Delta V, \Delta F)$ run statistical inference on the changed factor graph.

6.2.1.1 Standard Techniques: Delta Rules

Because DeepDive is based on SQL, we are able to take advantage of decades of work on incremental view maintenance. The input to this phase is the same as the input to the grounding phase, a set of SQL queries and the user schema. The output of this phase is how the output of grounding changes, i.e., a set of modified variables ΔV and their factors ΔF. Since V and F are simply views over the database, any view maintenance techniques can be applied to incremental grounding. DeepDive uses DRED algorithm [88] that handles both additions and deletions. Recall that in DRED, for each relation R_i in the user's schema, we create a *delta relation*, R_i^δ, with the same schema as R_i and an additional column $count$. For each tuple t, $t.count$ represents the number of derivations of t in R_i. On an update, DeepDive updates delta relations in two steps. First, for tuples in R_i^δ, DeepDive directly updates the corresponding counts. Second, a SQL query called a *"delta rule"*[19] is executed which processes these counts to generate modified variables ΔV and factors ΔF. We found that the overhead DRED is modest and the gains may be substantial, and so DeepDive always runs DRED–except on initial load.

6.2.1.2 Novel Techniques for Incremental Maintenance of Inference

We present three techniques for the incremental inference phase on factor graphs: given the set of modified variables ΔV and modified factors ΔF produced in the incremental grounding phase, our goal is to compute the new distribution. We split the problem into two phases. In the *materialization phase*, we are given access to the entire DeepDive program, and we attempt to store information about the original distribution, denoted $\Pr^{(0)}$. Each approach will store different information to use in the next phase, called the *inference phase*. The input to the inference phase is the materialized data from the preceding phase and the changes made to the factor graph, the modified variables ΔV and factors ΔF. Our goal is to perform inference with respect to the changed distribution, denoted $\Pr^{(\Delta)}$. For each approach, we study its space and time costs for materialization and the time cost for inference. We also analyze the empirical tradeoff between the approaches.

[19] For example, for the grounding procedure illustrated in Figure 3.3, the delta rule for $F1$ is $q^\delta(x) : -R^\delta(x, y)$.

Strawman: Complete Materialization The strawman approach, complete materialization, is computationally expensive and often infeasible. We use it to set a baseline for other approaches.

Materialization Phase We explicitly store the value of the probability $\Pr[I]$ for every possible world I. This approach has perfect fidelity, but storing all possible worlds takes an exponential amount of space and time in the number of variables in the original factor graph. Thus, the strawman approach is often infeasible on even moderate-sized graphs.[20]

Inference Phase We use Gibbs sampling: even if the distribution has changed to $\Pr^{(\Delta)}$, we only need access to the new factors in $\Delta\Pi_{\mathcal{F}}$ and to $\Pr[I]$ to perform the Gibbs update. The speed improvement arises from the fact that we do not need to access all factors from the original graph and perform a computation with them, since we can look them up in $\Pr[I]$.

Sampling Approach The sampling approach is a standard technique to improve over the strawman approach by storing a set of possible worlds sampled from the original distribution instead of storing all possible worlds. However, as the updated distribution $\Pr^{(\Delta)}$ is different from the distribution used to draw the stored samples, we cannot reuse them directly. We use a (standard) Metropolis-Hastings scheme to ensure convergence to the updated distribution.

Materialization Phase In the materialization phase, we store a set of possible worlds drawn from the original distribution. For each variable, we store the set of samples as a *tuple bundle*, as in MCDB [100]. A single sample for one random variable only requires 1 bit of storage. Therefore, the sampling approach can be efficient in terms of materialization space. In the KBC systems we evaluated, 100 samples require less than 5% of the space of the original factor graph.

Inference Phase We use the samples to generate *proposals* and adapt them to estimate the up-to-date distribution. This idea of using samples from similar distributions as proposals is standard in statistics, e.g., importance sampling, rejection sampling, and different variants of Metropolis-Hastings methods. After investigating these approaches, in DeepDive, we use the *independent Metropolis-Hastings* approach [15, 159], which generates proposal samples and accepts these samples with an

[20] Compared with running inference from scratch, the strawman approach does not materialize any factors. Therefore, it is necessary for strawman to enumerate each possible world and save their probability because we do not know *a priori* which possible world will be used in the inference phase.

Procedure 1 Variational Approach (Materialization)

Input: Factor graph $FG = (V, F)$, regularization parameter λ, number of samples N for approximation.

Output: An approximated factor graph $FG' = (V, F')$

1: $I_1, ..., I_N \leftarrow N$ samples drawn from FG.
2: $NZ \leftarrow \{(v_i, v_j)$: v_i and v_j are in some factor in $FG\}$.
3: $M \leftarrow$ covariance matrix estimated using $I_1, ..., I_N$, such that M_{ij} is the covariance between variable i and variable j. Set $M_{ij} = 0$ if $(v_i, v_j) \notin NZ$.
4: Solve the following optimization problem using gradient descent [22], and let the result be $\hat{X}$

$$\begin{aligned} \arg\max_X \quad & \log\det X \\ s.t., \quad & X_{kk} = M_{kk} + 1/3, \\ & |X_{kj} - M_{kj}| \leq \lambda \\ & X_{kj} = 0 \; if \; (v_k, v_j) \notin NZ \end{aligned}$$

5: **for all** i, j s.t. $\hat{X}_{ij} \neq 0$ **do**
6: Add in F' a factor from (v_i, v_j) with weight $\hat{X}_{ij}$.
7: **end for**
8: **return** $FG' = (V, F')$.

acceptance test. We choose this method only because the acceptance test can be evaluated using the sample, ΔV, and ΔF–without the entire factor graph. Thus, we may fetch many fewer factors than in the original graph, but we still converge to the correct answer.

The fraction of accepted samples is called the *acceptance rate*, and it is a key parameter in the efficiency of this approach. The approach may exhaust the stored samples, in which case the method resorts to another evaluation method or generates fresh samples.

Variational Approach The intuition behind our variational approach is as follows: rather than storing the exact original distribution, we store a factor graph with *fewer factors* that approximates the original distribution. On the smaller graph, running inference and learning is often faster.

Materialization Phase The key idea of the variational approach is to approximate the distribution using simpler or sparser correlations. To learn a sparser model, we use Procedure 1 which is a log-determinant relaxation [187] with a ℓ_1 penalty term [22]. We want to understand its strengths and limitations on KBC problems, which is novel. This approach uses standard techniques for learning that are already implemented in DeepDive [207].

The input is the original factor graph and two parameters: the number of samples N to use for

		Strawman	Sampling	Variational
Mat. Phase	Space	2^{n_a}	$S_I n_a/\rho$	$n_a{}^2$
	Cost	$2^{n_a} S_M \times C(n_a, f)$	$S_I C(n_a, f)/\rho$	$n_a{}^2 + S_M C(n_a, f)$
Inference Phase	Cost	$S_I \times C(n_a+n_f, 1+f')$	$S_I n_a/\rho + S_I C(n_f, f')/\rho$	$S_I \times C(n_a+n_f, n_a{}^2+f')$
Sensitivity	Size of the Graph	**High**	Low	Mid
	Amount of Change	Low	**High**	Low
	Sparsity of Correlation	Low	Low	**High**

n_a: # original vars f: # original factors ρ: acceptance rate
n_f: # modified vars f': # modified factors S_I: # samples for inference
S_M: # samples for materialization
$C(\#v, \#f)$: Cost of Gibbs with $\#v$ vars, and $\#f$ factors

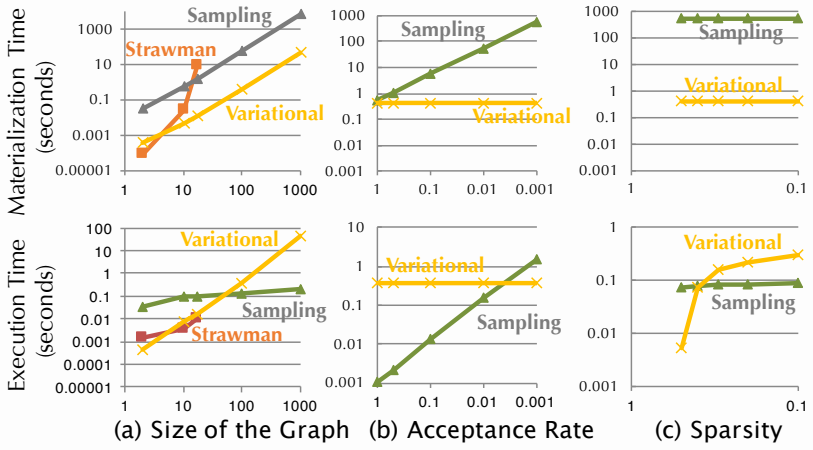

Figure 6.9: A Summary of the tradeoffs. Top: An analytical cost model for different approaches; Bottom: Empirical examples that illustrate the tradeoff space. All converge to <0.1% loss, and thus, have comparable quality.

approximating the covariance matrix, and the regularization parameter λ, which controls the sparsity of the approximation. The output is a new factor graph that has only binary potentials. The intuition for this procedure comes from graphical model structure learning: an entry (i, j) is present in the inverse covariance matrix only if variables i and j are connected in the factor graph. Given these inputs, the algorithm first draws a set of N possible worlds by running Gibbs sampling on the original factor graph. It then estimates the covariance matrix based on these samples (Lines 1-3). Using the estimated covariance matrix, our algorithms solves the optimization problem in Line 4 to estimate the inverse covariance matrix $\hat{X}$. Then, the algorithm creates one factor for each pair of variables such that the corresponding entry in $\hat{X}$ is non-zero, using the value in $\hat{X}$ as the new weight (Line

5-7). These are all the factors of the approximated factor graph (Line 8).

Inference Phase Given an update to the factor graph (e.g., new variables or new factors), we simply apply this update to the approximated graph, and run inference and learning directly on the resulting factor graph. As shown in Figure 6.9(c), the execution time of the variational approach is roughly linear in the sparsity of the approximated factor graph. Indeed, the execution time of running statistical inference using Gibbs sampling is dominated by the time needed to fetch the factors for each random variable, which is an expensive operation requiring random access. Therefore, as the approximated graph becomes sparser, the number of factors decreases and so does the running time.

Parameter Tuning We are among the first to use these methods in KBC applications, and there is little literature about tuning λ. Intuitively, the smaller λ is, the better the approximation is–but the less sparse the approximation is. To understand the impact of λ on quality, we show in Figure 6.10 the quality F1 score of a DeepDive program called News (see Section 6.2.2) as we vary the regularization parameter. As long as the regularization parameter λ is small (e.g., less than 0.1), the quality does not change significantly. In all of our applications we observe that there is a relatively large "safe" region from which to choose λ. In fact, for all five systems in Section 6.2.2, even if we set λ at 0.1 or 0.01, the impact on quality is minimal (within 1%), while the impact on speed is significant (up to an order of magnitude). Based on Figure 6.10, DeepDive supports a simple search protocol to set λ. We start with a small λ, e.g., 0.001, and increase it by $10\times$ until the KL-divergence is larger than a user-specified threshold, specified as a parameter in DeepDive.

Tradeoffs We studied the tradeoff between different approaches and summarize the empirical results of our study in Figure 6.9. The performance of different approaches may differ by more than two orders of magnitude, and neither of them dominates the other. We use a synthetic factor graph with pairwise factors[21] and control the following axes:

(1) Number of variables in the factor graph. In our experiments, we set the number of variables to values in {2, 10, 17, 100, 1000, 10000}.

[21] In Figure 6.9, the numbers are reported for a factor graph whose factor weights are sampled at random from $[-0.5, 0.5]$. We also experimented with different intervals ($[-0.1, 0.1]$, $[-1, 1]$, $[-10, 10]$), but these had no impact on the tradeoff

(2) Amount of change. How much the distribution changes affects efficiency, which manifests itself in the acceptance rate: the smaller the acceptance rate is, the more difference there will be in the distribution. We set the acceptance rate to values in {1.0, 0.5, 0.1, 0.01}.

(3) Sparsity of correlations. This is the ratio between the number of non-zero weights and the total weight. We set the sparsity to values in $\{0.1, 0.2, 0.3, 0.4, 0.5, 1.0\}$ by selecting uniformly at random a subset of factors and set their weight to zero.

We now discuss the results of our exploration of the tradeoff space, presented in Figure 6.9(a-c).

Size of the Factor Graph Since the materialization cost of the strawman is exponential in the size of the factor graph, we observe that, for graphs with more than 20 variables, the strawman is significantly slower than either the sampling approach or the variational approach. Factor graphs arising from KBC systems usually contain a much larger number of variables; therefore, from now on, we focus on the tradeoff between sampling and variational approaches.

Amount of Change As shown in Figure 6.9(b), when the acceptance rate is high, the sampling approach could outperform the variational one by more than two orders of magnitude. When the acceptance rate is high, the sampling approach requires no computation and so is much faster than Gibbs sampling. In contrast, when the acceptance rate is low, e.g., 0.1%, the variational approach could be more than 5$\times$ faster than the sampling approach. An acceptance rate lower than 0.1% occurs for KBC operations when one updates the training data, adds many new features, or concept drift happens during the development of KBC systems.

Sparsity of Correlations As shown in Figure 6.9(c), when the original factor graph is sparse, the variational approach can be 11$\times$ faster than the sampling approach. This is because the approximate factor graph contains less than 10% of the factors than the original graph, and it is therefore much faster to run inference on the approximate graph. On the other hand, if the original factor graph is too dense, the variational approach could be more than 7$\times$ slower than the sampling one, as it is essentially performing inference on a factor graph with a size similar to that of the original graph.

Discussion: Theoretical Guarantees We discuss the theoretical guarantee that each materialization strategy provides. Each materialization method inherits the guarantee of that inference

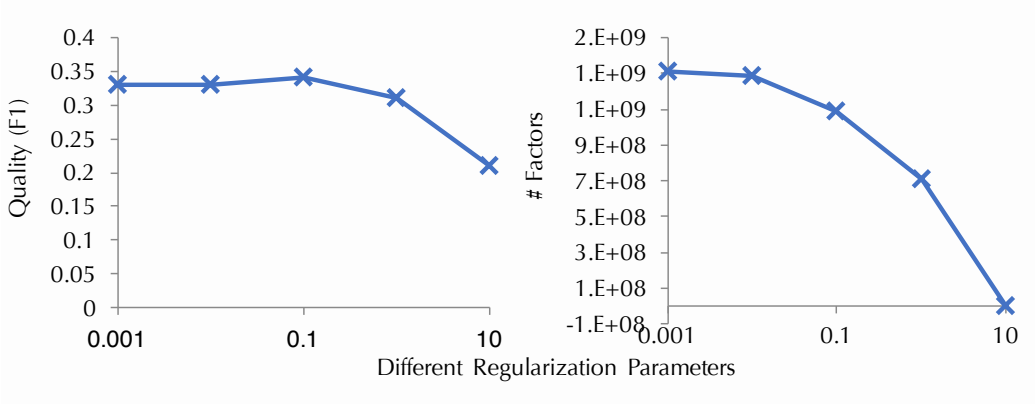

Figure 6.10: Quality and number of factors of the News corpus with different regularization parameters for the variational approach.

technique. The strawman approach retains the same guarantees as Gibbs sampling; For the sampling approach use standard Metropolis-Hasting scheme. Given enough time, this approach will converge to the true distribution. For the variational approach, the guarantees are more subtle and we point the reader to the consistency of structure estimation of Gaussian Markov random field [156] and log-determinate relaxation [187]. These results are theoretically incomparable, motivating our empirical study.

6.2.1.3 Choosing Between Different Approaches

From the study of the tradeoff space, neither the sampling approach nor the variational approach dominates the other, and their relative performance depends on how they are being used in KBC. We propose to materialize the factor graph using both the sampling approach *and* the variational approach, and defer the decision to the inference phase when we can observe the workload.

Materialization Phase Both approaches need samples from the original factor graph, and this is the dominant cost during materialization. A key question is *"How many samples should we collect?"* We experimented with several heuristic methods to estimate the number of samples that are needed, which requires understanding how likely future changes are, statistical considerations, etc. These approaches were difficult for users to understand, so DeepDive takes a best-effort approach: it generates as many samples as possible when idle or within a user-specified time interval.

System	# Docs	# Rels	# Rules	# vars	# factors
Adversarial	5M	1	10	0.1B	0.4B
News	1.8M	34	22	0.2B	1.2B
Genomics	0.2M	3	15	0.02B	0.1B
Pharma.	0.6M	9	24	0.2B	1.2B
Paleontology	0.3M	8	29	0.3B	0.4B

Table 6.4: Statistics of KBC systems we used in experiments. The # vars and # factors are for factor graphs that contain all rules.

Rule	Description
A1	Calculate marginal probability for variables or variable pairs.
FE1	Shallow NLP features (e.g., word sequence)
FE2	Deeper NLP features (e.g., dependency path)
I1	Inference rules (e.g., symmetrical HasSpouse).
S1	Positive examples
S2	Negative examples

Table 6.5: The set of rules in News. See Section 6.2.2.1

Inference Phase Based on the tradeoffs analysis, we developed a *rule-based optimizer* with the following set of rules:

- If an update does not change the structure of the graph, choose the sampling approach.
- If an update modifies the evidence, choose the variational approach.
- If an update introduces new features, choose the sampling approach.
- Finally, if we run out of samples, use the variational approach.

This simple set of rules is used in our experiments.

6.2.2 Experiments

We conducted an experimental evaluation of DeepDive for incremental maintenance of KBC systems.

6.2.2.1 Experimental Settings

To evaluate DeepDive, we used DeepDive programs developed by our users over the last three years from paleontologists, geologists, biologists, a defense contractor, and a KBC competition. These are high-quality KBC systems: two of our KBC systems for natural sciences achieved quality comparable to (and sometimes better than) human experts, as assessed by double-blind experiments, and our

KBC system for a KBC competition is the top system among all 45 submissions from 18 teams as assessed by professional annotators.[22] To simulate the development process, we took snapshots of DeepDive programs at the end of every development iteration, and we use this dataset of snapshots in the experiments to understand our hypothesis that incremental techniques can be used to improve development speed.

Datasets and Workloads To study the efficiency of DeepDive, we selected five KBC systems, namely (1) News, (2) Genomics, (3) Adversarial, (4) Pharmacogenomics, and (5) Paleontology. Their names refers to the specific domains on which they focus. Table 6.4 illustrates the statistics of these KBC systems and of their input datasets. We group all rules in each system into six rule templates with four workload categories. We focus on the News system below.

The News system builds a knowledge base between persons, locations, and organizations, and contains 34 different relations, e.g., HasSpouse or MemberOf. The input to the KBC system is a corpus that contains 1.8 million news articles and Web pages. We use four types of rules in News in our experiments, as shown in Table 6.5, error analysis (rule A1), candidate generation and feature extraction (FE1, FE2), supervision (S1, S2), and inference (I1), corresponding to the steps where these rules are used.

Other applications are different in terms of the quality of the text. We choose these systems as they span a large range in the spectrum of quality: Adversarial contains advertisements collected from websites where each document may have only 1-2 sentences with grammatical errors; in contrast, Paleontology contains well-curated journal articles with precise, unambiguous writing and simple relationships. Genomics and Pharma have precise texts, but the goal is to extract relationships that are more linguistically ambiguous compared to the Paleontology text. News has slightly degraded writing and ambiguous relationships, e.g., "member of." Rules with the same prefix, e.g., FE1 and FE2, belong to the same category, e.g., feature extraction.

DeepDive Details DeepDive is implemented in Scala and C++, and we use Greenplum to handle all SQL. All feature extractors are written in Python. The statistical inference and learning and the incremental maintenance component are all written in C++. All experiments are run on a machine with four CPUs (each CPU is a 12-core 2.40 GHz Xeon E5-4657L), 1 TB RAM, and 12×1TB hard

[22] http://surdeanu.info/kbp2014/index.php

Rule	Adversarial			News			Genomics			Pharma.			Paleontology		
	Rerun	Inc.	×	Rerun	Inc.	×	Rerun	Inc.	×	Rerun	Inc.	×	Rerun	Inc.	×
A1	1.0	0.03	33×	2.2	0.02	112×	0.3	0.01	30×	3.6	0.11	33×	2.8	0.3	10×
FE1	1.1	0.2	7×	2.7	0.3	10×	0.4	0.07	6×	3.8	0.3	12×	3.0	0.4	7×
FE2	1.2	0.2	6×	3.0	0.3	10×	0.4	0.07	6×	4.2	0.3	12×	3.3	0.4	8×
I1	1.3	0.2	6×	3.6	0.3	10×	0.5	0.09	6×	4.4	1.4	3×	3.8	0.5	8×
S1	1.3	0.2	6×	3.6	0.4	8×	0.6	0.1	6×	4.7	1.7	3×	4.0	0.5	7×
S2	1.3	0.3	5×	3.6	0.5	7×	0.7	0.1	7×	4.8	2.3	3×	4.1	0.6	7×

Table 6.6: End-to-end efficiency of incremental inference and learning. All execution times are in hours. The column × refers to the speedup of INCREMENTAL (Inc.) over RERUN.

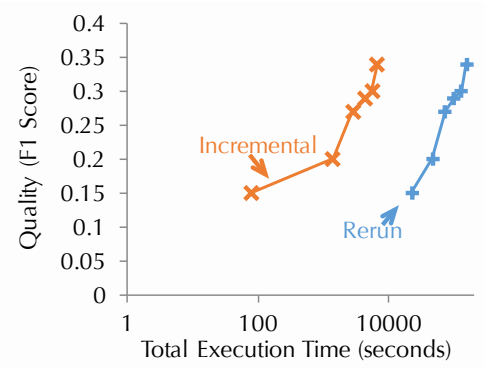

(a) Quality Improvement Over Time

	Adv	News	Gen	Pha	Pale
Linear	**0.33**	0.32	0.47	0.52	0.74
Logical	**0.33**	**0.34**	**0.53**	0.56	0.80
Ratio	**0.33**	**0.34**	**0.53**	**0.57**	**0.81**

(b) Quality (F1) of Different Semantics

Figure 6.11: (a) Quality improvement over time; (b) Quality for different semantics.

drives and running Ubuntu 12.04. For these experiments, we compiled DeepDive with Scala 2.11.2, g++-4.9.0 with -O3 optimization, and Python 2.7.3. In Genomics and Adversarial, Python 3.4.0 is used for feature extractors.

6.2.2.2 End-to-end Performance and Quality

We built a modified version of DeepDive called RERUN, which when given an update on the KBC system, runs the DeepDive program from scratch. DeepDive, which uses all techniques, is called INCREMENTAL. The results of our evaluation show that DeepDive is able to speed up the development of high-quality KBC systems through incremental maintenance with little impact on quality. We set the number of samples to collect during execution to {10, 100, 1000} and the number of samples to collect during materialization to {1000, 2000}. We report results for $(1000, 2000)$, as results for other combinations of parameters are similar.

Quality Over Time We first compare RERUN and INCREMENTAL in terms of the wait time that developers experience to improve the quality of a KBC system. We focus on News because it is a well-known benchmark competition. We run all six rules sequentially for both RERUN and INCREMENTAL, and after executing each rule, we report the quality of the system measured by the F1 score and the *cumulative* execution time. Materialization in the INCREMENTAL system is performed only once. Figure 6.11(a) shows the results. Using INCREMENTAL takes significantly less time than RERUN to achieve the same quality. To achieve an F1 score of 0.36 (a competition-winning score), INCREMENTAL is 22× faster than RERUN. Indeed, each run of RERUN takes ≈ 6 hours, while a run of INCREMENTAL

takes at most 30 minutes.

We further compare the facts extracted by INCREMENTAL and RERUN and find that these two systems not only have similar end-to-end quality, but are also similar enough to support common debugging tasks. We examine the facts with high-confidence in RERUN (> 0.9 probability), 99% of them also appear in INCREMENTAL, and vice versa. High confidence extractions are used by the developer to debug precision issues. Among all facts, we find that at most 4% of them have a probability that differs by more than 0.05. The similarity between snapshots suggests, our incremental maintenance techniques can be used for debugging.

Efficiency of Evaluating Updates We now compare RERUN and INCREMENTAL in terms of their speed in evaluating a given update to the KBC system. To better understand the impact of our technical contribution, we divide the total execution time into parts: (1) the time used for feature extraction and grounding; and (2) the time used for statistical inference and learning. We implemented classical incremental materialization techniques for feature extraction and grounding, which achieves up to a 360$\times$ speedup for rule FE1 in News. We get this speedup for free using standard RDBMS techniques, a key design decision in DeepDive.

Table 6.6 shows the execution time of statistical inference and learning for each update on different systems. We see from Table 6.6 that INCREMENTAL achieves a 7$\times$ to $112\times$ speedup for News across all categories of rules. The analysis rule A1 achieves the highest speedup – this is not surprising because, after applying A1, we do not need to rerun statistical learning, and the updated distribution does not change compared with the original distribution, so the sampling approach has a 100% acceptance rate. The execution of rules for feature extraction (FE1, FE2), supervision (S1, S2), and inference (I1) has a $10\times$ speedup. For these rules, the speedup over RERUN is to be attributed to the fact that the materialized graph contains only 10% of the factors in the full original graph. Below, we show that both the sampling approach and variational approach contribute to the speed-up. Compared with A1, the speedup is smaller because these rules produce a factor graph whose distribution changes more than A1. Because the difference in distribution is larger, the benefit of incremental evaluation is lower.

The execution of other KBC applications showed similar speedups, but there are also several interesting data points. For Pharmacogenomics, rule I1 speeds-up only $3\times$. This is caused by the fact that I1 introduces many new factors, and the new factor graph is 1.4$\times$ larger than the original one.

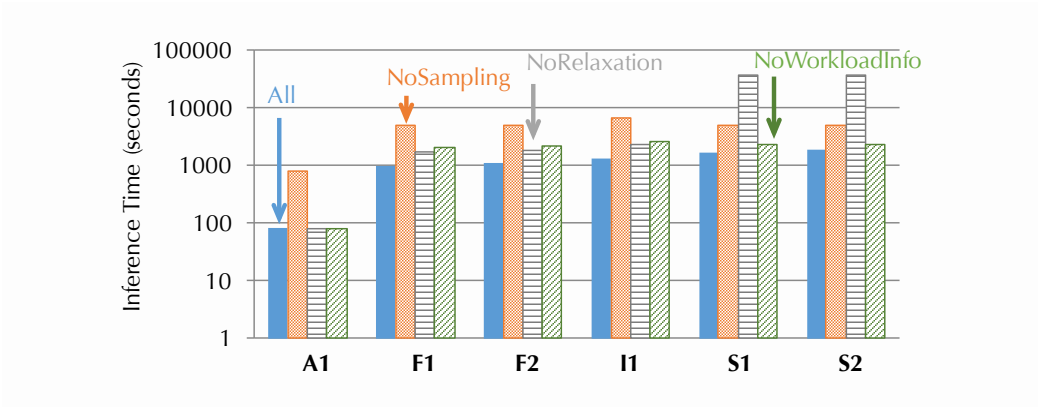

Figure 6.12: Study of the tradeoff space on News.

In this case, DeepDive needs to evaluate those new factors, which is expensive. For Paleontology, we see that the analysis rule A1 gets a $10\times$ speed-up because as illustrated in the corpus statistics (Table 6.4), the Paleontology factor graph has fewer factors for each variable than other systems. Therefore, executing inference on the whole factor graph is cheaper.

Materialization Time One factor that we need to consider is the materialization time for INCREMENTAL. INCREMENTAL took 12 hours to complete the materialization (2000 samples), for each of the five systems. Most of this time is spent in getting $2\times$ more samples than for a single run of RERUN. We argue that paying this cost is worthwhile given that it is a one-time cost and the materialization can be used for many successive updates, amortizing the one-time cost.

6.2.2.3 Lesion Studies

We conducted lesion studies to verify the effect of the tradeoff space on the performance of DeepDive. In each lesion study, we disable a component of DeepDive, and leave all other components untouched. We report the execution time for statistical inference and learning.

We evaluate the impact of each materialization strategy on the final end-to-end performance. We disabled either the sampling approach or the variational approach and left all other components of the system untouched. Figure 6.12 shows the results for News. Disabling either the sampling approach or the variational approach slows down the execution compared to the "full" system. For analysis rule A1, disabling the sampling approach leads to a more than $11\times$ slow down, because the sampling approach has, for this rule, a 100% acceptance rate because the distribution does not change. For

feature extraction rules, disabling the sampling approach slows down the system by $5\times$ because it forces the use of the variational approach even when the distribution for a group of variables does not change. For supervision rules, disabling the variational approach is $36\times$ slower because the introduction of training examples decreases the acceptance rate of the sampling approach.

Optimizer Using different materialization strategies for different groups of variables positively affects the performance of DeepDive. We compare INCREMENTAL with a strong baseline NOWORKLOADINFO which, for each group, first runs the sampling approach. After all samples have been used, we switch to the variational approach. Note that this baseline is stronger than the strategy that fixes the same strategy for all groups. Figure 6.12 shows the results of the experiment. We see that with the ability to choose between the sampling approach and variational approach according to the workload, DeepDive can be up to $2\times$ faster than NOWORKLOADINFO.

6.2.3 Conclusion to Incremental Feature Engineering

We described the DeepDive approach to incremental execution a series of KBC programs. By building on SQL, DeepDive is able to use classical techniques to provide incremental processing for the SQL components. However, these classical techniques do not help with statistical inference, and we described a novel tradeoff space for approximate inference techniques. We used these approximate inference techniques to improve end-to-end execution time in the face of changes both to the program and the data; they improved system performance by two orders of magnitude in five real KBC scenarios while keeping the quality high enough to aid in the development process.

6.3 Conclusion

In this chapter, we focus on speeding up the execution of a series of similar KBC systems to support a popular development pattern that we observe from users, i.e., the iterative exploration process to find or engineer the suitable set features to use in the system. We focus on two workloads, namely, feature selection and feature engineering, and develop techniques of materializing information that can be reused for a range of statistical models. With these materialization techniques, we obtain up to two to three orders of magnitude speedup on tasks that we collected from users.

7. Related Work

> *"The honour of the ancient authors stands firm, and so does everyones honour; we are not introducing a comparison of minds but a comparison of ways; and we are not taking the role of a judge but of a guide."*
>
> — Francis Bacon*, Novum Organum Scientiarum, 1620*

We present survey on two lines of related work to DeepDive. The first line is prior arts on knowledge base construction and information extraction. The second line is on speeding up and scaling up statistical inference and learning.

7.1 Knowledge Base Construction

KBC has been an area of intense study over the last decade [23, 32, 48, 54, 70, 71, 83, 105, 112, 134, 134, 149, 170, 179, 199, 200, 209], moving from pattern matching [92] and rule-based systems [120] to systems that use machine learning for KBC [32, 48, 71]. We survey these approaches by classifying them into two classes.

Rule-based Systems The earliest KBC systems used pattern matching to extract relationships from text. The most famous such example is the "Hearst Pattern" proposed by Hearst [92] in 1992. In her seminal work, Hearst observed that a large amount of hyponyms can be discovered by simple patterns, e.g., "X, such as Y". Hearst's technique forms the basis of many further techniques that attempt to extract high quality patterns from text. In industry, rule-based (pattern-matching-based) KBC systems, such as IBM's SystemT [112, 120], have been built to develop high quality patterns. These systems provide the user a (usually declarative) interface to specify a set of rules and patterns to derive relationships. These systems have achieved state-of-the-art quality after careful engineering effort as shown by Li et al. [120].

Statistical Approaches One limitation of rule-based systems is that the developer of a KBC system needs to ensure that all rules she provides to the system have high precision. For the last decade, probabilistic (or machine learning) approaches have been proposed to allow the system select

between a range of features provided by the developers automatically. For these approaches, the extracted tuple is associated with a marginal probability of that tuple to be true (i.e., appears in the KB). DeepDive, Google's knowledge graph, and IBM's Watson are built on this line of work. Within this space there are three styles of systems:

- **Classification-based Frameworks** One line of work uses traditional classifiers that assign each tuple a probability score, e.g., naïve Bayes classifier, and logistic regression classifier. For example, KnowItAll [71] and TextRunner [23, 200] use the naïve Bayes classifier and CMU's NELL [32, 48] uses logistic regression. Large-scale systems typically have used these types of approaches in sophisticated combinations, e.g., NELL or Watson.

- **Maximum a Posteriori (MAP)** One approach is to use the probabilistic approach but select the MAP or most likely world (which do differ slightly). Notable examples include the YAGO system [105],which uses a PageRank-based approach to assign the confident score. Other examples include the SOFIE [179] and Prospera [134] systems designed by researchers using an approach based on constraint satisfication.

- **Graphical Model Approaches** The classification-based methods ignore the interaction among predictions, and there is a hypothesis that modeling these correlations yields higher quality systems more quickly. There has been research that tries to use a generic graphical model to model the probabilistic distribution among all possible extractions. For example, Poon et al. [149] did work in using Markov logic networks (MLN) [69] for information extraction. Microsoft's StatisticalSnowBall/EntityCube [209] also uses an MLN-based approach. A key challenge with these systems is scalability. For example, Poon et al. approach was limited to 1.5K citations.

DeepDive is inspired by this line of work, however, is able to scale to a much larger databases. We also argue that probabilistic systems are easy to debug and to understand their results, as their answers can be meaningfully interpreted.

Knowledge bases have also been used wildly in supporting decision making, and related work include knowledge base model construction [191] and knowledge base compilation [95]. These work are orthogonal to our effort and we hope the knowledge bases constructed by DeepDive could also be used by these works.

7.1.1 Improving the Quality of KBC Systems

We survey recent efforts in knowledge base construction that focus on the methodology of how to improve the quality of a KBC system.

Rich Features In recent years, different researchers have noticed the importance of combining and using a rich set of features and signals to the quality of a KBC system.

Both two famous efforts, the Netflix challenge [45], and IBM's Watson [73] that won the Jeopardy gameshow, have identified the importance of features and signals:

> *Ferrucci et al. [73]: For the Jeopardy Challenge, we use more than 100 different techniques for analyzing natural language, identifying sources, finding and generating hypotheses, finding and scoring evidence, and merging and ranking hypotheses. What is far more important than any particular technique we use is how we combine them in DeepQA such that overlapping approaches can bring their strengths to bear and contribute to improvements in accuracy, confidence, or speed.*

> *Buskirk [45]: The top two teams beat the challenge by combining teams and their algorithms into more complex algorithms incorporating everybody's work. The more people joined, the more the resulting team's score would increase.*

For both efforts, the rich set of features and signals contribute the high-quality of the corresponding system. Apart from these two efforts, other researches also notice similar phenomenon. For example, Mintz et al. [131] finds that although both surface features and deep NLP features have similar quality for relation extraction tasks, combining both features achieves significant improvement over using either of these systems in isolation. Similar "feature-based" approach is also used in other domain, e.g., Finkel et al. [75] uses a diverse set of features to build a NLP parser with state-of-the-art quality. Also, in our own work [84], we also find that integrating a diverse set of deep NLP features can improve a table-extraction system significantly.

Joint Inference Another recent trend in building KBC system is to take advantage of *joint inference* [58, 59, 84, 127, 130, 142, 149, 150]. Different from traditional models [132], e.g., logistic regression or SVM, joint inference approaches have the emphasis of learning multiple targets together. For example, Poon et al. [149, 150] find that learning segmentation and extraction together in the

same Markov logic network significantly improves the quality of information extraction. Similar observations have been made by Min et al. [130] and McCallum [127] for information extraction. Our recent researches also show the empirical improvement of joint inference on the diverse set of tasks, including relation extraction [142] and table extraction [84].

Deep Learning and Joint Inference There has also been a recent emerging effort in the machine learning community to try to build a fully-joint model for NLP tasks [58,59]. The dream is to build a single joint model for NLP tasks from the lowest level, e.g., POS tagging, to the highest level, e.g., semantic role labeling. DeepDive is built in a similar spirit that tries to build a joint model for low-level tasks, e.g., optical character recognition, to high-level tasks, e.g., cross-document inference of relation extraction.

7.2 Performant and Scalable Statistical Analytics

Another line of work related to this dissertation is the work on speeding up and scaling up statistical inference and learning. We describe this line of related work in this section.

7.2.1 Probabilistic Graphical Models and Probabilistic Databases

Probabilistic graphical models [111] and factor graphs [188], in particular, are popular frameworks for statistical modeling. Gibbs sampling has been applied to a wide range of probabilistic models and applications [15], e.g., risk models in actuarial science [17], conditional random fields for information extraction [74], latent Dirichlet allocation for topic modeling [86,93], and Markov logic for text applications [69,140].

There are several recent general-purpose systems in which a user specifies a factor graph model and the system performs sampling-based inference. For example, Factorie [128] allows a user to specify arbitrary factor functions in Java; OpenBUGS [125] provides an interface for a user to specify arbitrary Bayes nets (which are also factor graphs) and performs Gibbs sampling on top of them; PGibbs [82] performs parallel Gibbs sampling over factor graphs on top of GraphLab [124].

To deploy sophisticated statistical analysis over increasingly data-intensive applications, there is a push to combine factor graphs and databases [165, 194]. Wick et al. [194] studies how to

construct a probabilistic database with factor graph, and perform blocked Gibbs sampling and exploit a connection to materialized view maintenance.

There is a rich literature on pushing probabilistic models and algorithms into database systems [5, 18, 62, 99, 144, 147, 162, 165, 189, 194]. Factor graphs are one of the most popular and general formalisms [165, 189, 194]. Although many of these systems rely on factor graph as their underlying representations, these probabilistic database systems usually contain high-level logic rules to specify a factor graph, which provides more information on the inference and learning process and enables optimization techniques like lifted inference [109]. There are also alternative representation frameworks to factor graphs. For example, BayesStore [190] uses Bayes nets; Trio [5, 162], MayBMS [18], and MystiQ [62] use c-tables [97]; MCDB [99] uses VG functions; and Markov logic systems such as Tuffy [140] use grounded-clause tables. We focus on factor graphs but speculate that our techniques could apply to other probabilistic frameworks as well. PrDB [165] uses factor graphs and casts SQL queries as inference problems in factor graphs.

7.2.2 In-database Statistical Analytics

There is a trend to integrate statistical analytics into data processing systems. Database vendors have recently put out new products in this space, including Oracle, Pivotal's MADlib [93], IBM's SystemML [80], SAP's HANA, and the RIOT project [208]. These systems support statistical analytics in existing data management systems. A key challenge for statistical analytics is performance. A handful of data processing frameworks have been developed in the last few years to support statistical analytics, including Mahout for Hadoop, MLI for Spark [176], GraphLab [123]. These systems have increased the performance of corresponding statistical analytics tasks significantly. The technique developed in the dissertation studies the tradeoff formed by the design decision made by these tools.

Other than statistical analytics, there has also been an intense effort to scale up individual linear algebra operations in data processing systems [33, 60, 208]. Constantine et al. [60] propose a distributed algorithm to calculate QR decomposition using MapReduce, while ScaLAPACK [33] uses a distributed main memory system to scale up linear algebra. The RIOT [208] system optimizes the I/O costs incurred during matrix calculations.

7.2.3 More Specific Related Work

Other than the related work that are boardly related as we described above, each prototype system is also related to more specific work. We survey these work in this section.

Efficient Gibbs Sampling Gibbs sampling is often optimized for specific applications of factors. For example, a popular technique for implementing Gibbs sampling for latent Dirichlet allocation [86, 122, 151, 173] is to only maintain the sum of a set of Boolean random variables instead of individual variable assignments. A more aggressive parallelization strategy allows non-atomic updates to the variables to increase throughput (possibly at the expense of sample quality) [122, 173]. Our Elementary prototype allows these optimization, but focuses on the scalability aspect of Gibbs sampling for general factor graphs.

Scalable Statistical Inference and Learning Three are work tries to scale up these main-memory systems to support analytics on data sets that are larger than main memory. For example, the Ricardo system [64] integrates R and Hadoop to process terabytes of data stored on HDFS. However, Ricardo spawns R processes on Hadoop worker nodes, and still assumes that statistical analytics happen in main memory on a single node. Our Elementary prototype studies how to scale up Gibbs sampling using both main memory and secondary storage. Systems like Ricardo could take advantage of our results to get higher scalability by improving single-node scalability. The MCDB system [100] is the seminal work of integrating sampling-based approaches into a database. MCDB scales up the sampling process using an RDBMS. However, it assumes that the classic I/O tradeoffs for an RDBMS work in the same way for sampling. Our work revisits these classical tradeoffs, and we hope that our study contributes to this line of work.

Shared-memory Multiprocessor Optimization. Performance optimization on shared-memory multiprocessors machines is a classical topic. Anderson and Lam [13] and Carr et al.'s [49] seminal work used complier techniques to improve locality on shared-memory multiprocessor machines. DimmWitted's *locality group* is inspired by Anderson and Lam's discussion of *computation decomposition* and *data decomposition*. These locality groups are the centerpiece of the Legion project [25].

Main-memory Databases. The database community has recognized that multi-socket, large-memory machines have changed the data processing landscape, and there has been a flurry of

recent work about how to build in-memory analytics systems [7, 20, 51, 108, 119, 152, 154, 186]. Classical tradeoffs have been revisited on modern architectures to gain significant improvement: Balkesen et al. [20], Albutiu et al. [7], Kim et al. [108], and Li [119] study the tradeoff for joins and shuffling, respectively. This work takes advantage of modern architectures, e.g., NUMA and SIMD, to increase memory bandwidth. We study a new tradeoff space for statistical analytics in which the performance of the system is affected by both hardware efficiency and statistical efficiency. The DimmWitted study is based on these related work but apply them to workload of statistical analytics.

Data Mining Algorithms DimmWitted focues on studying the impact of modern hardware on statistical analytics. The effort of applying modern hardware has also been studied for data mining algorithms. Probably the most related work is by Jin et al. [102], who consider how to take advantage of replication and different locking-based schemes with different caching behavior and locking granularity to increase the performance (hardware efficiency performance) for a range of data mining tasks including K-means, frequent pattern mining, and neural networks. Ghoting et al. [79] optimize cache-behavior of frequent pattern mining using novel cache-conscious techniques, including spatial and temporal locality, prefetching, and tiling. Tatikonda et al. [183] considers improving the performance of mining tree-structured data multicore systems by decreasing the spatial and temporal locality, and the technique they use is by careful study of different granularity and types of task and data chunking. Chu et al. [56] apply the MapReduce to a large range of statistical analytics tasks that fit into the statistical query model, and implements it on a multicore system and shows almost linear speed-up to the number of cores. Zaki et al. [202] study how to speed up classification tasks using decision trees on SMP machines, and their technique takes advantage data parallelism and task parallelism with lockings. Buehrer and Parthasarathy et al. [43] study how to build a distributed system for frequent pattern mining with terabytes of data. Their focus is to minimize the I/O cost and communication cost by optimizing the data placement and the number of passes over the dataset. Buehrer et al. [44] study implementing efficient graph mining algorithms over CMP and SMP machines with the focus on load balance, memory usage (i.e., size), spatial locality, and the tradeoff of pre-computing and re-computing. Zaki et al. [145, 203] study on how to implement parallel associated rule mining algorithms on shared memory systems by optimizing reference memory locality and data placement in the granularity of cachelines. This work also considers how to minimize the cost of coherent maintenance between multiple CPU caches. All of

these techniques are related and relevant to DimmWitted, but none consider optimizing first-order methods and the affect of these optimizations on their efficiency.

High Performance Computation DimmWitted's efficient implementation is borrowed from a wide range of literature in high performance computation, database, and systems. Locality is a classical technique: worker and data collocation technique has been advocated since at least 90s [13, 49] and is a common systems design principle [172].

The role of dense and sparse computation is well studied in the by the HPC community. For example, efficient computation kernels for matrix-vector and matrix-matrix multiplication [27, 28, 65, 196]. In this work, we only require dense-dense and dense-sparse matrix-vector multiplies. There is recent work on mapping sparse-sparse multiplies to GPUs and SIMD [198], which is useful for other data mining models beyond what we consider here. The row- vs. column-storage has been intensively studied by database community over traditional relational database [6] or Hadoop [91]. DimmWitted implements these techniques to make sure our study of hardware efficiency and statistical efficiency reflects the status of modern hardware, and we hope that future development on these topics can be applied to DimmWitted.

Domain Specific Languages In recent years, there have been a variety of *domain specific languages* (DSLs) to help the user extract parallelism; two examples of these DSLs include Galois [137, 138] and OptiML [181] for Delite [50]. With these DSLs, it is easier for the user to generate high-performant code by writing high-level specifications. To be effective, DSLs require the knowledge about the trade-off of the target domain to apply their compilation optimization, and we hope the insights from DimmWitted can be applied to these DSLs.

Array Databases Array databases were initiated by Sarawagi et al. [161], who studied how to efficiently organize *multidimensional arrays* in an RDBMS. Since then, there has been a recent resurgence in arrays as first-class citizens [42, 57, 178]. For example, Stonebraker et al. [178] recently envisioned the idea of using carefully optimized C++ code, e.g., ScaLAPACK, in array databases for matrix calculations. Many of these linear-algebra operations could also be used in Columbus, however, our Columbus system is complementary to these efforts, as we focus on how to optimize the execution of multiple operations to facilitate reuse. The materialization tradeoffs we explore are (largely) orthogonal to these lower-level tradeoffs.

Mathematical Optimization Many statistical analytics tasks are mathematical optimization problems. Recently, the mathematical optimization community has been looking at how to parallelize optimization problems [121, 141, 210]. For example, Niu et al. [141] for SGD and Shotgun [40] for SCD. A lock-free asynchronous variant was recently established by Ji et al. [121]. Using decompositions and subsampling-based approaches to solve linear algebra operations is not new. As far back as 1965, Golub [81] applied QR-decomposition to solve least squares problems. Coresets have also been intensively studied by different authors including Boutsidis et al. [38] and Langberg et al. [114]. These optimizations could be used in Columbus, whose focus in on studying how these optimizations impact the efficiency in terms of materialization and reuse.

Incremental Maintenance of Statistical Inference and Learning The task of incremental maintaining statistical inference and learning result over factor graphs is not new. Related work has focused on incremental inference for specific classes of graphs (tree-structured [67] or low-degree [1, 2] graphical models). Our focus instead is on the class of factor graphs that arise from the KBC process, which is much more general than the ones examined in previous approaches. Nath and Domingos [135] studied how to extend belief propagation on factor graphs with new evidence, but without any modification to the structure of the graph. Wick and McCallum [193] proposed a "query-aware MCMC" method. They designed a proposal scheme so that query variables tend to be sampled more frequently than other variables. We frame our problem as approximate inference, which allows us to handle changes to the program and the data in a single approach.

Our work also build on decades of study of incremental view maintenance [55, 87]: we rely on the classic incremental maintenance techniques to handle relational operations. Recently, others have proposed different approaches for incremental maintenance for individual analytics workflows like iterative linear algebra problems [139], classification as new training data arrived [110], or segmentation as new data arrives [52].

8. Conclusion and Future Work

> *It is just the fact that computers do not get confused by emotional factors, do not get bored with a lengthy problem, do not pursue hidden motives opposed to ours, that makes them safer agents than men for carrying out certain tasks.*
>
> — Edwin Thompson Jaynes*, Probability Theory: The Logic of Science, 2002*

In this dissertation, we introduce DeepDive, a data management system to make knowledge base construction easier. We describe a declarative language and an iterative debugging protocol that a user can use to build KBC systems, a set of high-quality KBC systems built with DeepDive, and techniques that we developed to make DeepDive scalable and efficient. These techniques optimize both batch execution and iterative execution, both of which are necessary, according to our experience observing users using DeepDive. With DeepDive, we hope to free domain experts from manually constructing knowledge bases, which is often tedious, expensive, and time consuming.

In future work on DeepDive, we shall continue to focus on tedious tasks that users are currently performing manually for their research and seek clean ways to automate them. With this goal in mind, we describe three possible directions as future work for DeepDive.

8.1 Deeper Fusion of Images and Text

As shown in Section 4.1.3, DeepDive is able to take advantage of state-of-the-art image-processing tools as feature extractors. This allows DeepDive to fuse text processing with the output of existing tools to jointly make predictions. One interesting direction is to study how to fuse image processing and text processing more deeply, which we call *feature-level fusion* and *fully-joint fusion*.

Feature-level Fusion Our work in extracting body size in Chapter 4 only uses image processing toolkits as a black box to generate prediction. One possible improvement is to take advantage of the features used in the image processing toolkits instead of just its outputs. For example, one future work would be to take both continuous features extracted by a convolutional neural network (CNN) [117] and high-level knowledge rules to improve the quality of a classic vision task. We are collaborating

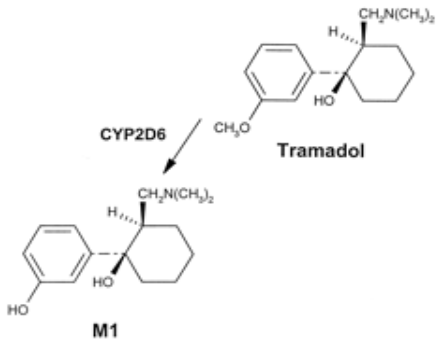

Figure 8.1: A sample pathway in a diagram.

with researchers in the vision community on applying this idea to a classic vision challenge, namely scene recognition.

Fully-joint Fusion Another natural step after the feature-level fusion is to fuse both features and predictions into the same framework. That is, some variables in the factor graph might correspond to visual predictions, while some variables in the factors might correspond to text predictions; and DeepDive allows the user to add factors cross all these variables. This system, if successfully, would allow us to build a fully-joint pipeline starting from OCR and ending at entity-level relation extraction.

To show off the benefit of this proposal, we consider genomic texts that often contain rich higher-level knowledge, but it is expressed only in diagrams and charts and so sits beyond the reach of today's text-only machine reading systems. Indeed, most fact-finding papers in biomedicine conclude with one or more diagrams featuring an updated model showing how their finding(s) fit into the broader scheme of the pathways and processes they study.

Example 8.1. *Figure 8.1 illustrates a diagram that contains a metabolic pathway [115]. This diagram expresses a relationship between the metabolites Tramadol and M1 via CYP2D6. In particular, it contains a pathway, which can be represented as* $\texttt{Pathway}(Tramadol, CYP2D6, M1)$. *In the same document, the text only reveals that there* exists *a pathway between Tramadol and M1 without the explicit mention of the role of CYP2D6.*

One challenge from the above example is the missing information that says *metabolites linked with an* $\rightarrow$ *indicate they participate in a* `Pathway`. As an analogy to extracting information from text, for this task we need at least two elements: (1) a set of "visual" words, and (2) a set of spatial relationships between those words. Such a formalism exists from Rosenfeld's seminal book *Picture*

Languages [160], in which an image is represented as a set of segments (as visual words), and their relationship specified as a two-dimensional context free grammar (2D-CFG). One possible future work is to exploit Rosenfeld's idea as the formal model to extend a machine reading system built with DeepDive to parsing diagrams. The 2D-CFG could be applied to extraction tasks for other tasks that rely on spatial relationships.

8.2 Effective Solvers for Hard Constraints

The current DeepDive engine relies on Gibbs sampling for statistical inference and learning. Gibbs sampling works well in models that do not have constraints. When there are hard constraints (e.g., from the domain), our current system struggles. However, in scientific domain, it is not uncommon for the user to specify hard constriants that must hold like "C as in benzene can only make four chemical bonds." One future work is to study how to enhance DeepDive with richer types of reasoning.

One direction of future work is to study how to integrate sampling strategies based on SAT-solver [164], which respects hard constraints, into DeepDive. Prior arts have already show potential solutions such as WalkSAT and MaxWalkSAT implemented in Alchemy [69] and Tuffy [140]. Our hope is that our study of speeding up and scaling up Gibbs sampling [206, 207] can be applied to these SAT-based samplers.

8.3 Performant and Scalable Image Processing

In recent years, image processing has been dominated by a resurgence of CNNs. On the other hand, to speed up DeepDive, we conduct a series of work of speeding up operations over factor graphs [206, 207]. Mathematically, neural networks and factor graphs are very close, to the point that it is possible to perform the underlying learning and inference tasks on them with the same engine, and we do so [207]. We propose to integrate these approaches at the application level.

Our preliminary work [90] indicates that to get peak performance from CNNs, one may want to re-explore subtle systems ideas about caching and batching. We show that by revisit these classic system ideas, we are able to get up to 4$\times$ speed up over popular CNN engine on CPU with a single machine. One natural future direction is to scale up this engine to multiple machines, and integrate it with DeepDive as first class citizen.

8.4 Conclusion

In this dissertation, we focus on supporting a workload called Knowledge base construction (KBC), the process of populating a knowledge base from unstructured inputs. One of the key challenge we aims at solving is how to help the developer of a KBC system to deal with data that are both diverse in type and large in size. After building more than ten KBC systems for a range of domain experts, we build DeepDive, a data management system to support KBC.

The thesis of DeepDive is that *it is feasible to build an efficient and scalable data management system for the end-to-end workflow of building KBC systems*. In DeepDive, we designed a declarative language to specify a KBC system and a concrete protocol that iteratively improves the quality of KBC systems. However, the flexibility of DeepDive introduces challenges of scalability and performance–Many KBC systems built with DeepDive contain statistical inference and learning tasks over terabytes of data, and the iterative protocol also requires executing similar inference problems multiple times. Motivated by these challenges, we designed techniques that make both the batch execution and incremental execution of a KBC program up to two orders of magnitude more efficient and/or scalable. In this dissertation, we described the DeepDive framework, its applications, and techniques to speed up and scale up statistical inference and learning. Our ultimate goal is that DeepDive can help scientists to build a KBC system by declaratively specifying domain knowledge without worrying about any algorithmic, performance, or scalability issues.

Bibliography

[1] U. A. Acar, A. Ihler, R. Mettu, and O. Sümer. Adaptive Bayesian inference. In *Annual Conference on Neural Information Processing Systems (NIPS)*, 2007.

[2] U. A. Acar, A. Ihler, R. Mettu, and O. Sümer. Adaptive inference on general graphical models. In *Conference on Uncertainty in Artificial Intelligence (UAI)*, 2008.

[3] J. M. Adrain and S. R. Westrop. An empirical assessment of taxic paleobiology. *Science*, 289(5476), Jul 2000.

[4] A. Agarwal, O. Chapelle, M. Dudík, and J. Langford. A reliable effective terascale linear learning system. *ArXiv e-prints*, 2011.

[5] P. Agrawal, O. Benjelloun, A. D. Sarma, C. Hayworth, S. Nabar, T. Sugihara, and J. Widom. Trio: A system for data, uncertainty, and lineage. In *International Conference on Very Large Data Bases (VLDB)*.

[6] A. Ailamaki, D. J. DeWitt, M. D. Hill, and M. Skounakis. Weaving relations for cache performance. In *International Conference on Very Large Data Bases (VLDB)*, 2001.

[7] M.-C. Albutiu, A. Kemper, and T. Neumann. Massively parallel sort-merge joins in main memory multi-core database systems. *Proceedings of the VLDB Endowment (PVLDB)*, 2012.

[8] J. Alroy. Cope's rule and the dynamics of body mass evolution in North American fossil mammals. *Science*, 280(5364), May 1998.

[9] J. ALROY. Geographical, environmental and intrinsic biotic controls on phanerozoic marine diversification. *Palaeontology*, 53(6), 2010.

[10] J. Alroy. The shifting balance of diversity among major marine animal groups. *Science*, 329(5996), Sep 2010.

[11] J. Alroy, M. Aberhan, D. J. Bottjer, M. Foote, F. T. Fursich, P. J. Harries, A. J. Hendy, S. M. Holland, L. C. Ivany, W. Kiessling, M. A. Kosnik, C. R. Marshall, A. J. McGowan, A. I. Miller, T. D. Olszewski, M. E. Patzkowsky, S. E. Peters, L. Villier, P. J. Wagner, N. Bonuso, P. S. Borkow, B. Brenneis, M. E. Clapham, L. M. Fall, C. A. Ferguson, V. L. Hanson, A. Z. Krug, K. M. Layou, E. H. Leckey, S. Nurnberg, C. M. Powers, J. A. Sessa, C. Simpson, A. Tomasovych, and C. C. Visaggi. Phanerozoic trends in the global diversity of marine invertebrates. *Science*, 321(5885), Jul 2008.

[12] J. Alroy, C. R. Marshall, R. K. Bambach, K. Bezusko, M. Foote, F. T. Fursich, T. A. Hansen, S. M. Holland, L. C. Ivany, D. Jablonski, D. K. Jacobs, D. C. Jones, M. A. Kosnik, S. Lidgard, S. Low,

A. I. Miller, P. M. Novack-Gottshall, T. D. Olszewski, M. E. Patzkowsky, D. M. Raup, K. Roy, J. J. Sepkoski, M. G. Sommers, P. J. Wagner, and A. Webber. Effects of sampling standardization on estimates of Phanerozoic marine diversification. *Proc. Natl. Acad. Sci.*, 98(11), May 2001.

[13] J. M. Anderson and M. S. Lam. Global optimizations for parallelism and locality on scalable parallel machines. In *ACM SIGPLAN Conference on Programming Language Design and Implementation (PLDI)*, 1993.

[14] K. Andreev and H. Räcke. Balanced graph partitioning. In *SPAA*, 2004.

[15] C. Andrieu, N. De Freitas, A. Doucet, and M. I. Jordan. An introduction to MCMC for machine learning. *Machine Learning*, 2003.

[16] G. Angeli, S. Gupta, M. J. Premkumar, C. D. Manning, C. Ré, J. Tibshirani, J. Y. Wu, S. Wu, and C. Zhang. Stanford's distantly supervised slot filling systems for KBP 2014. In *Text Analysis Conference (TAC-KBP)*, 2015.

[17] K. Antonio and J. Beirlant. Actuarial statistics with generalized linear mixed models. In *Insurance: Mathematics and Economics*, 2006.

[18] L. Antova, C. Koch, and D. Olteanu. Query language support for incomplete information in the MayBMS system. In *International Conference on Very Large Data Bases (VLDB)*, 2007.

[19] W. I. Ausich and S. E. Peters. A revised macroevolutionary history for Ordovician–Early Silurian crinoids. *Paleobiology*, 31(3), 2005.

[20] C. Balkesen, G. Alonso, J. Teubner, and M. T. Özsu. Multi-core, main-memory joins: Sort vs. hash revisited. *Proceedings of the VLDB Endowment (PVLDB)*, 2013.

[21] R. K. Bambach. Species richness in marine benthic habitats through the phanerozoic. *Paleobiology*, 3(2), 1977.

[22] O. Banerjee, L. El Ghaoui, and A. d'Aspremont. Model selection through sparse maximum likelihood estimation for multivariate Gaussian or binary data. *Journal of Machine Learning Research*, 2008.

[23] M. Banko, M. J. Cafarella, S. Soderland, M. Broadhead, and O. Etzioni. Open information extraction from the web. In *International Joint Conference on Artificial Intelligence (IJCAI)*, 2007.

[24] D. Barber. *Bayesian Reasoning and Machine Learning*. Cambridge University Press, 2012.

[25] M. Bauer, S. Treichler, E. Slaughter, and A. Aiken. Legion: expressing locality and independence with logical regions. In *International Conference for High Performance Computing, Networking, Storage and Analysis (SC)*, 2012.

[26] L. A. Belady. A study of replacement algorithms for a virtual-storage computer. *IBM Syst. J.*, 1966.

[27] N. Bell and M. Garland. Efficient sparse matrix-vector multiplication on CUDA. Technical report, NVIDIA Corporation, 2008.

[28] N. Bell and M. Garland. Implementing sparse matrix-vector multiplication on throughput-oriented processors. In *International Conference for High Performance Computing, Networking, Storage and Analysis (SC)*, 2009.

[29] M. J. Benton. Diversification and extinction in the history of life. *Science*, 268(5207), Apr 1995.

[30] L. Bergstrom. Measuring NUMA effects with the STREAM benchmark. *ArXiv e-prints*, 2011.

[31] D. Bertsekas. *Nonlinear Programming*. Athena Scientific, 1999.

[32] J. Betteridge, A. Carlson, S. A. Hong, E. R. Hruschka, E. L. M. Law, T. M. Mitchell, and S. H. Wang. Toward never ending language learning. In *AAAI Spring Symposium*, 2009.

[33] L. S. Blackford, J. Choi, A. Cleary, A. Petitet, R. C. Whaley, J. Demmel, I. Dhillon, K. Stanley, J. Dongarra, S. Hammarling, G. Henry, and D. Walker. ScaLAPACK: A portable linear algebra library for distributed memory computers - design issues and performance. In *SuperComputing*, 1996.

[34] D. M. Blei, A. Y. Ng, and M. I. Jordan. Latent Dirichlet allocation. *J. Mach. Learn. Res.*, 2003.

[35] J. L. Blois, P. L. Zarnetske, M. C. Fitzpatrick, and S. Finnegan. Climate change and the past, present, and future of biotic interactions. *Science*, 341(6145), 2013.

[36] E. Boschee, R. Weischedel, and A. Zamanian. Automatic information extraction. 2005.

[37] L. Bottou and O. Bousquet. The tradeoffs of large scale learning. In *Annual Conference on Neural Information Processing Systems (NIPS)*, 2007.

[38] C. Boutsidis, P. Drineas, and M. Magdon-Ismail. Near-optimal coresets for least-squares regression. *IEEE Transactions on Information Theory*, 2013.

[39] S. Boyd, N. Parikh, E. Chu, B. Peleato, and J. Eckstein. Distributed optimization and statistical learning via the alternating direction method of multipliers. *Foundations and Trends in Machine Learning*, 2011.

[40] J. K. Bradley, A. Kyrola, D. Bickson, and C. Guestrin. Parallel coordinate descent for l1-regularized loss minimization. In *International Conference on Machine Learning (ICML)*, 2011.

[41] S. Brin. Extracting patterns and relations from the world wide web. In *International Workshop on the Web and Databases (WebDB)*, 1999.

[42] P. G. Brown. Overview of sciDB: Large scale array storage, processing and analysis. In *ACM SIGMOD International Conference on Management of Data (SIGMOD)*, 2010.

[43] G. Buehrer, S. Parthasarathy, and Y.-K. Chen. Adaptive parallel graph mining for CMP architectures. In *IEEE International Conference on Data Mining (ICDM)*, 2006.

[44] G. Buehrer, S. Parthasarathy, S. Tatikonda, T. Kurc, and J. Saltz. Toward terabyte pattern mining: An architecture-conscious solution. In *ACM SIGPLAN Symposium on Principles & Practice of Parallel Programming (PPOPP)*, 2007.

[45] E. V. Buskirk. How the Netflix prize was won. *Wired*, 2009.

[46] E. Callaway. Computers read the fossil record. *Nature*, 523, Jun 2015.

[47] C. Callison-Burch and M. Dredze. Creating speech and language data with Amazon's Mechanical Turk. In *NAACL HLT 2010 Workshop on Creating Speech and Language Data with Amazon's Mechanical Turk (CSLDAMT)*, 2010.

[48] A. Carlson, J. Betteridge, B. Kisiel, B. Settles, E. R. Hruschka, and T. M. Mitchell. Toward an architecture for never-ending language learning. In *AAAI Conference on Artificial Intelligence (AAAI)*, 2010.

[49] S. Carr, K. S. McKinley, and C.-W. Tseng. Compiler optimizations for improving data locality. In *International Conference on Architectural Support for Programming Languages and Operating Systems (ASPLOS)*, 1994.

[50] H. Chafi, A. K. Sujeeth, K. J. Brown, H. Lee, A. R. Atreya, and K. Olukotun. A domain-specific approach to heterogeneous parallelism. In *ACM SIGPLAN Symposium on Principles & Practice of Parallel Programming (PPOPP)*, 2011.

[51] C. Chasseur and J. M. Patel. Design and evaluation of storage organizations for read-optimized main memory databases. *Proceedings of the VLDB Endowment (PVLDB)*, 2013.

[52] F. Chen, A. Doan, J. Yang, and R. Ramakrishnan. Efficient information extraction over evolving text data. In *IEEE International Conference on Data Engineering (ICDE)*, 2008.

[53] F. Chen, X. Feng, C. Ré, and M. Wang. Optimizing statistical information extraction programs over evolving text. In *IEEE International Conference on Data Engineering (ICDE)*, 2012.

[54] Y. Chen and D. Z. Wang. Knowledge expansion over probabilistic knowledge bases. In *ACM SIGMOD International Conference on Management of Data (SIGMOD)*, 2014.

[55] R. Chirkova and J. Yang. Materialized views. *Foundations and Trends in Databases*, 2012.

[56] C. Chu, S. K. Kim, Y. Lin, Y. Yu, G. R. Bradski, A. Y. Ng, and K. Olukotun. Map-reduce for machine learning on multicore. In *Annual Conference on Neural Information Processing Systems (NIPS)*, 2006.

[57] J. Cohen, B. Dolan, M. Dunlap, J. M. Hellerstein, and C. Welton. MAD skills: New analysis practices for big data. *Proceedings of the VLDB Endowment (PVLDB)*, 2009.

[58] R. Collobert and J. Weston. A unified architecture for natural language processing: Deep neural networks with multitask learning. In *International Conference on Machine Learning (ICML)*, 2008.

[59] R. Collobert, J. Weston, L. Bottou, M. Karlen, K. Kavukcuoglu, and P. Kuksa. Natural language processing (almost) from scratch. *Journal of Machine Learning Research*, 2011.

[60] P. G. Constantine and D. F. Gleich. Tall and skinny QR factorizations in MapReduce architectures. In *MapReduce*, 2011.

[61] M. Craven and J. Kumlien. Constructing biological knowledge bases by extracting information from text sources. In *International Conference on Intelligent Systems for Molecular Biology*, 1999.

[62] N. Dalvi, C. Re, and D. Suciu. Queries and materialized views on probabilistic databases. *Journal of Computer and System Sciences (JCSS)*, 2011.

[63] N. Dalvi and D. Suciu. The dichotomy of probabilistic inference for unions of conjunctive queries. *J. ACM*, 2013.

[64] S. Das, Y. Sismanis, K. S. Beyer, R. Gemulla, P. J. Haas, and J. McPherson. Ricardo: Integrating R and Hadoop. In *ACM SIGMOD International Conference on Management of Data (SIGMOD)*, 2010.

[65] E. F. D'Azevedo, M. R. Fahey, and R. T. Mills. Vectorized sparse matrix multiply for compressed row storage format. In *International Conference on Computational Science (ICCS)*, 2005.

[66] J. Dean, G. Corrado, R. Monga, K. Chen, M. Devin, Q. V. Le, M. Z. Mao, M. Ranzato, A. W. Senior, P. A. Tucker, K. Yang, and A. Y. Ng. Large scale distributed deep networks. In *Annual Conference on Neural Information Processing Systems (NIPS)*, 2012.

[67] A. L. Delcher, A. Grove, S. Kasif, and J. Pearl. Logarithmic-time updates and queries in probabilistic networks. *J. Artif. Intell. Res.*, 1996.

[68] F. den Hollander. *Probability Theory: The Coupling Method*. 2012.

[69] P. Domingos and D. Lowd. *Markov Logic: An Interface Layer for Artificial Intelligence*. Synthesis Lectures on Artificial Intelligence and Machine Learning. Morgan & Claypool Publishers, 2009.

[70] X. L. Dong, E. Gabrilovich, G. Heitz, W. Horn, K. Murphy, S. Sun, and W. Zhang. From data fusion to knowledge fusion. In *International Conference on Very Large Data Bases (VLDB)*, 2014.

[71] O. Etzioni, M. Cafarella, D. Downey, S. Kok, A.-M. Popescu, T. Shaked, S. Soderland, D. S. Weld, and A. Yates. Web-scale information extraction in KnowItAll: (preliminary results). In *International Conference on World Wide Web (WWW)*, 2004.

[72] N. Fenton and M. Neil. Combining evidence in risk analysis using Bayesian networks. *Agena*, 2004.

[73] D. A. Ferrucci, E. W. Brown, J. Chu-Carroll, J. Fan, D. Gondek, A. Kalyanpur, A. Lally, J. W. Murdock, E. Nyberg, J. M. Prager, N. Schlaefer, and C. A. Welty. Building Watson: An overview of the DeepQA project. *AI Magazine*, 2010.

[74] J. Finkel, T. Grenager, and C. Manning. Incorporating non-local information into information extraction systems by Gibbs sampling. In *Annual Meeting of the Association for Computational Linguistics (ACL)*, 2005.

[75] J. R. Finkel, A. Kleeman, and C. D. Manning. Efficient, feature-based, conditional random field parsing. In *Annual Meeting of the Association for Computational Linguistics (ACL)*, 2008.

[76] S. Finnegan, N. A. Heim, S. E. Peters, and W. W. Fischer. Climate change and the selective signature of the late ordovician mass extinction. *Proc. Natl. Acad. Sci.*, 109(18), 2012.

[77] M. Foote. Origination and extinction components of taxonomic diversity: general problems. *Paleobiology*, 26(sp4), 2014/07/11 2000.

[78] J. a. Gama, I. Žliobaitė, A. Bifet, M. Pechenizkiy, and A. Bouchachia. A survey on concept drift adaptation. *ACM Comput. Surv.*, 2014.

[79] A. Ghoting, G. Buehrer, S. Parthasarathy, D. Kim, A. Nguyen, Y.-K. Chen, and P. Dubey. Cache-conscious frequent pattern mining on modern and emerging processors. *The VLDB Journal*, 2007.

[80] A. Ghoting, R. Krishnamurthy, E. Pednault, B. Reinwald, V. Sindhwani, S. Tatikonda, Y. Tian, and S. Vaithyanathan. SystemML: Declarative machine learning on MapReduce. In *IEEE International Conference on Data Engineering (ICDE)*, 2011.

[81] G. Golub. Numerical methods for solving linear least squares problems. *Numerische Mathematik*, 1965.

[82] J. Gonzalez, Y. Low, A. Gretton, and C. Guestrin. Parallel Gibbs sampling: From colored fields to thin junction trees. In *International Conference on Artificial Intelligence and Statistics (AISTATS)*, 2011.

[83] G. Gottlob, C. Koch, R. Baumgartner, M. Herzog, and S. Flesca. The Lixto data extraction project: Back and forth between theory and practice. In *ACM Symposium on Principles of Database Systems (PODS)*, 2004.

[84] V. Govindaraju, C. Zhang, and C. Ré. Understanding tables in context using standard NLP toolkits. In *Annual Meeting of the Association for Computational Linguistics (ACL)*, 2013.

[85] G. Graefe and W. J. McKenna. The Volcano optimizer generator: Extensibility and efficient search. In *IEEE International Conference on Data Engineering (ICDE)*, 1993.

[86] T. L. Griffiths and M. Steyvers. Finding scientific topics. *Proc. Natl. Acad. Sci.*, 2004.

[87] A. Gupta and I. S. Mumick, editors. *Materialized Views: Techniques, Implementations, and Applications*. MIT Press, Cambridge, MA, USA, 1999.

[88] A. Gupta, I. S. Mumick, and V. S. Subrahmanian. Maintaining views incrementally. *SIGMOD Rec.*, 1993.

[89] I. Guyon and A. Elisseeff. An introduction to variable and feature selection. *Journal of Machine Learning Research*, 2003.

[90] S. Hadjis, F. Abuzaid, C. Zhang, and C. Ré. Caffe con Troll: Shallow ideas to speed up deep learning. In *Workshop on Data analytics in the Cloud (DanaC)*, 2015.

[91] Y. He, R. Lee, Y. Huai, Z. Shao, N. Jain, X. Zhang, and Z. Xu. RCFile: A fast and space-efficient data placement structure in MapReduce-based warehouse systems. In *IEEE International Conference on Data Engineering (ICDE)*, 2011.

[92] M. A. Hearst. Automatic acquisition of hyponyms from large text corpora. In *International Conference on Computational Linguistics (COLING)*, 1992.

[93] J. M. Hellerstein, C. Ré, F. Schoppmann, D. Z. Wang, E. Fratkin, A. Gorajek, K. S. Ng, C. Welton, X. Feng, K. Li, and A. Kumar. The MADlib analytics library: Or MAD skills, the SQL. *Proceedings of the VLDB Endowment (PVLDB)*, 2012.

[94] M. Hewett, D. E. Oliver, D. L. Rubin, K. L. Easton, J. M. Stuart, R. B. Altman, and T. E. Klein. PharmGKB: The Pharmacogenetics Knowledge Base. *Nucleic Acids Res.*, 2002.

[95] F. D. Highland and C. T. Iwaskiw. Knowledge base compilation. In *International Joint Conference on Artificial Intelligence (IJCAI)*, 1989.

[96] R. Hoffmann, C. Zhang, X. Ling, L. Zettlemoyer, and D. Weld. Knowledge-based weak supervision for information extraction of overlapping relations. In *Annual Meeting of the Association for Computational Linguistics (ACL)*, 2011.

[97] T. Imieliński and W. Lipski, Jr. Incomplete information in relational databases. *J. ACM*, 1984.

[98] D. Jablonski, K. Roy, and J. W. Valentine. Out of the tropics: Evolutionary dynamics of the latitudinal diversity gradient. *Science*, 314(5796), Oct 2006.

[99] R. Jampani, F. Xu, M. Wu, L. Perez, C. Jermaine, and P. J. Haas. The Monte Carlo database system: Stochastic analysis close to the data. *ACM Transactions on Database Systems (TODS)*, 2011.

[100] R. Jampani, F. Xu, M. Wu, L. L. Perez, C. Jermaine, and P. J. Haas. MCDB: A Monte Carlo approach to managing uncertain data. In *ACM SIGMOD International Conference on Management of Data (SIGMOD)*, 2008.

[101] M. Jerrum and A. Sinclair. Polynomial-time approximation algorithms for the Ising model. *SIAM J. Comput.*, 1993.

[102] R. Jin, G. Yang, and G. Agrawal. Shared memory parallelization of data mining algorithms: Techniques, programming interface, and performance. *IEEE Transactions on Knowledge and Data Engineering (TKDE)*, 2005.

[103] M. J. Johnson, J. Saunderson, and A. S. Willsky. Analyzing Hogwild parallel Gaussian Gibbs sampling. In *Annual Conference on Neural Information Processing Systems (NIPS)*, 2013.

[104] S. Kandel, A. Paepcke, J. M. Hellerstein, and J. Heer. Enterprise data analysis and visualization: An interview study. *IEEE Trans. Vis. Comput. Graph.*, 2012.

[105] G. Kasneci, M. Ramanath, F. Suchanek, and G. Weikum. The YAGO-NAGA approach to knowledge discovery. *SIGMOD Rec.*, 2009.

[106] I. Katakis, G. Tsoumakas, E. Banos, N. Bassiliades, and I. Vlahavas. An adaptive personalized news dissemination system. *J. Intell. Inf. Syst.*, 2009.

[107] W. Kiessling. Long-term relationships between ecological stability and biodiversity in phanerozoic reefs. *Nature*, 433(7024), 01 2005.

[108] C. Kim, T. Kaldewey, V. W. Lee, E. Sedlar, A. D. Nguyen, N. Satish, J. Chhugani, A. Di Blas, and P. Dubey. Sort vs. hash revisited: Fast join implementation on modern multi-core CPUs. *Proceedings of the VLDB Endowment (PVLDB)*, 2009.

[109] A. Kimmig, L. Mihalkova, and L. Getoor. Lifted graphical models: a survey. *Maching Learning*, 99, 2015.

[110] M. L. Koc and C. Ré. Incrementally maintaining classification using an RDBMS. *Proceedings of the VLDB Endowment (PVLDB)*, 2011.

[111] D. Koller and N. Friedman. *Probabilistic Graphical Models: Principles and Techniques*. MIT Press, 2009.

[112] R. Krishnamurthy, Y. Li, S. Raghavan, F. Reiss, S. Vaithyanathan, and H. Zhu. SystemT: A system for declarative information extraction. *SIGMOD Rec.*, 2009.

[113] A. Kyrola, G. Blelloch, and C. Guestrin. GraphChi: Large-scale graph computation on just a PC. In *USENIX Symposium on Operating Systems Design and Implementation (OSDI)*, 2012.

[114] M. Langberg and L. J. Schulman. Universal ϵ-approximators for integrals. In *Annual ACM-SIAM Symposium on Discrete Algorithms (SODA)*, 2010.

[115] S. Laugesen et al. Paroxetine, a cytochrome P450 2D6 inhibitor, diminishes the stereoselective O-demethylation and reduces the hypoalgesic effect of tramadol. *Clin. Pharmacol. Ther.*, 2005.

[116] Q. V. Le, M. Ranzato, R. Monga, M. Devin, G. Corrado, K. Chen, J. Dean, and A. Y. Ng. Building high-level features using large scale unsupervised learning. In *International Conference on Machine Learning (ICML)*, 2012.

[117] Y. LeCun, L. Bottou, Y. Bengio, and P. Haffner. Gradient-based learning applied to document recognition. In *Intelligent Signal Processing*. 2001.

[118] D. A. Levin, Y. Peres, and E. L. Wilmer. *Markov Chains and Mixing Times*. American Mathematical Society, 2006.

[119] Y. Li, I. Pandis, R. Müller, V. Raman, and G. M. Lohman. NUMA-aware algorithms: the case of data shuffling. In *Biennial Conference on Innovative Data Systems Research (CIDR)*, 2013.

[120] Y. Li, F. R. Reiss, and L. Chiticariu. SystemT: A declarative information extraction system. In *Conference of the North American Chapter of the Association for Computational Linguistics: Human Language Technologies (NAACL)*, 2011.

[121] J. Liu, S. Wright, C. Ré, V. Bittorf, and S. Sridhar. An asynchronous parallel stochastic coordinate descent algorithm. *International Conference on Machine Learning (ICML)*, 2014.

[122] Z. Liu, Y. Zhang, E. Y. Chang, and M. Sun. PLDA+: Parallel latent Dirichlet allocation with data placement and pipeline processing. *ACM Transactions on Intelligent Systems and Technology*, 2011.

[123] Y. Low, D. Bickson, J. Gonzalez, C. Guestrin, A. Kyrola, and J. M. Hellerstein. Distributed GraphLab: A framework for machine learning in the cloud. *Proceedings of the VLDB Endowment (PVLDB)*, 2012.

[124] Y. Low, J. Gonzalez, A. Kyrola, D. Bickson, C. Guestrin, and J. M. Hellerstein. Graphlab: A new parallel framework for machine learning. In *Conference on Uncertainty in Artificial Intelligence (UAI)*, 2010.

[125] D. Lunn, D. Spiegelhalter, A. Thomas, and N. Best. The BUGS project: Evolution, critique and future directions. *Statistics in Medicine*, 2009.

[126] C. D. Manning, M. Surdeanu, J. Bauer, J. Finkel, S. J. Bethard, and D. McClosky. The Stanford CoreNLP natural language processing toolkit. In *Annual Meeting of the Association for Computational Linguistics (ACL)*, 2014.

[127] A. McCallum. Joint inference for natural language processing. In *Conference on Computational Natural Language Learning (CONLL)*, 2009.

[128] A. McCallum, K. Schultz, and S. Singh. Factorie: Probabilistic programming via imperatively defined factor graphs. In *Annual Conference on Neural Information Processing Systems (NIPS)*, 2009.

[129] A. I. Miller, M. Foote, and A. I. Miller. Calibrating the Ordovician Radiation of marine life: Implications for Phanerozoic diversity trends. *Paleobiology*, 22(2), 1996.

[130] B. Min, R. Grishman, L. Wan, C. Wang, and D. Gondek. Distant supervision for relation extraction with an incomplete knowledge base. In *Conference of the North American Chapter of the Association for Computational Linguistics: Human Language Technologies (NAACL)*, 2013.

[131] M. Mintz, S. Bills, R. Snow, and D. Jurafsky. Distant supervision for relation extraction without labeled data. In *Annual Meeting of the Association for Computational Linguistics (ACL)*, 2009.

[132] T. M. Mitchell. *Machine Learning*. McGraw-Hill, USA, 1997.

[133] K. Murphy. From big data to big knowledge. In *ACM International Conference on Conference on Information and Knowledge Management (CIKM)*, New York, NY, USA, 2013. ACM.

[134] N. Nakashole, M. Theobald, and G. Weikum. Scalable knowledge harvesting with high precision and high recall. In *WSDM*, 2011.

[135] A. Nath and P. Domingos. Efficient belief propagation for utility maximization and repeated inference. In *AAAI Conference on Artificial Intelligence (AAAI)*, 2010.

[136] D. Newman, P. Smyth, and M. Steyvers. Scalable parallel topic models. *Journal of Intelligence Community Research and Development*, 2006.

[137] D. Nguyen, A. Lenharth, and K. Pingali. A lightweight infrastructure for graph analytics. In *ACM SIGOPS Symposium on Operating Systems Principles (SOSP)*, 2013.

[138] D. Nguyen, A. Lenharth, and K. Pingali. Deterministic Galois: On-demand, portable and parameterless. In *International Conference on Architectural Support for Programming Languages and Operating Systems (ASPLOS)*, 2014.

[139] M. Nikolic, M. ElSeidy, and C. Koch. LINVIEW: incremental view maintenance for complex analytical queries. In *ACM SIGMOD International Conference on Management of Data (SIGMOD)*, 2014.

[140] F. Niu, C. Ré, A. Doan, and J. Shavlik. Tuffy: Scaling up statistical inference in Markov logic networks using an RDBMS. *Proceedings of the VLDB Endowment (PVLDB)*, 2011.

[141] F. Niu, B. Recht, C. Re, and S. J. Wright. Hogwild: A lock-free approach to parallelizing stochastic gradient descent. In *Annual Conference on Neural Information Processing Systems (NIPS)*, 2011.

[142] F. Niu, C. Zhang, C. Ré, and J. W. Shavlik. Elementary: Large-scale knowledge-base construction via machine learning and statistical inference. *Int. J. Semantic Web Inf. Syst.*, 2012.

[143] J. Nivre, J. Hall, and J. Nilsson. MaltParser: A data-driven parser-generator for dependency parsing. In *International Conference on Language Resources and Evaluation (LREC)*, 2006.

[144] D. Olteanu, J. Huang, and C. Koch. Sprout: Lazy vs. eager query plans for tuple-independent probabilistic databases. In *IEEE International Conference on Data Engineering (ICDE)*, 2009.

[145] S. Parthasarathy, M. J. Zaki, M. Ogihara, and W. Li. Parallel data mining for association rules on shared memory systems. *Knowl. Inf. Syst.*, 2001.

[146] J. Pearl. *Probabilistic Reasoning in Intelligent Systems: Networks of Plausible Inference*. Morgan Kaufmann, 1988.

[147] L. Peng, Y. Diao, and A. Liu. Optimizing probabilistic query processing on continuous uncertain data. *Proceedings of the VLDB Endowment (PVLDB)*, 2011.

[148] S. E. Peters, C. Zhang, M. Livny, and C. Ré. A machine reading system for assembling synthetic paleontological databases. *PLoS ONE*, 2014.

[149] H. Poon and P. Domingos. Joint inference in information extraction. In *AAAI Conference on Artificial Intelligence (AAAI)*, 2007.

[150] H. Poon and L. Vanderwende. Joint inference for knowledge extraction from biomedical literature. In *Conference of the North American Chapter of the Association for Computational Linguistics: Human Language Technologies (NAACL)*, Stroudsburg, PA, USA, 2010.

[151] I. Porteous, D. Newman, A. Ihler, A. Asuncion, P. Smyth, and M. Welling. Fast collapsed Gibbs sampling for latent Dirichlet allocation. In *ACM SIGKDD International Conference on Knowledge Discovery and Data Mining (KDD)*, 2008.

[152] L. Qiao, V. Raman, F. Reiss, P. J. Haas, and G. M. Lohman. Main-memory scan sharing for multi-core CPUs. *Proceedings of the VLDB Endowment (PVLDB)*, 2008.

[153] R. Ramakrishnan and J. Gehrke. *Database Management Systems*. Osborne/McGraw-Hill, 2000.

[154] V. Raman, G. Attaluri, R. Barber, N. Chainani, D. Kalmuk, V. KulandaiSamy, J. Leenstra, S. Lightstone, S. Liu, G. M. Lohman, T. Malkemus, R. Mueller, I. Pandis, B. Schiefer, D. Sharpe, R. Sidle, A. Storm, and L. Zhang. DB2 with BLU acceleration: So much more than just a column store. *Proceedings of the VLDB Endowment (PVLDB)*, 2013.

[155] D. M. Raup. Species diversity in the phanerozoic: A tabulation. *Paleobiology*, 2(4), 1976.

[156] P. D. Ravikumar, G. Raskutti, M. J. Wainwright, and B. Yu. Model selection in Gaussian graphical models: High-dimensional consistency of ℓ_1-regularized MLE. In *Annual Conference on Neural Information Processing Systems (NIPS)*, 2008.

[157] C. Ré, A. A. Sadeghian, Z. Shan, J. Shin, F. Wang, S. Wu, and C. Zhang. Feature engineering for knowledge base construction. *IEEE Data Eng. Bull.*, 2014.

[158] P. Richtárik and M. Takáč. Parallel coordinate descent methods for big data optimization. *ArXiv e-prints*, 2012.

[159] C. P. Robert and G. Casella. *Monte Carlo Statistical Methods (Springer Texts in Statistics)*. Springer-Verlag New York, Inc., 2005.

[160] A. Rosenfeld. *Picture Languages: Formal Models for Picture Recognition*. Academic Press, Inc., 1979.

[161] S. Sarawagi and M. Stonebraker. Efficient organization of large multidimensional arrays. In *IEEE International Conference on Data Engineering (ICDE)*, 1994.

[162] A. D. Sarma, O. Benjelloun, A. Halevy, S. Nabar, and J. Widom. Representing uncertain data: Models, properties, and algorithms. *The VLDB Journal*, 2009.

[163] S. Satpal, S. Bhadra, S. Sellamanickam, R. Rastogi, and P. Sen. Web information extraction using Markov logic networks. In *International Conference on World Wide Web (WWW)*, 2011.

[164] U. Schöning and J. Torán. *The Satisfiability Problem: Algorithms and Analyses*. Mathematik für Anwendungen. Lehmanns Media, 2013.

[165] P. Sen, A. Deshpande, and L. Getoor. PrDB: Managing and exploiting rich correlations in probabilistic databases. *The VLDB Journal*, 2009.

[166] J. J. Sepkoski and J. J. Sepkoski, Jr. Rates of speciation in the fossil record. *Philos. Trans. R. Soc. Lond., B, Biol. Sci.*, 353(1366), Feb 1998.

[167] J. J. Sepkoski, Jr. A factor analytic description of the phanerozoic marine fossil record. *Paleobiology*, 1981.

[168] J. J. Sepkoski, Jr. Ten years in the library: New data confirm paleontological patterns. *Paleobiology*, 19(1), 1993.

[169] S. Shalev-Shwartz and N. Srebro. SVM optimization: Inverse dependence on training set size. In *International Conference on Machine Learning (ICML)*, 2008.

[170] W. Shen, A. Doan, J. F. Naughton, and R. Ramakrishnan. Declarative information extraction using datalog with embedded extraction predicates. In *International Conference on Very Large Data Bases (VLDB)*, 2007.

[171] J. Shin, S. Wu, F. Wang, C. D. Sa, C. Zhang, and C. Ré. Incremental knowledge base construction using DeepDive. *Proceedings of the VLDB Endowment (PVLDB)*, 2015.

[172] A. Silberschatz, J. L. Peterson, and P. B. Galvin. *Operating System Concepts (3rd Ed.)*. Addison-Wesley Longman Publishing Co., Inc., 1991.

[173] A. Smola and S. Narayanamurthy. An architecture for parallel topic models. *Proceedings of the VLDB Endowment (PVLDB)*, 2010.

[174] J. R. Sobehart, R. Stein, V. Mikityanskaya, and L. Li. Moody's public firm risk model: A hybrid approach to modeling short term default risk. *Moody's Investors Service, Global Credit Research, Rating Methodology*, 2000.

[175] S. Sonnenburg, G. Rätsch, S. Henschel, C. Widmer, J. Behr, A. Zien, F. D. Bona, A. Binder, C. Gehl, and V. Franc. The SHOGUN machine learning toolbox. *Journal of Machine Learning Research*, 2010.

[176] E. R. Sparks, A. Talwalkar, V. Smith, J. Kottalam, X. Pan, J. Gonzalez, M. J. Franklin, M. I. Jordan, and T. Kraska. MLI: An API for distributed machine learning. In *IEEE International Conference on Data Mining (ICDM)*, 2013.

[177] S. Sridhar, S. J. Wright, C. Re, J. Liu, V. Bittorf, and C. Zhang. An approximate, efficient LP solver for LP rounding. In *Annual Conference on Neural Information Processing Systems (NIPS)*, 2013.

[178] M. Stonebraker, S. Madden, and P. Dubey. Intel "Big Data" science and technology center vision and execution plan. *SIGMOD Rec.*, 2013.

[179] F. M. Suchanek, M. Sozio, and G. Weikum. SOFIE: A self-organizing framework for information extraction. In *International Conference on World Wide Web (WWW)*, 2009.

[180] D. Suciu, D. Olteanu, C. Ré, and C. Koch. *Probabilistic Databases*. Morgan & Claypool, 2011.

[181] A. K. Sujeeth, H. Lee, K. J. Brown, T. Rompf, H. Chafi, M. Wu, A. R. Atreya, M. Odersky, and K. Olukotun. OptiML: An Implicitly Parallel Domain-Specific Language for Machine Learning. In *International Conference on Machine Learning (ICML)*, 2011.

[182] C. Sutton and A. McCallum. Collective segmentation and labeling of distant entities in information extraction. Technical report, U. Mass, 2004.

[183] S. Tatikonda and S. Parthasarathy. Mining tree-structured data on multicore systems. *Proceedings of the VLDB Endowment (PVLDB)*, 2009.

[184] R. Tibshirani. Regression shrinkage and selection via the Lasso. *Journal of the Royal Statistical Society (Series B)*, 58:267–288, 1996.

[185] M. M. Tsangaris and J. F. Naughton. A stochastic approach for clustering in object bases. In *ACM SIGMOD International Conference on Management of Data (SIGMOD)*, 1991.

[186] S. Tu, W. Zheng, E. Kohler, B. Liskov, and S. Madden. Speedy transactions in multicore in-memory databases. In *ACM SIGOPS Symposium on Operating Systems Principles (SOSP)*, 2013.

[187] M. Wainwright and M. Jordan. Log-determinant relaxation for approximate inference in discrete Markov random fields. *Trans. Sig. Proc.*, 2006.

[188] M. J. Wainwright and M. I. Jordan. Graphical models, exponential families, and variational inference. *Foundations and Trends in Machine Learning*, 2008.

[189] D. Z. Wang, M. J. Franklin, M. Garofalakis, J. M. Hellerstein, and M. L. Wick. Hybrid in-database inference for declarative information extraction. In *ACM SIGMOD International Conference on Management of Data (SIGMOD)*, 2011.

[190] D. Z. Wang, E. Michelakis, M. Garofalakis, and J. M. Hellerstein. BayesStore: Managing large, uncertain data repositories with probabilistic graphical models. *Proceedings of the VLDB Endowment (PVLDB)*, 2008.

[191] M. P. Wellman, J. S. Breese, and R. P. Goldman. From knowledge bases to decision models. *The Knowledge Engineering Review*, 7, 1992.

[192] R. West, E. Gabrilovich, K. Murphy, S. Sun, R. Gupta, and D. Lin. Knowledge base completion via search-based question answering. In *International Conference on World Wide Web (WWW)*, New York, NY, USA, 2014. ACM.

[193] M. Wick and A. McCallum. Query-aware MCMC. In *Annual Conference on Neural Information Processing Systems (NIPS)*, 2011.

[194] M. Wick, A. McCallum, and G. Miklau. Scalable probabilistic databases with factor graphs and MCMC. *Proceedings of the VLDB Endowment (PVLDB)*, 2010.

[195] M. L. Wick, A. McCallum, and G. Miklau. Scalable probabilistic databases with factor graphs and MCMC. *Proceedings of the VLDB Endowment (PVLDB)*, 2010.

[196] S. Williams, L. Oliker, R. Vuduc, J. Shalf, K. Yelick, and J. Demmel. Optimization of sparse matrix-vector multiplication on emerging multicore platforms. In *International Conference for High Performance Computing, Networking, Storage and Analysis (SC)*, 2007.

[197] T. Xu and A. T. Ihler. Multicore Gibbs sampling in dense, unstructured graphs. *International Conference on Artificial Intelligence and Statistics (AISTATS)*, 2011.

[198] X. Yang, S. Parthasarathy, and P. Sadayappan. Fast sparse matrix-vector multiplication on gpus: Implications for graph mining. *Proceedings of the VLDB Endowment (PVLDB)*, 2011.

[199] L. Yao, S. Riedel, and A. McCallum. Collective cross-document relation extraction without labelled data. In *Conference on Empirical Methods in Natural Language Processing (EMNLP)*, 2010.

[200] A. Yates, M. Cafarella, M. Banko, O. Etzioni, M. Broadhead, and S. Soderland. TextRunner: Open information extraction on the Web. In *Conference of the North American Chapter of the Association for Computational Linguistics: Human Language Technologies (NAACL)*, 2007.

[201] M. Zaharia, M. Chowdhury, T. Das, A. Dave, J. Ma, M. McCauley, M. J. Franklin, S. Shenker, and I. Stoica. Resilient distributed datasets: A fault-tolerant abstraction for in-memory cluster computing. In *USENIX Symposium on Networked Systems Design and Implementation (NSDI)*, 2012.

[202] M. J. Zaki, C. Ho, and R. Agrawal. Parallel classification for data mining on shared-memory multiprocessors. In *IEEE International Conference on Data Engineering (ICDE)*, 1999.

[203] M. J. Zaki, S. Parthasarathy, M. Ogihara, and W. Li. New algorithms for fast discovery of association rules. In *ACM SIGKDD International Conference on Knowledge Discovery and Data Mining (KDD)*, 1997.

[204] C. Zhang, A. Kumar, and C. Ré. Materialization optimizations for feature selection workloads. In *ACM SIGMOD International Conference on Management of Data (SIGMOD)*, 2014.

[205] C. Zhang, F. Niu, C. Ré, and J. Shavlik. Big data versus the crowd: Looking for relationships in all the right places. In *Annual Meeting of the Association for Computational Linguistics (ACL)*, 2012.

[206] C. Zhang and C. Ré. Towards high-throughput Gibbs sampling at scale: a study across storage managers. In *ACM SIGMOD International Conference on Management of Data (SIGMOD)*, 2013.

[207] C. Zhang and C. Ré. DimmWitted: A study of main-memory statistical analytics. *Proceedings of the VLDB Endowment (PVLDB)*, 2014.

[208] Y. Zhang, W. Zhang, and J. Yang. I/O-efficient statistical computing with RIOT. In *IEEE International Conference on Data Engineering (ICDE)*, 2010.

[209] J. Zhu, Z. Nie, X. Liu, B. Zhang, and J.-R. Wen. StatSnowball: A statistical approach to extracting entity relationships. In *International Conference on World Wide Web (WWW)*, 2009.

[210] M. Zinkevich, M. Weimer, A. J. Smola, and L. Li. Parallelized stochastic gradient descent. In *Annual Conference on Neural Information Processing Systems (NIPS)*, 2010.

A. Appendix

A.1 Scalable Gibbs Sampling

A.1.1 Theoretical Hardness of I/O Optimization

We prove the following proposition which appears in Chapter 5.1.

Proposition A.1. *Assuming $|F| \geq 2S$ and all factor pages must be full ($|F| = kS$ for some integer k), there exist factor graphs (V, F, E) and variable orders μ such that there is no polynomial time approximation algorithm with finite approximation ratio for the following I/O optimization problem unless P=NP:*

$$\operatorname*{argmin}_{\pi \in S(\mu), \beta: F \mapsto \{1,\ldots,k\}} \textit{cost}(\pi, \beta).$$

Proof. Balanced Graph Partitioning (BGP) [14] has been proven to have no polynomial time approximation algorithm with finite approximation ratio unless P=NP. We reduce BGP to the I/O optimization problem in two steps: (1) we reduce BGP to a Eulerian-graph BGP problem; and (2) we reduce the Eulerian-graph BGP problem to the above I/O optimization problem.

First, let $G = (W, C)$ be a graph such that k divides $|W|$. There is no polynomial time algorithm with finite approximation ratio to partition W into k components of equal sizes with minimum cut size, a problem called BGP [14]. Let $G' = (W', C')$ be a copy of G; i.e., there is a bijection $\sigma : W \mapsto W'$ such that $w' = \sigma(w) \in W'$ for each $w \in W$. Let $H = (W \cup W', C \cup C' \cup D)$ where D contains $2|C| + \deg(w)$ copies of (w, w') for each corresponding $w \in W$ and $w' = \sigma(w) \in W'$; $\deg(w)$ denotes the degree of w in G. If there is an P-Time θ-approx algorithm to compute a k-way balanced partitioning of H, then the same algorithm would approximates BGP with the same ratio: it is easy to see that any partitioning of H that cuts (resp. does not cut) edges in D have cost at least $2|C| + 1$ (resp. at most $2|C|$). Therefore, an optimal partitioning of H does not cut edges in D, which together with the balance requirement implies that the projection of this partitioning on G is also a optimal k-way balanaced partitioning for G. Noting that H is an Eulerian graph (each node an even degree), we conclude that BSG on Eulerian graphs is as hard as BSG in general.

Next we reduce Eulerian-graph BSG to the I/O minimization problem. Let $H = (W, C)$ be an

Eulerian graph, $c_1, \ldots, c_n$ be an Eulerian path in H, and denote by $w_0, w_1, \ldots, w_n$ the corresponding sequence of nodes being visited (i.e., $c_i = (w_{i-1}, w_i)$). We can construct a disk layout problem as follows. Let variables $V = C$ and $c_1, \ldots, c_n$ the required variable order (i.e., μ). Let factors $F = W$ and $E = \{(c_i, w_{i-1}), (c_i, w_i) \mid 1 \leq i \leq n\}$. To minize I/O for this factor graph, it is not hard to see that (1) The visiting order of F is the same as $w_0, w_1, \ldots, w_n$ (otherwise, the same page mapping β would result in higher or the same I/O cost); and (2) β maps F to exactly k pages (because every factor page must be full). Thus, β must also be a balanced partitioning of H. Let $\pi = (\ldots, (c_i, w_{i-1}), (c_i, w_i), (c_{i+1}, w_i), \ldots)$. Among the two types of edges, (c_{i+1}, w_i) edges do not incur any I/O cost since w_i was just visited; (c_i, w_i) incurs an I/O fetch if and only if w_{i-1} and w_i are on different pages, i.e., when c_i is cut by β. Thus, cost(π, β) is equal to the cut size of β on H. If we can solve $\arg\min_{\pi,\beta}$ cost(π, β), we would be able to solve Eulerian graph BSG and thereby BSG just as efficiently. The approximability result is based on the facts that (1) the above construction is in polynomial time; and (2) the costs in all three problems are affinely related. □

A.1.2 Buffer Management

When a data set does not fit in memory, a classical challenge is to choose the replacement policy for the buffer manager. A key twist here is that we will be going over the same data set many times, and so we have access to the full reference stream. Thus, we can use a classical result from Belady in 60s [26] to define a theoretical optimal eviction strategy: *evict the item that will be used latest in the future*.

Recall that for each iteration our system performs a scan over $E = \{(v, f) | v \in \text{vars}(f)\}$ in an order $\pi = (e_1, ..., e_L)$. Therefore, we know an access order of all factors $\pi_f = (f_{\gamma_1}, ..., f_{\gamma_L})$, where $e_j.f = f_{\gamma_j}$. Given the set of factors F, we assume that we have a fixed-size buffer $B \subseteq F$ (let K be the size of the buffer). We define two operations over B:

1. **Evict** f**.** $B \leftarrow B - \{f\}$.
2. **Insert** f**.** $B \leftarrow B \cup \{f\}$.

Before we process f_{γ_j}, the buffer is in the state $B^{(j-1)}$ (let $B^{(0)} = \emptyset$). We pay an I/O cost if $f_{\gamma_j} \notin B^{(j-1)}$. We then insert f_{γ_j} into $B^{(j-1)}$, and if $|B^{(j-1)} \cup \{f_{\gamma_j}\}| > K$ select one factor

$f^{(j)} \in B^{(j-1)} \cup \{f_{\gamma_j}\}$ to evict, to get $B^{(j)}$. We want to optimize the selection of $f^{(j)}$ to minimize the I/O cost:

$$\min_{f^{(1)},\ldots f^{(L)}} \sum_j \mathbb{I}(f_{\gamma_j} \notin B^{(j-1)}).$$

where $\mathbb{I}(f_{\gamma_j} \notin B^{(j-1)}) = 1$ if $f_{\gamma_j} \notin B^{(j-1)}$ evaluates to true; otherwise 0. This problem has been studied by Belady [26] and we construct an algorithm that forms the optimal solution of this optimization problem. First, for each f_{γ_j} we associate a number $\rho_j = \min(\{\gamma_t | t > j \wedge f_{\gamma j} = f_{\gamma_t}\} \cup \{L+1\})$. In other words, ρ_j is the index of the nearest next usage of factor f_{γ_j}. The smaller the ρ_j, the sooner that factor f_{γ_j} will be used later. The optimal strategy of selecting a factor in the buffer to evict is to select a factor with largest ρ value.

We implement this buffer manager in our system and run experiments to validate its efficiency. To implement this buffer manager, we maintain the ρ numbers in an array. We go through the data set by one pass to calculate these ρ's. When we process an (v, f) pair, we also fetch its ρ value. The array of ρ is stored on disk and we need one sequential scan over the array for every epoch of sampling.

A.2 Implementation Details of DimmWitted

In DimmWitted (Chapter 5.2), we implement optimizations that are part of scientific computation and analytics systems. While these optimizations are not new, they are not universally implemented in analytics systems. We briefly describes each optimization and its impact.

Data and Worker Collocation We observe that different strategies of locating data and workers affect the performance of DimmWitted. One standard technique is to collocate the worker and the data on the same NUMA node. In this way, the worker in each node will pull data from its own DRAM region, and does not need to occupy the node-DRAM bandwidth of other nodes. In DimmWitted, we tried two different placement strategies for data and workers. The first protocol, called OS, relies on the operating system to allocate data and threads for workers. The operating system will usually locate data on one single NUMA node, and worker threads to different NUMA nodes using heuristics that are not exposed to the user. The second protocol, called NUMA, evenly distributes worker threads across NUMA nodes, and for each worker, replicates the data on the same NUMA node. We find that for SVM on RCV1, the strategy NUMA can be up to 2$\times$ faster than OS. Here are two reasons

for this improvement. First, by locating data on the same NUMA node to workers, we achieve 1.24× improvement on the throughput of reading data. Second, by not asking the operating system to allocate workers, we actually have a more balanced allocation of workers on NUMA nodes.

Dense and Sparse For statistical analytics workloads, it is not uncommon for the data matrix A to be sparse, especially for applications such as information extraction and text mining. In DimmWitted, we implement two protocols, Dense and Sparse, which store the data matrix A as a dense or sparse matrix, respectively. A Dense storage format has two advantages: (1) if storing a fully dense vector, it requires $\frac{1}{2}$ the space as a sparse representation, and (2) Dense is able to leverage hardware SIMD instructions, which allows multiple floating point operations to be performed in parallel. A Sparse storage format can use a BLAS-style scatter-gather to incorporate SIMD, which can improve cache performance and memory throughput; this approach has the additional overhead for the gather operation. We find on a synthetic dataset in which we vary the sparsity from 0.01 to 1.0, Dense can be up to 2× faster than Sparse (for sparsity=1.0) while Sparse can be up to 4× faster than Dense (for sparsity=0.01).

The dense vs. sparse tradeoff might change on newer CPUs with VGATHERDPD intrinsic designed to specifically speed up the gather operation. However, our current machines do not support this intrinsics and how to optimize sparse and dense computation kernel is orthogonal to the main goals of this paper.

Row-major and Column-major Storage There are two well-studied strategies to store a data matrix A: Row-major and Column-major storage. Not surprisingly, we observed that choosing an incorrect data storage strategy can cause a large slowdown. We conduct a simple experiment where we multiply a matrix and a vector using row-access method, where the matrix is stored in column- and row-major order. We find that the Column-major could resulting $9\times$ more L1 data load misses than using Row-major for two reasons: (1) our architectures fetch four doubles in a cacheline, only one of which is useful for the current operation. The prefetcher in Intel machines does not prefetch across page boundaries, and so it is unable to pick up significant portions of the strided access; (2) On the first access, the Data cache unit (DCU) prefetcher also gets the next cacheline compounding the problem, and so it runs $8\times$ slower. Therefore, DimmWitted always stores the dataset in a way that is consistent with the access method—no matter how the input data is stored

A.3 Additional Details of Incremental Feature Engineering

A.3.1 Additional Theoretical Details

We find that the three semantics that we defined, namely, Linear, Logical, and Ratio, have impact to the convergence speed of the sampling procedure. We describe these results in Section A.3.1.1 and provide proof in Section A.3.1.2.

A.3.1.1 Convergence Results

We describe our results on convergence rates, which are summarized in Figure A.1. We first describe results for the Voting program from Example 3.4, and summarize those results in a theorem. We now introduce the standard metric of convergence in Markov Chain theory [101].

Definition A.2. *The* total variation distance *between two probability measures $\mathbb{P}$ and $\mathbb{P}'$ over the same sample space Ω is defined as*

$$\|\mathbb{P} - \mathbb{P}'\|_{\text{tv}} = \sup_{A \subset \Omega} |\mathbb{P}(A) - \mathbb{P}'(A)|,$$

that is, it represents the largest difference in the probabilities that $\mathbb{P}$ and $\mathbb{P}'$ assign to the same event.

In Gibbs sampling, the total variation distance is a metric of comparison between the actual distribution $\mathbb{P}_k$ achieved at some timestep k and the equilibrium distribution π.

Types of Programs We consider two families of programs motivated by our work in KBC: voting programs and hierarchical programs. The voting program is used to continue the example, but some KBC programs are hierarchical (13/14 KBC systems from the literature). We consider some enhancements that make our programs more realistic. We allow every tuple (IDB or EDB) to have its own weight, i.e., we allow every ground atom $R(a)$ to have a rule $w_a \ : R(a)$. Moreover, we allow any atom to be marked as evidence (or not), which means its value is fixed. We assume that all weights are *not* functions of the number of variables (and so are $O(1)$). Finally, we consider two types of programs. The first we call *voting programs*, which are a generalization of Example 3.4 in which any subset of variables may be evidence and the weights may be distinct.

Proposition A.3. *Let $\varepsilon > 0$. Consider Gibbs sampling running on a particular factor graph with n variables, there exists a $\tau(n)$ that satisfies the upper bounds in Figure A.1 and such that $\|\mathbb{P}_k - \pi\|_{\text{tv}} \leq \varepsilon$*

Problem	OR Semantic	Upper Bound	Lower Bound
Voting	Logical	$O(n \log n)$	$\Omega(n \log n)$
	Ratio	$O(n \log n)$	$\Omega(n \log n)$
	Linear	$2^{O(n)}$	$2^{\Omega(n)}$

Figure A.1: Bounds on $\tau(n)$. The O notation hides constants that depend the query and the weights.

after $\tau(n) \log(1 + \varepsilon^{-1})$ steps. Furthermore, for each of the classes, we can construct a graph on which the minimum time to achieve total variation distance ε is at least the lower bound in Figure A.1.

For example, for the voting example with logical semantics, $\tau(n) = O(n \log n)$. The lower bounds are demonstrated with explicit examples and analysis. The upper bounds use the special form of Gibbs sampling on these factor graphs, and then use a standard argument based on *coupling* [68] and an analysis very similar to a generalized coupon collector process. This argument is sufficient to analyze the voting program in all three semantics.

We consider a generalization of the voting program in which each tuple is a random variable (possibly with a weight); specifically, the program consists of a variable Q, a set of "Up" variables U, and a set of "Down" variables D. Experimentally, we compute how different semantics converges on the voting program as illustrated in Figure A.2. In this figure, we vary the size of $|U| + |D|$ with $|U| = |D|$ and all variables to be non-evidence variables and measure the time that Gibbs sampling converges to 1% within the correct marginal probability of Q. We see that empirically, these semantics do have an effect on Gibbs sampling performance (Linear converges much slower than either Ratio or Logical) and we seek to give some insight into this phenomenon for KBC programs.

We analyze more general *hierarchical* programs in an asymptotic setting.

Definition A.4. *A rule $q(\bar{x}) :\text{-} p_1(\bar{x}_1), \ldots, p_k(x_k)$ is hierarchical if either $\bar{x} = \emptyset$ or there is a single variable $x \in \bar{x}$ such that $x \in \bar{x}_i$ for $i = 1, \ldots, k$. A set of rules (or a Datalog program) is hierarchical if each rule is hierarchical and they can be stratified.*

Evaluation of hierarchical programs is ♯P-hard, e.g., any Boolean query is hierarchical, but there are ♯P-hard Boolean queries [180]. Using a similar argument, we show that any set of hierarchical rules that have non-overlapping bodies converges in time $O(N \log N \log(1 + \varepsilon^{-1}))$ for either Logical or Ratio semantics, where N is the number of factors. This statement is not trivial, as we show that Gibbs sampling on the simplest non-hierarchical programs may take exponential time to converge. Our definition is more general than the typical notions of *safety* [63]: we consider multiple rules with

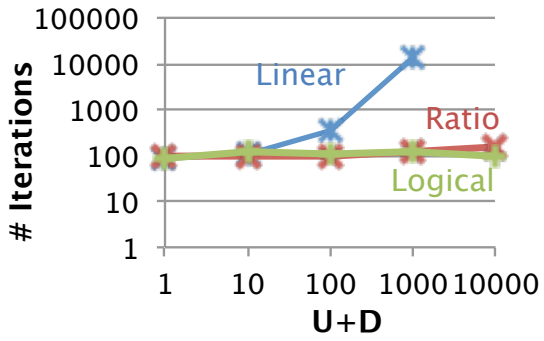

Figure A.2: Convergence of different semantics.

rich correlations rather than a single query over a tuple independent database. However, we only provide guarantees about sampling (not exact evaluation) and have no dichotomy theorem.

We also analyze an asymptotic setting, in which the domain size grows, and we show that hierarchical programs also converge in polynomial time in the Logical semantics. This result is a theoretical example that suggests that the more data we have, the better Gibbs sampling will behave. The key technical idea is that for the hierarchical programs no variable has unbounded influence on the final result, i.e., no variable contributes an amount depending on N to the final joint probability.

A.3.1.2 Proofs of Convergence Rates

Here, we prove the convergence rates stated in Proposition A.3. The strategy for the upper bound proofs involves constructing a *coupling* between the Gibbs sampler and another process that attains the equilibrium distribution at each step. First, we define a coupling [68, 118].

Definition A.5 (Coupling)**.** *A coupling of two random variables X and X' defined on some separate probability spaces $\mathbb{P}$ and $\mathbb{P}'$ is any new probability space $\hat{\mathbb{P}}$ over which there are two random variables $\hat{X}$ and $\hat{X}'$ such that X has the same distribution as $\hat{X}$ and X' has the same distribution as $\hat{X}'$.*

Given a coupling of two sequences of random variables X_k and X'_k, the *coupling time* is defined as the first time T when $\hat{X}_k = \hat{X}'_k$. The following theorem lets us bound the total variance distance in terms of the coupling time.

Theorem A.6. *For any coupling $(\hat{X}_k, \hat{X}'_k)$ with coupling time T,*

$$\|\mathbb{P}(X_k \in \cdot) - \mathbb{P}'(X'_k \in \cdot)\|_{\text{tv}} \leq 2\hat{\mathbb{P}}(T > k).$$

All of the coupling examples in this section use a *correlated flip coupler*, which consists of two Gibbs samplers $\hat{X}$ and $\hat{X}'$, each of which is running with the same random inputs. Specifically, both samplers choose to sample the same variable at each timestep. Then, if we define p as the probability of sampling 1 for $\hat{X}$, and p' similarly, it assigns both variables to 1 with probability $\min(p, p')$, both variables to 0 with probability $\min(1-p, 1-p')$, and assigns different values with probability $|p - p'|$. If we initialize $\hat{X}$ with an arbitrary distribution and $\hat{X}'$ with the stationary distribution π, it is trivial to check that $\hat{X}_k$ has distribution $\mathbb{P}_k$, and $\hat{X}'_k$ always has distribution π. Applying Theorem A.6 results in

$$\|\mathbb{P}_k - \pi\|_{\mathrm{tv}} \leq 2\hat{\mathbb{P}}(T > k).$$

Now, we prove the bounds in Figure A.1.

Theorem A.7 (UB for Voting: Logical and Ratio)**.** *For the voting example, if all the weights on the variables are bounded independently of the number of variables n, and $|U| = \Omega(n)$, and $|D| = \Omega(n)$, then for either the logical or ratio projection semantics, there exists a $\tau(n) = O(n \log n)$ such that for any $\varepsilon > 0$, $\|\mathbb{P}_k - \pi\|_{\mathrm{tv}} \leq \varepsilon$ for any $k \geq \tau(n) \log(\epsilon^{-1})$.*

Proof. For the voting problem, if we let f denote the projection semantic we are using, then for any possible world I the weight can be written as

$$W = \sum_{u \in U \cap I} w_u + \sum_{d \in D \cap I} w_d + w\sigma f(|U \cap I|) - w\sigma f(|D \cap I|),$$

where $\sigma = \mathsf{sign}(Q, I)$. Let I denote the world at the current timestep, I' be the world at the next timestep, and I_- be I with the variable we choose to sample removed. Then if we sample a variable $u \in U$, and let $m_U = |U \cap I_-|$, then

$$\begin{aligned}\mathbb{P}(u \in I') &= \frac{\exp(w_u + w\sigma f(m_U + 1))}{\exp(w_u + w\sigma f(m_U + 1)) + \exp(w\sigma f(m_U))} \\ &= (1 + \exp(-w_u - w\sigma(f(m_U + 1) - f(m_U))))^{-1}.\end{aligned}$$

Since $f(x+1) - f(x) < 1$ for any x, it follows that $\sigma(f(m_U + 1) - f(m_U)) \geq -1$. Furthermore, since w_u is bounded independently of n, we know that $w_u \geq w_{\min}$ for some constant $w_{\min}$. Substituting

this results in

$$\mathbb{P}\left(u \in I'\right) \geq \frac{1}{1+\exp\left(-w_{\min}+w\right)} = p_{\min},$$

for some constant $p_{\min}$ independent of n. The same argument will show that, if we sample $d \in D$,

$$\mathbb{P}\left(d \in I'\right) \geq p_{\min}.$$

Now, if $|U \cap I| > \frac{p_{\min}|U|}{2}$, it follows that, for both the logical and ratio semantics, $f(m_U+1)-f(m_U) \leq \frac{2}{p_{\min}|U|}$. Under these conditions, then if we sample u, we will have

$$\begin{aligned}
&\frac{1}{1+\exp\left(-w_u + w\frac{2}{p_{\min}|U|}\right)} \\
&\quad \leq \mathbb{P}\left(u \in I'\right) \\
&\quad \leq \frac{1}{1+\exp\left(-w_u - w\frac{2}{p_{\min}|U|}\right)},
\end{aligned}$$

The same argument applies to sampling d.

Next, consider the situation if we sample Q.

$$\mathbb{P}\left(Q \in I'\right) = \left(1+\exp\left(-2wf(|U \cap I|) + 2wf(|D \cap I|)\right)\right)^{-1}.$$

Under the condition that $|U \cap I| > \frac{p_{\min}|U|}{2}$, and similarly for D, this is bounded by

$$\begin{aligned}
&\left(1+\exp\left(-2wf\left(\frac{p_{\min}|U|}{2}\right) + 2wf(|D|)\right)\right)^{-1} \\
&\quad \leq \mathbb{P}\left(Q \in I'\right) \\
&\quad \leq \left(1+\exp\left(2wf\left(\frac{p_{\min}|D|}{2}\right) - 2wf(|U|)\right)\right)^{-1}.
\end{aligned}$$

But, for both logical and ratio semantics, we have that $f(cn) - f(n) = O(1)$, and so for some q_+ and q_- independent of n,

$$q_- \leq \mathbb{P}\left(Q \in I'\right) \leq q_+.$$

Now, consider a correlated-flip coupler running for $4n\log n$ steps on the Gibbs sampler. Let E_1 be the event that, after the first $2n\log n$ steps, each of the variables has been sampled at least once. (This

will have probability at least $\frac{1}{2}$ by the coupon collector's problem.) Let E_U be the event that, after the first $2n \log n$ steps, $|U \cap I| \geq \frac{p_{\min}|U|}{2}$ for the next $2n \log n$ steps for both samplers, and similarly for E_D. After all the entries have been sampled, $|U \cap I|$ and $|D \cap I|$ will each be bounded from below by a binomial random variable with parameter $p_{\min}$ at each timestep, so from Hoeffding's inequality, the probability that this constraint will be violated by a sampler at any particular step is less than $\exp(-\frac{1}{2}p_{\min}|U|)$. Therefore,

$$\hat{\mathbb{P}}(E_U|E_1) \geq \left(1 - \exp\left(-\frac{1}{2}p_{\min}|U|\right)\right)^{4n \log n} = \Omega(1).$$

The same argument shows that $E_D = \Omega(1)$. Let E_2 be the event that all the variables are resampled at least once between time $2n \log n$ and $4n \log n$. Again this event has probability at least $\frac{1}{2}$. Finally, let C be the event that coupling occurs at time $4n \log n$. Given E_1, E_2, E_U, and E_D, this probability is equal to the probability that each variable coupled individually the last time it was sampled. For u, this probability is

$$1 - \frac{1}{1 + \exp\left(-w_u - w\frac{2}{p_{\min}n}\right)} + \frac{1}{1 + \exp\left(-w_u + w\frac{2}{p_{\min}n}\right)},$$

and similarly for d. We know this probability is $1 - O(\frac{1}{n})$ by Taylor's theorem. Meanwhile, for Q, the probability of coupling is $1 - q_+ + q_-$, which is always $\Omega(1)$. Therefore,

$$\hat{\mathbb{P}}(C|E_1, E_2, E_U, E_D) \geq \Omega(1)\left(1 - O\left(\frac{1}{n}\right)\right)^{n-1} = \Omega(1),$$

and since

$$\hat{\mathbb{P}}(C) = \hat{\mathbb{P}}(C|E_1, E_2, E_U, E_D)\hat{\mathbb{P}}(E_U|E_1)\hat{\mathbb{P}}(E_D|E_1)\hat{\mathbb{P}}(E_2|E_1)\hat{\mathbb{P}}(E_1),$$

we can conclude that $\hat{\mathbb{P}}(C) = \Omega(1)$.

Therefore, this process couples with at least some constant probability p_C after $4n \log n$ steps. Since we can run this coupling argument independently an arbitrary number of times, it follows that, after $4Ln \log n$ steps, the probability of coupling will be at least $1 - (1 - p_C)^L$. Therefore,

$$\|\mathbb{P}_{4Ln \log n} - \pi\|_{\text{tv}} \leq \hat{\mathbb{P}}(T > 4Ln \log n) \leq (1 - p_C)^L.$$

This will be less than ϵ when $L \geq \frac{\log(\epsilon)}{\log(1-p_C)}$, which occurs when $k \geq 4n \log n \frac{\log(\epsilon)}{\log(1-p_C)}$. Letting $\tau(n) = \frac{4n \log n}{-\log(1-p_C)}$ proves the theorem. □

Theorem A.8 (LB for Voting: Logical and Ratio)**.** *For the voting example, using either the logical or ratio projection semantics, the minimum time to achieve total variation distance ε is $O(n \log n)$.*

Proof. At a minimum, in order to converge, we must sample all the variables. From the coupon collector's problem, this requires $O(n \log n)$ time. □

Theorem A.9 (UB for Voting: Linear)**.** *For the voting example, if all the weights on the variables are bounded independently of n, then for linear projection semantics, there exists a $\tau(n) = 2^{O(n)}$ such that for any $\varepsilon > 0$, $\|\mathbb{P}_k - \pi\|_{\text{tv}} \leq \varepsilon$ for any $k \geq \tau(n) \log(\epsilon^{-1})$.*

Proof. If at some timestep we choose to sample variable u,

$$\mathbb{P}\left(u \in I'\right) = \frac{\exp\left(w_u + wq\right)}{\exp\left(w_u + wq\right) + \exp(0)} = \Omega(1),$$

where $q = \text{sign}(Q, I)$. The same is true for sampling d. If we choose to sample Q,

$$\begin{aligned}
&\mathbb{P}\left(Q \in I'\right) \\
&\quad = \frac{\exp\left(w|U \cap I| - w|D \cap I|\right)}{\exp\left(w|U \cap I| - w|D \cap I|\right) + \exp\left(-w|U \cap I| + w|D \cap I|\right)} \\
&\quad = \left(1 + \exp\left(-2w(|U \cap I| - |D \cap I|)\right)\right)^{-1} = \exp(-O(n)).
\end{aligned}$$

Therefore, if we run a correlated-flip coupler for $2n \log n$ timesteps, the probability that coupling will have occured is greater the probability that all variables have been sampled (which is $\Omega(1)$) times the probability that all variables were sampled as 1 in both samplers. Thus if p_C is the probability of coupling,

$$p_C \geq \Omega(1) \left(\exp(-O(n))\right)^2 \left(\Omega(1)\right)^{2O(n)} = \exp(-O(n)).$$

Therefore, if we run for some $\tau(n) = 2^{O(n)}$ timesteps, coupling will have occurred at least once with high probability. The statements in terms of total variance distance follow via the same argument used in the previous lower bound proof. □

Theorem A.10 (LB for Voting: Linear)**.** *For the voting example using linear projection semantics, the minimum time to achieve total variation distance ε is $2^{O(n)}$.*

Proof. Consider a sampler with unary weights all zero that starts in the state $I = Q \cup U$. We will show that it takes an exponential amount of time until $Q \notin I$. From above, the probability of flipping Q will be

$$\mathbb{P}\left(Q \notin I'\right) = \left(1 + \exp\left(2w(|U \cap I| - |D \cap I|)\right)\right)^{-1}.$$

Meanwhile, the probability to flip any u while $Q \in I$ is

$$\mathbb{P}\left(u \notin I'\right) = \frac{\exp\left(0\right)}{\exp\left(w\right) + \exp(0)} = \left(\exp\left(w\right) + 1\right)^{-1} = p,$$

for some p, and the probability of flipping d is similarly

$$\mathbb{P}\left(d \in I'\right) = \frac{\exp\left(-w\right)}{\exp\left(-w\right) + \exp(0)} = p.$$

Now, consider the following events which could happen at any timestep. While $Q \in I$, let E_U be the event that $|U \cap I| \leq (1-2p)n$, and let E_D be the event that $|D \cap I| \geq 2pn$. Since $|U \cap I|$ and $|D \cap I|$ are both bounded by binomial random variables with parameters $1-p$ and p respectively, Hoeffding's inequality states that, at any timestep,

$$\mathbb{P}\left(|U \cap I| \leq (1-2p)n\right) \leq \exp(-2p^2 n),$$

and similarly

$$\mathbb{P}\left(|D \cap I| \geq 2pn\right) \leq \exp(-2p^2 n).$$

Now, while these bounds are satisfied, let E_Q be the event that $Q \notin I'$. This will be bounded by

$$\mathbb{P}\left(E_Q\right) = \left(1 + \exp\left(2w(1-4p)n\right)\right)^{-1} \leq \exp(-2w(1-4p)n).$$

It follows that at any timestep, $\mathbb{P}\left(E_U \vee E_D \vee E_Q\right) = \exp(-\Omega(n))$. So, at any timestep k, $\mathbb{P}\left(Q \in I\right) = k\exp(-\Omega(n))$. However, by symmetry the stationary distribution π must have $\pi\left(Q \in I\right) = \frac{1}{2}$.

Therefore, the total variation distance is bounded by

$$\|\mathbb{P}_k - \pi\|_{\text{tv}} \geq \frac{1}{2} - k \exp(-\Omega(n)).$$

So, for convergence to less than ε, we must require at least $2^{O(n)}$ steps. □

A.3.2 Additional System Details

A.3.2.1 Decomposition with Inactive Variables

Our system also uses the following heuristic. The intuition behind this heuristic is that, the fewer variables we materialize, the faster all approaches are. DeepDive allows the user to specify a set of rules (the "interest area") that identify a set of relations that she will focus on in the next iteration of the development. Given the set of rules, we use the standard *dependency graph* to find relations that could be changed by the rules. We call variables in the relations that the developer wants to improve *active variables*, and we call *inactive variables* those that are not needed in the next KBC iteration. Our previous discussion assumes that all the variables are active. The intuition is that we only require the active variables, but we first need to marginalize out the inactive variables to create a new factor graph. If done naively, this new factor graph can be excessively large. The observation that serves as the basis of our optimization is as follows: conditioning on all active variables, we can partition all inactive variables into sets that are conditionally independent from each other. Then, by appropriately grouping together some of the sets, we can create a more succinct factor graph to materialize.

Procedure We now describe in detail our procedure to decompose a graph in the presence of inactive variables, as illustrated in Algorithm 2. Let $\{\mathcal{V}_j^{(i)}\}$ be the collection of all the sets of inactive variables that are conditionally independent for all other inactive variables, *given the active variables*. This is effectively a partitioning of all the inactive variables (Line 1). For each set $\mathcal{V}_j^{(i)}$, let $\mathcal{V}_j^{(a)}$ be the *minimal* set of active variables conditioning on which the variables in $\mathcal{V}_j^{(i)}$ are independent of all other inactive variables (Line 2). Consider now the set $\mathcal{G}$ of pairs $(\mathcal{V}_j^{(i)}, \mathcal{V}_j^{(a)})$. It is easy to see that we can materialize each pair separately from other pairs. Following this approach to the letter, some active random variables may be materialized multiple times, once for each pair they belong to, with an impact on performance. This can be avoided by grouping some pairs together, with the

Procedure 2 Heuristic for Decomposition with Inactive Variables

Input: Factor graph $FG = (\mathcal{V}, \mathcal{F})$, active variables $\mathcal{V}^{(a)}$, and inactive variables $\mathcal{V}^{(i)}$.

Output: Set of groups of variables $\mathcal{G} = \{(\mathcal{V}_i^{(i)}, \mathcal{V}_i^{(a)})\}$ that will be materialized independently with other groups.

1: $\{\mathcal{V}_j^{(i)}\} \leftarrow$ connected components of the factor graph after removing all active variables, i.e., $\mathcal{V} - \mathcal{V}^{(a)}$.
2: $\mathcal{V}_j^{(a)} \leftarrow$ minimal set of active variables conditioned on which $\mathcal{V}_j^{(i)}$ is independent of other inactive variables.
3: $\mathcal{G} \leftarrow \{(\mathcal{V}_j^{(i)}, \mathcal{V}_j^{(a)})\}$.
4: **for all** $j \neq k$ s.t. $|\mathcal{V}_j^{(a)} \cup \mathcal{V}_k^{(a)}| = \max\{|\mathcal{V}_j^{(a)}|, |\mathcal{V}_k^{(a)}|\}$ **do**
5: $\quad \mathcal{G} \leftarrow \mathcal{G} \cup \{(\mathcal{V}_j^{(i)} \cup \mathcal{V}_k^{(i)}, \mathcal{V}_j^{(a)} \cup \mathcal{V}_k^{(a)})\}$
6: $\quad \mathcal{G} \leftarrow \mathcal{G} - \{(\mathcal{V}_j^{(i)}, \mathcal{V}_j^{(a)}), (\mathcal{V}_k^{(i)}, \mathcal{V}_k^{(a)})\}$
7: **end for**

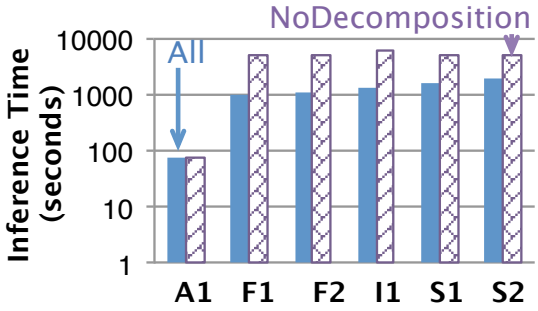

Figure A.3: The Lesion Study of Decomposition.

goal of minimizing the runtime of inference on the materialized graph. Finding the optimal grouping is actually NP-hard, even if we make the simplification that each group $g = (\mathcal{V}^{(i)}, \mathcal{V}^{(a)})$ has a cost function $c(g)$ that specifies the inference time, and the total inference time is the sum of the cost of all groups. The key observation concerning the NP-hardness is that two arbitrary groups $g_1 = (\mathcal{V}_1^{(i)}, \mathcal{V}_1^{(a)})$ and $g_2 = (\mathcal{V}_2^{(i)}, \mathcal{V}_2^{(a)})$ can be materialized together to form a new group $g_3 = (\mathcal{V}_1^{(i)} \cup \mathcal{V}_2^{(i)}, \mathcal{V}_1^{(a)} \cup \mathcal{V}_2^{(a)})$, and $c(g_3)$ could be smaller than $c(g_1) + c(g_2)$ when g_1 and g_2 share most of the active variables. This allows us to reduce the problem to WEIGHTEDSETCOVER. Therefore, we use a greedy heuristic that starts with groups, each containing one inactive variable, and iteratively merges two groups $(\mathcal{V}_1^{(i)}, \mathcal{V}_1^{(a)})$ and $(\mathcal{V}_2^{(i)}, \mathcal{V}_2^{(a)})$ if $|\mathcal{V}_1^{(a)} \cup \mathcal{V}_2^{(a)}| = \max\{|\mathcal{V}_1^{(a)}|, |\mathcal{V}_2^{(a)}|\}$ (Line 4-6). The intuition behind this heuristic is that, according to our study of the tradeoff between different materialization approaches, the fewer variables we materialize, the greater the speedup for all materialization approaches will be.

	Adv.	News	Gen.	Pharma.	Paleo.
# Samples	2083	3007	22162	1852	2375

Figure A.4: Number of Samples We can Materialize in 8 Hours.

Experimental Validation We also verified that using the decomposition technique has a positive impact on the performance of the system. We built NoDecomposition that does not decompose the factor graph and select either the sampling approach or the variational approach for the whole factor graph. We report the *best* of these two strategies as the performance of NoDecomposition in Figure A.3. We found that, for A1, removing structural decomposition does not slow down compared with DeepDive, and it is actually 2% faster because it involves less computation for determining sample acceptance. However, for both feature extraction and supervision rules, NoDecomposition is at least $6\times$ slower. For both types of rules, the NoDecomposition costs corresponds to the cost of the variational approach. In contrast, the sampling approach has near-zero acceptance rate because of a large change in the distribution.

A.3.2.2 Materialization Time

We show how materialization time changes across different systems. In the following experiment, we set the total materialization time to 8 hours, a common time budget that our users often used for overnight runs. We execute the *whole* materialization phase of DeepDivefor all systems, which will materialize both the sampling approach and the variational approach, and we require the whole process to finish in 8 hours. Figure A.4 shows how many samples we can collect given this 8-hour budget: for all five systems, in 8 hours, we can store more than 2000 samples, from which to generate 1000 samples during inference if the acceptance rate for the sampling approach is 0.5.

A.3.2.3 Incremental Learning

Rerunning learning happens when one labels new documents (typically an analyst in the loop), so one would like this to be an efficient procedure. One interesting observation is that a popular technique called distant supervision (used in DeepDive) is able to label new documents heuristically using rules, so that new labeled data is created without human intervention. Thus, we study how to incrementally perform learning. This is well studied in the online learning community, and here we adapt essentially standard techniques. We essentially get this for free because we choose to adapt

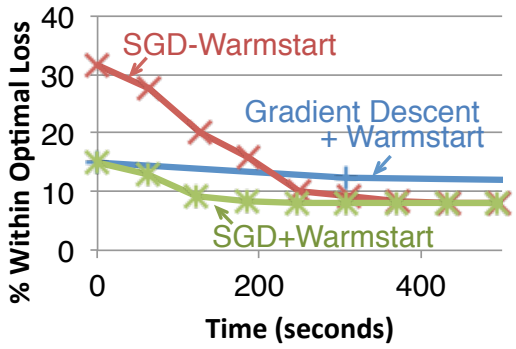

Figure A.5: Convergence of Different Incremental Learning Strategies.

standard online methods, such as stochastic gradient descent with warmstart, for our training system. Here, warmstart means that DeepDiveuses the learned model in the last run as the starting point instead of initializing the model to start randomly.

Experimental Validation We validate that, by adapting standard online learning methods, DeepDiveis able to outperform baseline approaches. We compare DeepDivewith two baseline approaches, namely (1) stochastic gradient descent without warmstart and (2) gradient descent with warmstart. We run on the dataset News with rules F2 and S2, introduces *both* new features and new training examples with labels. We obtain a proxy for the optimal loss by running both stochastic gradient descent and gradient descent separately for 24 hours and picking the lowest loss. For each learning approach, we grid search its step size in {1.0, 0.1, 0.01, 0.001, 0.0001}, run for 1 hour, and pick the fastest one to reach a loss that is within 10% of the optimal loss. We estimate the loss after each learning epoch and report the percentage within the optimal loss in Figure A.5.

As shown in Figure A.5, the loss of all learning approaches decrease, with more learning epochs. However, DeepDive's SGD+Warmstart approach reaches a loss that achieves a loss within 10% optimal loss faster than other approaches. Compared with SGD-Warmstart, SGD+Warmstart is 2× faster in reaching a loss that is within 10% of the optimal loss because it starts with a model that has lower loss because of warmstart. Compared with gradient descent, SGD+Warmstart is about 10× faster. Although SGD+Warmstart and gradient descent with warmstart have the same initial loss, SGD converges faster than gradient descent in our example.

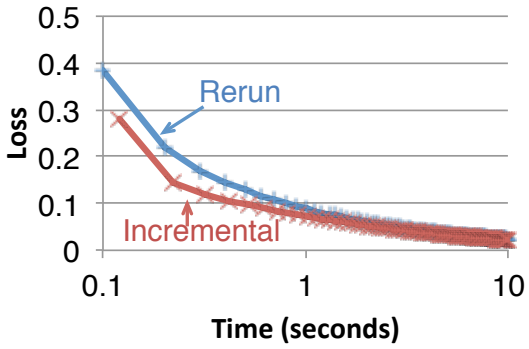

Figure A.6: Impact of Concept Drifts.

A.3.2.4 Discussion of Concept Drift

Concept drift [78, 106] refers to the scenario that arises in online learning when the training examples become available as a stream, and the distribution from which these examples are generated keeps changing overtime. Therefore, the key technique in how to resolve the problem of concept drift is premarily in how to design a machine learning system to automatically *detect* and *adapt to* the changes. The design needs to consider how to not only update the model incrementally, but also "forget the old information" [78]. Although we have not observed quality issues caused by concept drift in our KBC applications, it is possible for DeepDive to encounter this issue in other applications. Thus, we study the impact of concept drift to our incremental inference and learning approach.

Impact on Performance In this work, we solely focus on the efficiency of updating the model incrementally. When concept drift happens, the new distribution and new target model would be significantly different from the materialized distribution as well as the learned model from last iteration. From our previous analysis, we hypothesize there are two impacts of concept drift that require consideration in DeepDive. First, the difference between materialized distribution and the target distributed is modeled as the amount of change, and therefore, in the case of concept drift, we expect our system favors variational approach more than sampling approach. Second, because the difference between the learned model and target model is large, it is not clear whether the warmstart scheme we discussed in Section A.3.2.3 will work.

Experimental Validation As our workloads do not have concept drift, we follow prior art [106], we use its dataset that contains 9,324 emails ordered chronologically, and predict exactly the same

task that for each email predict whether it is spam or not. We implement a logistic regression classifier in DeepDive with a rule similar to Example 3.5. We use the first 10% emails and first 30% emails as training sets, respectively, and use the remaining 70% as the testing set. We construct two systems in a similar way as Section 6.2.2: RERUN that trains directly on 30% emails, and INCREMENTAL that materialize using 10% emails and incrementally train on 30% emails. We run both systems and measure the test set loss after each learning epoch.

Figure A.6 shows the result. We see that even with concept drift, both systems converge to the same loss. INCREMENTAL converges faster than RERUN, and it is because even with concept drift, warmstart still allows INCREMENTAL to start from a lower loss at the first iteration. In terms of the time used for each iteration, INCREMENTAL and RERUN uses roughly the same amount of time for each iteration. This is expected because INCREMENTAL rejects almost all samples due to the large difference between distributions and switch to variational approach, which, for a logistic regression model where all variables are active and all weights have been changed, is very similar to the original model. From these result we see that, even with concept drifts, INCREMENTAL still provides benefit over rerunning the system from scratch due to warmstart; however, as expected, the benefit from incremental inference is smaller.